Role of KCNE4 on the voltage gated potassium channel Kv1.3

Paper de KCNE4 en el canal de potassi dependent de voltage Kv1.3

Laura Solé Codina

ADVERTIMENT. La consulta d'aquesta tesi queda condicionada a l'acceptació de les següents condicions d'ús: La difusió d'aquesta tesi per mitjà del servei TDX (**www.tdx.cat**) i a través del Dipòsit Digital de la UB (**diposit.ub.edu**) ha estat autoritzada pels titulars dels drets de propietat intel·lectual únicament per a usos privats emmarcats en activitats d'investigació i docència. No s'autoritza la seva reproducció amb finalitats de lucre ni la seva difusió i posada a disposició des d'un lloc aliè al servei TDX ni al Dipòsit Digital de la UB. No s'autoritza la presentació del seu contingut en una finestra o marc aliè a TDX o al Dipòsit Digital de la UB (framing). Aquesta reserva de drets afecta tant al resum de presentació de la tesi com als seus continguts. En la utilització o cita de parts de la tesi és obligat indicar el nom de la persona autora.

ADVERTENCIA. La consulta de esta tesis queda condicionada a la aceptación de las siguientes condiciones de uso: La difusión de esta tesis por medio del servicio TDR (**www.tdx.cat**) y a través del Repositorio Digital de la UB (**diposit.ub.edu**) ha sido autorizada por los titulares de los derechos de propiedad intelectual únicamente para usos privados enmarcados en actividades de investigación y docencia. No se autoriza su reproducción con finalidades de lucro ni su difusión y puesta a disposición desde un sitio ajeno al servicio TDR o al Repositorio Digital de la UB. No se autoriza la presentación de su contenido en una ventana o marco ajeno a TDR o al Repositorio Digital de la UB (framing). Esta reserva de derechos afecta tanto al resumen de presentación de la tesis como a sus contenidos. En la utilización o cita de partes de la tesis es obligado indicar el nombre de la persona autora.

WARNING. On having consulted this thesis you're accepting the following use conditions: Spreading this thesis by the TDX (**www.tdx.cat**) service and by the UB Digital Repository (**diposit.ub.edu**) has been authorized by the titular of the intellectual property rights only for private uses placed in investigation and teaching activities. Reproduction with lucrative aims is not authorized nor its spreading and availability from a site foreign to the TDX service or to the UB Digital Repository. Introducing its content in a window or frame foreign to the TDX service or to the UB Digital Repository is not authorized (framing). Those rights affect to the presentation summary of the thesis as well as to its contents. In the using or citation of parts of the thesis it's obliged to indicate the name of the author.

Role of KCNE4 on the voltage gated potassium channel Kv1.3

Paper de KCNE4 en el canal de potassi dependent de voltage Kv1.3

Laura Solé Codina

PhD Thesis, Barcelona 2013

Universitat de Barcelona
Facultat de Biologia
Departament de Bioquímica i Biologia Molecular
Programa de Doctorat en Biomedicina
Bienni 2007-2008

Role of KCNE4 on the voltage gated potassium channel Kv1.3

Paper de KCNE4 en el canal de potassi dependent de voltage Kv1.3

Tesi Doctoral
Memoria presentada per Laura Solé Codina
per tal d'optar al grau de Doctor per la Universitat de Barcelona

Barcelona, Setembre 2013

La interessada,

Laura Solé Codina

Vist i plau del director de la Tesi,

Antonoio Felipe Campo
Professor Titular de Bioquímica
Departament de Bioquímica i Biologia Molecular
Universitat de Barcelona

Agraïments

Sembla mentida que hagin passat més de 10 anys des d'aquell primer dia d'estiu a primer de carrera en que vaig entrar per la porta de MP amb tota la il·lusió del món per començar a col·laborar amb aquest grup. Així que primer de tot, haig de donar les gràcies al Doctor Antonio Felipe per donar-me aquesta oportunitat, per seleccionar-me entre tots els que va entrevistar i per a confiar en mi per a realitzar un doctorat en el seu grup. També li haig de donar les gràcies per tot els suport que m'ha donat, la força i ganes de ciència que m'ha transmès durant tots aquests anys, i per esforçar-ce en ensenyar-me el cantó positiu dels resultats, tot i que jo sempre veiés el negatiu. Gràcies també per les portes que se m'obren al marxar d'aquí, ja que sense la teva ajuda durant tots aquests anys no tindria les oportunitats que ara tinc.

En 10 anys per MP he treballat i he tingut el privilegi d'aprendre de la mà molta gent, molt bona, i no només sobre ciència, tant dels Seniors passats com dels Juniors presents. Gràcies a tots plegats (Rubén, Txell, Nuria, Ramón, Joasia, Mireia, Anna, Núria, Albert, Sara, Kasia i Antonio) per fer que el laboratori fos com una segona casa (i només per la quantitat d'hores que ens hi estem). Gràcies pels riures de cada dia, pels consells en experiments, per les ajudes en acabar experiments quan fa una hora que hauries d'haver marxat, per les cerveses en moments difícils i també en celebracions, i finalment, gràcies per "aguantar-me", ja que després de tant de temps qui més qui menys ha hagut de patir alguna de les meves borderies en els dies més estrès, sabeu que molts cops ni em dono conte, em sap greu. Després de tant de temps a MP, sincerament se'm fa difícil pensar en estar en un altre laboratori que no sigui aquest, ja que ha estat la meva casa per molts anys, però una cosa que m'alegra saber, i que té de bó la investigació, que sé que més o menys ens anirem veient o seguint la pista, mitjançant congressos, estances, etc. i que sempre que els ens trobem serà com si no hagués marxat mai i ens enrecordarem de tot aquest temps.

Al llarg d'aquesta tesi he pogut realitzar dues estances, una a Madrid i una altra a Fort Collins. Gracias a Pilar, Carolina, Miguel y Sebastián por tener paciencia conmigo y explicarme una y otra vez anisotropías y dudas y por hacer que la física no sea tan compleja para una bioquímica. Gracias también por, a pesar de la gran cantidad de horas dedicadas, descubrirme Madrid y lo maravillosa que es su gente. Aquí también incluyo a Cristina, que hizo que los fines de semana en Madrid lejos de casa fueran más llevaderos. Now is turn for Fort Collins: thanks Mike, Phil and Liz. Thanks for teaching me in only three months electrophysiology and single bleaching steps and giving me so many advices. Thanks for your patience, every time I came saying that I did not know why the patch was not working. Furthermore, thanks for letting me enjoy Colorado with you, thanks for those many beers,

backpacking and fishing trips, Yellowstone... It was amazing. Thanks also to my “crazy” American flat-mates. It was a great time, and I am happy to know that soon we will be able to do all the to-do list things that we left.

Agrair també a tota la gent que m’ha acompanyat al llarg d’aquest anys fora del laboratori, amb molt dels quals hem anat madurant junts. No us puc anomenar a tots, però ja sabeu qui sou: gràcies als de Canet, als de Mataró, als de Biologia i als de Bioquímica. Gràcies per tots els moments, alguns d’ells inoblidables, viscuts durant aquest temps. Gràcies també per està allà en moments dolents, per estar sempre disponibles a escoltar i donar el vostre consell (especialment Gemma, Sara i Xavi).

Res de tot això tampoc hagués estat possible sense el recolzament de la meva família. Gràcies als meus pares per estar allà sempre, per inculcar-me els valors que m’heu transmès, ja que segurament sense ells no hagués arribat aquí. Gràcies per recolzar-me i facilitar-me sempre els estudis i l’entrada en el món de la investigació/doctorat, tot i que fos un món desconegut per a vosaltres. Gràcies a la meva germana per estar també sempre allà, segurament tampoc seria qui sóc si no fos per ella, ja que les germanes grans sempre són un model a seguir. Gràcies també Ginés per fer-me com de germà gran.

Finalment gràcies a tu, Xevi, per estar sempre al meu costat, per la paciència, per el escoltar-me fins i tot quan dorms o simplement per intentar-me fer riure després d’un dia dolent de laboratori. Sense el teu recolzament no hagués pogut arribar aquí. Gràcies per tots els anys, moments i viatges compartits, i gràcies per voler continuar compartint la teva vida amb mi, encara que sigui a “l’altra banda del xarco”. Gràcies un cop més, tot i que per més que ho digui, mai seran suficients.

TABLE OF CONTENTS

1. Introduction

1.1. Voltage-gated potassium channels

Potassium-selective channels are the largest and most diverse group of ion channels Potassium channel are transmembrane proteins which allow the selective crossing of potassium ions through the plasmatic membrane and are crucial for life. Potassium channel play important roles in different biological process at the organism level (generation and propagation of the nerve pulse and the cardiac action potential, promotion of insulin secretion), and also at the cellular level (cell volume control, induction of cell proliferation, apoptosis, migration and initiation of many signaling pathways).

Potassium channels can be subdivided in different families, depending on the architecture of their conducting subunits: two transmembrane domains and one pore channels (2TM/1P), four transmembrane domains and two pore channels (4TM/2P) and six transmembrane domains and one pore channels (6TM/1P). The aim of the current dissertation is the voltage-gated potassium channels (Kv), which belong to the last cited group.

The voltage-gated Kv channels form the largest family among the group of human potassium channels, comprising 40 of the 90 potassium channels described genes. According to the International Union of Pharmacology (IUPHAR) they are divided into twelve families (Kv1-12), each of one can present different isoforms. In a phylogenetic way, Kv channels can be grouped into two groups: the first one, comprised by Kv1-9; and the second one, comprised by Kv10-12 (Fig. 1). This last group of channels also possesses a potential cyclic-nucleotide binding site in their C-terminus (Gutman et al. 2003).

Apart from comprising one of the largest families, Kv channels can also multiply their diversity due to the combination of different processes such as:

a) Alternative splicing phenomena of the mRNA. Kv3, 4, 6, 7, 9, 10 and 11 are code by exons and introns which may lead to different variants (Jenkinson 2006).
b) Homo- and hetero-tetramerization between subunits of different Kv members. The assembly can be between members from the same family, as for example Kv1.1-Kv1.4 (Shamotienko et al. 1997), Kv1.3-Kv1.5 (Vicente et al. 2006; Villalonga et al. 2007), or with silent subunits (Kv5, Kv6, Kv8 and Kv9). These silent subunits, do not homo-tetramerize, but can assemble to some members of Kv2 and Kv3 families in order to modulate their current (Hugnot et al. 1996; Post et al. 1996; Salinas et al. 1997).
c) Post-translational such as phosphorylation, glycosylation, ubiquitination, palmitoylation, oxidation, etc. (Nitabach et al. 2002; Zhang et al. 2007; Jindal et al. 2008; Noma et al. 2009)

d) Assembly of regulatory subunits which modulate the Kv characteristics (traffic, current density and gating) such as AKAP proteins, Kvβ, KCNEs, etc (Pongs et al. 1999; Pourrier et al. 2003).

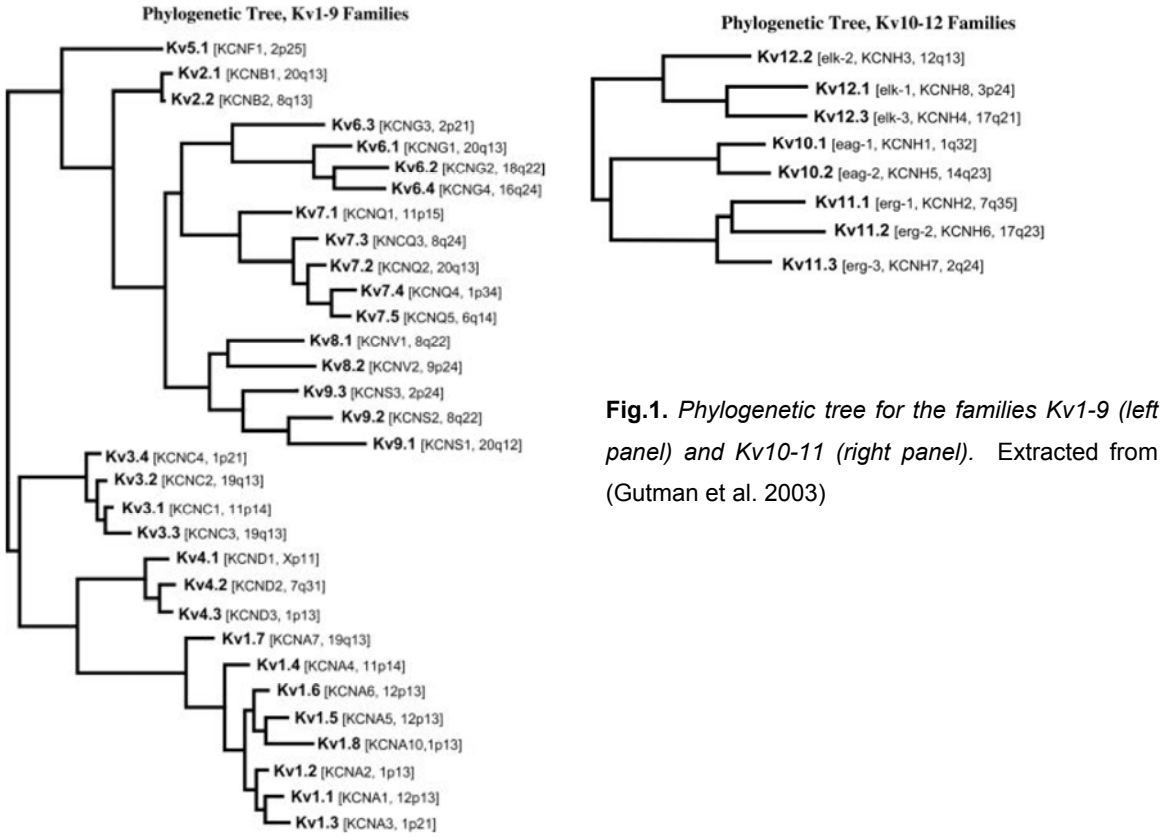

Fig.1. *Phylogenetic tree for the families Kv1-9 (left panel) and Kv10-11 (right panel).* Extracted from (Gutman et al. 2003)

1.1.1. Basic principles of Kv channels

Kv channels are made up of the tetramerization of 4 α subunits (MacKinnon 1991). Each of these subunits is composed by six transmembrane domains (S1-S6), which are connected by an intra or extracellular loops. The first four helices (S1-S4) form the voltage sensor domain, whereas the S5-S6 form the ion conducting pore. X-ray crystal structures of bacterial and eukaryotic Kv channels have been solved and show that the pore domains are arranged with four-folds symmetry around the ion conduction pathway, while the voltage-sensing domains lies at the periphery (Fig. 2) (Jiang et al. 2002; Jiang et al. 2003; Long et al. 2005; Long et al. 2007; Tao et al. 2009). The Nt- and Ct- domains are both intracellular, and their structure was more difficult to be solved. For Nt- structure resolution the crystallization of Kv1.2 in presence of Kvβ2.1 was needed (Long et al. 2005). For the entire KcsA C-terminus was needed, as crystallographic chaperones, the use of antigen-binding fragments (Fabs) (Uysal et al. 2009).

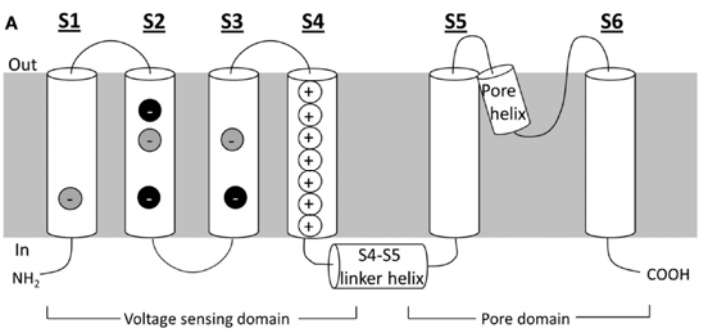

Fig 2. *Schematic representation of the membrane topology of a Kv α subunit*. Kv channels are composed by 6 trasnmembrane domains. S1-S4 segments form the voltage sensor domain. The positive residues of S4 are highlighted. S5-S6 segments compose the pore domain. Extracted from (Cheng and Claydon 2012)

1.1.1.1. The pore and ion selectivity

The pore domain of an α-subunit is formed by the S5 and S6 segments, which are joined by a re-entrant pore helix and loop (P-loop). The P-loop of Kv channels is characterized for containing a highly conserved motif: TVGYGG, which is crucial for the selectivity filter of the channel (Heginbotham et al. 1994). In fact, mutations in this sequence lead to a lack of K^+ ion selectivity (Heginbotham et al. 1994; Aiyar et al. 1996).

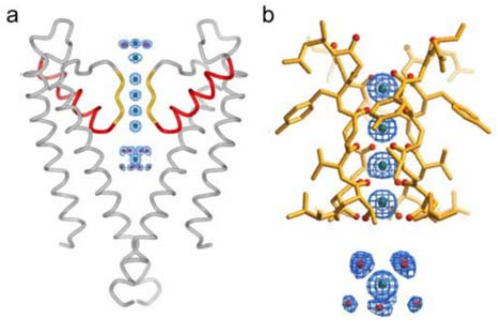

Fig. 3. *Strucutural model of the KcsA pore.* Left panel: conformation acquired of two subunits. The selectivity filter is highlighted in yellow. Right panel: Conformation acquired by the selectivity filter and dehydrated potassium ions. (MacKinnon 2003)

Crystal structures of the voltage-gated potassium channel allowed understanding the mechanism of the pore. The pore is about 45Å, and contains (from inside to outside) a 18Å tunnel, followed by a more open cavity of 10Å, and then, for about 12Å, the selectivity filter is located in another narrower conduct, with the carbonyl groups facing the conducting pathway (Fig.3). The selectivity of Kv channels rise in the size of K^+ ions, which fits perfectly between the carbonyl groups present at the selectivity filter (Doyle et al. 1998; Zhou and MacKinnon 2003).

The access to the ion conducting pore is controlled by an intracellular gate comprised of the S6 C-terminal end, which form a bundle crossing that obstructs the pore when the channel is closed (Holmgren et al. 1997; Doyle et al. 1998). It is worthy to mention that this is possible due to the presence of a flexible high conserved sequence among S6 segment (which in general is more rigid): PxP, which acts as a hinge, allowing the opening or

closing of the intracellular part of the S6 domain, in front of changes in the membrane voltage, detected by the VSD (del Camino et al. 2000; del Camino and Yellen 2001).

1.1.1.2. The voltage sensor

Kv channels respond to membrane potential changes. The voltage sensor domain which comprises the S1-S4 α helixes, is the responsible of this sensing. High conserved sequences throughout S1, S2, S3 are also involved in the voltage-dependent conformational change, but S4 playing a major role. S4 sequence contains a positive charged amino acid (Arg or Lys) every two hydrophobic amino acids, repetitively, 4 to 8 times (Liman et al. 1991; Logothetis et al. 1992; Papazian et al. 1995). This creates a positively charged surface along the S4 which senses the membrane potential. S1-S3 segments, plenty of negative charges, complete the voltage-sensing domain and help to stabilize the positively charged S4 segment in the lipid bilayer and to define the pathway for its movement through the electric field (Papazian et al. 2002; Borjesson and Elinder 2008).

1.1.1.3. Gating

Among the last decade, many X-ray crystal structures from different channels in open or close state have been obtained, and an extended debate about the gating movement of the voltage sensor have been performed. Three main models were proposed: a) the helical-screw or sliding helix model, where S4 rotates along its axis while being translated across the membrane to move gating charges across the electric field (Larsson et al. 1996; Durell et al. 1998; Keynes and Elinder 1999); b) the transporter-like model, where a mostly rotational movement of S4 essentially flips S4 charges from one side of the membrane to the other (Starace and Bezanilla 2001; Chanda et al. 2004; Starace and Bezanilla 2004; Chanda et al. 2005), and c) the paddle model, initially based on the crystal structure of KvAP in which a voltage sensor paddle comprised of S4 and the C-terminal half of S3 form a rigid structure that moves through the membrane an in close proximity to S1 and S2 (Jiang et al. 2003; Ruta et al. 2005). But the current understandings (Fig. 4) seem to converge toward a single consensus model for the gating movement of the voltage sensor: the movement of S4 upon activation seems to be a combination of a tilt of the S4 helix in the membrane, a rotation around the helix axis, and small vertical and radial translations. Movement of the voltage-sensing unit in response to changes in membrane potential is translated into the opening or closing of the activation gate within the pore domain, through and electromechanical coupling. The outward movement of S4 upon depolarization may create tension in the α-helical S4-S5linker, which appears to lie across the distal S6 helix below the PxP motif within the same subunit. Then, upon depolarization, S4-S5 linker is predicted to cause radial

displacement of the the C-terminal end of S6, moving away from the central axis of the pore to open the activation gate, permitting ion permeation. (Chen et al. 2001; Ding and Horn 2002; Lu et al. 2002; Long et al. 2005; Labro et al. 2008).This movement is in part allowed for the presence of the highly conserved PxP motif at S6 that introduces a kink in the α-helical structure, allowing the electromechanical coupling with the S4-S5 linker.

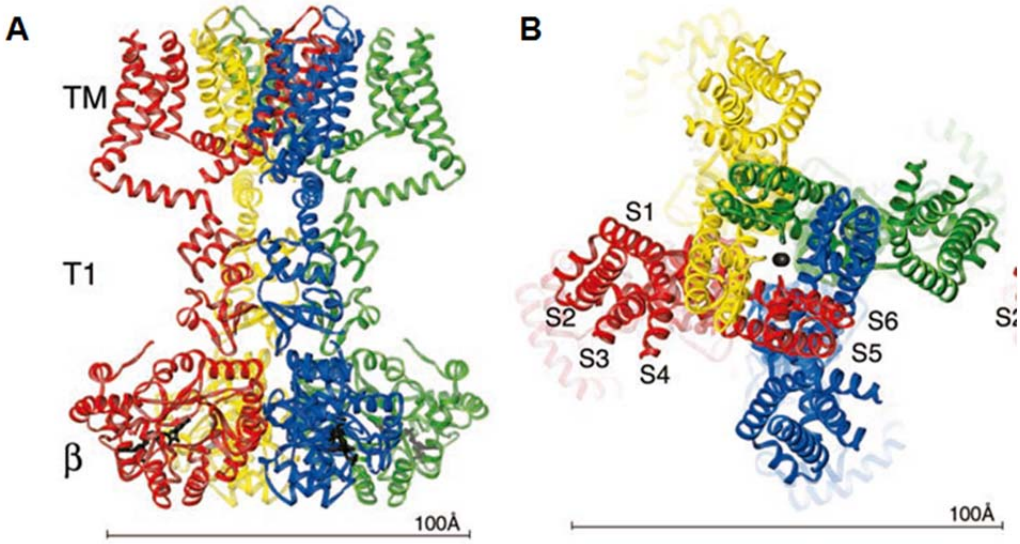

Fig.4. *Crystal structure of the Kv1.2–β2 subunit complex.* A. Stereoview from the side, four subunits of the channel are colored uniquely. B. Stereoview of a ribbon representation viewed from the extracellular side of the pore. Extracted from (Long et al. 2005)

Once opened, channels can be closed thanks of different processes voltage-independent: inactivation of the channel. Different kinds of inactivation have been described (Fig. 5). N-type inactivation ("ball and chain" inactivation type) is characteristic from Kv1.4, Kv3.3, Kv3.4 and Kv4 family, for example. During the fast, N-type inactivation, a ball peptide tethered to the N-terminus of the Kv channels enters the open pore when the channel is still open and blocks access to it (Hoshi et al. 1990; Zagotta et al. 1990; Zhou et al. 2001). Kvβ can mimic this kind of fast inactivation (Rettig et al. 1994; Morales et al. 1995). Another kind of inactivation is the

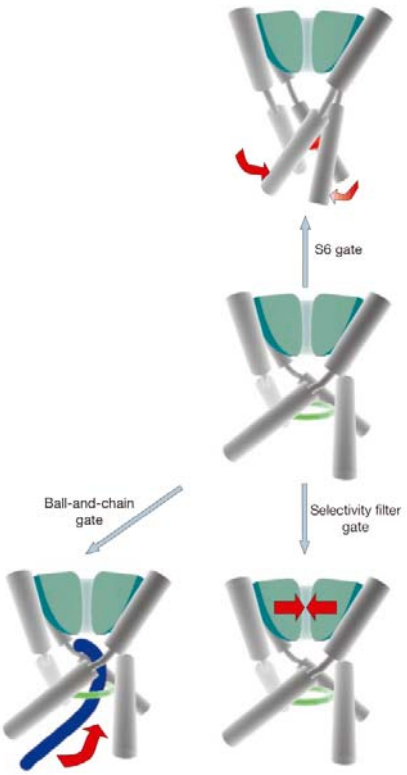

Fig. 5. *Representation of the conformational changes that gate the Kv channel pore.* The pore is colored in green, and the grey helices represent the S6 segments. In the middle panel, the channel is in an open conformation. In the upper panel, channel is in a closed conformation, according to KcsA crystal. In the bottom panels, the channel adopts an inactivated conformation trough N-type (right) and C-type (left) inactivation processes. (Yellen 2002)

C-type, which is slower than the N-type, and it seems is due to movements in the residues near the selectivity filter of the channel (Blunck et al. 2006; Wang et al. 2011) . It appears that the selectivity filter acts as a second gate and prevents ions from passing through. Kv7 channels seem also to possess one kind of inactivation which differs from the two mentioned before (Jensen et al. 2007).

1.1.2. Biogenesis and traffic of Kv channels

Kv channels are synthesized in the rough endoplasmic reticulum (ER) (Palade 1975). Although Kv channels do not possess the typical ER targeted signal sequence, they undergo ER targeting by a S2 transmembrane domain, found for Kv1.3 (Tu et al. 2000). Kv channels are synthesized and assembled as tetrameric complexes in the ER (Schulteis et al. 1998; Papazian 1999; Lu et al. 2001). In fact, the T1 domain (tetramerization domain located at the Nt) association takes place while nascent polypeptide chains are still attached to synthetizing ribosomes (Lu et al. 2001). Kv complexes are further subjected to a quality control checkpoint (Braakman and Bulleid 2011), which allows tetrameric configurations to exit the ER. The composition and stoichiometric assembly of Kv1 hetero-tetrameric channels have been demonstrated to have major effects on ER export of the channels (Manganas and Trimmer 2000; Vicente et al. 2008).

The correct folding of Kv may require the intervention of chaperones such as Heat shock proteins (Hsp) or calnexin. For example, Kv1.5 stability increases when interacting with Hsp70 (Hirota et al. 2008) and Kv1.2 surface levels increases when co-expressed with calnexin (Manganas and Trimmer 2004). Sometimes, regulatory subunits also play as chaperones. Kvβ2 stabilizes Kv1.2 and also increases membrane surface targeting (Shi et al. 1996). Other regulatory subunits, which play a similar role to chaperones are KChAP, KChIP and dippetidyl aminopeptidase (DPPL)-like proteins (Kuryshev et al. 2000; Kuryshev et al. 2001; Nadal et al. 2003; Shibata et al. 2003).

Signal sequences, such as R-X-R, K-K-X-X and K-D-E-L, are responsible for ER retention of Kv, (Zerangue et al. 1999; Ma et al. 2001; Kupershmidt et al. 2002). In most of the cases, their accessibility becomes hidden when the channels acquire their proper folding, and then, the channels can leave the ER. If these sequences are exposed, the channel is retained at the ER. Apart from this generic ER retention signals, Some Kv also possess an anterograde trafficking signal (V-X-X-S-L or similar) in their C-terminal domain (Li et al. 2000) (Steele et al. 2007). Furthermore, in some Kv members, ER retention signals located at the extracellular face of the pore, between S5 and S6, have also been described (Manganas et al. 2001; Zhu et al. 2003; Zhu et al. 2003; Zhu et al. 2005). The effects of this ER retention

signal is dominant respect other signals or even association with regulatory subunits, such as Kvβ(Manganas et al. 2001).

The traffic of the final heteromeric complex (different α and β subunits) will depend on the balance of signals of each subunit. For example, the combination of Kv1.1 (strong retention signals) with Kv1.4 (good surface targeting) leads to a complex with ER retention but high glycosylation (Zhu et al. 2003). Changes in the stoichiometry between the different subunits will alter the traffic, depending on the more abundant subunit (Manganas et al. 2001).

From the ER, Kv channel complexes continue on their journey to the plasma membrane, passing through cis-medial-, and trans-Golgi elements. Some membrane proteins need a selective transport from the ER to the Golgi apparatus, for example via COPII vesicles. This process is complex and requires the coordinated activity of different proteins such as Sec and SarI, the cytoskeleton, etc. In general, COPII recognition sites are characterized for containing di-hydrophobic (F-F, Y-Y, L-L, or F-Y) or di-acidic (D/E-X-(D/E) motifs. Few potassium channels have been described to interact directly with COPII anterograde mechanism ($K_{AT}1$, $K_{2P}9.1$) (Zuzarte et al. 2007; Sieben et al. 2008). Kv1.3 contains an anterograde signature motif (YMVIEE) in its C-terminus domain which involves COPII interaction (Martínez-Mármol et al. 2013).

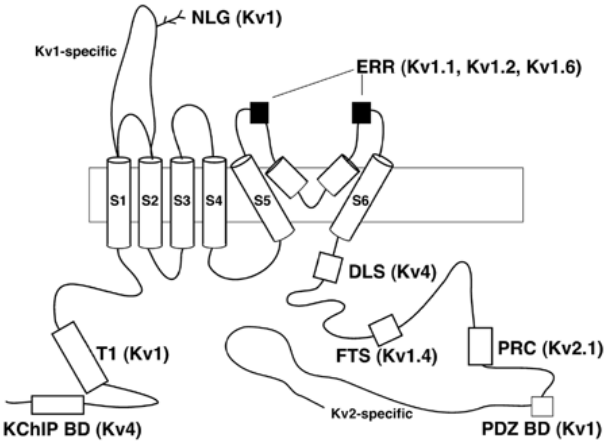

Fig. 6. *Cartoon summarizing of trafficking signals on Kv α subunits.* KChIP BD, KChIP binding domain; T1, tetramerization; NLG, N-linked glycosylation site; ERR, ER retention motif; DLS, dendritic localization signal; FTS, forward-trafficking signal; PRC, proximal dendritic clustering signal; PDZ BD, PDZ-binding domain. Extracted from (Misonou and Trimmer 2004)

Along this forward trafficking to Golgi apparatus, Kv channels undergo further modification, such as N-linked glycosylation, tyrosine, serine or threonine's phosphorylation. Phosphorylation modify channel's activity (Bowlby et al. 1997; Fadool et al. 1997; Nitabach et al. 2002; Misonou et al. 2004), as well as surface membrane targeting (Misonou et al. 2004; Yang et al. 2007) and recycling (Sterling et al. 2002; Nesti et al. 2004). Finally, ubiquitination also regulates Kv's membrane levels. In this vein, ENaC, Kv1.5, Kv7.2, Kv7.3, Kv7.5 are

ubiquitinated triggering endocytic signals and downregulating membrane abundance (Staub et al. 1997; Abriel et al. 2000; Ekberg et al. 2007; Boehmer et al. 2008).

1.1.3. Subcellular localization of Kv channels: lipid rafts microdomains

Plasma membranes are not a homogenous bilayer. In a membrane exist different regions which differ in lipid composition and structure, creating a patchwork of different lipid environments at the cell surface. These different domains, known as lipid rafts, are characterized for being rich in cholesterol, sphingolipids and phospholipids with saturated acyl tails, forming tightly packed aggregates (Harder and Simons 1997; Simons and Ikonen 1997). These domains, which a size of 10-200 nm, are relatively more rigid, ordered structures than the more fluid and bulk regions of the bilayer where the kinked hydrocarbon chains of the largely unsaturated phospholipids prevent close packing (Brown and London 1998; Simons and Toomre 2000). Despite their high packed structure, lipid rafts are a very dynamic domains which participate in the recruitment of a wide range of proteins, and at the same time, these proteins suffer a dynamic exchange with the neighborhood (O'Connell et al. 2006; Tamkun et al. 2007). Many functions have been associational to lipid rafts, such as: endocytosis and exocytosis (Anderson 1998), internalization of virus and toxins (Brown and London 1998; Herreros et al. 2001; Triantafilou and Triantafilou 2004), cell migration (Hanzal-Bayer and Hancock 2007), polarization of cell functions (Simons and Ikonen 1997; Guirland and Zheng 2007), cell signal transduction (Shaul and Anderson 1998; Simons and Toomre 2000; Patel et al. 2008), etc. Then, lipid raft are like protein recruitment platforms, which selectively aggregate interacting signaling molecules, allowing to the different proteins involved in a same signal transduction pathway to become really close and facilitating the coordination of the signaling pathways in front of specific stimulus.

Multiples types of rafts exist with differences in lipid and protein composition. The only morphologically identifiable raft-like domain are caveolas, where association with the specific protein caveolin causes the cholesterol- and sphingolipid-enriched regions of the membrane to bend into the cell forming a small flask-shape invagination (Fig. 7.), visible in scanning electron microscope (Yamada 1955; Scherer et al. 1994; Parton et al. 1997).

Raft-enriched lipids, such as cholesterol and sphingolipids, affect channel activity either via direct protein-lipid interaction (Epshtein et al. 2009) or by influencing the physical characteristics of the bilayer (Andersen and Koeppe 2007). Ion channels can be also affected by the interaction of proteins present in the lipid rafts, such caveolin or other scaffolding proteins (Jiao et al. 2008; Garg et al. 2009).

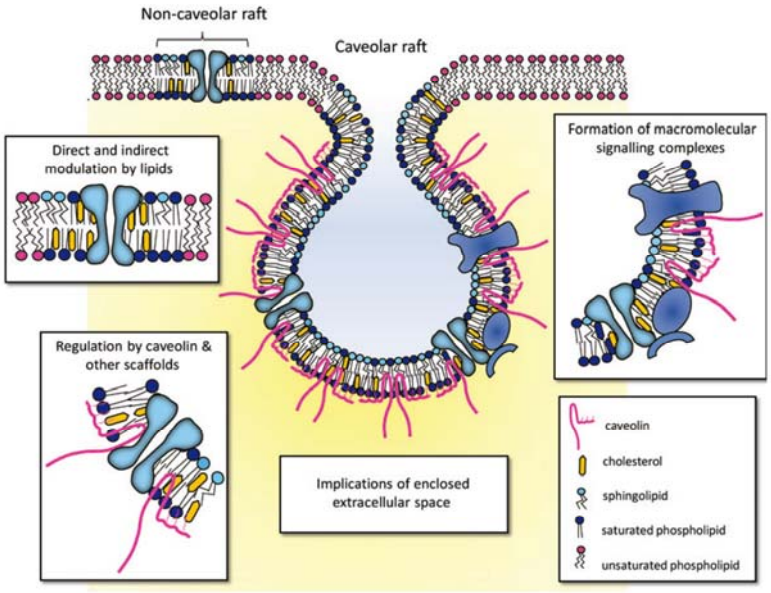

Fig. 7. *Representation of the plasma membrane with different lipid raft microdomains.* A caveola is represented in the center of the scheme, with the characteristic flask-shape, and several channels and proteins recruited in there. Cholesterol is colored in yellow, sphingolipids and saturated phospholipids in blue, and caveolin in pink. Extracted from (Dart 2010)

A number of ion channels locate at lipid raft microdomains (table 1). Evidence for the association of ion channels with membrane rafts comes mainly from three different approaches: (i) biochemical techniques that exploit the unusual properties of these domains to isolate them and from the rest of the cell membrane; (ii) microscopic approaches designed to directly visualize rafts; and (iii) functional approaches that destroy these domains, through the depletion of cellular cholesterol by agents such as methyl-β-cyclodextrin. The isolation of lipid raft is based in the resistance to solubilization by cold non-ionic detergents, such as 1% Triton X-100, due to the tight packing and the high lipid content of the complexes, which also enables rafts to float on a low density sucrose gradient centrifugation (Brown and Rose 1992; Sargiacomo et al. 1993). Appropriate fractions can be isolated from the density gradient and proteins associated with these fractions characterized by Western blot analysis.

As mentioned before, a range of signaling proteins are recruited into lipid rafts, including G-protein coupled receptors, various classes of G protein, adenylyl cyclase, protein kinase C, nitric oxide synthase, tyrosine kinases, H-ras and mitogen-activated protein kinase (Patel et al. 2008). Protein recruitment to raft microdomains may result from specific targeting signals, such as palmitoylation and myristoylation (Zacharias et al. 2002). Additionally, targeting may be through association with caveolae-associated scaffolding proteins, like caveolin or membrane-associated guanylate kinase (MAGUK) proteins such as postsynaptic density protein-95 (PSD-95) and synapse-associated protein-97 (SAP97),which have been

suggested to be important in the localization of Kv1.4 and Kv1.5, respectively, to membrane rafts (Folco et al. 2004; Wong and Schlichter 2004).

Caveolin is a small protein (21-24KDa), which possess intracellular Nt- and Ct-terminal domains, with an embedded hairpin into the membrane. There are three caveolin isoforms (cav-1, 2 and 3) (Rothberg et al. 1992; Scherer et al. 1995; Tang et al. 1996). While cav1 and 2 are ubiquitous, cav3 is muscle specific (Razani et al. 2002). The N-terminal domain of caveolin interacts with other proteins via a Caveolin-Scaffolding Domain (CSD). Therefore, caveolin can act as an anchoring point to the membrane for G proteins, kinases, etc. In many proteins which interact with caveolin, a consensus caveolin binding sequence has been identified (Cavelin-Binding Domain, CBD). The motif of CBD may be φxφxxxxφ, φxxxxφxxφ and φxφxxxxφxxφ, where φ corresponds to an aromatic amino acid (trp, phe, tyr) (Couet et al. 1997).

Channel	Tissue	Comments	References
Kv1.3	Jurkat T-lymphocytes HEK-293	Constitutively present in rafts. Hydrolysis of sphingomyelin causes rafts to merge into large ceramide-enriched domains. Association of Kv1.3 with ceramide-enriched domains inhibits channel activity	(Bock et al. 2003) (Vicente et al. 2008)
Kv1.4	Brain HEK293Tcells Pancreatic β cells	Requires PSD-95 for raft targeting	(Wong and Schlichter 2004) (Xia et al. 2004)
Kv1.5	Heart Cell lines	Cholesterol depletion modulates gating Interaction with SAP-97 and caveolin-3 involved in raft targeting. Coexpression with caveolin or addition of exogenous cholesterol causes a depolarizing shift in steady-state activation and inactivation	(Abi-Char et al. 2007) (Folco et al. 2004) (Martens et al. 2001)
Kv2.1	L cell fibroblasts Pancreatic β cells Oocytes	Cholesterol depletion causes hyperpolarizing shift in the inactivation curve Cholesterol depletion reduces current amplitude and causes hyperpolarizing shift in inactivation curve Regulation of gating by sphingomyelin	(Martens et al. 2000) (Xia et al. 2004) (Ramu et al. 2006)
Kv4.2	Brain		(Wong and Schlichter 2004)
Kv7.1	Heart HEK293 cells		(Balijepalli et al. 2007)
Kv11.1	Heart HEK293 cells	Cholesterol depletion causes positive shift in voltage dependence of activation and accelerates deactivation kinetics	(Balijepalli et al. 2007)
K_{Ca}1.1	Aorta Myometrium Aortic endothelial	Caveolin-regulated surface expression Knockdown of caveolin with siRNA suppresses total BK current Channel inactive under control conditions but activated by cholesterol depletion or knockdown of caveolin	(Alioua et al. 2008) (Brainard et al. 2009) (Wang et al. 2005)
Kir2.1	Aortic endothelial	Cholesterol depletion increases current density. Single channel properties unaffected – cholesterol may modulate number of active	(Romanenko et al. 2002)

		channels	
Kir3.1/Kir3.2	Neurones CHO cells	Rafts may be involved in surface delivery	(Delling et al. 2002)
Kir4.1	Astrocytes HEK293 cells	Associate with non-caveolar lipid rafts. Cholesterol depletion results in loss of channel activity	(Hibino and Kurachi 2007)
Kir6.1	Aorta Vascular smooth muscle HEK293 cells	Cholesterol depletion abolishes cAMP/PKA regulation of channel PKC-mediated caveolin-dependent Internalization	(Sampson et al. 2004; Sampson et al. 2007) (Jiao et al. 2008)
Kir6.2	Heart	Currents suppressed by association with caveolin-3, but not caveolin-1	(Garg et al. 2009)
Nav1.5	Heart	Gαs-mediated recruitment of Nav1.5-containing caveolae to surface membrane -increase in current density	(Yarbrough et al. 2002; Balijepalli and Kamp 2008)
ENaC	Cell lines	Caveolin-dependent ubiquitination and subsequent internalization	(Hill et al. 2007; Lee et al. 2009)
$Ca_V1.2$	Pancreatic β cells Smooth muscle Heart	 Destruction of caveolae causes loss in β2AR regulation (neonatal mice myocytes) or enhanced β2AR regulation (adult rat myocytes)	(Xia et al. 2004) (Darby et al. 2000) (O'Connell et al. 2004; Balijepalli et al. 2006) (Calaghan and White 2006)
HCN4	Sinus node	Cholesterol depletion causes positive shift in activation; reduces deactivation; loss of β2AR regulation Disruption of caveolae by expression of dominant negative caveolin mutants shifts voltage dependence of activation to more negative potentials and increases time constant of activation	(Barbuti et al. 2004)
Connexin-43	Cell lines	Sucrose density gradients also suggest that Cx32, Cx36, and Cx46 are targeted to lipid rafts, while Cx26 and Cx50 are specifically excluded	(Schubert et al. 2002)
CFTR	Epithelial cells	Raft association required for CFTR-dependent bacterial internalization and activation of innate immune response	(Kowalski and Pier 2004)
CLIC4	HEK293 cells		(Suginta et al. 2001)
TRPC	Submandibular gland cells Smooth muscle Platelets	Cholesterol depletion inhibits TRPC1-store operated Ca2+ signals	(Kwiatek et al. 2006; Pani et al. 2009; Sundivakkam et al. 2009)
P2X1	Platelets Vascular smooth muscle	Cholesterol depletion inhibits P2X1-mediated currents and artery contraction	(Vial and Evans 2005)
P2X3	Neurones		(Vacca et al. 2004)
P2X4	Epithelial cells		(Barth et al. 2008)
P2X7	Submandibular cells	Cholesterol depletion inhibits P2X7-mediated lipid signaling	(Barth et al. 2007; Barth et al. 2008)

Table 1. *Summary of the ion channels located in lipid raft microdomains*. Adapted from (Dart 2010)

1.1.4. Regulatory subunits

Channelosomes are multi-subunit complexes formed by membrane-integrated Kv-subunits (α subunits) and accessory subunits. Accessory subunits influence a wide range of

Kv channel properties, such as gating, post-translational modifications, traffic and subcellular localization, pharmacology, etc. Different kind of regulatory subunits have been described (Fig. 8.), which some of them are cytoplasmic (Kvβ subunits, KChIP (K^+ Channel Interacting Proteins) and KChAP (K^+ Channel Associated Proteins) and others are transmembrane proteins (KCNEs and dipeptidyl aminopeptidase-like proteins (DPPLs)) (Li et al. 2006).

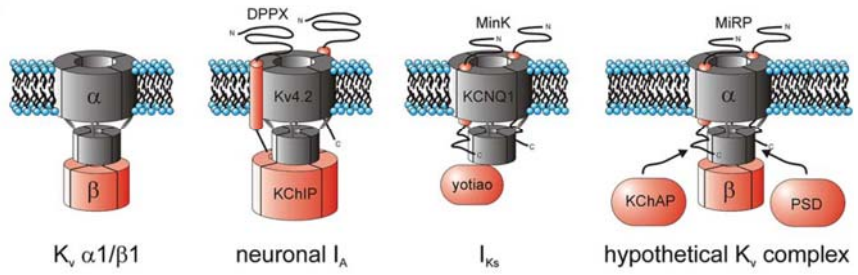

Fig 8. *Cartoon representing different regulatory subunits associated to Kv channels.* Kv channels are colored in grey and regulatory subunits are highlighted in red. See the different localization, depending on the family of auxiliary subunits: Kvβ, KChIP, KChAP are associated to the intracellular domains of Kv, while DPPX and KCNEs (MinK and MIRP) are located between the transmembrane segments of the channel. Extracted from (McCrossan and Abbott 2004)

Kvβ are cytoplasmic regulatory subunits which interact with Kv channels (Kv1.x, Kv2.2 and Kv4.x, specifically), assembling in the early synthesis at the ER (Nagaya and Papazian 1997). There are three subfamilies: Kvβ1 (Kvβ1.1-1.3), Kvβ2 (Kvβ2.1, Kvβ2.2) and Kvβ3. Kvβ have a size of 300 aa and a very conserved Ct domain which interacts with the T1-domain of the Nt- domain of Kv channels (Pongs et al. 1999; Wissmann et al. 1999; Long et al. 2005). Stoichiometry association with Kv channels is 1:1 (Long et al. 2005). Kvβ1 interacts with all the members of Kv1 family; Kvβ2 associates with Kv1 and Kv4 members; while Kvβ3 interacts with Kv1.2, Kv1.3, Kv1.4 and Kv1.5 (Pongs and Schwarz 2010). In general, their effect is to introduce ball-chain type inactivation to the channels (Heinemann et al. 1994; Rettig et al. 1994; Leicher et al. 1998), or accelerate the inactivation of the N-type inactivation channels (McIntosh et al. 1997). Some Kvβ, working as a chaperone, also increase the membrane surface expression of the functional complex (Shi et al. 1996; Accili et al. 1997). Kvβ sense the redox state of the cell. For instance, Kvβ2 possess a NADPH oxido-reductase domain, which could lead the coupling between the membrane potential with the cell redox state (Bahring et al. 2001; Weng et al. 2006).

KChIP regulatory subunits possess a conserved Ct- domain, where four EF-hand Ca^{2+} binding domains are located (Pongs and Schwarz 2010). KChIPs interact specifically with Kv4 members, especially with Kv4.2 and Kv4.3. These proteins play an important role in heart, where are necessary to generate I_{to} currents (An et al. 2000; Nerbonne and Kass 2005). KChIPs slow the inactivation, affect traffic and localization, and modulate the

membrane mobility and endocytosis of Kv4 channels. It is important to mention that KChIP2 is not restricted to Kv4 channels (Li et al. 2006; Pongs and Schwarz 2010). KChIP2 also impairs trafficking and cell surface expression of Kv1.5 (Li et al. 2005). KChIP assemble to T1 domain of Kv channels at the ER in a 1:1 stoichiometry (Kim et al. 2004; Wang et al. 2007).

KChAP regulatory subunits enhance the current amplitude of Kv channels, due to a chaperone role, leading to an increase in the surface expression of the channel (Li et al. 2006). They are expressed in heart, brain, kidney and lung. They can associate to Kv1.1-1.5 and Kv2.1-2.2 (Kuryshev et al. 2000). A competitive interaction with Kvβ subunits has been proposed (Kuryshev et al. 2001).

DPPLs are dipeptidyl aminopeptidase-like proteins without serine protease activity due to mutations in the highly conserved serine residue in the catalytic site of the DPP serine proteases (Nadal et al. 2003). Two DPPL families have been described, DPP6 (DPPX) and DPP10 (DPPY). The general topology reveals a relatively short cytoplasmic N-terminus, a single transmembrane segment, and a large extracellular C-terminus, which displays a glycosylation domain, a cysteine-rich domain, and an aminopeptidase-like domainDPP (Nadal et al. 2003). It has been proposed that the single DPPL-transmembrane domain binds to the voltage sensors of the Kv4 channels (Strop et al. 2004). The stoichiometry of the complex has not been decipher yet, despite that DPPL can homo- and hetero-dimerize (Strop et al. 2004; Soh and Goldstein 2008). In general, DPPL interact with Kv4 channels (most of the time overlapping with KChIPs regulatory subunits) and lead to a great increase in surface expression and to a significant acceleration of the inactivation time course of channels (Jerng et al. 2005; Zagha et al. 2005; Dougherty and Covarrubias 2006). DPPL slow retrograde trafficking by stimulating Kv4 channel retention in the plasma membrane by binding to components of the extracellular matrix (Nadal et al. 2003).

KCNEs are small transmebrane proteins (14-20 KDa or 103-170aa) which interact with a wide range of Kv channels. These regulatory subunits are one of the most promiscuous auxiliary subunits described. Not only one member of the CKNE family can regulate multiple different Kv channels, but also one Kv family member can be regulated by different KCNEs. The family is composed of five members (KCNE1-5) and has a very ubiquitous expression (McCrossan and Abbott 2004). Each member will be detailed below.

1.2. KCNEs

KCNE family is a composed of 5 members (KCNE1-5) of single spanned transmembrane proteins. Their Nt-domain is extracellular and the Ct-domain intracellular. KCNE4 is the more divergent, especially the Ct-domain (Fig. 9). All five members are able to

interact with a wide range of potassium channels. Promiscuity in co-assembly and diversity of regulation allows different tissues to carry unique electrophysiological phenotypes by expressing different KCNE-Kv combinations.

The first cloned member was KCNE1 (Takumi et al. 1988), which was called MinK (minimal K^+ channel), because it was thought that was able to generate currents. Some years later, it was discovered that the currents detected were due to endogenous potassium channels from *Xenopus* oocytes, and that KCNE1 was just an accessory subunit. KCNE2, 3 and 4 were cloned, for KCNE1 homology and they were called MinK Related Peptides (MIRP) 1, 2 and 3, respectively (Abbott and Goldstein 1998; Abbott et al. 1999). Finally, KCNE5 (MIRP4 or KCNE1-like) is one of the genes involved in the AMME disease (Alport syndrome, Mental retardation, Midface hypoplasia and Elliptocytosis), caused for huge genes deletions (Piccini et al. 1999).

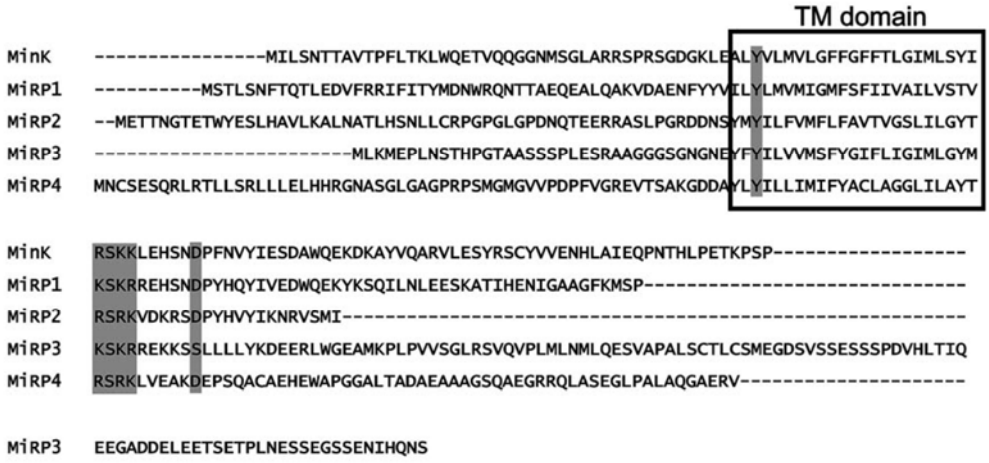

Fig. 9. *Sequence alignment of the human KCNE family.* The squared region corresponds to the transmembrane domains. Three conserved regions are highlighted in grey. Adapted from (McCrossan and Abbott 2004)

1.2.1. KNCE1

As previously mentioned, KCNE1 was cloned as the responsible for the cardiac I_{ks} current (Takumi et al. 1988). However, *Xenopus* oocites express endogenous potassium channels (Kv7.1) which co-assemble with the KCNE1 generating an I_{Ks} resembling current (Barhanin et al. 1996; Anantharam et al. 2003; Gordon et al. 2006). KCNE1 is a regulatory subunit of 15KDa approximately. Two splicing isoforms have been described: KCNE1b, which seems a heart specific isoform, and KCNE1a, which is more ubiquitously expressed (Lundquist et al. 2006). Curiously, KCNE1, as KCNE2, undergoes a sequential cleavage mediated by different secretases which is involved in the regulation of Kv channels (Sachse et al. 2013).

KCNE1 association to Kv7.1 shifts the voltage-dependence of activation towards more depolarized potentials, slows activation and deactivation kinetics, removes inactivation and raises Kv7.1 currents by an increase in the single channel conductance (Barhanin et al. 1996; Sanguinetti et al. 1996; Pusch et al. 1998; Tristani-Firouzi and Sanguinetti 1998; Yang and Sigworth 1998). In addition, KCNE1 increases Kv7.1 the sensitivity to PIP2 (Li et al. 2011) and to chromanol 293B (Lerche et al. 2000).

KCNE1 modulates Kv11.1 enhancing current density and shifting the voltage-dependence activation to more hyperpolarized values (McDonald et al. 1997), resembling cardiac I_{Kr} current. In addition, KCNE1 also modulates Kv3.1 and Kv3.2, slowing the activation and deactivation kinetics (Lewis et al. 2004). Curiously, while Kv3.3 and Kv3.4 currents are suppressed by KCNE1 by an inhibition of their forward trafficking, Kv3.1 and Kv3.2 hetero-oligomerization with Kv3.3 and Kv3.4 prevented this inhibition (Kanda et al. 2011). Kv2.1 activity is also impaired by the presence of KCNE1, leading to a reduction of current, slowing the activation and deactivation (McCrossan et al. 2009). Furthermore, KCNE1 accelerates Kv4.3 inactivation (Radicke et al. 2006).

Most of the KCNE1 mutations described, which compromise I_{Ks} function, cause Long QT syndrome (LQTS) (Splawski et al. 1997; Bianchi et al. 1999; Hoppe et al. 2001; Wu et al. 2006; Ohno et al. 2007) and raises the risk of ventricular arrhythmias and sudden death. Most common mutations include: S74L, D76N, V47F, L51H, G52R, D85N, A8V, R98W and Y81C. In some cases, the cardiac phenotype can be accompanied by congenital deafness, such as the Jervell and Lange-Nielsen syndrome (Jervell and Lange-Nielsen 1957; Schulze-Bahr et al. 1997; Duggal et al. 1998). There are some cases of drug-induced LQTS (D85N) (Paulussen et al. 2004; Kaab et al. 2012) or exercise-induced LQTS (V47I) (Ryan et al. 2012) associated to KCNE1 mutations. KNCE1 single nucleotide polymorphisms have also been associated to Méniere's disease (Doi et al. 2005). Finally, some KCNE1 mutations (G25V,G60D, S38G) are associated to atrial fibrillation (AF) (Ehrlich et al. 2005; Olesen et al. 2012; Liang et al. 2013) and heart failure (Fatini et al. 2010).

KCNE1 kcnock-out mice exhibited spontaneous episodes of atrial fibrillation despite normal atrial size and structure. KCNE1$^{-/-}$ mice display increased outward current in atrial myocytes, shorten atrial action potentials, and enhanced susceptibility to atrial fibrillation. (Balasubramaniam et al. 2003; Temple et al. 2005). KCNE1$^{-/-}$ also presented an ear epithelium degeneration along post-natal development, leading to a collapse of the endolymphatic spaces, similarly to what happens in the Jervell and Lange-Nielsen syndrome (Nicolas et al. 2001).

In 2008, Kang et al, presented a three-dimensial structure of KCNE1 (Fig. 10), arguing that is a curved α–helix, flanked by intra- and extracelluar domains comprised of α–helices joined by flexible linkers (Kang et al. 2008).

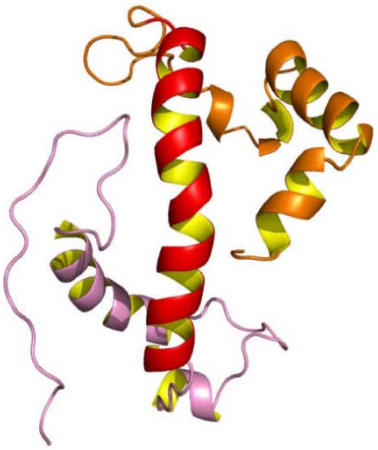

Fig. 10. *Structure proposed of KCNE1 determined by NMR and molecular dynamics analysis.* The transmembrane domain is colored in red, while the N-terminus and C-terminus domain are orange and pink, respectively. (Kang et al. 2008)

1.2.2. KCNE2

KCNE2 (15 KDa) is expressed in heart, brain, kidney, small intestine, among others tissues (Lundquist et al. 2006). Genetic variations in KCNE2 have been linked to LQTS and AF, suggesting that proper functioning of KCNE2 is necessary for cardiac electrical stability.

KCNE2 associates to Kv11.1 and resembled the native cardiac I_{Kr} current. In presence of KCNE2, Kv11.1 exhibits a slower activation, faster inactivation and deactivation, a shift to more hyperpolarized voltages and smaller currents (Abbott et al. 1999). This interaction is also important for regulation of the resting potential of the stomach smooth muscle (Ohya et al. 2002). In addition, KCNE2 associates to Kv7.1, leading to smaller and time-independent currents (Tinel et al. 2000). KCNE2 also associates to Kv4.2, being responsible for the cardiac I_{to} current, together with KChIP (Liu et al. 2008). KCNE2 slows the rates of Kv4.2 activation and inactivation and shifts the voltage dependence to more depolarized voltages (Zhang et al. 2001). Kv4.3, is also modulated by KCNE2 (Liu et al. 2006; Radicke et al. 2008). Kv3.1 and Kv3.2 slow activation and deactivation in the presence of KCNE2, as well as shift the voltage dependence to more negative potentials (Lewis et al. 2004). KCNE2 also forms native cardiac complexes with Kv2.1, reducing the current density and slowing the activation and deactivation (McCrossan et al. 2009). Furthermore, KCNE2 suppresses Kv1.4, Kv3.3 and Kv3.4 by inhibiting their forward trafficking (Kanda et al. 2011) Curiously, KCNE2 traffic effect on Kv1.4 and Kv3.4 is prevented by Kv1.1 and Kv3.1 hetero-oligomerization, respectively (Kanda et al. 2011). An interaction between KCNE2 and Kv1.5 has been suggested since *kcne2*$^{-/-}$ mice exhibited decreased K_{slow1} currents (Roepke et al. 2008). Animals exhibit an increase in margatoxin-sensitive currents in choroid plexus epithelium suggesting a Kv1.3-KCNE2 interaction yet to be deciphered. In this work, a partial inhibition of Kv1.3 by KCNE2 in CHO cells was proposed (Roepke et al. 2011), although others demonstrate that KCNE2 do not modulate

Kv1.3 in *Xenopus* oocytes and HEK-293 cells (Grunnet et al. 2003). Finally, KCNE2 is not restricted to the Kv family, since may also modulate HCN channels (Decher et al. 2003; Brandt et al. 2009).

Unlike KCNE1 and KCNE3, KCNE2 alone has the capability to travel to the surface in the absence of Kv subunits (Um and McDonald 2007; Kanda et al. 2011; Kanda et al. 2011). KCNE2 mediates the internalization of some Kv partners, such as Kv11.1, but not Kv4.3, decreasing the amount of channel at the cell surface and accelerating the degradation (Zhang et al. 2012).

KCNE2 mutations are associated with cardiac arrhythmias, long QT syndrome (LQT6) (Abbott et al. 1999; Splawski et al. 2000; Isbrandt et al. 2002; Paulussen et al. 2004; Tester et al. 2005), drug-induced LQT (Sesti et al. 2000) or T10M mutation was associated with auditory stimulus-induced LQTS (Gordon et al. 2008). A specific KNCE2 mutation (R27C) was also associated to atrial fibrillation. Curiously, this mutation displayed a gain-of-function effect on Kv7.1/KCNE2, although did not alter Kv11.1-KCNE2 (Yang et al. 2004). KCNE2(Q9E) is a rare genetic variant which impairs I_{Kr} activation and is associated with some cases of sudden infant death syndrome (SIDS) (Arnestad et al. 2007). A LQTS KCNE2 mutation (I57T) is also associated to Brugada Syndrome triggering a gain-of-function on I_{to} currens by Kv4.3 (Wu et al. 2010). Finally, some KCNE2 mutations have also been related with some cases of unexplained nocturnal death syndrome (SUNDS) (Liu et al. 2013).

KCNE2 kcnock-out mice exhibit prolonged ventricular action potentials, suggesting a reduced repolarizing capacity. In fact, KCNE2$^{-/-}$ mice exhibited decreased I_{Kslow1} and I_{to} ventricular currents, mediated by Kv1.5 and Kv4.3 channels, respectively (Roepke et al. 2008). Furthermore, animals presented striking gastric morphological and functional abnormalities, including achlorhydria, gastric hyperplasia, and abnormal parietal cell architecture (Roepke et al. 2010). KCNE2$^{-/-}$ mice suffer also hypothyroidism, dwarfism, alopecia, goiter and cardiac abnormalities including hypertrophy and fibrosis. The authors suggested that Kv7.1-KCNE2 may be required for normal thyroid hormone biosynthesis (Roepke et al. 2009). In addition, loss of KCNE2 leads to a down-regulation of HCN channel function associated with an increased excitability in neurons from the cortico-thalamo-cortical loop (Ying et al. 2012).

1.2.3. KCNE3

KCNE3 (12 KDa) is ubiquously expressed throughout the body (Lundquist et al. 2006) and has two splicing isoforms.

,KCNE3 plays an important role in skeletal muscle in association to Kv3.4. This interaction increases the unitary conductance, accelerates the inactivation recovery and

decreases the cumulative inactivation. Furthermore, a *KCNE3* missense mutation is associated to hyperkalemic periodic paralysis (Abbott et al. 2001). However KCNE3 mutations responsibility on Familial Hypokalemic Periodic Paralysis and Thyrotoxic Hypokalemic Periodic Paralysis raises controversy (Abbott et al. 2001; Dias Da Silva et al. 2002; Silva et al. 2004) (Sternberg et al. 2003; Tang et al. 2004; Vendrame et al. 2008). β-amyloid peptide-dependent Up-regulation of Kv3.4 channels and KCNE3 are involved in apoptotic neuronal death. In fact, Kv3.4-KCNE3 channels have been proposed for a novel target for Alzheimer's disease and potentially other neurodegenerative disorders (Pannaccione et al. 2007). Finally, Kv3.4-KCNE3 channels play an important role in the proliferation of artery smooth muscle cells (Leblanc 2010; Miguel-Velado et al. 2010).

KCNE3 inhibits neuronal Kv2.1, Kv3.1 and Kv3.2 channels (McCrossan et al. 2003; Lewis et al. 2004). Moreover, KCNE3, together with KCNE1, inhibits Kv12.2 and modulates the surface expression (Clancy et al. 2009).

Kv7.1 is another target of KCNE3, triggering instantaneous high density Kv7.1 currents. KCNE3 increases the potassium selectivity of Kv7.1 and the sensitivity to chromanol 293B and XE991 (Schroeder et al. 2000; MacVinish et al. 2001; Bendahhou et al. 2005).

KCNE3, as well as Kv7.1, is present in lateral membrane of crypt and surface cells in distal colon and small intestine (Liao et al. 2005). Both proteins are crucial for forming the basolateral potassium conductance that is required for trans-epithelial cAMP-stimulated chloride secretion, through basolateral recycling of K^+ ions and by increasing the electrochemical driving force for apical Cl^- exit (Dedek and Waldegger 2001). They are also located in parietal stomach cells playing an important role in acid secretion (Grahammer et al. 2001). In fact, despite of KCNE3 knock-out mice are viable, fertile and displayed neither periodic paralysis nor other obvious skeletal muscle abnormalities, cAMP-stimulated electrogenic Cl^- secretion across tracheal and intestinal epithelia was drastically reduced. Interestingly, the abundance and subcellular localization of Kv7.1 is normal (Preston et al. 2010).

KCNE3 also modulates Kv4.3, which responsible of the cardiac I_{to} current. KCNE3 (R99H) missense mutation was detected in a patient with Brugada Syndrome. Co-transfection of R99H KCNE3 with Kv4.3 leads to an increase of Kv4.3 currents (Delpon et al. 2008). Other mutations on KCNE3, which also resulted in a gain of function of I_{to} currents, are also associated to Brugada Syndrome (Nakajima et al. 2012). KCNE3 (V17M) mutation is associated to gain of function of Kv4.3/KCNE3 and Kv11.1/KCNE3 currents triggering atrial fibrillation. (Lundby et al. 2008).

KCNE3 mutations may be associated to Méniere's disease, characterized by a disorder of the inner ear that can affect hearing and balance to a varying degree. Some

studies find that a single-nucleotide polymorphism (SNP) in the KCNE3 gene (198T/C) increases the susceptibility to develop this disease (Doi et al. 2005), although other studies do not (Campbell et al. 2010). Finally, two other missense mutations on KCNE3 located in the N- and C-terminal domains were associated with a long QT syndrome, due to a reduction of the repolarizing potassium current (Ohno et al. 2009).

1.2.4. KCNE4

KCNE4 (20 KDa) is the biggest member of the family with a C-terminus domain being the more extended and divergent domain. KCNE4 is expressed strongly in heart, skeletal muscle, uterus and kidney, less in placenta, lung, and liver, and weakly in brain and blood cells (Grunnet et al. 2002; Grunnet et al. 2003; Teng et al. 2003; McCallum et al. 2009).

KCNE4 mostly acts a dominant-negative regulatory subunit. KCNE4 inhibits Kv7.1 currents, in *Xenopus* oocytes and HEK-293 cells with slightly discrepancies in the activation kinetics (Grunnet et al. 2002; Teng et al. 2003; Grunnet et al. 2005). Kv1.1, Kv1.3, $K_{Ca}1.1$ and Kv4.2 (in a KChIP2-dependent manner) channels are also inhibited by KCNE4 (Grunnet et al. 2003; Levy et al. 2008; Levy et al. 2010) (Fig. 11). Furthermore, KCNE4 inhibits heterotetrameric Kv1.1/Kv1.2 and Kv1.3/Kv1.2 channels.

While KCNE4 inhibits $K_{Ca}1.1$ expression and surface abundance by a decrease in channel half-life, the effects observed on Kv7.1 and Kv1.1 are not mediated by an intracellular retention (Levy et al. 2008).

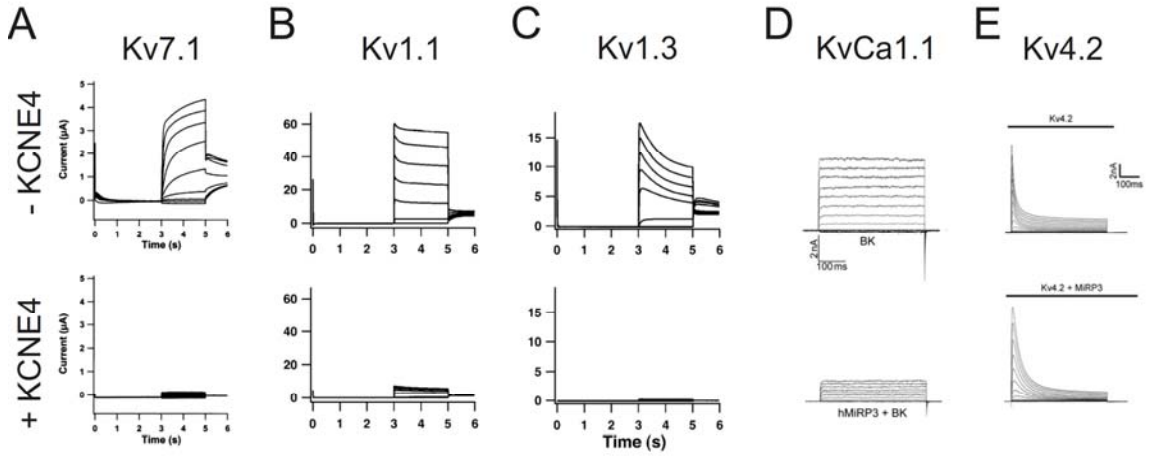

Fig. 11. *Effect of KCNE4 on different potassium channels.* Potassium currents recorded of A. Kv7.1 B. Kv1.1 C. Kv1.3 D.$K_{Ca}1.1$ E.Kv4.2, in the abscense (top panels) or in the presence (bottom panels) of KCNE4. Adapted from (Grunnet et al. 2002; Grunnet et al. 2003; Levy et al. 2008; Levy et al. 2010)

Interestingly, a putative calmodulin binding domain (CaMBD) is present in KCNE4. The CaMBD (amino acids 44 to 73) is located at the transmembrane-proximal C-terminus boundary. Calcium-dependent association of Calmodulin to KCNE4 and the Kv7.1-KCNE4

inhibition was located in a tetra-leucine motif within the putative CaMBD (L69-72) (Ciampa et al. 2011).

A (SNP) of KCNE4(E145D) is associated with atrial fibrillation phenotype (Zeng et al. 2007). KCNE4(145E/D) exerts a "gain of function" of Kv7.1, and alters the half time activation voltage, activation and deactivation kinetics (Ma et al. 2007).

A genome-wide association study with the Russian population suggested that *KCNE4* gene is involved in allergic rhinitis disease (Freidin et al. 2011).

1.2.5. KCNE5

KCNE5 (15KDa) was the last member to be discovered. The gene is situated in a chromosome region which contains several brain-related genes (Lundquist et al. 2006).

KCNE5-Kv7.1 complex raises controversial results. Initially, it was described that KCNE5 did not modify Kv7.1 currents, in *Xenopus* oocytes (Piccini et al. 1999). However, later on in CHO cells, it was described that KCNE5 shifted the voltage activation curve of Kv7.1 by more than 140 mV in the positive direction, and the activation time constant of the Kv7.1-KCNE5 current decreased, suppressing Kv7.1 currents (Angelo et al. 2002; Bendahhou et al. 2005). This modulation seemed to be specific because neither other members of the Kv7 family nor Kv11.1 were affected by the presence of KCNE5 (Angelo et al. 2002).

KCNE5 is expressed in heart, skeletal muscle, brain, spinal cord and placenta (Lundquist et al. 2006). Although at the beginning the cardiac role was not understood, recently, KCNE5 mutations are associated with cardiac pathologies. A missense mutation in KCNE5 (L65F) is associated with non-familial or acquired forms of atrial fibrillation, due to a gain of function of I_{Ks} current (Ravn et al. 2008). Furthermore, a KCNE5 polymorphism (97T) confers protection against AF and contribute to sex differences in AF (Ravn et al. 2005). KCNE5 also modulates I_{to} currents (Kv4.3+KChIP2), and novel KCNE5 variants appeared to cause idiopathic ventricular fibrilation, especially Brugada Syndrome, in male patients through gain-of-function of I_{to} (Ohno et al. 2011).

1.2.6. Molecular determinants of KCNEs

Kv7.1/KCNE1 association deserves the major part of studies focused on a KCNE interaction. The structural basis of this interaction has been extensively studied over the last two decades. Motifs, from both Kv7.1 and KCNE1, crucial for association and modulation have been identified by experimental data obtained from combination of paradigms. The transmembrane segment and the C-terminal domain of KCNE1 are crucial for modulation of

Kv7.1 (Takumi et al. 1991; Tapper and George 2000). While some reports support that the KCNE1 C-terminal domain modulates but not associates Kv7.1 (Tapper and George 2000), other studies indicate that this domain only plays a role in positioning or anchoring KCNE1 to the complex (Melman et al. 2001; Melman et al. 2002; Melman et al. 2004). In addition, the absence of the C-terminus of KCNE3 does not impair Kv7.1 modulation (Gage and Kobertz 2004). Finally, other studies proposed that KCNE1 C-terminus is crucial for channel assembly, open state destabilization and kinetics of deactivation (Chen et al. 2009). More recently, it has been demonstated though that C-terminus of Kv7.1 is also in close proximity with the KCNE1 C-terminus domain. In fact, a physical interaction has been proved by FRET and co-immunoprecipitation experiments (Haitin et al. 2009; Zheng et al. 2010).

Molecular key elements of KCNE1 function are three Gly, several aromatic Phe and a Thr 58 located at the KCNE1 transmembrane. Amino acids similarly located in KCNE3 are also important. In KCNE3 though, a Val 72, instead of Thr 58, plays a major role in Kv7.1 modulation (Melman et al. 2001; Melman et al. 2002; Melman et al. 2002). Regarding KCNE4, the transmembrane domain also modulates the voltage dependence of Kv7.1 (Ciampa et al. 2011). Different KCNEs may contact different regions of Kv7.1 within the trasmembrane segments. The C-terminus and S5-S6 domains of Kv7.1 are also required for KCNE1 and KCNE3 modulation (Melman et al. 2004). Other evidence supports that the C-terminus of Kv7.1 acts as anchoring and correct positioning of the regulatory subunit. In the S6 of Kv7.1, three amino acids (S338, F339, and F340) are the site of specific interaction with KCNE1 and KCNE3. S338 and F339 play a crucial role more for KCNE3 modulation by V72, whereas F340 is important for the KCNE1 modulation by T58 (Melman et al. 2004; Panaghie et al. 2006). Others residues, such as F270, G272 and L273 (in the S5 segment); V307, V310 and T310 (in the pore helix); and V324 and V334 (in the S6 segment) are also important for an accurate modulation by KCNE1, (Seebohm et al. 2001; Seebohm et al. 2003; Nakajo et al. 2011). Regarding KCNE2, residues which play a role in Kv7.1 modulation are L51, Y52, L53, M59, F60, S61, I63 and I67. M59 and S61 being functionally coupled to the C331 position of Kv7.1 (Liu et al. 2007).

Furthermore, whether KCNE1 was located on the pore of Kv7.1, or outside, is subject of debate. Some preliminary studies pointed out that KCNE1 lines the conduction pathway (Wang et al. 1996; Tai and Goldstein 1998). However recently, studies suggest that is located outside the pore (Lerche et al. 2000; Kurokawa et al. 2001; Tapper and George 2001; Chung et al. 2009), but in close proximity, since interacts with S1, S5 and S6 segments of Kv7.1 (Franqueza et al. 1999; Chouabe et al. 2000; Melman et al. 2004; Panaghie et al. 2006; Chan et al. 2012). In addition, KCNE1 constrains the VSD of Kv7.1 (Shamgar et al. 2008). KCNE1 also alters the coupling between the voltage sensor and the Kv7.1 gate. (Osteen et al. 2010; Wu et al. 2010; Wu et al. 2010).

In 2008, Kang et al, proposed a KCNE1 model, showing that is a curved α–helix, flanked by intra- and extracellular domains comprised of α–helices joined by flexible linkers. Furthermore, a 3D model of the Kv7.1/KCNE complex was generated, based in experimental data and homology modeling and Rosetta-based docking of KCNE1 to Kv7.1 (Kang et al. 2008). In this model (Fig.12), where an open and a close state channel, are presented, KCNE1 directly contacts with the S5-P-S6 domain and lies in a cleft between this pore domain and an adjacent voltage sensor. The experimentally-restrained docking of the KCNE1 TMD to a closed state model of Kv7.1 suggests that KCNE1 slows channel activation by sitting on and restricting the movement of the S4-S5 linker that connects the voltage sensor to the pore domain. The intracellular end of the KCNE1 TMD sits on the S5 end of the critical S4-S5 linker of KCNQ1 that connects the voltage sensor to the pore domain and is thought to press downward on the cytosolic end of the S6 helix to hold the channel gate in a closed position. In addition, the proximal end of the KCNE1 TMD contacts with a cleft formed between the upper part of S3, on the voltage sensor of one Kv7.1 subunit, and the S5/S6 segments of another. Authors postulate that this interaction must be disrupted before the channel can be opened in response to membrane depolarization. Docking to open Kv7.1 indicates that the N-terminus of the KCNE1 TMD forms an interface with an inter-subunit cleft in the channel (S1 from one subunit, S5 and the end of the pore helix from a second subunit, and S6 from a third subunit) that is associated with most known gain-of-function disease mutations. The C-terminus of the KCNE1 TMD sits at an interface between the cytosolic end of S1 in one subunit and S5 in another.

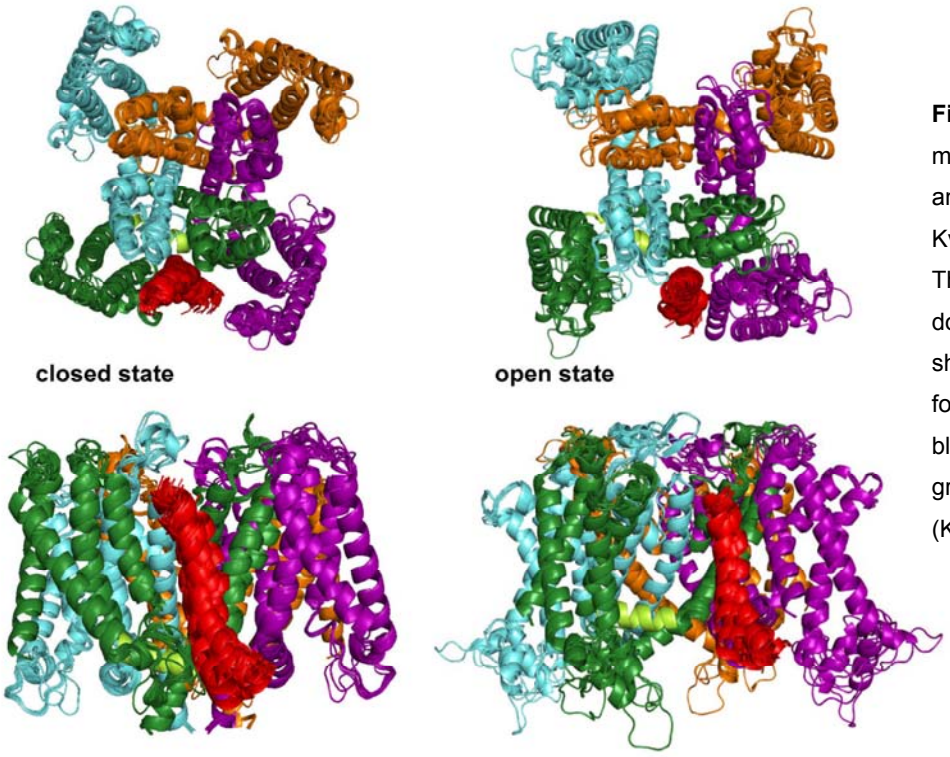

Fig. 12 Structure of the most possible open (right) and closed (left) states of Kv7.1-KCNE1 complex. The trans-membrane domain of KCNE1 is is shown in red, while the four Kv7.1 subunits are blue, orange, purple, and green. Extracted from (Kang et al. 2008)

1.2.7. Association and Stoichiometry of KCNE-Kv7.1 complex

The subcellular localization where the KCNE association takes place opens an interesting debate. Some KCNEs possess the ability of trafficking to the plasma membrane and some studies point to a reversible interaction between KCNE1 and Kv7.1 located in the surface. (Poulsen and Klaerke 2007). In addition, KCNE4 inhibits Kv7.1 already present at the membrane of *Xenopus* oocytes (Grunnet et al. 2002), and similar results have been reported by using free vesicle-mediated-delivered KCNE2 or KCNE1 on Kv7.1 expressing cells (Jiang et al. 2009). On the other hand, evidences argue against an earlier interaction, in the endoplasmic reticulum, before glycosylation. In support of this, KCNE1 (L51H) mutation, which retains the peptide and Kv7.1 at the ER, decreases I_{ks} currents (Krumerman et al. 2004; Chandrasekhar et al. 2006). Contrarily, Kv7.1-KCNE1 assembly takes place in a post-ER event in MDCK cells, but previous to the plasma membrane (David et al. 2013). KCNE2 associates to Kv channels in the ER, though few KCNE2 subunits are still able to reach to the membrane surface (Jiang et al. 2009; Kanda and Abbott 2012).

Since the identification of KCNE1, previous to the knowledge that was a Kv7.1 regulatory subunit, different stoichiometries were postulated. Up to 14 KCNEs were suggested to be present in the complex (Tzounopoulos et al. 1995). Later, more evidence suggested two KCNE subunits by channel (Wang and Goldstein 1995). Since KCNE1 was identified as no channel, different stoichiometry has been also suggested by complex. In fact, two different schools suggested that (i) four Kv7.1 α subunits associate in a fixed way with two KCNE1 subunits (stoichiometry of 4:2); and (ii) an open Kv7.1/KCNE1 stoichiometry. Experimental evidences support the fixed stoichiometry (4:2) via charybdotoxin (^{3}H-CTX) binding to Kv7.1/KCNE1 and chimeric Kv7.1-Kv7.1-KCNE1 (Chen et al. 2003). In addition, two KCNE1 (fixed stoichiometry 4:2) subunits associated to Kv7.1, by toxin-chemical-mediated subunit counting experiments (Morin and Kobertz 2008). However, other evidence proposed an open Kv7.1/KCNE1 stoichiometry (up to 4:4) by tandem fusion constructs combined with electrophysiological studies. These demonstrated that additional KCNE1 to Kv7.1-KCNE1 fusion proteins are able to produce currents with activation kinetics and voltage dependence similar to naturally assembled Kv7.1/KCNE1 channels. The voltage dependence of activation of Kv7.1/KCNE1 channels also depend on the amount of KCNE1 (Wang et al. 1998; Nakajo et al. 2010). Moreover, single-molecule fluorescent bleaching studies indicate that up to four KCNE1 subunits are present in a Kv7.1 tetramer, depending on the relative densities of the two subunits (Nakajo et al. 2010). Furthermore, the over-expression of KCNE1, which markedly changes the activation kinetics and the voltage dependence of native I_{ks} currents in cardiomyocytes, supports a variable stoichiometry

(Wang et al. 2011). Lately, the hypothesis of a variable stoichiometry, up to 4 KCNEs/complex, is gaining more strength.

It is worth to mention that not only one kind of KCNE isoform can associate to the channel. As commented before, KCNE is a very promiscuous family, and the same channel can be modulated by different KCNE member at the same time. KCNE4 may co-associates to Kv7.1, while KCNE1 is present in the complex (Manderfield and George 2008). However, there are some discrepancies about whether the KCNE4 inhibitor effect is dominant on KCNE1 modulation (Lundquist et al. 2005; Morin and Kobertz 2007). KCNE3, KCNE4 and KCNE5 are also able to modulate the I_{ks} current in cell lines stably expressing Kv7.1/KCNE1 (Lundquist et al. 2005). Kv7.1/KCNE1/KCNE3, Kv7.1/KCNE1/KCNE4 and Kv7.1/KCNE3/KCNE4 complexes have also reported by derived scorpion toxin-based experiments (Morin and Kobertz 2007). In addition, co-immunoprecipitation experiments suggested that Kv7.1, KCNE1, and KCNE2 can form a tripartite complex and that the presence of KCNE2 leads to a decrease in the I_{Ks} current (Wu et al. 2006; Jiang et al. 2009). Kv7.1 is not unique interacting with different KCNE simultaneosly. Native co-immunoprecipitation assays from mouse brain membranes showed that KCNE1 and KCNE3 interact with Kv12.2 simultaneously suggesting the existence of KCNE1-KCNE3-Kv12.2 channel tripartite complexes (Clancy et al. 2009).

1.3. Several Kv subfamilies are regulated by KCNEs

As previously mentioned, KCNEs modulate a spread range of Kv channels. One aim of this dissertation has been the analysis of classical interactions Kv7.1-KCNE and, in addition, to also identify other Kv7.5 (homologous to Kv7.1) interactions not yet described. Finally, to extend this study to not related and novel KCNE-Kv1.3 interaction, specially focused on KCNE4, which may be relevant in leukocytes. Therefore, we are going to focus on Kv7.1, Kv7.5, Kv1.3 and Kv1.5 in the next lines.

Despite of being from the the same superfamily of Kv channels, enormous structural differences between Kv1 and Kv7 members exist (Fig. 13). While Kv1 channels tetramerize via a tetramerization domain (T1) of about 100 amino acids located at the intracellular N-terminus domain (Li et al. 1992; Xu et al. 1995), Kv7 members, which exhibit a larger C-terminus domain, use this segment for assembly, traffic and gating (Cushman et al. 2000; Gulbis et al. 2000; Minor et al. 2000; Haitin and Attali 2008).

The C-terminus of Kv7 channels is composed of 4 α helixes (A-D). The distal Ct domain (helixes C and D) is also called A-domain. Helix C dimerizes and undergoes concentration-dependent self-association to form a dimer of dimers (Wiener et al. 2008). The helix C module is strongly conserved throughout the Kv7 subfamily, suggesting a general

role in promoting oligomerization and association with proteins involved in trafficking and/or regulation. Crystallographic studies on Kv7.1 reveal that helix D is a tetrameric parallel-orientated coiled-coil quaternary structure playing a role in the hetero-tetramerization (Howard et al. 2007; Wiener et al. 2008). Proximal helixes A and B form the site for calmodulin (CaM) binding (Haitin and Attali 2008; Wiener et al. 2008). CaM seems to be an essential auxiliary subunit of all Kv7 channels (Wen and Levitan 2002; Yus-Najera et al. 2002; Gamper and Shapiro 2003; Gamper et al. 2005; Shamgar et al. 2006). Kv1 channels do not possess any of these domains throughout their structure.

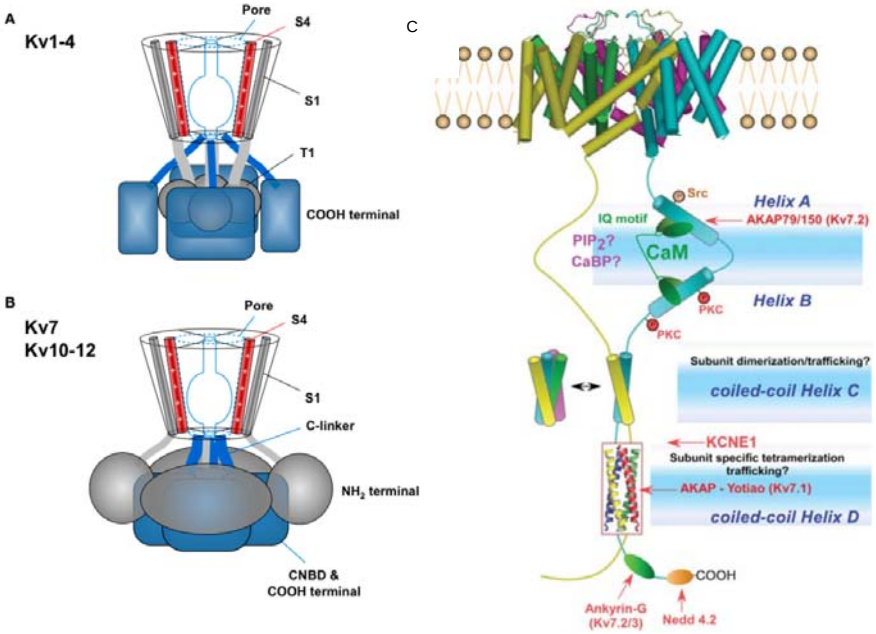

Fig. 13. *Scheme the main topological characteristics of Kv1 and Kv7.* A. Kv1 family tetramerize through T1 domain, located in N-terminus domain. B. Kv7 family tetramerizes through the C-terminus domain. C. Diagram of the different motifs located in the C-terminus domain of Kv7 channels and its major partners. Adapted from (Barros et al. 2012) and (Haitin and Attali 2008)

Kv7.1 C-terminus also conveys modulation by PIP_2, which stabilizes the open state of the channel (Loussouarn et al. 2003; Zhang et al. 2003; Park et al. 2005). In addition, the helix D serves as the interface to the AKAP scaffold protein YOTIAO (Marx et al. 2002), needed for PKC-dependent phosphorylation (Higashida et al. 2005).

Some Kv1 and Kv7 members share a SH3 domain (i.e. Kv1.5, Kv7.3-7.5), which play an important role for their modulation by tyrosine kinase Src (Holmes et al. 1996; Gamper et al. 2003). Furthermore, Kv1 channels possess a PDZ-binding domain (S/T-X-V/L) in their C-terminus domain, where PSD-95 can associate. PSD-95 is a member of the MAGUK (membrane-associated guanylate kinase) family of genes, which encode proteins (i.e. SAP-97 and PSD-93) containing a guanylate kinase domain, an SH3 domain, and at least one

PDZ domain. MAGUK proteins may determine the subcellular distribution of channels. For instance, PSD-95 mediates clustering of ion channels into raft-like structures (Kim et al. 1995). Kv1.4 forms clusters at the membrane in the presence of SAP-97 or PSD-95 (Kim and Sheng 1996) and PSD-95 stabilizes Kv1.4 in lipid-raft microdomains (Wong and Schlichter 2004). SAP-97 also interacts with Kv1.5, though due to the N-terminus of the channel (Eldstrom et al. 2003).

As previously mentioned, both families can hetero-tetramerize. Some described hetero-oligomers described are Kv1.2/Kv1.5, Kv1.1/Kv1.2, Kv1.2/Kv1.3, Kv1.2/Kv1.6, Kv1.3/Kv1.5, Kv1.1/Kv1.4, Kv1.2/Kv1.4 (Koch et al. 1997; Albarwani et al. 2003; Fergus et al. 2003; Vicente et al. 2006; Vicente et al. 2008; Imbrici et al. 2011). Some Kv7.2/Kv7.3, Kv7.3/Kv7.5, Kv7.2/Kv7.5, Kv7.4/Kv7.5, Kv7.3/Kv7.4 chanelosomes have also been reported (Wang et al. 1998; Lerche et al. 2000; Schroeder et al. 2000; Bal et al. 2008).

1.3.1. Kv7.1

Kv7.1, also called KvLQT1 and KCNQ1, was first identified in a linkage study of patients with long QT syndrome (LQTS1) (Wang et al. 1996). Subsequently, human and murine Kv7.1 was cloned (Sanguinetti et al. 1996) (Barhanin et al. 1996). The *KCNQ1* gene encodes a potassium channel whose properties do not resemble any cardiac potassium channel. However, Kv7.1 recapitulates properties similar to the cardiac slow delayed rectifier (I_{Ks}) channel in the presence of KCNE1 (Barhanin et al. 1996; Sanguinetti et al. 1996). Although 5 isoforms of Kv7.1 exist only two are functional. Kv7.1 (0), which corresponds to the one initially discovered by Barhanin and Sanguinetti, and Kv7.1 (1), lately detected by Wang and colleagues (Lee et al. 1997; Wollnik et al. 1997). In heart and skeletal muscle, a subunit which represents half of 0 and 1 isoforms is expressed (Yang et al. 1997). In heart, isoform 2 is also expressed. This isoform has no activity, because does not contain the entire N-terminus domain and inhibits Kv7.1 currents (Jiang et al. 1997). The relative expression of these different subunits in the same tissue may be a mechanism of controlling the intensity and heterogeneity of Kv7.1/I_{Ks} currents.

Kv7.1 (676 amino acids) is the unique Kv7 member with a glycosylation site (N160). In addition, Kv7.1 N-terminus domain also contains a PKA target site (S95) (Barhanin et al. 1996; Wang et al. 1996). Kv7.1 is also the member which contains less positive charges in the S4 segment (only 4) among all the Kv7 members.

Kv7.1 electrophysiological properties differ between the different reports. Kv7.1 generates a voltage-dependent, slowly activating and slowly deactivating outward potassium current, with a half-activation voltage -12 to -36 mV. Channels are activated between 100 and 200 ms, exhibiting an exponential curve and up to 3 seconds are needed to achieve the

maximal activation in *Xenopus* oocytes (Barhanin et al. 1996; Tristani-Firouzi and Sanguinetti 1998; Schroeder et al. 2000). Kv7.1 single unit conductance is 1.8 pS.. Though, hetero-oligomeric Kv7.1/KCNE1 channels expressed show a conductance of 5.8pS in *Xenopus* oocytes (Pusch 1998).

Kv7.1 is inhibited by XE991 (IC_{50} of 0.8 μM). Interestingly, Kv7.1-KCNE1 complex is more resistant (IC_{50} of 11 μM) (Wang et al. 2000). Chromanol 293B also inhibits Kv7.1 with a 80% of efficiency for 100 μM. In this case, KCNE1, enhances Kv7.1 sensitivity to this drug (Robbins 2001).

Kv7.1 and KCNE1 share expression in heart but also in many organs and very often separate Kv7.1 from KCNE1 is not easy due to the physiological importance as a complex. In heart, Kv7.1 is involved in the termination of the cardiac action potential, mediated by the repolarizing potassium current I_{ks} (Sanguinetti and Jurkiewicz 1990; Barhanin et al. 1996; Sanguinetti et al. 1996). In addition, Kv7.1 and KCNE1 play a crucial role in the hearing process and the maintenance of endolymph potassium homeostasis (Marcus and Shen 1994; Shen et al. 1995; Wangemann et al. 1995; Sunose et al. 1997). Kv7.1 has also been detected in kidney, where it plays an important role in conduction a K^+ current to counterbalance membrane depolarization induced by electrogenic Na^+-coupled transport of glucose or amino acids (Vallon et al. 2001; Vallon et al. 2005). Colon and small intestine also express Kv7.1, KCNE1 and KCNE3. In colonic crypt cells, Kv7.1 seems to assemble with KCNE3 and mediate a K^+ conductance that provides the driving force for chloride secretion (Schroeder et al. 2000; Kunzelmann et al. 2001). Kv7.1 is also related with other chloride-secreting tissues such as pancreatic acinar cells and airway epithelium (Kim and Greger 1999; Mall et al. 2000). Kv7.1/KCNE2 complex is also crucial for gastric acid secretion in stomach parietal cells (Dedek and Waldegger 2001; Demolombe et al. 2001; Heitzmann et al. 2004). Kv7.1 has also been detected in the human thyroid gland, smooth muscle of different vessels and skeletal muscle (Roura-Ferrer et al. 2008; Zhong et al. 2010; Frohlich et al. 2011; Chadha et al. 2012). It is important to mention the possible role of Kv7.1, coordinated also with Kv7.4 and Kv7.5, in vasodilatation processes (Zhong et al. 2010). Kv7.1 mRNA has also been detected in liver, lungs, thymus, exocrine pancreas, salivary glands, and uterus (Demolombe et al. 2001; Grunnet et al. 2002).

All this functional processes in which Kv7.1 is involved are highlighted by the Kv7.1 knock-out mice (Lee et al. 2000; Arrighi et al. 2001; Casimiro et al. 2001). These mice present hypokalemia, urinary and fecal salt wasting and volume depletion. In addition, gastric hyperplasia and profound hypochlorhydria have been observed in Kv7.1 knock-out mice, indicating the importance of Kv7.1 in normal stomach development and function. Hypertension and deafness are also characteristic malfunctions of these mice. The physiological importance of this channel is also demonstrated by the different mutations

association with many diseases. Mutations in Kv7.1 compromise I_{ks} function and can cause long QT syndromes and sudden death (Wang et al. 1996; Donger et al. 1997; Bokil et al. 2010). In some case, LQTS are also accompanied by congenital deafness (Neyroud et al. 1997). In contrast, I_{ks} gain-of-function mutations cause premature repolarization and are associated with short QT syndromes (SQTS) and atrial fibrillation (AF) (Loussouarn et al. 2006).

As mentioned before, Kv7.1 is modulated by all the KCNE family members (Fig. 14). KCNE1 drastically modifies Kv7.1 activity by increasing its unitary conductance as well as macroscopic currents, slowing activation, right-shifting the voltage dependence of activation, suppressing partial inactivation and modulating the pharmacology of the channel. KCNE2 gives rise to currents with decreased amplitude, instantaneous activation, rapid partial deactivation and a linear current-voltage relationship. Moreover, KCNE3 converts Kv7.1 to a channel with nearly instantaneous activation and a linear current-voltage relationship. KCNE4 completely suppresses Kv7.1 currents. Finally, KCNE5, in addition to inhibiting Kv7.1 currents, shifts the voltage dependence of Kv7.1 activation to more positive potentials.

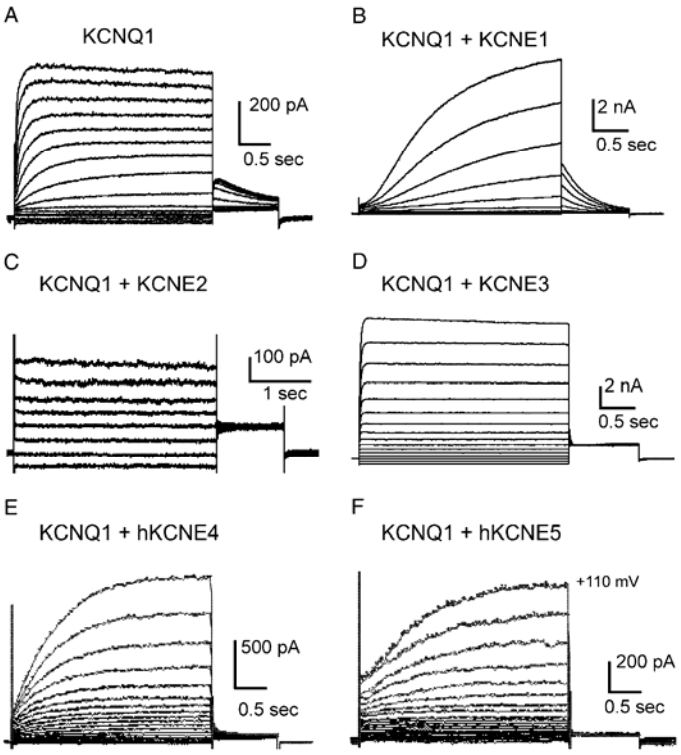

Fig. 14. *Kv7.1 activity modulation by KCNE family.* Whole cell patch clamp recordings from COS-7 cells transfected with (A) Kv7.1 alone or (B–F) with Kv7.1 and each of the 5 KCNE subunits. Extracted from (Bendahhou et al. 2005).

In addition to associations with KCNEs, Kv7.1 channels are modulated via different mechanisms. Kv7.1 is inhibited by PKC (Barhanin et al. 1996; Kurokawa et al. 2001; Li et al. 2005). Furthermore, high AMPc levels enhances the activity of Kv7.1 (Yang et al. 1997). Ser71 of Kv7.1 is phosphorylated by PKA when β-adrenergic receptors are activated, leading to an increase in Kv7.1 currents in the presence of KCNE1 (Kurokawa et al. 2001; Kurokawa et al. 2003). A platform protein from AKAP family (Yotiao), binding to C-terminus of Kv7.1, is also needed for this process. Yotiao works as an association platform for many proteins,

such as PKA and phosphatase1. In addition, Yotiao, undergoes phosphorylation for proper regulation of I_{ks} current (Chen and Kass 2006). PIP_2 also modulates Kv7.1 currents in a KCNE1-dependent manner, stabilizing its open state (Loussouarn et al. 2003). As mentioned before, Kv7.1 has been detected in lipid raft micro domains (Balijepalli et al. 2007).

1.3.2. Kv7.5

Kv7.5 was the latest discovered member of the Kv7 family. It was characterized from brain extracts by two groups simultaneously (Lerche et al. 2000; Schroeder et al. 2000). Three isoforms (I, II and III) of Kv7.5 exist. Isoform I is mainly expressed in brain, while the isoforms II and III show a more skeletal muscle distribution. Kv7.5 is expressed in brain with a similar pattern to Kv7.2 and Kv7.3, the hippocampus and the neocortex region containing higher expression (Schroeder et al. 2000; Yus-Najera et al. 2003).

Kv7.5 activates at around −60 mV and presents a decrease in apparent P_{open} at positive voltages than +20 mV due to inactivation. The apparent half-maximal activation is −46 and −48 mV for isoforms I and III, respectively. While the isoform III shows a faster initial activation and takes more time to stabilize, the isoform I shows a slower initial activation, but reaches the plateau earlier than III (Schroeder et al. 2000). The single channel conductance is 2.2 pS (Li et al. 2004).

Kv7.5 is inhibited by TEA (IC_{50} 70 mM), linopirdine (IC_{50} 16 mM) and XE991 (IC_{50} 70 mM) (Lerche et al. 2000; Schroeder et al. 2000). Kv7.5 currents are activated by BMS-204352 (Dupuis et al. 2002), retigabine (Schenzer et al. 2005) and NS15370, a novel high-potency chemical analogue of retigabine (Dalby-Brown et al. 2013).

Kv7.5 can form hetero-tetramers with Kv7.2-Kv7.3. Hetero-oligomerization with Kv7.1 and Kv7.4 was proposed not to be possible, but recently, Kv7.4/Kv7.5 assembly has been demonstrated (Lerche et al. 2000; Schroeder et al. 2000; Bal et al. 2008).

Regarding possible KCNEs-Kv7.5 modulation, preliminary studies of Kv7.5+KCNEs in *Xenopus oocytes* were performed and suggested that KCNE1 was able to inhibit Kv7.5 current slowing the activation (Fig. 15.). Since KCNE1 could not be detected at that time in brain and skeletal muscle by Northern blot analysis, an interaction with Kv7.5 was unlikely of physiological relevance. KCNE3 may also inhibit Kv7.5, but KCNE2 leads to a faster activation of the channel (Schroeder et al. 2000). On the contrary, other groups postulated that KCNEs did not exert any effect upon Kv7.5 channel gating (Lerche et al. 2000; Grunnet et al. 2002).

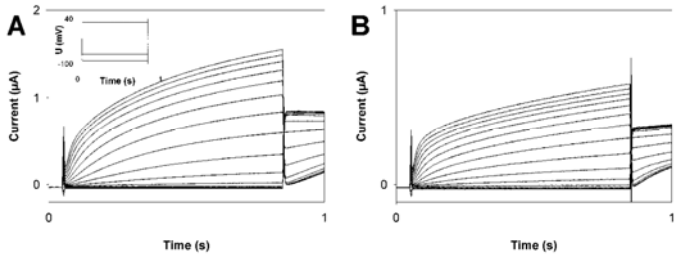

Fig. 15. *Electrophysiological records of Kv7.5 and Kv75+KCNE1).* Records from A. Kv7.5, and B. Kv7.5+KCNE1, obtained in Xenopus oocytes. Extracted from (Schroeder et al. 2000).

Kv7.5 plays an important physiological role in the generation of M-current, which is mediated by hetero-tetrameric channels formed by Kv7.3 subunits associated with either Kv7.2 or Kv7.5 (Wang et al. 1998; Lerche et al. 2000; Schroeder et al. 2000). The M-current is a slowly activating and deactivating potassium conductance that plays a critical role in determining the sub-threshold excitability of neurons as well as the responsiveness to synaptic inputs. The M-current was first described in peripheral sympathetic neurons, and differential expression of this conductance produces subtypes of sympathetic neurons with distinct firing patterns. The M-current is also expressed in many neurons in the central nervous system. In neurons, Kv7.2, Kv7.3 and Kv7.5 can be detected in soma and perisoma (Hu et al. 2007). This is the only study focus on Kv7.5 traffic or subcellular localization.

Kv7.5 plays also an important role in smooth muscle cells, where is involved in the maintenance of the vascular muscle tone. Kv7-mediated currents sensible to Arg8-vasopressin (AVP) hormone in A7r5 cells (vascular smooth muscle cells) were detected. These currents were inhibited by linopirdine and XE991, and only Kv7.5 mRNA was detected (Brueggemann et al. 2007). However, the effects of AVP were apparently protein kinase C (PKC)-dependent. Furthermore, splice variants of Kv7.5 were detected in murine thoracic aorta, carotid and mesenteric arteries, and portal vein (Yeung et al. 2007; Yeung et al. 2008).

Recently a dysfunction of the hetero-oligomeric Kv7.3/Kv7.5 has been proposed in association with autism spectrum disorders (Gilling et al. 2013). C-fibers in association with small-diameter neurons in the dorsal root ganglia express Kv7.5, but not Kv7.2 and Kv7.3 (King and Scherer 2012). This may explain why Kv7 potassium channel openers decrease neuropathic pain in experimental models (Passmore et al. 2003; Roza and Lopez-Garcia 2008).

1.3.3. Kv1.3

Kv1.3 was cloned almost simultaneously from brain of different species (Christie et al. 1990; Grupe et al. 1990; Swanson et al. 1990) and human T lymphocytes (Grissmer et al. 1990; Attali et al. 1992; Cai et al. 1992). All this clones, codified for the same protein, of 575

amino acids (the human isoform). The distribution of this channel is mainly in the immune system, where it is expressed in T, B lymphocytes and microglia (Cahalan et al. 2001), and in the nervous system.

Kv1.3 is a voltage gated potassium channel which is activated by depolarization of the membrane. The threshold of activation is around -50 mV, exhibiting a voltage half activation voltage of -35 mV. Kv1.3 characterizes for reaching the maximum peak of conductance about 10 ms after a depolarizing stimulus. Kv1.3 exhibits a marked C-type

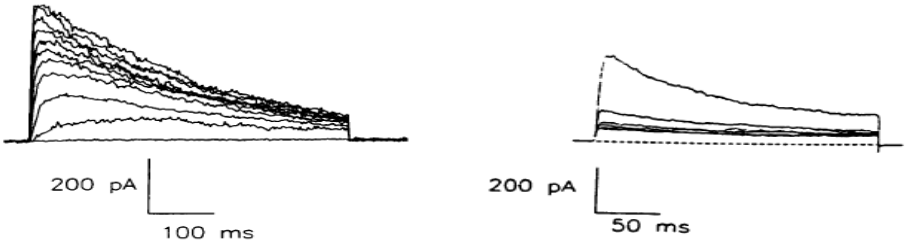

inactivation, in front a sustained depolarization with a $T_{inactivation}$ between 200 and 400 ms (Fig. 16A). Kv1.3 is also characterized for presenting cumulative inactivation, which consist in a progressive decrease in the potassium current after the application of successive depolarizing pulse trains (Fig. 16B). The single-channel conductance of Kv1.3 is about 13pS (Cahalan et al. 1985; Grissmer et al. 1990).

Fig. 16. *Kv1.3 inactivation processes.* A. Characteristic Kv1.3 current, showing the C-type inactivation. B. Kv1.3's current density decreases in front of a repetitive depolarizing pulse train, due to cumulative inactivation. Extracted from (Grissmer et al. 1990).

Kv1.3 forms heteromeric complexes with Kv1.1 Kv1.2 and Kv1.4, in the brain grey matter (Coleman et al. 1999), whereas in the bovine cortex, Kv1.3 hetero-oligomerize with Kv1.6, Kv1.2, and Kv1.4 (Shamotienko et al. 1997). In the immune system, Kv1.3 forms hetero-tetramers in cells where Kv1.5 is also co-expressed such as macrophages and microglia (Vicente et al. 2006; Villalonga et al. 2007).

Kv1.3 is inhibited by general blockers of potassium channels such as quinidine, TEA and 4-aminopiridine (4-AP). Other Kv1.3 inhibitors are benzamide derivatives (Miao et al. 2003) or derivatives from 5-(4-phenyl-butoxy psoralen (Psora-4) (Vennekamp et al. 2004). However, the more effective Kv1.3 inhibitors come from natural venom derivatives. Some of them proceed from venom scorpions such as margatoxin (*Centruroides margaritatus*) (Garcia-Calvo et al. 1993), which exhibits a IC_{50} in the picomolar range. Charybdotoxin (*Leiurus quinquestriatus*) (Miller et al. 1985; MacKinnon et al. 1988) and the Pi2 and Pi3 toxins (*Pandimius imperator*) (Peter et al. 2001) are other examples of venom scorpion which inhibit Kv1.3, among other potassium channels. α-dendrotoxin is a green mamba (*Dendroaspis angusticeps*) venom derivative which blocks Kv1.1-1.3 and Kv1.6 (Harvey

2001). One of the most specific peptide toxins is Shk, from the sea anemone *Stichodactyla helianthus*, which blocks Kv1.3 in a nanomolar concentration, although some effect upon Kv1.1, Kv1.4 and Kv1.6 has also been described (Pennington et al. 1996). Different chemically and modified derivatives of ShK peptide have been developed, in order to increase its selectivity and efficiency inhibiting Kv1.3 to target autoimmune diseases (Lanigan et al. 2002; Beeton et al. 2003; Beeton et al. 2005; Beeton et al. 2011; Chi et al. 2012).

As previously mentioned, Kv1.3 can be modulated by association with auxiliary subunits, such as the KCNE4 regulatory subunit (Grunnet et al. 2003). Other interacting regulatory subunits are Kvβ1.1 and Kvβ2.1, which enhance Kv1.3 currents (Autieri et al. 1997; McCormack et al. 1999). Kv1.3 activity is also modulated by PKA and PKC which decrease the activity (Payet and Dupuis 1992; Cai and Douglass 1993). Kv1.3 can be also inhibited by tyrosine kinase phosphorylation, such as by Src kinases (Holmes et al. 1996; Fadool et al. 1997) or tyrosine kinase-activity receptors (EGF or insulin receptors) (Bowlby et al. 1997). A Ca^{++}-dependendent regulation of Kv1.3 was also suggested in lymphoblast together with an association with the type II CAM kinase (Chang et al. 2001), but no Calmodulin association (Fanger et al. 1999). Recently, a Ca^{+}-dependent reduction of Kv1.3 inhibition in megakaryocytes and heterologous expression system has also been described (Martínez-Pinna 2012).

In the nervous system, Kv1.3 presents a restricted expression pattern in hippocampus, striatum corpus, piriform cortex and olfactory bulb (Swanson et al. 1990; Kues and Wunder 1992; Mourre et al. 1999).

In the immune system, Kv1.3 is expressed in T, B lymphocytes, macrophages, dendritic cells, microglia etc. Kv1.3 plays an important role in immune system during activation and proliferation of leukocytes (Beeton and Chandy 2005). After TCR activation and subsequent release of endoplasmic reticulum calcium, Kv1.3, together with $K_{Ca}3.1$, play a crucial role in providing the sufficient driving force for further Ca^{2+} to entry the cell via Ora1. The sustained calcium signal is needed to the T-cell activated transduction signal. Calcium signal is needed for activation of calcineurin and the NFAT translocation to the nucleus, which leads to the transcription of specific T-cell activation and proliferation genes (Fig. 17). Moreover, Kv1.3 has also been related to many autoimmune diseases such as multiple sclerosis, diabetes mellitus, arthritis rheumatoid, etc. and for this reason there is a lot of effort in searching a specific inhibitor of Kv1.3 as an immunotherapeutic (Beeton and Chandy 2005; Beeton et al. 2005; Varga et al. 2010; Beeton et al. 2011). Furthermore, Kv1.3 overreactivity has been also described in T_{EM} cells from patients with autoimmune diseases (Rus et al. 2005; Varga et al. 2009). In this context, blocking Kv1.3 ameliorates the animal model for multiple sclerosis (EAE) (Beeton et al. 2001).

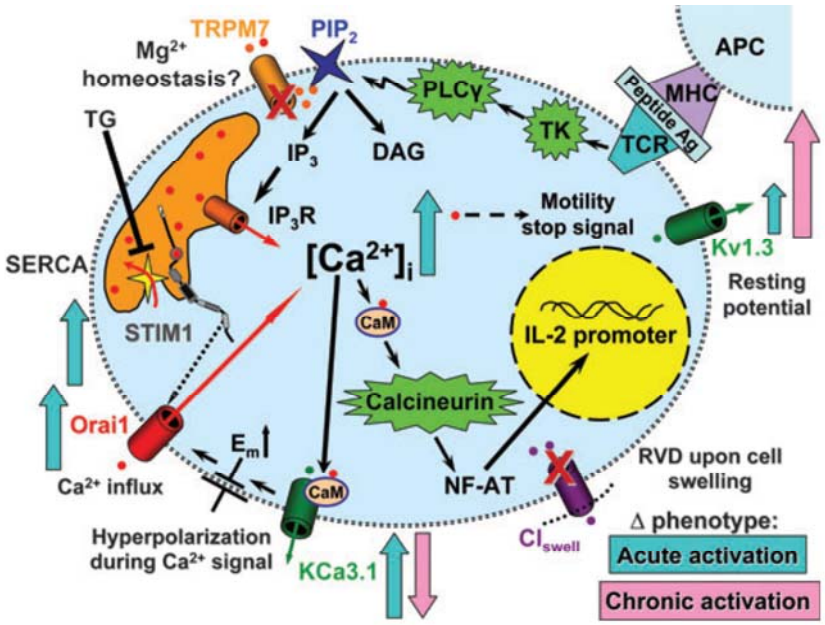

Fig. 17. *Signaling cascade triggered by T lymphocyte activation.* Activation of TCR leads to IP_3 formation through PLC, which triggers calcium ER depletion. The elevated intracellular calcium concentration activates Kv1.3 and $K_{Ca}3.1$ channels, which promote the sustained calcium entrance through Orai1, which is need for the activation of nuclear factors and transcription of pro-inflamation genes. Extracted from (Cahalan and Chandy 2009)

Kv1.3, as well as Kv1.5, plays also an important role in the maintenance of the membrane potential, proliferation and activation of macrophages (Vicente et al. 2006; Villalonga et al. 2007). In addition, Kv1.3 is also important for the production of ROS by microglia and the capacity for killing neurons (Khanna et al. 2001; Fordyce et al. 2005). In dendritic cells, both channels are involved in the regulation of inflammatory cytokines (Mullen et al. 2006).

As mentioned before, Kv1.3 is a channel that partially targets to lipid raft microdomains. In fact, lymphocytic Kv1.3 rearranges around the immunological synapse (IS), within lipid rafts, co-localizing with the TCR, CD3. An association between Kv1.3 and the TCR/CD3 receptor has been demonstrated by FRET experiments (Panyi et al. 2004). Also, molecular interactions between Kv1.3 and β1-integrin, SAP-97 and PSD-95 and Kvβ2 regulatory subunits have been also reported in these microdomains (Panyi et al. 2004; Cahalan and Chandy 2009; Szilagyi et al. 2013). Kv1.3 localization in lipid rafts is crucial, because methyl-beta-cyclodextrin treatment, which depletes the membrane from cholesterol, disrupts lipid rafts and causes a depolarizing shift of the Kv1.3 channel activation and inactivation and more than two-fold decrease in Kv1.3 currents (Pottosin et al. 2007). Furthermore, segregation of Kv1.3 channels into the IS modifies the gating properties (Toth et al. 2009). In addition, an alteration in lipid raft formation in some autoimmune diseases such as Sistemic Lupus Erythematous (SLE) has been reported (Nicolaou et al. 2007; Nicolaou et al. 2010).

Kv1.3 is also expressed in other tissues, but with less abundance (Bielanska et al. 2009), such as kidney (Yao et al. 1996), bladder (Davies et al. 2002), adipose tissue (Xu et al. 2003), smooth muscle (Cox et al. 2001; Miguel-Velado et al. 2005) and skeletal muscle (Villalonga et al. 2008), osteoclasts (Arkett et al. 1994), testis (Jacob et al. 2000), etc. Kv1.3 expression has been related to many cancers (Bielanska et al. 2009; Bielanska et al. 2012; Bielanska et al. 2012) and plays a role in apopotosis (Bock et al. 2002; Bock et al. 2003; Gulbins et al. 2010; Leanza et al. 2012). In fact, the presence of Kv1.3 in the mithocondrial membrane has been described (Szabo et al. 2005; Szabo et al. 2008).

Kv1.3 knock-down mice present a hyperdeveloped olfactory sense and impaired action potentials in the bulb olfactory neurons (Fadool et al. 2004). Though, recently an enhancement of K_{Na} currents (Slack channel) have been detected in olfactory bulb Kv1.3$^{-/-}$ mice, which may explain part of the olfactory phenotype of these mice (Lu et al. 2010). In addition, Kv1.3$^{-/-}$ presented a decreased body mass, and in the number of fat bodies, due to probably the enhanced nocturnal motor activity and metabolism which these mice exhibit. These mice also present higher longevity. (Tucker et al. 2008). Furthermore, animals present an increased expression in some adaptor proteins such as PSD-95, Src, Grb, or 14-3-3, which some of them are involved directly or indirectly with the Kv1.3 activity (Fadool et al. 2004). The immune system of Kv1.3 knock-out mice developed properly, because similar number of lymphocytes in the spleen and thymus and no significant difference upon proliferation in response to anti-CD3 were initially found. However, a compensatory up-regulation of chloride currents (Koni et al. 2003) in lymphocytes was detected. Although a more evidence demonstrate that Kv1.3$^{-/-}$ mice exhibited a decreased incidence and severity of experimental autoimmune encephalomyelitis (EAE) and a limited proliferative capacity of lymphocytes. Kv1.3$^{-/-}$ mice present significantly more naïve and T_{CM} cells and fewer T_{EM} cells in the lymph node at seven days after immunization than WT, despite of exhibiting similar percentages of $CD4^+$ and $CD8^+$ T cells in spleen and lymph node (Gocke et al. 2012).

1.3.4. Kv1.5

Kv1.5 channel was cloned from a human ventricular myocardium (Tamkun et al. 1991) and rat brain (Swanson et al. 1990).

Kv1.5 responds to membrane potential depolarizations and exhibits an activation threshold more hyperpolarized than Kv1.3, being -14mV the voltage half activation. Kv1.5 channels activate very fast and presents a conductance of 8pS (Snyders et al. 1993; Grissmer et al. 1994). In addition, Kv1.5 is characterized for

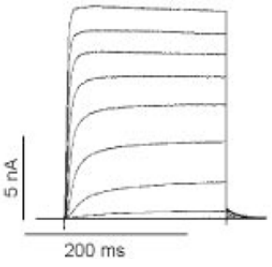

Fig. 18. K*v1.5 electro-physiological currents.* (transient transfected HEK-293 cells). Extracted from (Vicente et al. 2006)

presenting a very slow inactivation (T>5s). Kv1.5 does not present cumulative inactivation (Snyders et al. 1993).

Kv1.5 is inhibited at high doses of different generic drugs such as 4-AP, TEA or quinidine (μM). Some new chemicals have been discovered that inhibits Kv1.5, such as S0100176 (from Sanofi-Aventis), AVE0118 or diphenyl phosphine oxide-1 (DPO-1) (Decher et al. 2004; Villalonga et al. 2008; Du et al. 2010). These compounds block the channel in open-conformation, but recognizing the conserved residues among Kv, which leads to unspecific inhibition of other potassium channels. A lot of effort is being implied in the study of Kv1.5 inhibitors in order to develop an anti-arrhythmic drug, due to the importance of this channel in cardiovascular physiology. Kv1.5 plays an important role in the heart action potential, since is the responsible of the I_{kur} current (Feng et al. 1997).

Kv1.5 is mainly expressed in smooth, skeletal and cardiac muscle. Kv1.5 it has been found in pulmonary artery smooth muscle, where it is involved in the maintenance of the membrane potential and vasoconstriction of these cells (Hong et al. 2005; Wang et al. 2005). In heart, Kv1.5 expression is higher in auricula than ventricle (Tamkun et al. 1991; Mays et al. 1995). As previously mentioned, Kv1.5 generates I_{kur} current which is fast activated and slow inactivated during the plateaus phase of the action potential in auricular cells (Fedida et al. 1993; Snyders et al. 1993; Nattel et al. 1999). Kv1.5 is expressed either in embrionary or adult cardiomyocytes (Mays et al. 1995), as well as in myoblasts and contractile myotubes (Levitan and Takimoto 1998).

Kv1.5 also plays an important role in immune system because is expressed in macrophages, where associates to Kv1.3 forming Kv1.3/Kv1.5 hetero-tetramers (Vicente et al. 2003; Vicente et al. 2005; Vicente et al. 2006). Kv1.5 is involved in migration and phagocytosis processes (Park et al. 2006). Kv1.5 is also expressed in microglia playing a role in proliferation (Pannasch et al. 2006). It is also present in dendritic cells, where, together with Kv1.3, are involved in the production of inflammatory cytokines (Mullen et al. 2006).

Kv1.5 channel expression is more ubiquitous. Thus, it is present in kidney, alveolar pulmonary epithelia, brain (pituitary, microglia and Schawnn cells), testis, kidney, bladder, colon, etc (Takimoto et al. 1995; Sobko et al. 1998; Bielanska et al. 2009).

Apart from hetero-tetramerize with Kv1.3 and other Kv1 subunits, Kvβ2.1 and Kvβ1 can also be present in the channelosome modifying gating properties (Heinemann et al. 1996; Sewing et al. 1996; Uebele et al. 1996). Kv1.5 also associates to KChAP, although no functional changes have been detected (Wible et al. 1998). KCNE1 was also able to co-immunoprecipitate with Kv1.5, although no functional effects have been reported (Melman et al. 2004).

Kv1.5 partially localizes to lipid raft microdomains, in caveolaes in mouse Ltk cells (Martens et al. 2001) but not in rat and canine heart (Eldstrom et al. 2006). Also, Kv1.5 targets to lipid raft in heterologous system expression such as HEK-293 cells, but not in macrophages or L6E9 skeletal myoblasts, heart membranes or cardiomyocites. Furthermore, Kvβ2.1 presence impaired Kv1.5 localization to lipid raft microdomains (Martinez-Marmol et al. 2008).

Kv1.5 is also inhibited by phosphorylation via PKA, PKC and tyrosine kinases (Li et al. 1996; Sobko et al. 1998). Contrary to Kv1.3, Kv1.5 which possesses a SH3 domain and a direct interaction between Src and the channel have been proposed (Holmes et al. 1996). Modulation by kinases may also be dependent of Kvβ presence in the Kv1.5 channelosome (Williams et al. 2002).

2. Objectives

OBJECTIVES

Voltage-dependent potassium (Kv) channels play important roles in the maintenance of resting membrane potential and many other physiological functions such as propagation of the nerve impulse, generation of the cardiac action potential, muscular contraction, proliferation, cell volume control, etc. However, all these processes are generated by oligomeric complexes (chanelosomes) formed by Kv conducting subunits in association with ancillary subunits. Auxiliary subunits are able to modify traffic, current density, gating kinetics and pharmacology of the channels. In fact, native currents such as I_{Kr}, I_{Ks} or I_{to} currents have been recapitulated in heterologous systems only when co-expression of Kv channels with regulatory subunits have been performed.

KCNE peptides are one of these regulatory subunit families, which is comprised by five members of single spanned transmembrane proteins (KCNE1-5). KCNEs peptides interact and modify many types of Kv channels. Among all the possible interactions, Kv7.1-KCNE1 is the most analyzed channelosome. In addition, a large body of information is available about the gating modulation of KCNEs on Kv channels. However, scarce information is known about the modulation of Kv traffic and subcellular localization.

The current dissertation aims to further the knowledge of the KCNE modulation on Kv channels. To that end we also analyzed their interaction with Kv7.5, which is the last and less studied member from the Kv7 family. In addition, we focused on the KCNE4-dependent Kv1.3 regulation. Therefore, the specific objectives of the PhD dissertation are:

1. KCNE modulation on Kv7.1 traffic and membrane localization.
2. KCNE modulation on Kv7.5
3. KCNE modulation of the Kv1.3 channelosome in leukocytes.

3. Results

3.1. Block 1:

KCNE modulation of Kv7 channels

3.1.1. Resum de la contribució 1

Article publicat en J Cell Physiol, 2010, 225:692-700

Impacte de les subunitats KCNE en el tràfic a superfície de membrana del canal KCNQ1 (Kv7.1)

Mertixell Roura-Ferrer, Laura Solé, Anna Oliveras, Rinat Dahan, Joanna Bielanska, Álvaro Villarroel, Nuria Comes, Antonio Felipe

El canal KCNQ1 (Kv7.1) juga un paper molt important en la fisiologia cardiovascular. Els cardiomiòcits co-expressen el canal KCNQ1 i les subunitats reguladores KCNE1-5. S'ha descrit com el canal KCNQ1 pot associar-se amb els diferents membres de la família KCNE, generant oligomers amb diferents propietats biofísiques i farmacològiques.

Són molts els resultats que en els darrers anys indiquen com la localització dels canals és un dels factors determinants per a la seva correcta funció. En aquest context, la presència de canals de potassi en microdominis de membrana rics en esfingolípids i colesterol (*lipid rafts*) és el centre de molts estudis. S'ha descrit com els *lipid rafts* són importants pel funcionament cardiovascular.

En el present treball ens vam preguntar si les subunitats KCNE modificaven la localització del canal KNCQ1 en els microdominis del tipus *lipid raft*. Cèl·lules HEK-293 es van transfectar de manera transitòria amb KCNQ1 i KCNE1-5, i es va analitzar el tràfic i la presència a *lipid rafts* de cadascuna de les proteïnes, per separat i co-expressades. Només KCNQ1 i KCNE3, quan s'expressaven per separat, co-localitzaren amb les fraccions riques en *lipid rafts*. A més a més, mentre que KCNE2 i KCNE5 s'observaven notablement a la superfície cel·lular, KCNQ1 i la resta de KCNEs mostraven un marcada retenció intracel·lular. Es va poder observar però com KCNQ1 es localitza en diferents microdominis de la membrana en funció de la seva associació amb els pèptids KCNE. Així, per exemple, mentre que KCNQ1/KCNE1 i KCNQ1/ KCNE2 es localitzen en *lipid rafts*, KCNQ1 associat amb KCNE3-5 no s'hi localitza. Aquests resultats es van poder corroborar a més a més mitjançant l'anàlisi d'experiments de recuperació de la fluorescència després del cremat o *Fluorescence Recovery After Photobleaching* (FRAP), on s'estudia la dinàmica de membrana del canal.

En conclusió, el tràfic i la localització del canal KCNQ1 pot ser modificat per la seva associació amb KCNEs. Degut a que KCNQ1 juga un paper crucial en la fisiologia cardiovascular, la regulació temporal i espacial que les diferents subunitats KCNE poden conferir als canals pot tenir un impacte dramàtic en l'activitat elèctrica de la membrana i la seva regulació endocrina.

3.1.2. Report of the PhD student participation in the article

Informe de la participació de la doctoranda en l'article

Impact of KCNE subunits on KCNQ1 (Kv7.1) channel membrane surface targeting.

Published in Journal of Cellular Physiology, **Impact Factor (2010): 4.59**

Laura Solé Codina performed confocal co-localization experiments and lipid raft purification experiments of KCNEs, as well as participated in FRAP experiments.

Laura Solé Codina ha participat en la realitazació dels expermints de co-localització dels KCNEs amb confocal, l'extracció de lipid rafts dels KCNEs, així com en alguns experiments de FRAP.

Thesis director

El director de la tesi

Dr. Antonio Felipe Campo

ORIGINAL ARTICLE

692

Journal of Cellular Physiology

Impact of KCNE Subunits on KCNQ1 (Kv7.1) Channel Membrane Surface Targeting

MERITXELL ROURA-FERRER,[1,2] LAURA SOLÉ,[1] ANNA OLIVERAS,[1] RINAT DAHAN,[1] JOANNA BIELANSKA,[1] ÁLVARO VILLARROEL,[2] NÚRIA COMES,[1] AND ANTONIO FELIPE[1]*

[1]*Molecular Physiology Laboratory, Departament de Bioquímica i Biologia Molecular, Institut de Biomedicina (IBUB), Universitat de Barcelona, Barcelona, Spain*

[2]*Unidad de Biofísica, CSIC-UPV/EHU, Universidad del País Vasco, Leioa, Spain*

The KCNQ1 (Kv7.1) channel plays an important role in cardiovascular physiology. Cardiomyocytes co-express KCNQ1 with KCNE1-5 proteins. KCNQ1 may co-associate with multiple KCNE regulatory subunits to generate different biophysically and pharmacologically distinct channels. Increasing evidence indicates that the location and targeting of channels are important determinants of their function. In this context, the presence of K^+ channels in sphingolipid–cholesterol-enriched membrane microdomains (lipid rafts) is under investigation. Lipid rafts are important for cardiovascular functioning. We aimed to determine whether KCNE subunits modify the localization and targeting of KCNQ1 channels in lipid rafts microdomains. HEK-293 cells were transiently transfected with KCNQ1 and KCNE1–5, and their traffic and presence in lipid rafts were analyzed. Only KCNQ1 and KCNE3, when expressed alone, co-localized in raft fractions. In addition, while KCNE2 and KCNE5 notably stained the cell surface, KCNQ1 and the rest of the KCNEs showed strong intracellular retention. KCNQ1 targets multiple membrane surface microdomains upon association with KCNE peptides. Thus, while KCNQ1/KCNE1 and KCNQ1/KCNE2 channels target lipid rafts, KCNQ1 associated with KCNE3–5 did not. Channel membrane dynamics, analyzed by fluorescence recovery after photobleaching (FRAP) experiments, further supported these results. In conclusion, the trafficking and targeting pattern of KCNQ1 can be influenced by its association with KCNEs. Since KCNQ1 is crucial for cardiovascular physiology, the temporal and spatial regulations that different KCNE subunits may confer to the channels could have a dramatic impact on membrane electrical activity and putative endocrine regulation.

J. Cell. Physiol. 225: 692–700, 2010. © 2010 Wiley-Liss, Inc.

Many types of ion channels determine the configuration and duration of the cardiac action potential. Potassium channels control membrane potential, thereby playing a crucial role in cellular excitability (Hille, 2001). KCNQ1, also named Kv7.1 (IUPHAR, www.iuphar.org), is a voltage-gated potassium channel expressed in muscle cells that plays a central role for myocardial repolarization. In addition, KCNQ1 is involved in different physiological functions because is expressed in several epithelia, where it is involved in water and salt transport (Jespersen et al., 2005). In the heart, KCNQ1 associates with the KCNE1 ancillary subunit (minK). KCNQ1/KCNE1 oligomeric association forms a channel that conducts the cardiac I_{Ks} current. I_{Ks} activates slowly in response to changes in the membrane potential and is partly responsible for terminating the cardiac action potential. The physiological importance of these channels is emphasized by the fact that mutations in KCNQ1 or KCNE1 can cause cardiac arrhythmias and hearing loss in humans (Jespersen et al., 2005; Peroz et al., 2008).

The KCNE family (encoded by five genes designated KCNE1–5) is a group of small single transmembrane peptides that function as ancillary β-subunits to modulate voltage-dependent K^+ channels in muscle and epithelia (Abbott and Goldstein, 2001; McCrossan and Abbott, 2004). The first member of the KCNE family (KCNE1), originally cloned from rat kidney (Takumi et al., 1988), is expressed ubiquitously (McCrossan and Abbott, 2004). It was designated minK for minimal K^+ channel. KCNE1 associates with KCNQ1 to recapitulate many properties of the slowly activating and deactivating cardiac delayed rectifier K^+ current (I_{Ks}; Melman et al., 2002). KCNE2, first designated as MiRP1, for MinK-related peptide 1, regulates the Kv11.1 (HERG) channel to form a rapid component of cardiac delayed rectifier K^+ current (I_{Kr}; Abbott et al., 1999). While KCNE3 (MiRP2) is expressed in nerve, muscle and epithelia, KCNE4 (MiRP3) and KCNE5 (MiRP4) are also present in nerve and heart (Piccini et al., 1999; Abbott and Goldstein, 2001; Melman et al., 2002; McCrossan et al., 2003; McCrossan and Abbott, 2004). In addition to KCNE1, KCNE2–5 peptides also modulate KCNQ1 channels (Angelo et al., 2002; Grunnet et al., 2002; Melman et al., 2002; McCrossan and Abbott, 2004). KCNE2 and KCNE3 alter activation and confer constitutive activity when co-expressed with KCNQ1 (Melman et al., 2002). By contrast, KCNE4 and KCNE5 inhibit heterologously expressed KCNQ1 channel activity (Grunnet et al., 2002). The importance of KCNE genes is supported by mutations associated with inherited human diseases (Abbott and Goldstein, 2001). Although the physiological relevance of KCNE3–5 to cardiac ionic currents is still under debate, evidence indicates that different KCNE subunits may interact simultaneously with KCNQ1, thereby modulating current and traffic (Manderfield and George, 2008).

Subcellular localization of ion channels is crucial for adequate electrical signaling in the cardiovascular system (Steele et al., 2007; Cusdin et al., 2008). Besides biophysics, distinct accessory

Contract grant sponsor: Ministerio de Ciencia e Innovación (MICINN), Spain;
Contract grant numbers: BFU2008-00431, CSD2008-00005.

*Correspondence to: Antonio Felipe, Molecular Physiology Laboratory, Departament de Bioquímica i Biologia Molecular, Universitat de Barcelona, Avda Diagonal 645, E-08028 Barcelona, Spain. E-mail: afelipe@ub.edu

Received 13 January 2010; Accepted 25 May 2010

Published online in Wiley Online Library (wileyonlinelibrary.com.), 7 June 2010.
DOI: 10.1002/jcp.22265

© 2010 WILEY-LISS, INC.

β-subunits have important effects on Kv trafficking and surface expression (Martens et al., 1999; Abbott et al., 2007). Ion channels have specific surface distributions. Lipid rafts are specialized membrane microdomains rich in sphingolipids and cholesterol. Many signal transduction enzymes known to modulate ion channels are concentrated in these domains (Martens et al., 2004; O'Connell et al., 2004). Recently, there has been interest in the channel targeting to the membrane that defines the protein microenvironment. Lipid rafts work as platforms on which signal transduction pathways converge. Multiple Kv channels have affinities for lipid rafts, and different isoforms target distinct lipid microdomains (O'Connell et al., 2004; Maguy et al., 2006). However, oligomeric associations may impair these locations, causing notable effects on channel physiology (Martinez-Marmol et al., 2008; Vicente et al., 2008; Sole et al., 2009).

Because of the importance of a proper membrane surface expression of cardiac KCNQ1, we analyzed the impact of the oligomeric association with KCNE subunits on KCNQ1 channel membrane surface targeting. We investigated the localization of heteromeric complexes in lipid raft microdomains and analyzed surface dynamics. We describe, for the first time, that KCNQ1 targets non-caveolar rafts. Interestingly, KCNE3 is the unique KCNE peptide that localizes in lipid rafts. Association of KCNQ1 with KCNE1 and KCNE2 partially relocalizes these ancillary subunits in rafts. On the other hand, KCNQ1–KCNE3–5 heteromers were absent at low-buoyant density fractions. Membrane dynamics analyzed by FRAP further support these results. This is the first study demonstrating that cardiac KCNQ1 channels differentially target lipid rafts upon KCNE association.

Materials and Methods

Expression plasmids

hKCNQ1 cDNA in the pTNL vector was kindly provided by T. Jentsch (Leibniz-Institut für Molekulare Pharmakologie and Max-Delbrück-Centrum für Molekulare Medizin, Berlin, Germany). hKCNE1 and hKCNE2 in pHA were obtained from S. de la Luna (Centro de Regulación Genómica-CRG, Barcelona, Spain). Human KCNE3 and KCNE5 in pXOOM were provided by J. Barhanin (Institut de Pharmacologie Moléculaire et Cellulaire, CNRS and Université de Nice Sophia Antipolis, Valbonne Sophia Antipolis, France). hKCNE4-pXOOM cDNA was obtained from M. Grunnet (Danish National Research Foundation Centre for Cardiac Arrhythmia, University of Copenhagen, Copenhagen, Denmark). For expression studies, proteins were cloned into pCDNA3, pEYFP, and pECFP (Clontech, Mountain View, CA). All constructs were verified by sequencing.

Cell culture and transient transfections in HEK-293 cells

HEK-293 cells were grown on poly-lysine-coated coverslips in DMEM medium containing 10% FBS and supplemented with antibiotics, 10 U/ml penicillin and streptomycin.

Transient transfection was performed using Metafectene™ Pro (Biontex) at nearly 80% confluence (Sole et al., 2009). Twenty-four hours after transfection, cells were washed in phosphate-buffered saline (PBS), fixed with 4% paraformaldehyde in PBS for 10 min and mounted with Aqua Poly/Mount from Polysciences, Inc., Warrington, PA.

Protein extraction, co-immunoprecipitation, and Western blot

Twenty-four hours after transfection cells were processed for Western blot analysis. Cells were washed twice in cold PBS and lysed on ice with lysis solution (1% Triton X-100, 50 mmol/L Tris, pH 7.2, 150 mmol/L NaCl, 1 mmol/L EDTA) supplemented with 1 μg/ml aprotinin, 1 μg/ml leupeptin, 1 μg/ml pepstatin, and 1 mM phenylmethylsulfonyl fluoride as protease inhibitors. Homogenates were centrifuged at 3,000*g* for 10 min, and the supernatant was aliquoted and stored at −20°C. Protein content was determined by the Bio-Rad Protein Assay (Bio-Rad, Hercules, CA).

For co-immunoprecipitation, samples (1 mg) were precleared with 25 μl of protein G-Sepharose beads for 2 h at 4°C with gentle mixing. The beads were then removed by centrifugation at 1,000*g* for 30 sec at 4°C. The sample was then incubated overnight with the desired antibody (4 ng/μg protein) at 4°C with gentle mixing. Thirty microliters of protein G-Sepharose was added to each sample for 4 h at 4°C. The beads were removed by centrifugation at 1,000*g* for 30 sec at 4°C, washed four times in NGH buffer (50 mM HEPES, 150 mM NaCl, 1% Triton X-100, 10% glycerol, pH 7.2), and resuspended in 70 μl of SDS sample buffer.

Protein samples (50 μg) and immunoprecipitates were boiled in Laemmli SDS loading buffer and separated on 10% SDS–PAGE. Next, they were transferred to nitrocellulose membranes (Immobilon-P; Millipore, Billerica, MA) and blocked in 5% dry milk-supplemented 0.05% Tween 20 PBS before immunoreaction. Filters were immunoblotted with antibodies against GFP (1/1,000; Roche, Mannhein, Germany) or KCNQ1 (1/200; Alomone, Jerusalem, Israel). Anti-pan-caveolin antibody was used as a marker of lipid raft fractions (1/1,000; BD Transduction Laboratories, Franklin Lakes, NJ), and anti-clathrin antibody was used to characterize non-floating fractions (1/1,000; Chemicon, Temecula, CA).

Raft isolation and immunoisolation of caveolae

Low density, Triton-insoluble complexes were isolated as previously described (Vicente et al., 2008) from HEK cells transient transfected with either KCNQ1-CFP or double transfected KCNQ1-CFP/KCNEs-YFP. Cells were homogenized in 1 ml of 1% Triton X-100, and sucrose was added to a final concentration of 40%. A 5–30% linear sucrose gradient was layered on top and further centrifuged (39,000 rpm) for 20–22 h at 4°C in a Beckman SW41TI rotor. Gradient fractions (1 ml) were collected from the top and 50 μl were analyzed by Western blot.

Immunoisolation of caveolae has been described previously (Vicente et al., 2008). Following sucrose gradient sedimentation, floating membranes were collected and pooled. Samples were diluted with Mes-buffered saline (25 mM Mes, pH 6.5, 0.15 M NaCl) containing 0.05% Triton X-100 and precleared with 25 μl of protein A-Sepharose beads for 2 h at 4°C with gentle mixing. The beads were then removed by centrifugation at 1,000*g* for 30 sec at 4°C. The sample was then incubated overnight with anti-caveolin polyclonal antibodies (2.5 μg) at 4°C with gentle mixing. Thirty microliters of protein A-Sepharose was added to each sample for 2 h at 4°C. The beads were removed by centrifugation at 1,000*g* for 30 sec at 4°C, washed three times in NGH, and resuspended in 50 μl of SDS sample buffer.

Confocal microscopy and FRAP

Fluorescence recovery after photobleaching (FRAP) experiments were performed 1 day after transfection at room temperature (Sole et al., 2009). Dishes were replaced every 2 h. Time series were taken with 20 scans before bleaching, which was accomplished by 20 iterations of bleaching with 100% laser power of the 514-nm line, followed by 100 scans every 0.36 sec and 100 scans every second (2.5 min in total) of the bleached region with 6% laser power. In each cell, a circular region of interest (ROI) of 6.57 μm^2 was bleached. Experiments were performed with $n = 4$–10 cells per group. Fluorescence intensity was normalized to the prebleach intensity. Any loss of fluorescence during the recording was corrected with unbleached regions of the cell. Mobile fraction (F_M) was calculated according to the following equation:

$$F_M = \frac{(F_\infty - F_i)}{(F_0 - F_i)}$$

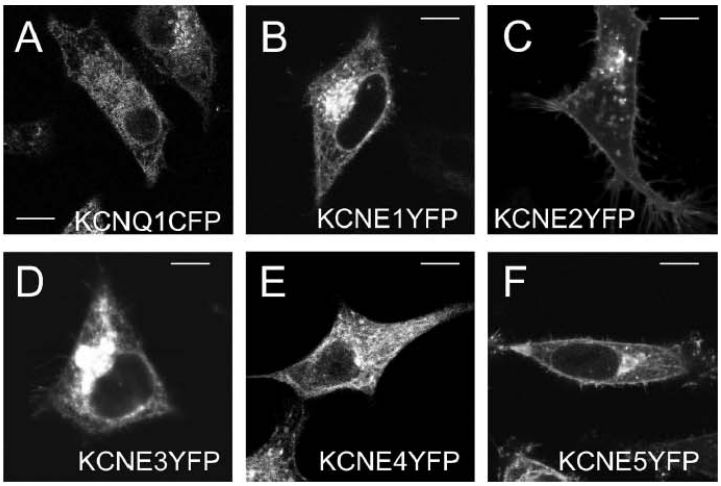

Fig. 1. KCNQ1-CFP and KCNEs-YFP have distinct cellular distributions and membrane targeting. HEK cells were transient transfected with KCNQ1 (A) and KCNE1–5 (B–F). The bars represent 10 μm.

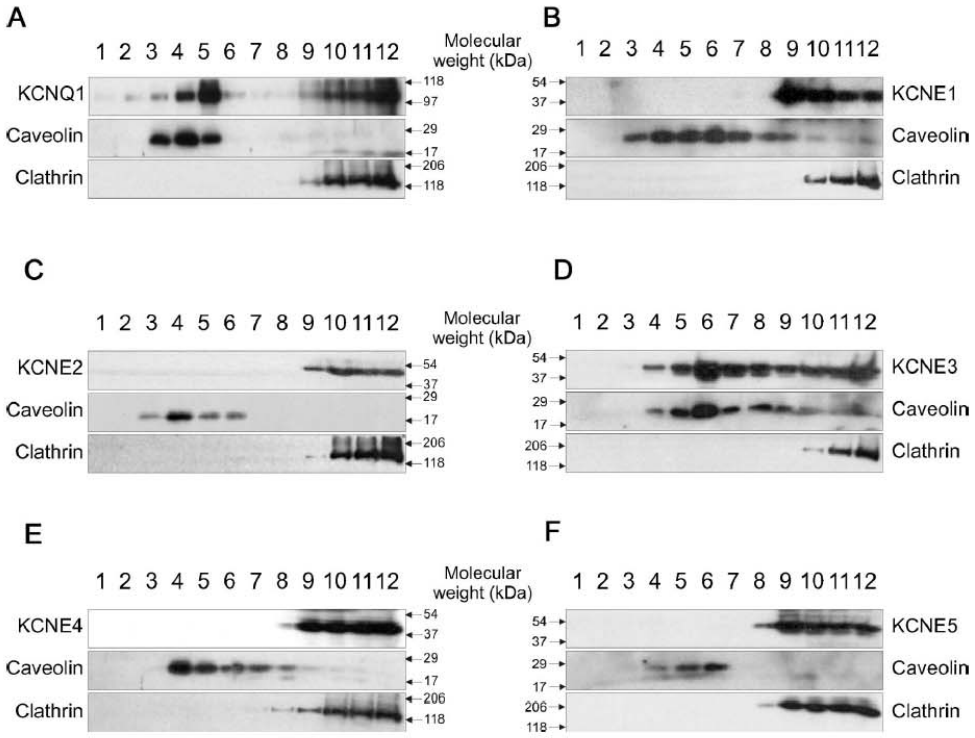

Fig. 2. KCNQ1 and KCNE1–5 differentially target lipid rafts in HEK-293 cells. Cells were transfected with KCNQ1 (A), KCNE1 (B), KCNE2 (C), KCNE3 (D), KCNE4 (E), and KCNE5 (F). Sucrose density gradient fractions of HEK transfected cells were isolated and blotted against KCNQ1, KCNEs, caveolin, and clathrin. While caveolin was used as a low-buoyant density fractions marker, clathrin identified non-raft fractions.

where F_∞ is the fluorescence at the end of the steady state, F_i is the fluorescence intensity post-bleaching, and F_0 is the fluorescence of the ROI previous to the bleaching.

Values were fitted to a nonlinear regression equation, $F(t) = F_M [1 - \exp(-t/t_{1/2})]$, where F is the fluorescence intensity, F_M is the mobile fraction, and $t_{1/2}$ is the time constant. Data are shown as the mean ± SEM. Statistical analysis was performed by Student's *t*-test (GraphPad Prism, La Jolla, CA™).

For image processing and quantification analysis we measured the degree of overlap of the red and green spots calculating the Pearson's correlation coefficient (r) between the red and the green component of each dual-channel image (Manders et al., 1993). Furthermore, percentage of co-localization was calculated on a pixel by pixel analysis from confocal images (Sole et al., 2009).

Cells were examined with a 63× oil immersion objective on a Leica TCS SL laser scanning confocal microscope. All offline image analysis was done using Leica confocal Image J software and Sigmaplot.

Results

Traffic and membrane surface targeting of KCNQ1 and KCNE peptides

The modulation of KCNQ1 channels by KCNE accessory subunits is under investigation and the functional consequences of their association widely described (Melman et al., 2002; McCrossan and Abbott, 2004). Therefore, we first corroborated the effects of our KCNE constructs on KCNQ1 currents. All KCNQ1/KCNE combinations gave the expected results (Melman et al., 2002; McCrossan and Abbott, 2004; data not shown).

Voltage-dependent K^+ channels have different traffic phenotypes, and this is important to cell physiology (Misonou and Trimmer, 2004; Vacher et al., 2008). We analyzed the cellular localization of KCNQ1 and KCNEs expressed individually in the mammalian cell line HEK-293 (Fig. 1). KCNQ1, KCNE1, KCNE3, and KCNE4 showed intracellular retention (Fig. 1A,B,D,E, respectively). Contrarily, KCNE2 and KCNE5 presented membrane targeting (Fig. 1C,F, respectively). Because the crucial role of ion channel surface location in specific membrane microdomains is worthy of considerable effort (O'Connell et al., 2004; Maguy et al., 2006), we next studied the raft microdomain localization of individually expressed KCNQ1 and KCNE peptides (Fig. 2). KCNQ1 co-localized in caveolin-enriched low-buoyant density fractions, indicating that this channel partially targets lipid rafts. Contrarily, KCNE1, 2, 4, and 5 targeted out-of-raft microdomains. Surprisingly, KCNE3 showed notable expression in low-buoyant sucrose fractions, demonstrating that, unlike other KCNE subunits, this protein efficiently targets lipid rafts. Caveolae are specialized membrane lipid rafts enriched in caveolins, where many signal transduction proteins and their targets interface (O'Connell et al., 2004; Maguy et al., 2006). While some Kv channels associate with these structures, some others remain in caveolae-free rafts (O'Connell et al., 2004; Maguy et al., 2006). Since KCNQ1 and KCNE3 were located in lipid rafts, we next investigated whether these Kv channel subunits were associated with caveolin. Co-immunoprecipitation studies from the caveolin-enriched pooled fraction from the lipid raft isolation studies in Figure 2 demonstrated that KCNQ1 and KCNE3 were not associated with caveolin (data not shown). These data indicate that similar to other Kv channels (Martens et al., 2000), KCNQ1 and KCNE3 may be located in non-caveolar lipid rafts.

KCNQ1 associates with all KCNE peptides

KCNQ1 forms heteromeric channels with all KCNE peptides. However, the physiological role of some oligomers is under debate. We studied the association of KCNQ1 with KCNE peptides and analyzed their traffic (Fig. 3). All KCNE ancillary subunits strongly co-localized with KCNQ1, and channel complexes were mainly retained intracellularly. Evidence indicates that regulatory subunits are involved in Kv channel targeting (Martens et al., 1999; Abbott et al., 2007). In this context, mutations on KCNE1 impair KCNQ1 surface expression (Krumerman et al., 2004). The co-expression of KCNE1 and KCNQ1 (Fig. 3A–D) slightly improved the surface staining of KCNQ1 (see Fig. 1A). Contrarily, KCNQ1 association impaired KCNE2 membrane location (Fig. 3E–H). Similar results were obtained with KCNE3 (Fig. 3I–L), KCNE4 (Fig. 3M–P), and KCNE5 (Fig. 3Q–T). It is noteworthy that KCNE2 and KCNE5, which showed membrane staining when expressed alone, suffered strong intracellular retention in the presence of KCNQ1. The quantitative co-localization analysis was performed calculating the Pearson's correlation coefficient (r) and the percentage of co-localization (Manders et al., 1993; Sole et al., 2009). Values indicated high co-localization between KCNQ1 and KCNEs. For instance, 77% of KCNQ1/KCNE1 cells (37/48) showed that 61% of KCNQ1 co-localized with KCNE1 with an r value of 0.68 ± 0.03. Similar values were obtained with the rest of KCNEs [KCNQ1/KCNE2: 82% of cells (42/51), 68% of co-localization, r = 0.67 ± 0.06; KCNQ1/KCNE3: 84% of cells (38/45), 55% of co-localization, r = 0.65 ± 0.04; KCNQ1/KCNE4: 83% of cells (40/48), 61% of co-localization, r = 0.64 ± 0.04; KCNQ1/KCNE5: 58% of cells (28/48), 50% of co-localization, r = 0.66 ± 0.05]. The widely recognized association of KCNQ1 with all KCNE peptides was further supported by co-immunoprecipitation studies (not shown).

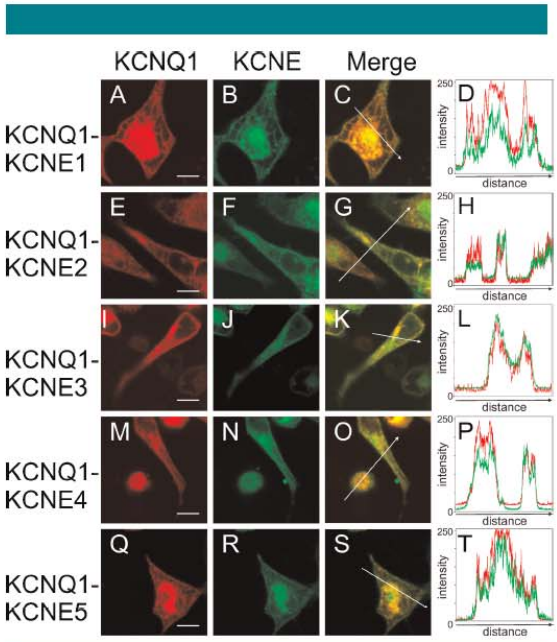

Fig. 3. KCNQ1 co-localizes with all KCNE subunits. HEK-293 cells were doubly transfected with KCNQ1-CFP and KCNE1–5-YFP. While the red panel shows KCNQ1-CFP (A,E,I,M,Q), the green panel depicts KCNE peptides (B,F,J,N,R). The merge panels show co-localization in yellow (C,G,K,O,S). (D,H,L,P,T) Histograms of the pixel by pixel analysis of the section indicated by arrows in merge panels C, G, K, O, and S, respectively. Red, KCNQ1; green, KCNEs. The bars represent 10 μm.

KCNQ1/KCNE oligomeric channels target multiple membrane surface microdomains

Great emphasis is being placed on the elements involved in channel targeting and anchoring to the membrane (Misonou and Trimmer, 2004; Steele et al., 2007; Vacher et al., 2008). The subcellular localization of Kv channels is critical for proper signaling in the cardiovascular system, and the compartmentalization of cardiac ion channels illustrates lipid raft heterogeneity (O'Connell et al., 2004; Maguy et al., 2006). Therefore, we analyzed the membrane localization of KCNQ1/KCNE channels. Figure 4 shows the membrane microdomain targeting and the surface dynamics of oligomeric KCNQ1/KCNE1 and KCNQ1/KCNE2 channels. Similar to KCNQ1 homomers, oligomeric KCNQ1 channels were partly located in low-buoyant density fractions (Fig. 4A,B, top panels). However, unlike KCNE1 and KCNE2 alone, oligomeric forms of these ancillary subunits associated with KCNQ1 were in part relocated in lipid rafts. While KCNE1 did not alter the KCNQ1 relative abundance in floating fractions (40 ± 6% and 48 ± 9% in the absence or the presence of KCNE1, respectively), KCNE2 diminished the localization of KCNQ1 in low-buoyant rafts (16 ± 3%, $P < 0.01$ vs. KCNQ1 in the absence of KCNE2, n = 4). Furthermore, KCNQ1 association partly target KCNE1 and KCNE2 to rafts (35 ± 7% and 28 ± 6%, respectively). FRAP studies further demonstrated that KCNE1 and KCNE2 membrane dynamics were also modified by the presence of KCNQ1. The data shown in Figure 4C,D,G,H demonstrate that while the percentage of KCNE1 mobile fraction was roughly similar (62 ± 10% and 76 ± 3% for KCNE1 and KCNE1/KCNQ1, respectively), the recovery time constant slowed from 8 ± 2 sec to 22 ± 3 sec for KCNE1 and KCNE1/KCNQ1, respectively ($P < 0.05$, n = 4–6; Fig. 4K). Similarly, KCNE2 parameters also suggest that the KCNE peptide was relocated to less dynamic microdomains (Fig. 4E,F,I,J). While mobile fractions were 58 ± 7% and 70 ± 4% for KCNE2 and KCNE2/KCNQ1, respectively, the recovery time constant rose from 8 ± 2 sec to 17 ± 3 sec ($P < 0.05$, n = 8–10) for KCNE2 and KCNE2/KCNQ1, respectively (Fig. 4K).

Unlike KCNE1 and KCNE2, KCNE3 targeted lipid rafts (see Fig. 2B–D). However, the presence of KCNQ1 impaired this location (Fig. 5A). In addition, the association of KCNQ1 with KCNE3 also altered the KCNQ1 location. Thus, KCNE3 triggered a decrease of KCNQ1 in floating fractions (35 ± 1% to 25 ± 4% for KCNQ1 and KCNQ1/KCNE3, respectively, $P < 0.05$, n = 4–6; Fig. 5B). Furthermore, KCNQ1 association drastically relocated KCNE3 in non-raft domains (Fig. 5C). FRAP analysis revealed that KCNQ1 membrane dynamics were slightly affected by the presence of KCNE3 (Fig. 5D,E,H,I). However, the membrane dynamics of KCNE3 were altered in the presence of KCNQ1 (Fig. 5F,G,J,K). Thus, the mobile

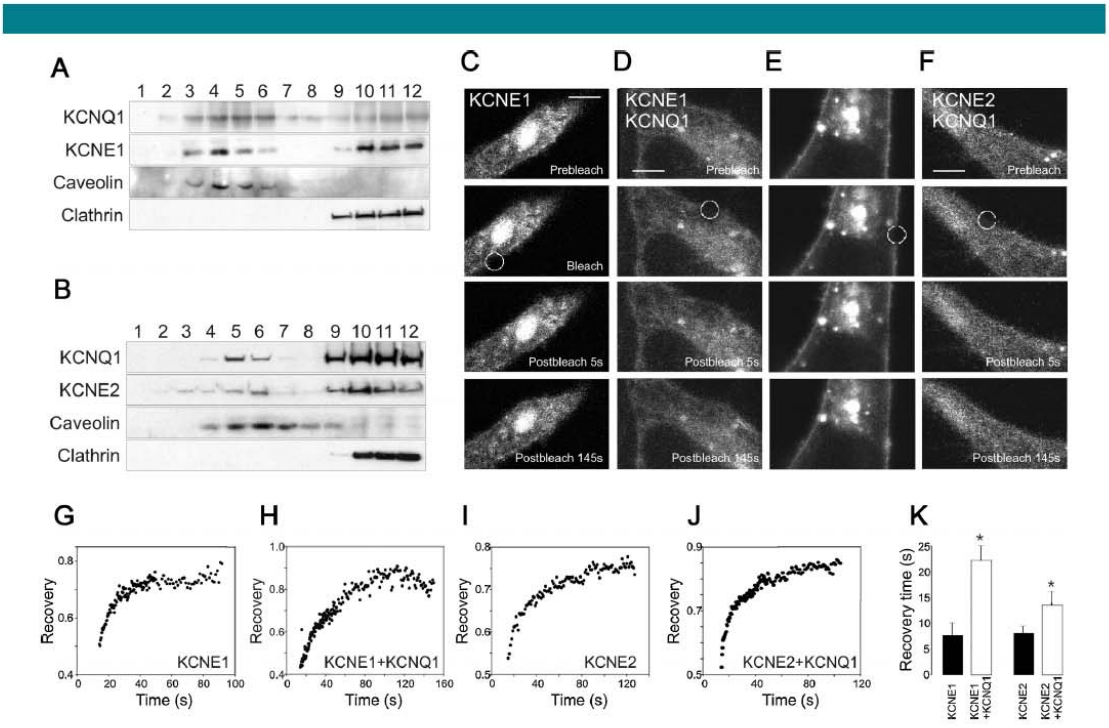

Fig. 4. Association of KCNQ1 with KCNE1 and KCNE2 partly targets KCNE peptides to different membrane microdomains with lower mobility. HEK-293 cells were doubly transfected with either KCNQ1-CFP and KCNE1-YFP or KCNQ1-CFP and KCNE2-YFP. A: Sucrose density gradient fractions of KCNQ1/KCNE1. B: Sucrose density gradient fractions of KCNQ1/KCNE2. C,D: Fluorescence recovery after photobleaching (FRAP) of KCNE1 and KCNQ1/KCNE1. FRAP experiments monitored YFP intensity after 20 iterations of bleaching with 100% laser power. Representative images of KCNE1-YFP at different times. Circles indicate regions of interest. C: KCNE1; D: KCNE1+KCNQ1. E,F: FRAP of KCNE2 and KCNQ1/KCNE2. Representative images of KCNE2-YFP at different times. E: KCNE2; F: KCNE2+KCNQ1. Scale bars: 10 μm. G,H: Graphs of the average (n > 8) intensity from KCNE1 (G) and KCNE1+KCNQ1 (H). I,J: Graphs of the average (n > 6) intensity from KCNE2 (G) and KCNE2+KCNQ1 (H). K: The recovery time was calculated as the time constant ($t_{1/2}$) of KCNE1 and KCNE2 in the absence (black bars) or the presence (white bars) of KCNQ1. *$P < 0.05$ versus KCNE1 and KCNE2.

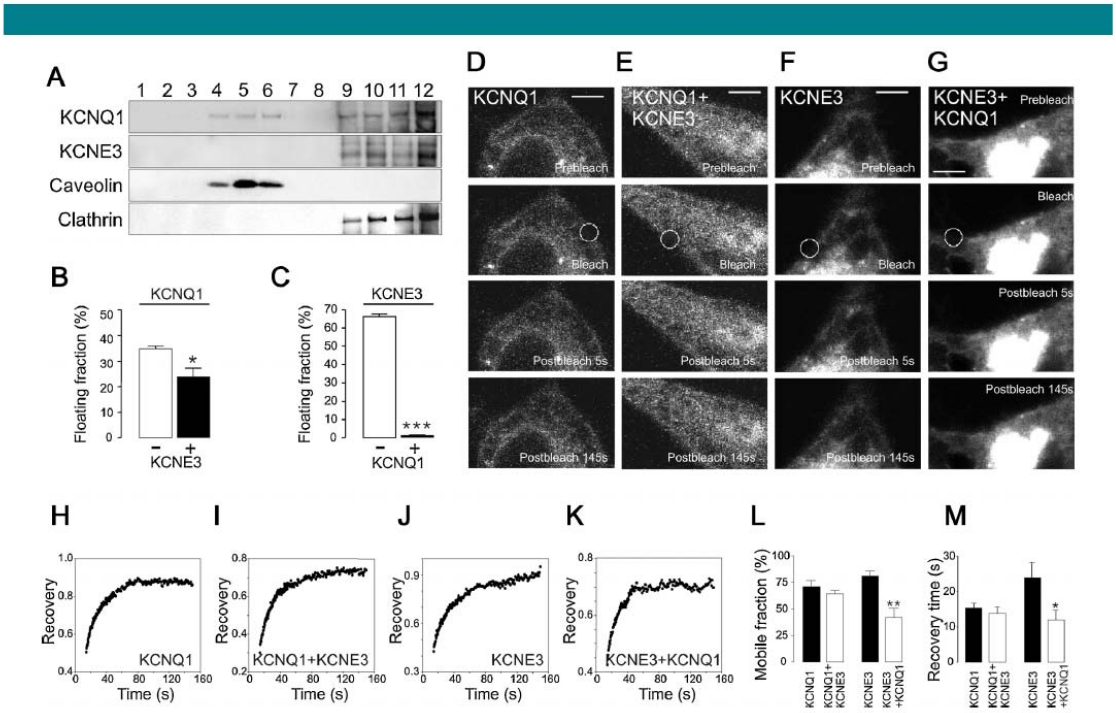

Fig. 5. Association of KCNQ1 with KCNE3 alters the location of KCNQ1/KCNE3 channels. HEK-293 cells were transfected with either KCNQ1-YFP or KCNE3-YFP and doubly transfected with KCNQ1-CFP and KCNE3-YFP. A: Sucrose density gradient fractions of KCNQ1/KCNE3. B: Percentage of KCNQ1 relative abundance in floating fractions in the absence (−, white bars) and the presence (+, black bars) of KCNE3 [*$P < 0.05$ vs. in the absence (−) of KCNE3]. C: Percentage of KCNE3 relative abundance in floating fractions in the absence (white bars) and the presence (black bars) of KCNQ1 [*$P < 0.001$ vs. in the absence (−) of KCNQ1]. D,E: FRAP of KCNQ1 and KCNQ1/KCNE3. Representative images of the KCNQ1-YFP intensity at different times. Circles indicate regions of interest. D: KCNQ1; E: KCNQ1+KCNE3. F,G: FRAP of KCNE3 and KCNQ1/KCNE3. Representative images of KCNE3-YFP at different times. F: KCNE3; G: KCNE3+KCNq1. Scale bars: 10 μm. H,I: Graphs of the average (n > 6) intensity from KCNQ1 (H) and KCNQ1+KCNE3 (I). J,K: Graphs of the average (n > 4) intensity from KCNE3 (J) and KCNE3+KCNQ1 (K). L: Mobile fraction in percentage of KCNQ1 and KCNE3 in the absence (black bars) and the presence (white bars) of KCNE3 or KCNQ1, respectively. **$P < 0.01$ versus in the absence of KCNQ1. M: The recovery time was calculated as the time constant ($t_{1/2}$) of KCNQ1 and KCNE3 in the absence (black bars) or the presence (white bars) of KCNE3 or KCNQ1, respectively. *$P < 0.05$ versus KCNE3.**

fraction and the recovery time constant decreased in association with KCNQ1 (Fig. 5L,M).

KCNQ1 was differentially located in low-buoyant density sucrose fractions upon association with KCNE2 and 3. However, interactions with KCNE4 and KCNE5 impaired KCNQ1 co-localization with rafts (Fig. 6A,B). This surprising result was further supported by KCNQ1 membrane dynamics. KCNE4 (Fig. 6C,D,H) and KCNE5 (Fig. 6E,F,I) slightly diminished the mobile fraction (Fig. 6J), but notably speeded the KCNQ1 recovery time constant (Fig. 6K).

Discussion

Voltage-dependent K^+ channels play a pivotal role during the action potential in the cardiovascular system. In this context, the subunit composition of the channelosome and specific subcellular localizations allow for precise regulation of cardiac excitability. Evidence indicates that the physiological function of Kv channels is affected by interactions with accessory proteins that modulate their activity and localization. In this scenario, channel targeting to lipid rafts is a novel and important spatial factor in cardiovascular physiology (O'Connell et al., 2004; Maguy et al., 2006).

In the present study, we demonstrate that KCNQ1 channels target multiple membrane surface microdomains upon association with KCNE subunits. KCNQ1 partly located in lipid rafts. However, KCNE peptides showed different targeting. Thus, while KCNE3 strongly co-localized with raft domains, the rest of the KCNE isoforms did not. KCNQ1 partly relocalized KCNE1 and KCNE2 subunits in low-buoyant density fractions. Surprisingly, the association of KCNQ1 with KCNE3 targeted the complex out of rafts. In addition, the association of KCNE4 and KCNE5 impaired KCNQ1 targeting to lipid rafts.

The targeting of ion channels to cholesterol-rich membrane microdomains has emerged as a novel mechanism of ion channel regulation in the cardiovascular system (O'Connell et al., 2004; Maguy et al., 2006). However, limited information about cardiac KCNQ1 and KCNE partners is available. Low-buoyant density fraction isolations from cardiac samples demonstrate that KCNQ1, KCNE1, and KCNE2 localize in lipid rafts (Balijepalli et al., 2007; Nakamura et al., 2007). Endocrine signals known to regulate KCNQ1 also localize in raft domains (Callera et al., 2007). For instance, β-adrenergic signaling, which modulates I_{Ks} currents contributing to ventricular repolarization during rapid heart rate, regulates cardiac Nav1.5 regulation via a G-protein mechanism associated with lipid rafts (Yarbrough et al., 2002). In addition, progesterone acutely modulates I_{Ks} through a non-genomic pathway involving c-Src/PI3K/Akt-dependent endothelial nitric oxide (NO) synthase (eNOS) activation (Nakamura et al., 2007). However,

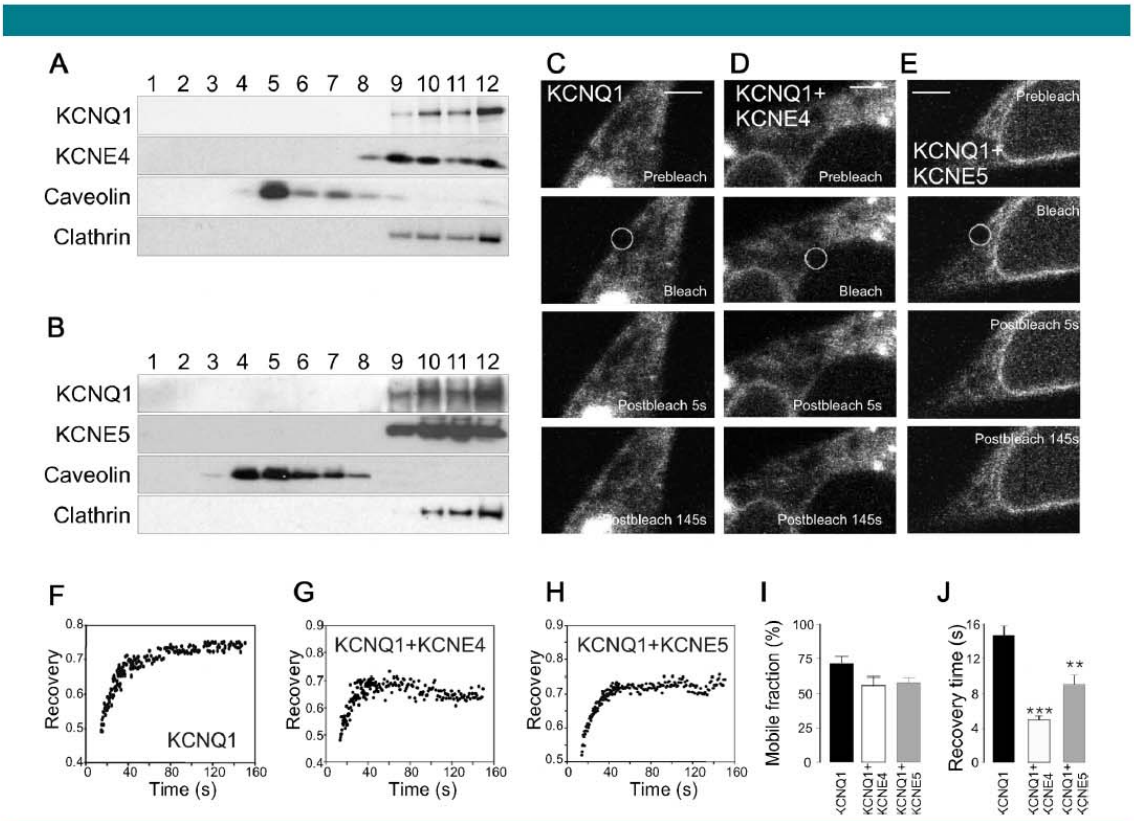

Fig. 6. KCNE4 and KCNE5 impair KCNQ1 localization in lipid rafts. HEK-293 cells were transfected with KCNQ1 or doubly transfected with either KCNQ1-YFP and KCNE4-CFP or KCNQ1-YFP and KCNE5-CFP. A: Sucrose density gradient fractions of KCNQ1/KCNE4. B: Sucrose density gradient fractions of KCNQ1/KCNE5. C: FRAP experiment of KCNQ1. D: FRAP experiment of KCNQ1/KCNE4. E: FRAP experiment of KCNQ1/KCNE5. FRAP representative images of KCNQ1-YFP at different times are shown. Circles indicate regions of interest. Scale bars: 10 μm. F–H: Graphs of the average (n > 6) intensity from KCNQ1 (F) and KCNQ1+KCNE4 (G) and KCNQ1+KCNE5 (H). I: Percentage of KCNQ1 mobile fraction (black bars) in the presence of KCNE4 (white bars) or KCNE5 (gray bars). J: The recovery time was calculated as the time constant ($t_{1/2}$) of KCNQ1 (black bars) in the presence of KCNE4 (white bars) or KCNE5 (gray bars). $^{**}P < 0.01$; $^{***}P < 0.001$ versus KCNQ1.

although progesterone does not alter KCNQ1/KCNE1 localization in rafts, molecules involved in the downstream pathway of progesterone, such as eNOS, co-localize in caveolae-raft fractions (Callera et al., 2007; Nakamura et al., 2007). Lipid rafts ensure close proximity between signaling molecules and their targets. eNOS and KCNQ1, sharing membrane microdomains, function as a co-ordinated mechanism that ensures correct modulation. We found that KCNE1 is only located in rafts when associated with KCNQ1, which generates functional I_{Ks} channels. To what extent the presence of inherited mutations of KCNE1, which impairs KCNQ1 membrane surface expression and triggers cardiac LQT1 syndrome, alters KCNQ1 signaling is not known (Krumerman et al., 2004), but clinical data suggest protective effects of progesterone against LQTS-associated arrhythmias (Nakamura et al., 2007).

Although KCNE1 is an obligate I_{Ks} component (Barhanin et al., 1996), KCNE2 is also expressed in the human heart (Melman et al., 2002; Lundquist et al., 2005). KCNE2, a recognized partner of Kv11.1 (HERG; Abbott et al., 1999), also associates with KCNQ1 within the cardiovascular system (Melman et al., 2002; Bendahhou et al., 2005; Lundquist et al., 2005). Although the physiological significance of cardiac KCNQ1/KCNE2 oligomeric channels is not clear, human *KCNE2* gene variants in association with KCNQ1 have been tentatively associated with atrial fibrillation (Yang et al., 2004). Furthermore, KCNE2 associates with KCNQ1/KCNE1 channels to suppress the current amplitude without altering the slow gating kinetics (Jiang et al., 2009). In this context, similar to Um and McDonald (2007), we found that KCNE2 stains more cell surface compared to KCNE1, which is mostly retained in the endoplasmic reticulum. In addition, Chandrasekhar et al. (2006) support that KCNE1 remains mostly intracellular but the presence of KCNQ1 increases the surface expression. Our results agree with these previous works indicating that the association with KCNQ1 improves the membrane targeting. Contrarily, we demonstrate that KCNE2 membrane surface expression is impaired by the presence of KCNQ1. Kv11.1/KCNE2 channels have been localized in lipid rafts (Balijepalli et al., 2007). However, similar to KCNE1, KCNE2 alone did not co-localize with rafts. Our data indicate that similar to KCNQ1/KCNE1, KCNQ1/KCNE2 channels partly target rafts. However, it is worth mentioning that the amount of KCNQ1 present in rafts decreases in combination with KCNE2. The final channel subunit composition is likely to be determined by a combination of subunit expression rates and differential protein processing and trafficking. For instance, in the *Kcne2*$^{-/-}$ null mouse, the traffic of Kv1.5 to the intercalated discs is disrupted,

concomitant with a prolonged ventricular action potential duration, which triggers an extended QT interval under sevoflurane anesthesia (Roepke et al., 2008). Although the role of KCNE2 in the heart is still under debate, the physiological relevance of KCNQ1/KCNE2 channels for maintaining K^+ conductance in epithelial cells, such as acid secretory gastric parietal cells and thyrocytes, is crucial (Lee et al., 2000; Roepke et al., 2006; Roepke et al., 2009).

The expression of multiple KCNE genes in the human heart may enable variable modulation of I_{Ks}. KCNE3 is highly expressed in muscle, and inherited mutations trigger severe myopathies (Abbott et al., 2001). If human cardiac myocytes co-express KCNQ1 with KCNE1–KCNE5, changing the pattern of KCNQ1/KCNE associations can have a dramatic impact on the membrane electrical activity. However, the role of KCNQ1/KCNE3 channels has only been deciphered in the gastrointestinal epithelia (Schroeder et al., 2000; Grahammer et al., 2001). It is generally accepted that the tissue expression modulates the activity of ion channels. Our results may bring some light to this issue. While KCNQ1 relocalized KCNE1 and KCNE2 in rafts to generate cardiac currents, KCNE3 association impairs KCNQ1 localization in rafts. Because the biophysics and pharmacology of KCNQ1/KCNE3 complexes are markedly different from those of KCNQ1/KCNE1 and KCNQ1/KCNE2 channels (Melman et al., 2002; McCrossan and Abbott, 2004), their association may mask important elements eliciting different membrane targeting surface phenotypes. Multiple KCNQ1 targeting phenotypes may account for specific tissue roles.

Less is known about the physiological significance of KCNE4 and KCNE5 in combination with KCNQ1 (Angelo et al., 2002; Grunnet et al., 2002). Both KCNE peptides are expressed in the cardiovascular system (McCrossan and Abbott, 2004; Abbott et al., 2007). Although the two KCNE peptides differentially target the membrane surface, neither KCNE4 nor KCNE5 was present in lipid rafts. In addition, KCNQ1 association with KCNE4 or KCNE5 targets KCNQ1 heteromeric channels out of rafts. Similarly, Kv1.3/KCNE4 association impairs Kv1.3 localization in caveolar raft domains (Sole et al., 2009). In addition, KCNQ1 may form a heterooligomeric complex with KCNE1 and KCNE4 (Manderfield and George, 2008). Although KCNE4 suppresses channel activity by a mechanism that does not impair cell surface expression, we demonstrated that microdomain targeting is clearly affected. Therefore, the effect of KCNE4 may serve as an accessory negative regulatory mechanism.

Our results further suggest that KCNQ1 and KCNE3 are associated with non-caveolar rafts. Kv2.1 was the first channel to be localized in non-caveolar cholesterol-enriched membrane domains (Martens et al., 2000) but other Kv, such as cardiac Kv1.5 and leukocytic Kv1.3, co-localize in caveolar domains (Martens et al., 2000; Martinez-Marmol et al., 2008; Vicente et al., 2008). The presence of Kv1.5 modulates Kv1.3 traffic and membrane surface expression (Vicente et al., 2008). In addition, Kv1.5 targets multiple membrane surface microdomains upon its partnership association (Martinez-Marmol et al., 2008). Similarly, the presence of partner subunits may modulate the KCNQ1 channel-raft association.

To what extent the localization in caveolar or non-caveolar rafts is determinant of cell physiology is still under investigation. However, the importance of lipid-raft integrity in the cardiovascular system is demonstrated by the appearance of cardiomyopathies and impaired vasoconstriction in null animal models (O'Connell et al., 2004; Maguy et al., 2006). Lipid rafts are specific domains for co-ordinating signaling molecules with targets and to promote interactions with accessory proteins. The precise location of KCNQ1/KCNE oligomeric channels may contribute to fine-tuning the regulation of KCNQ1 signaling in the heart. Since the comprehension of the role of ion channels in multiple membrane microdomains is still in its infancy, a better understanding of how Kv channels compartmentalize in lipid rafts, in close proximity to signaling molecules, will provide further insights into the molecular mechanisms underlying cardiovascular diseases.

Acknowledgments

M.R.-F. hold a fellowship from the Generalitat de Catalunya. LS, JB, and AO are fellows from MICINN. N.C. is supported by the Juan de la Cierva program (MICINN). We thank M. Calvo (Unitat de Microscòpia Confocal, Serveis Cientificotècnics, Facultat de Medicina, Universitat de Barcelona) for the confocal microscopy experiments. We also thank the editorial assistance of American Journal Experts. M.R.-F. and L.S. contributed equally to this work.

Literature Cited

Abbott GW, Goldstein SA. 2001. Potassium channel subunits encoded by the KCNE gene family: Physiology and pathophysiology of the MinK-related peptides (MiRPs). Mol Interv 1:95–107.

Abbott GW, Sesti F, Splawski I, Buck ME, Lehmann MH, Timothy KW, Keating MT, Goldstein SA. 1999. MiRP1 forms IKr potassium channels with HERG and is associated with cardiac arrhythmia. Cell 97:175–187.

Abbott GW, Butler MH, Bendahhou S, Dalakas MC, Ptacek LJ, Goldstein SA. 2001. MiRP2 forms potassium channels in skeletal muscle with Kv3.4 and is associated with periodic paralysis. Cell 104:217–231.

Abbott GW, Xu X, Roepke TK. 2007. Impact of ancillary subunits on ventricular repolarization. J Electrocardiol 40:S42–S46.

Angelo K, Jespersen T, Grunnet M, Nielsen MS, Klaerke DA, Olesen SP. 2002. KCNE5 induces time- and voltage-dependent modulation of the KCNQ1 current. Biophys J 83:1997–2006.

Balijepalli RC, Delisle BP, Balijepalli SY, Foell JD, Slind JK, Kamp TJ, January CT. 2007. Kv11.1 (ERG1) K+ channels localize in cholesterol and sphingolipid enriched membranes and are modulated by membrane cholesterol. Channels (Austin) 1:263–272.

Barhanin J, Lesage F, Guillemare E, Fink M, Lazdunski M, Romey G. 1996. K(V)LQT1 and IsK (minK) proteins associate to form the I(Ks) cardiac potassium current. Nature 384:78–80.

Bendahhou S, Marionneau C, Haurogne K, Larroque MM, Derand R, Szuts V, Escande D, Demolombe S, Barhanin J. 2005. In vitro molecular interactions and distribution of KCNE family with KCNQ1 in the human heart. Cardiovasc Res 67:529–538.

Callera GE, Montezano AC, Yogi A, Tostes RC, Touyz RM. 2007. Vascular signaling through cholesterol-rich domains: Implications in hypertension. Curr Opin Nephrol Hypertens 16:90–104.

Chandrasekhar KD, Bas T, Kobertz WR. 2006. KCNE1 subunits require co-assembly with K+ channels for efficient trafficking and cell surface expression. J Biol Chem 281:40015–40023.

Cusdin FS, Clare JJ, Jackson AP. 2008. Trafficking and cellular distribution of voltage-gated sodium channels. Traffic 9:17–26.

Grahammer F, Herling AW, Lang HJ, Schmitt-Graff A, Wittekindt OH, Nitschke R, Bleich M, Barhanin J, Warth R. 2001. The cardiac K+ channel KCNQ1 is essential for gastric acid secretion. Gastroenterology 120:1363–1371.

Grunnet M, Jespersen T, Rasmussen HB, Ljungstrom T, Jorgensen NK, Olesen SP, Klaerke DA. 2002. KCNE4 is an inhibitory subunit to the KCNQ1 channel. J Physiol 542:119–130.

Hille B. 2001. Ion channels of excitable membranes. Sunderland, MA: Sinauer. p 814.

Jespersen T, Grunnet M, Olesen SP. 2005. The KCNQ1 potassium channel: From gene to physiological function. Physiology (Bethesda) 20:408–416.

Jiang M, Xu X, Wang Y, Toyoda F, Liu XS, Zhang M, Robinson RB, Tseng GN. 2009. Dynamic partnership between KCNQ1 and KCNE1 and influence on cardiac IKs current amplitude by KCNE2. J Biol Chem 284:16452–16462.

Krumerman A, Gao X, Bian JS, Melman YF, Kagan A, McDonald TV. 2004. An LQT mutant minK alters KvLQT1 trafficking. Am J Physiol Cell Physiol 286:C1453–C1463.

Lee MP, Ravenel JD, Hu RJ, Lustig LR, Tomaselli G, Berger RD, Brandenburg SA, Litzi TJ, Bunton TE, Limb C, Francis H, Gorelikow M, Gu H, Washington K, Argani P, Goldenring JR, Coffey RJ, Feinberg AP. 2000. Targeted disruption of the Kvlqt1 gene causes deafness and gastric hyperplasia in mice. J Clin Invest 106:1447–1455.

Lundquist AL, Manderfield LJ, Vanoye CG, Rogers CS, Donahue BS, Chang PA, Drinkwater DC, Murray KT, George AL, Jr. 2005. Expression of multiple KCNE genes in human heart may enable variable modulation of I(Ks). J Mol Cell Cardiol 38:277–287.

Maguy A, Hebert TE, Nattel S. 2006. Involvement of lipid rafts and caveolae in cardiac ion channel function. Cardiovasc Res 69:798–807.

Manderfield LJ, George AL, Jr. 2008. KCNE4 can co-associate with the I(Ks) (KCNQ1–KCNE1) channel complex. FEBS J 275:1336–1349.

Manders EMM, Verbeek FJ, Aten JA. 1993. Measurement of co-localization of objects in dual-colour confocal images. J Microsc 169:375–382.

Martens JR, Kwak YG, Tamkun MM. 1999. Modulation of Kv channel alpha/beta subunit interactions. Trends Cardiovasc Med 9:253–258.

Martens JR, Navarro-Polanco R, Coppock EA, Nishiyama A, Parshley L, Grobaski TD, Tamkun MM. 2000. Differential targeting of Shaker-like potassium channels to lipid rafts. J Biol Chem 275:7443–7446.

Martens JR, O'Connell K, Tamkun M. 2004. Targeting of ion channels to membrane microdomains: Localization of KV channels to lipid rafts. Trends Pharmacol Sci 25:16–21.

Martinez-Marmol R, Villalonga N, Sole L, Vicente R, Tamkun MM, Soler C, Felipe A. 2008. Multiple Kv1.5 targeting to membrane surface microdomains. J Cell Physiol 217:667–673.

McCrossan ZA, Abbott GW. 2004. The MinK-related peptides. Neuropharmacology 47:787–821.

McCrossan ZA, Lewis A, Panaghie G, Jordan PN, Christini DJ, Lerner DJ, Abbott GW. 2003. MinK-related peptide 2 modulates Kv2.1 and Kv3.1 potassium channels in mammalian brain. J Neurosci 23:8077–8091.

Melman YF, Krummerman A, McDonald TV. 2002. KCNE regulation of KvLQT1 channels: Structure–function correlates. Trends Cardiovasc Med 12:182–187.
Misonou H, Trimmer JS. 2004. Determinants of voltage-gated potassium channel surface expression and localization in Mammalian neurons. Crit Rev Biochem Mol Biol 39:125–145.
Nakamura H, Kurokawa J, Bai CX, Asada K, Xu J, Oren RV, Zhu ZI, Clancy CE, Isobe M, Furukawa T. 2007. Progesterone regulates cardiac repolarization through a nongenomic pathway: An in vitro patch-clamp and computational modeling study. Circulation 116:2913–2922.
O'Connell KM, Martens JR, Tamkun MM. 2004. Localization of ion channels to lipid raft domains within the cardiovascular system. Trends Cardiovasc Med 14:37–42.
Peroz D, Rodriguez N, Choveau F, Baro I, Merot J, Loussouarn G. 2008. Kv7.1 (KCNQ1) properties and channelopathies. J Physiol 586:1785–1789.
Piccini M, Vitelli F, Seri M, Galietta LJ, Moran O, Bulfone A, Banfi S, Pober B, Renieri A. 1999. KCNE1-like gene is deleted in AMME contiguous gene syndrome: Identification and characterization of the human and mouse homologs. Genomics 60:251–257.
Roepke TK, Anantharam A, Kirchhoff P, Busque SM, Young JB, Geibel JP, Lerner DJ, Abbott GW. 2006. The KCNE2 potassium channel ancillary subunit is essential for gastric acid secretion. J Biol Chem 281:23740–23747.
Roepke TK, Kontogeorgis A, Ovanez C, Xu X, Young JB, Purtell K, Goldstein PA, Christini DJ, Peters NS, Akar FG, Gutstein DE, Lerner DJ, Abbott GW. 2008. Targeted deletion of kcne2 impairs ventricular repolarization via disruption of I(K,slow1) and I(to,f). FASEB J 22:3648–3660.
Roepke TK, King EC, Reyna-Neyra A, Paroder M, Purtell K, Koba W, Fine E, Lerner DJ, Carrasco N, Abbott GW. 2009. Kcne2 deletion uncovers its crucial role in thyroid hormone biosynthesis. Nat Med 15:1186–1194.
Schroeder BC, Waldegger S, Fehr S, Bleich M, Warth R, Greger R, Jentsch TJ. 2000. A constitutively open potassium channel formed by KCNQ1 and KCNE3. Nature 403:196–199.
Sole L, Roura-Ferrer M, Perez-Verdaguer M, Oliveras A, Calvo M, Fernandez-Fernandez JM, Felipe A. 2009. KCNE4 suppresses Kv1.3 currents by modulating trafficking, surface expression and channel gating. J Cell Sci 122:3738–3748.
Steele DF, Zadeh AD, Loewen ME, Fedida D. 2007. Localization and trafficking of cardiac voltage-gated potassium channels. Biochem Soc Trans 35:1069–1073.
Takumi T, Ohkubo H, Nakanishi S. 1988. Cloning of a membrane protein that induces a slow voltage-gated potassium current. Science 242:1042–1045.
Um SY, McDonald TV. 2007. Differential association between HERG and KCNE1 or KCNE2. PLoS One 2:e933.
Vacher H, Mohapatra DP, Trimmer JS. 2008. Localization and targeting of voltage-dependent ion channels in mammalian central neurons. Physiol Rev 88:1407–1447.
Vicente R, Villalonga N, Calvo M, Escalada A, Solsona C, Soler C, Tamkun MM, Felipe A. 2008. Kv1.5 association modifies Kv1.3 traffic and membrane localization. J Biol Chem 283:8756–8764.
Yang Y, Xia M, Jin Q, Bendahhou S, Shi J, Chen Y, Liang B, Lin J, Liu Y, Liu B, Zhou Q, Zhang D, Wang R, Ma N, Su X, Niu K, Pei Y, Xu W, Chen Z, Wan H, Cui J, Barhanin J, Chen Y. 2004. Identification of a KCNE2 gain-of-function mutation in patients with familial atrial fibrillation. Am J Hum Genet 75:899–905.
Yarbrough TL, Lu T, Lee HC, Shibata EF. 2002. Localization of cardiac sodium channels in caveolin-rich membrane domains: Regulation of sodium current amplitude. Circ Res 90:443–449.

3.1.4. Resum de la contribució 2

Publicat en Cell Physiol Biochem, 2009, 24:325-34.

Implicacions funcionals de l'expressió de les subunitats KCNE sobre el canal Kv7.5 (KCNQ5)

Meritxell Roura-Ferrer, Ainhoa Etxebarria, Laura Solé, Anna Oliveras, Nuria Comes, Álvaro Villarroel, Antonio Felipe

Les proteïnes Kv7 (KCNQ) formen part d'una família de canals de potassi dependents de voltatge que consta de cinc membres (Kv7.1-Kv7.5). Mentre que Kv7.1 és crucial en el cor, els canals Kv7.2, Kv7.3, Kv7.4 i Kv7.5 participen en la corrent de tipus M en el sistema nerviós. A més a més de al cervell, Kv7.5 és expressat en múscul esquelètic i llis, on el seu paper fisiològic està sent encara avaluat. S'ha descrit com els membres de la família Kv7 es poden associar a subunitats accessòries KCNE (KCNE1-5). Aquestes interaccions augmenten la diversitat dels canals i els proporciona mecanismes per respondre a d'una gran varietat d'estímuls. S'ha observat com els pèptids KCNE controlen l'expressió a superfície, dependència a voltatge, cinètica d'obertura, conductància unitària, selectivitat iònica i farmacologia de diferents canals. Els KCNE però han estat bàsicament estudiats en el cor, d'altra banda però, la seva activitat en el cervell i molts altres teixits està sent reconeguda cada cop més.

En aquest treball, descrivim com Kv7.5 i les subunitats KCNE estan presents en mioblasts. Per tant, associacions oligomèriques entre aquestes proteïnes podrien proporcionar una gran diversitat funcional al canal Kv7.5 en múscul esquelètic.

Un extens estudi en oòcits de Xenopus i cèl·lules HEK-293 demostra com KCNE1 i KCNE3, però no cap altre membre de la família KCNE, afecten al corrent del canal Kv7.5. Per una banda, KCNE1 alenteix l'activació i suprimeix la rectificació inversa de Kv7.5. Per l'altra, KCNE3 inhibeix dràsticament els corrents de Kv7.5. A més a més, KCNE1 augmenta l'amplitud de corrent del canal Kv7.5, en cèl•lules HEK-293.

En conclusió, els canvis observats tant en la cinètica o obertura del canal, com en l'amplitud de corrent suggereixen interaccions funcionals entre Kv7.5 i KCNE1 i Kv7.5 i KCNE3. Els nostres resultats tenen importància fisiològica ja que Kv7.5 és molt abundant en musculatura esquelètica i llisa, i la seva associació amb les subunitats KCNEs podria regular de manera precisa diferents respostes cel•lulars.

3.1.5. Report of the PhD student participation in the article

Informe de la participació de la doctoranda en l'article

Functional implications of KCNE subunit expression for the Kv7.5 (KCNQ5) channel.

Published in Cellular Physiology and Biochemistry, **Impact Factor (2009): 3.56**

Laura Solé Codina participated in the experiments of KCNEs expression in skeletal muscle (Fig1).

Laura Solé Codina ha realitzat els experiments de detecció de l'expressió dels KCNEs en el múscul esqueletic (Fig1).

Thesis director

El director de la tesi

Dr. Antonio Felipe Campo

Original Paper

Cellular Physiology and Biochemistry

Cell Physiol Biochem 2009;24:325-334

Accepted: July 28, 2009

Functional Implications of KCNE Subunit Expression for the Kv7.5 (KCNQ5) Channel

Meritxell Roura-Ferrer[1,2], Ainhoa Etxebarria[2], Laura Solé[1], Anna Oliveras[1], Núria Comes[1], Álvaro Villarroel[2] and Antonio Felipe[1]

[1]Molecular Physiology Laboratory, Departament de Bioquímica i Biologia Molecular, Universitat de Barcelona, Avda. Diagonal 645, Barcelona, [2]Unidad de Biofísica, CSIC-UPV/EHU, Universidad del País Vasco, Barrio Sarriena s/n, Leioa

Key Words
Voltage-dependent channels • Regulatory subunits • Skeletal muscle

Abstract
Kv7 (KCNQ) proteins form a family of voltage-gated potassium channels that is comprised of five members, Kv7.1-Kv7.5. While Kv7.1 is crucial in the heart, the Kv7.2, Kv7.3, Kv7.4 and Kv7.5 channels contribute to the M-current in the nervous system. In addition to the brain, Kv7.5 is expressed in skeletal and smooth muscle, where its physiological role is currently under evaluation. Kv7 associations with KCNE accessory subunits (KCNE1-5) enhance channel diversity and their interaction provides mechanisms to respond to a variety of stimuli. KCNE peptides control the surface expression, voltage-dependence, kinetics of gating, unitary conductance, ion selectivity and pharmacology of several channels. KCNE subunits have been primarily studied in the heart; however, their activity in the brain and in many other tissues is being increasingly recognized. Here, we found that Kv7.5 and KCNE subunits are present in myoblasts. Therefore, oligomeric associations may underlie some Kv7.5 functional diversity in skeletal muscle. An extensive study in *Xenopus* oocytes and HEK-293 cells demonstrates that KCNE1 and KCNE3, but none of the other KCNE subunits, affect Kv7.5 currents. While KCNE1 slows activation and suppresses inward rectification, KCNE3 drastically inhibits Kv7.5 currents. In addition, KCNE1 increases Kv7.5 currents in HEK cells. Changes in gating and amplitude indicate functional interactions. Our results have physiological relevance since Kv7.5 is abundant in skeletal and smooth muscle and its association with KCNE peptides may fine-tune cellular responses.

Copyright © 2009 S. Karger AG, Basel

Introduction

Potassium channels are one of the most diverse classes of membrane proteins in terms of function and structure. They establish the resting membrane potential and modulate the duration of the action potential in nerves and muscle. They are also involved in the maintenance of vascular smooth muscle tone, cell volume regulation, and leukocyte activation and proliferation, among other physiological responses [1]. More than 80 different genes

KARGER
Fax +41 61 306 12 34
E-Mail karger@karger.ch
www.karger.com

© 2009 S. Karger AG, Basel
1015-8987/09/0246-0325$26.00/0

Accessible online at:
www.karger.com/cpb

Antonio Felipe
Mol Physiol Lab, Departament de Bioquímica i Biología Molecular
Institut de Biomedicina, Universitat de Barcelona
Avda Diagonal 645, E-08028 Barcelona (Spain)
Tel. +34-934034616, Fax +34-934021559, E-Mail afelipe@ub.edu

have been classified and have been distributed into 4 superfamilies. The voltage-dependent potassium (Kv) superfamily may be further subdivided into seven conserved gene families. These comprise the voltage-dependent channels Kv1-4 (Shaker, Shab, Shaw, Shal-like subunits), the KCNQ channels (Kv7), the silent Kv5, Kv6, Kv8 and Kv9 subunits (modulators), and the eag-like channels (Kv10-12) [2].

The Kv7 family consists of five members (Kv7.1-Kv7.5), encoded by single genes that all give rise to proteins that form slowly activating potassium selective ion channels [2]. The fact that mutations in four genes of these subunits (Kv7.1-Kv7.4) give rise to human genetic disorders highlights the physiological relevance of this family [3, 4]. Kv7.1, mostly expressed in heart, is present in several tissues, including testis and skeletal muscle [5]. Kv7.2 and Kv7.3 channels are confined to the nervous system, where they have been found in various cell types, including hippocampus, cortex and dorsal root ganglia [6]. Kv7.2-Kv7.5 channels have been proposed to constitute the M-current. This current is central in the control of neuronal firing due to its modulation by neurotransmitters and voltage-sensitivity [3]. While Kv7.5 might produce different variants of M-current in different parts of the nervous system, its role in skeletal and smooth muscle, where is expressed, is currently under investigation [7-10]. In this context, we have recently described that Kv7.5 is involved in myoblast proliferation [11].

The interaction of Kv channels with accessory subunits provides a mechanism for channels to respond to a variety of stimuli beyond changes in membrane potential. Kv7 channels associate with KCNE proteins, contributing to the functional diversity of K^+ currents. The significance of these interactions is manifest in reports of genetic disorders such as the Long QT Syndrome, linked to KCNE mutations [12, 13]. The KCNE gene family also comprises five known members, *KCNE1* to *KCNE5* [12, 13]. KCNE regulatory subunits have been primarily studied in association with cardiac Kv7.1. Thus, the Kv7.1-KCNE1 interaction was identified as the molecular basis underlying the cardiac I_{ks} current. However, KCNE activity in the brain and in many other tissues is being increasingly recognized [12, 13]. Several KCNE proteins interact not only with Kv7.1, but also with other Kv7 members. While KCNE1 and KCNE2 have been shown to mainly function in the heart and KCNE3 functions in skeletal muscle, the roles of KCNE4 and KCNE5 are not yet understood [12, 13]. Although Kv7.5 is highly expressed in skeletal muscle, preliminary reports on the Kv7.5-KCNE interaction are contradictory and have argued against any physiological relevance because, at that time, the presence of most KCNEs in skeletal muscle was controversial [14, 15]. However, it is clear today that missense mutations of KCNE3 lead to the dysregulation of muscular excitability, triggering a form of hereditary Familial Periodic Paralysis [16].

In light of this, we aimed to study whether the co-expression of KCNE1-5 proteins can affect the characteristics of Kv7.5. We here describe that all five KCNE proteins are expressed in skeletal muscle, indicating that a physiological interaction with Kv7.5 may occur. However, only KCNE1 and KCNE3 alter the gating of the Kv7.5 channel in *Xenopus* oocytes and HEK-293 cells,. While KCNE1 slows activation and inhibits inward rectification, KCNE3 inhibits the current amplitude and differentially affects activation. Furthermore, KCNE1 increases Kv7.5 currents, when co-expressed in HEK cells. Our results have physiological relevance since Kv7.5 is involved during cell cycle progression in skeletal myoblasts [11], KCNE1 is induced in atrial tumors and germ cell neoplastic growth [5, 17], and KCNE3 is associated with skeletal muscle channelopathies [16].

Materials and Methods

RNA isolation and RT-PCR analysis

Total RNA from rat tissues (brain, heart, and skeletal muscle) and L6E9 cells was isolated using the Tripure reagent (Roche Diagnostics). All animal handling was approved by the ethics committee of the University of Barcelona. RNA was treated with DNaseI and PCR controls were performed in the absence of reverse transcriptase. cDNA synthesis was performed with transcriptor reverse transcriptase (Roche) with a random hexanucleotide and oligo dT, according to the manufacturer's instructions. Once cDNA was synthesized, the PCR conditions used were 94°C for 1 min, 1 min at the optimal annealing temperature (see Table 1 for temperatures and primers), and 72°C for 1 min. These settings were applied for 30 cycles. DNA from 10 µl of the total reaction was separated by gel electrophoresis in a 1.2% agarose 0.5X TBE (50 mM Tris, 50 mM boric acid, 1 mM EDTA, pH 8.0) gel.

Molecular Biology

Human Kv7.5 cDNA in the pTNL vector was kindly provided by T. Jentsch (Leibniz-Institut für Molekulare Pharmakologie and Max-Delbrück-Centrum für Molekulare Medizin, Berlin, Germany). Human KCNE1 and KCNE2 were obtained from S. de la Luna (Centro de Regulación Genómica-CRG, Barcelona, Spain) and were subcloned between the BamHI and XhoI sites and the BamHI and XbaI sites in the pXOOM vector, respectively. Human KCNE3 and KCNE5 in pXOOM were provided by J. Barhanin (Institut de Pharmacologie Moléculaire

Gene	Accession number	Sequence [a]	base pairs	length (bp)[b]	annealing (ºC)[c]
Kv7.5	XM_001071249	F: 5'-ACATGAAAGGCCATGTATACGC -3'	3061-3083		
		R: 5'-TATCCCGACATCTTCACACACC -3'	3240-3218	180	55
KCNE1	NM_000219	F: 5'-TGACAGCAAGCTGGAGGCTCT-3'	738-759		
		R: 5'-GCTTCAGAGCTTGCTATGTC -3'	949-929	211	50
KCNE2	NM_172201	F: 5'-GTCATCCTGTACCTCATGGT -3'	284-304		
		R: 5'-AAGGCCACCATCCATGAGAA -3'	478-458	194	60
KCNE3	NM_005472	F: 5'-CGTAATGACAACTCCTACATG -3'	441- 462		
		R: 5'-TAGTGACCCCTATCATGTGT -3'	568-548	126	60
KCNE4	NM_080671	F: 5'-TCCAGCAGCCCCCTTGAGTC-3'	138-158		
		R: 5'-CGGGAGAAGAAGTCCAGCCT-3'	295-275	157	55
KCNE5	NM_012282	F: 5'-CCCCTACCCCGCACATC -3'	789-806		
		R: 5'-GAACTGAATCCAACACGTCCAA -3'	896-874	107	55

Table 1. Genes, accession numbers, sequences of oligonucleotide primers, base pairs in the accession and cDNA length. [a] F, forward; R, reverse. [b] bp, base pair. [c] annealing PCR temperature

et Cellulaire, CNRS and Université de Nice Sophia Antipolis, Valbonne Sophia Antipolis, France). hKCNE4-pXOOM cDNA was obtained from M. Grunnet (Danish National Research Foundation Centre for Cardiac Arrhythmia, University of Copenhagen, Copenhagen, Denmark).

Channel expression and electrophysiology in Xenopus oocytes

After linearizing the cDNAs, the cRNAs were generated with T7 and SP6 RNA polymerase by using the mMESSAGE mMACHINE kit, according to the manufacturer's instructions (Ambion). Oocyte preparation was performed as described previously [18]. Stage V or VI oocytes were enzymatically defolliculated with collagenase (Sigma), 1 mg/ml in Ca^{2+}-free solution, in a solution containing, in mM, 82.5 NaCl, 2.5 KCl, 1 $MgCl_2$, and 5 HEPES, pH 7.5. They were then transferred to a Ca^{2+}-containing solution, ND96, consisting of, in mM, 96 NaCl, 2 KCl, 1.8 $CaCl_2$, 1 $MgCl_2$, and 5 HEPES, pH 7.5. The oocytes were injected with 50 nl of Kv7 or KCNE cRNA solution, containing 5 ng of Kv7.1 or Kv7.5, or 7.5 ng of a 1:0.5 mixture of Kv and KCNE in coexpression experiments. For unknown reasons, higher doses of some KCNEs killed oocytes, as has been previously described [19]. Oocytes were kept in ND96 buffer at 18ºC and used for recording two to four days after injection.

Whole-cell currents were recorded in oocytes at room temperature (22ºC) with a two-electrode voltage clamp using a virtual-ground Geneclamp 500B amplifier (Axon Instruments). Borosilicate electrodes were filled with 3 M KCl and had resistances of 1 MΩ. The oocytes were perfused continuously in *Xenopus* saline comprising, in mM, 100 NaCl, 2.5 KCl, 1 $MgCl_2$, 2 $MnCl_2$, and 5 HEPES, pH 7.5. All chemicals, except where otherwise stated, were from Sigma. Data were acquired at a sampling rate of 1 KHz and filtered at 100 Hz. Voltage-step protocols and current analysis were performed with pCLAMP 8.2 software (Axon Instruments). The voltage activation was determined as follows: oocytes were clamped for 3 s from a holding potential of -50 mV to voltages between -100 to +60 mV in 10 mV steps, and followed by a constant pulse to -20 mV of 1 s duration. The current activated at different voltage test pulses was estimated by measuring the amplitude of corresponding tail currents at -20 mV. For each oocyte, the current (I), was normalized relative to its maximal value. To evaluate the voltage dependence of potassium channels, the mean values of currents (±SE) were plotted versus voltage, and the I/V relationship was fitted to a Boltzmann function of the form:

$$I = I_{max}/[1 + \exp((V_{1/2}-V_m)/slope)],$$

where I_{max} is the maximal current and $V_{1/2}$ is the membrane potential (V_m) at which $I=I_{max}/2$. Fits were made by treating I_{max}, $V_{1/2}$ and slope as free parameters, and the best values of constants were obtained by applying an iterative procedure of fitting to minimize the least-squares error between the data and the calculated fit point. Data were normalized in Excel and plotted with SigmaPlot. For statistical evaluation, the unpaired Student's t-test was applied. A $p<0.05$ was considered significant.

Cell culture, transient transfection and electrophysiology in HEK-293 cells

HEK-293 cells were grown on poly-lysine-coated coverslips in DMEM medium containing 10% FBS with 10U/ml penicillin and streptomycin, and 2mM L-glutamine. Transient transfection was performed using Metafectene™Pro (Biontex) at nearly 80% confluence. Kv7.5 and KCNE cDNAs were used at 1:1 ratio. Two to three days after transfection, coverslips were transferred to a special chamber (Harvard Apparatus) mounted on the stage of an inverted microscope (Olympus IX-50) to perform the recordings. Whole cell currents were measured with an Axopatch-1D (Axon Instruments) amplifier using the patch clamp technique. WinWCP Strathclyde Whole Cell Program 3.8.2 (John Dempster, University of Strathclyde. U.K) was used for pulse generation, data acquisition and, subsequent analysis through a 1320A Axon Digidata A/D interface. After achieving the whole-cell configuration, currents were recorded at 2-10 KHz and low-pass filtered at 1-2 kHz

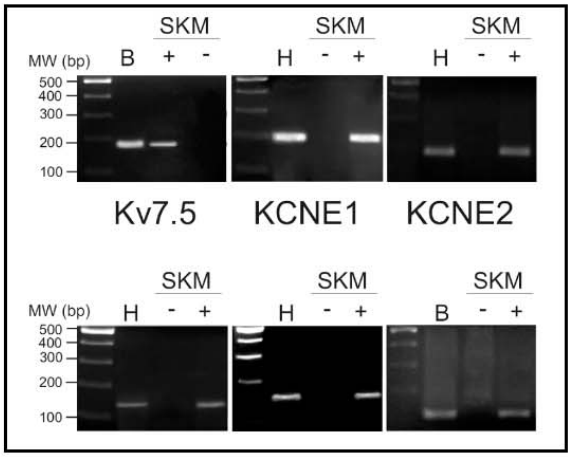

Fig. 1. Skeletal muscle expresses Kv7.5 and KCNE modulatory subunits. mRNA expression of Kv7.5 and KCNE modulatory subunits in skeletal muscle (SK) and tissues from adult rat. RNA from rat brain (B) and heart (H) was used as positive controls. PCR reactions were performed in the presence (+) or absence (-) of the retrotranscriptase reaction.

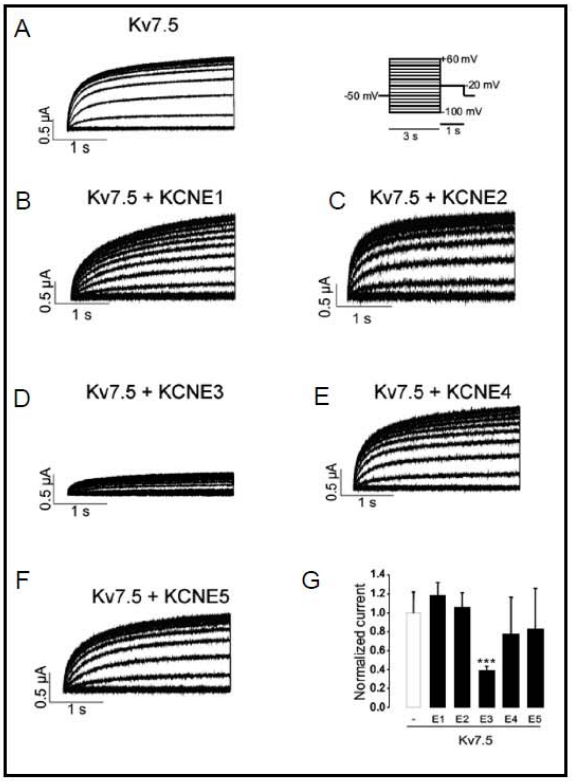

Fig. 2. KCNE subunit modulation of Kv7.5 currents. Voltage clamp recordings from Xenopus oocytes injected with cRNA encoding (A) Kv7.5 alone or (B-F) Kv7.5 and one of the five KCNE subunits. Oocytes were clamped for 3 s from a holding potential of -50 mV to voltages between -100 to +60 mV in 10 mV steps, followed by a constant pulse to -20 mV of 1 s duration, and then back to holding potential. The current activated at different voltage test pulses was estimated by measuring the amplitude of corresponding tail currents at -20 mV. (G) Mean current values of oocytes expressing either Kv7.5 (-) or Kv7.5 together with KCNE (1-5). Peak currents were measured at + 20 mV. Values are the mean ± SEM (n>12). ***, $p<0.001$ vs. Kv7.5 alone (-) by Student's *t*-test.

without leak substraction. Series resistance compensation was always above 70%. All experiments were performed at room temperature. Electrodes were fabricated from borosilicate glass capillaries (Harvard Apparatus) using a P-97 micropipette puller (Sutter Instruments) and fire polished. Pipettes had a resistance of 2-4 MΩ when filled with a solution containing (in mM): 120 KCl, 5.37 $CaCl_2$, 2 $MgCl_2$, 10 EGTA, 10 HEPES, 2 ATP (pH 7.2 by KOH). The extracellular solution contained (in mM): 140 NaCl, 4 KCl, 2 $CaCl_2$, 1 $MgCl_2$, 10 HEPES (pH 7.4 by NaOH). Cells were clamped to a holding potential of -90 mV. To evoke voltage-gated currents, all cells were stimulated with 2000-ms square pulses ranging from -80 to +60 mV in 10 mV steps. Traces were fitted with Sigma Plot 10.0 (SPSS Inc.).

Results and Discussion

Kv7.5 and KCNE peptides are coexpressed in skeletal muscle

The complexity of Kv7 channels may be further increased by their associations with KCNE modulatory subunits. Studies in heterologous expression systems have highlighted the wide variety of biophysically and pharmacologically distinct Kv7 channels that carry out diverse functions as key determinants of membrane excitability [16]. Kv7.5 is expressed in the brain, skeletal and vascular smooth muscle [7-10, 14, 15]. While Kv7.5 function has been evaluated in brain, where, in combination with Kv7.3, it contributes to neuronal excitability, its role in skeletal muscle is unknown [14, 15]. However, recent data in vascular smooth muscle identify Kv7.5 as target for vasoconstrictor signal transduction [7-10]. Kv7.5 is inhibited by M1 muscarinic receptor activation and shows pharmacological properties suggesting that it plays a role in generating M-like currents in different parts of the nervous system [20]. In muscle, we have recently described cell-cycle-dependent regulation of Kv7.5. Kv7.5 is induced prior to the S-phase and is involved in cell cycle progression [11]. Since Kv7

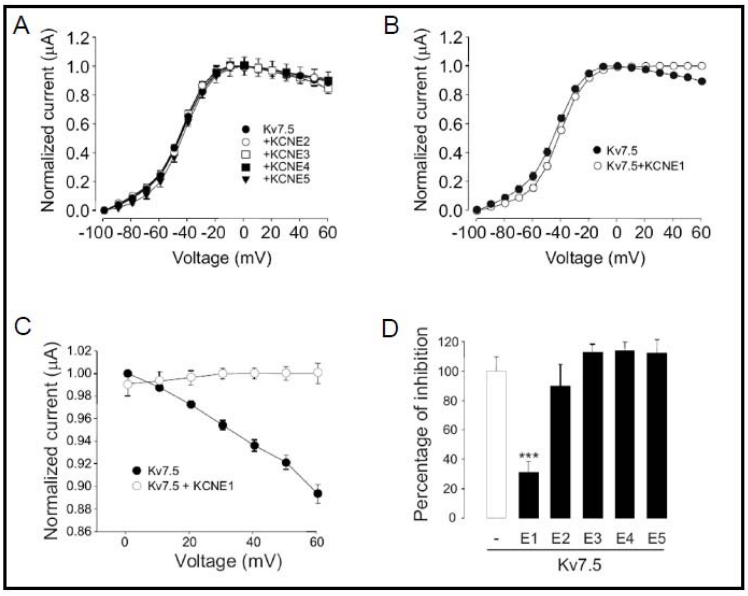

Fig. 3. Kv7.5 current-voltage relationships in the presence of KCNE subunits. (A) I-V relationships from Kv7.5 currents recorded in oocytes (n>12) in the presence or absence of KCNE2, KCNE3, KCNE4, or KCNE5. (B) Similar I-V relationships in the presence of KCNE1 (n=14). The pulse protocols are the same as in Figure 2. Current amplitudes were normalized to the maximum value. (C) I-V relationships from Kv7.5 currents in the presence or absence of KCNE1 following depolarizing pulses from 0 to +60 mV. Current amplitudes were normalized to the maximum value as in panels A and B. (D) Percentage of inward rectification at +60 mV from Kv7.5-injected oocytes in the presence (E1 to E5) or in the absence of KCNE (-). Values were normalized to 100% of inward rectification in the absence of KCNE (maximal Kv7.5 inward rectification at +60 mV). Values are the mean ± SEM of n>14 oocytes. ***, $p<0.001$ vs. Kv7.5 alone (-) by Student's *t*-test.

channels are tightly modulated upon association with KCNE subunits, we aimed to analyze how all five KCNE subunits modulate Kv7.5. The cloning of Kv7.5 was simultaneously described by two laboratories and preliminary KCNE coexpression data led to controversy [14, 15]. While Lerche et al. failed to detect evidence for functional interactions with KCNE peptides [14], Schroeder et al. argued against any physiological relevance of KCNE proteins in conjunction with Kv7.5 since KCNE1 is not present in the brain and had not yet been detected in skeletal muscle by northern blot analysis [15]. However, Lazdunski and coworkers found KCNE1 mRNA in mouse skeletal muscle by PCR [21]. Additionally, Figure 1 shows that Kv7.5 and KCNE subunits are present in rat skeletal muscle. Likewise, all five KCNE subunits are coexpressed with Kv7.5 in vascular smooth muscle [9].

Effects of KCNE subunits on Kv7.5 currents

The significance of Kv7.5-KCNE interactions is clear since these proteins are coexpressed in skeletal and smooth muscle and since KCNE peptides affect the gating of Kv channels. KCNE1 functions in the heart and ear, KCNE2 in the heart and stomach, and KCNE3 in the colon, ear, and skeletal muscle [12, 13]. Although roles for KCNE4 and KCNE5 are under investigation, KCNE5 is associated with AMME syndrome (Alport syndrome, mental retardation, midface hypoplasia, and elliptocytosis) [22]. Preliminary Kv7.5-KCNE studies have revealed important discrepancies between laboratories and a full characterization had not been undertaken [14, 15]. Therefore, we wanted to analyze whether Kv7.5 channels can be functionally modulated by KCNE accessory subunits. To that end, we undertook a complete analysis in *Xenopus* oocytes and HEK-293 cells. Since the modulation of Kv7 channels by KCNE accessory subunits is currently under investigation, we first controlled the effects of our KCNE constructs on Kv7.1 currents. As expected, KCNE subunits modulated Kv7.1 currents as previously described (not shown) [22-29]. Figure 2 illustrates representative K^+ current tracings and normalized peak-current densities obtained from Kv7.5-injected oocytes in the presence or the absence of KCNE. The electrophysiological analysis took place two to four days after injection, and no currents were detected in water-injected control oocytes (not shown). Kv7.5-injected oocytes yielded currents that needed several seconds to fully activate upon depolarization (Fig. 2 A). Activation of Kv7.5 ($V_{1/2}$, -46.7±1.6 mV; *k*, 11.8±0.8 mV) currents was in the range of previous works and generally faster than that of other Kv7 currents. Thus, the half-maximal activation of Kv7.5 was more negative than that of Kv7.2 (-37 mV), Kv7.4 (~11 mV), and Kv7.3/Kv7.5 heterotetramers (-35 mV), but in the range of that of Kv7.2/Kv7.3 (-40 mV) [6, 30-32]. Hyperpolarizing test pulses in Kv7.5-KCNE-injected oocytes failed to indicate relevant change in K^+ current amplitude with most KCNEs (Fig. 2B, C, E and F). However, coexpression with KCNE3 significantly suppressed more than 60% of Kv7.5 currents (Fig. 2 D and G). While Schroeder and

coworkers suggest similar results, Lerche et al. detected no evidence for a functional interaction [14, 15]. However, Schroeder et al. argued against any physiological significance due to the small magnitude of the effects [15]. Our results indicate that a 1:1 ratio (in kilobases) of KCNE3-Kv7.5 cRNA drastically inhibited Kv7.5. Similar inhibitory effects of KCNE3 have been also observed on Kv7.4 currents [31]. KCNE3 and Kv7.4 are coexpressed in the inner and outer hair cells of the inner ear, and a functional interaction may influence electrical excitability and cell survival [31, 33]. In addition, KCNE3 also modulates Kv members from other families. Thus, KCNE3 alters the gating of Kv3.4 and reduces Kv2.1 and Kv3.1 currents in the brain and skeletal muscle [16, 34]. Since KCNE3 turns out to be essential for regulating membrane potential in skeletal muscle [16], our results point to a functional interaction of this subunit with Kv7.5.

Tail current analysis was used to estimate activation parameters. Current-voltage relationships of Kv7.5 currents in the presence or absence of KCNE subunits are shown in Figure 3. Currents were activated at positive depolarizing potentials above -80 mV and displayed a "crossover" phenomenon that was observed at potentials greater than 0 mV and independent of current amplitudes (Fig. 3 A). This inward rectification [14] was suppressed in the presence of KCNE1 (Fig. 3 B). This KCNE1-dependent process is specific since similar results have also been observed with Kv7.1, but not Kv7.4 currents [31, 35]. Normalizing currents against test potentials showed that KCNE1 suppressed the inward rectification more than 70 % (Fig. 3 C and D), a phenomenon that may have physiological relevance. For instance, KCNE1 abundance increases during neoplastic growth in atrial and germinal tumours [5, 17]. To what extent a lack of inward rectification would support a sustained outward K^+ flux in proliferating cells is not known, but Kv7.5, which is induced during the G1/S phase of the myoblast cell cycle, may contribute to a transient hyperpolarization in cell cycle progression like other Kv channels [11, 36-38].

No important differences were observed in the half-maximal activation of Kv7.5 in the presence or absence of KCNE (Fig. 3A, B and Table 2). However, KCNE1 significantly shifted the $V_{1/2}$ to depolarised values (-42.4 ± 0.9 mV vs. -46.7 ± 1.6 mV, $p<0.05$) (Table 2). This depolarized shift is again shared with Kv7.1 [25, 26, 35]. In contrast, KCNE1 hyperpolarizes the half point of voltage-dependent activation of Kv7.4 [31]. This modulation of activation by KCNE1 seems specific to Kv7 channels since no significant differences for time constants of activation were found when KCNE1 was coexpressed with hERG, Kv3.1 and Kv3.2 channels [39, 40]. Similar to our findings, Schroeder et al. indicate that KCNE1 slowly activates Kv7.5, whereas Lerche et al. describe no such effects [14, 15]. Our results indicate that only KCNE1 and KCNE3 alter Kv7.5 currents.

	$V_{½}$ (mV)	Slope (k)
Kv7.5	-46.7 ± 1.6	11.8
Kv7.5 + KCNE1	-42.2 ± 0.9*	11.3
Kv7.5 + KCNE2	-46.4 ± 1.2	11.4
Kv7.5 + KCNE3	-45.9 ± 0.9	11.5
Kv7.5 + KCNE4	-45.1 ± 1.4	11.5
Kv7.5 + KCNE5	-44.0 ± 1.2	10.5

Table 2. Activation of Kv7.5 currents in the presence of KCNE subunits. Currents were evoked in Kv7.5-injected oocytes in the presence or absence of KCNE. Voltage for half-maximal activation ($V_{1/2}$) and slope values were calculated following the pulse protocol described in Figures 2 and 3. Values are the mean ± SEM of 10 to 15 oocytes. *, $p<0.05$ vs. Kv7.5, Student's t-test.

Next, we further analyzed the effects of these KCNE subunits on Kv7.5 activation at different voltages. Kv7.5 currents were evoked in the presence or absence of KCNE by 3 s depolarizing pulses at -30 mV (close to the $V_{1/2}$ of activation), 0 mV (peak current) and +60 mV (inward rectification). While KCNE1 slowed Kv7.5 activation at all voltages, KCNE3 exerts a crossover phenomenon (Fig. 4). KCNE3 accelerated activation at -30 mV and 0 mV, although it slowed the activation at +60 mV. No other KCNE subunits modified Kv7.5 activation (not shown). Similar KCNE1 and KCNE3 differential tuning occurs with other Kv members. KCNE1 slows Kv3.1 and Kv3.2 activation [40]. KCNE3 increases the activation time constants of Kv2.1, Kv3.1 and Kv3.2 [34, 40]. However, while KCNE3 exerts profound effects on Kv3.4 current has no significant effect on either Kv1.4 or Kv4.1 [16, 34, 40]. Since channel activation could be analysed by a sum of three exponential functions [15], traces evoked by 3 s depolarizing pulses at -30 mV, 0 mV and +60 mV were further analyzed (Table 3). For a step to -30mV, the presence of KCNE1 raised τ2 and τ3 rate constants, whereas KCNE3 significantly diminished τ1. A 0 mV step showed similar consequences. Thus, while KCNE1 slowed τ2 and τ3 activation constants, KCNE3 accelerated the activation at τ1 and τ2. At the +60 mV step, KCNE1 increased the activation constants τ2 and

	-30 mV			0 mV			+60 mV		
	τ1	τ2	τ3	τ1	τ2	τ3	τ1	τ2	τ3
Kv7.5	93.7±7	328±22	1561±104	66.9±4	307±14	1590±70	35.8±2	210±17	921±61
+ KCNE1	79.3±8	401±21*	1819±56*	72.8±3	350±15*	1930±62***	36.1±2	324±29**	1310±118**
+ KCNE2	79.4±13	332±12	1565±56	65±3	293±12	1579±52	32.1±2	207±14	848±36
+ KCNE3	69.4±9*	326±10	1777±81	50.2±2**	262±6*	1470±50	42.7±4	241±28	1235±109*
+ KCNE4	104.9±14	336±19	1813±115	65.1±2	268±12	1533±53	29.9±2	221±18	1053±85
+ KCNE5	111.2±14	309±18	1781±99	62.6±1	302±5	1526±51	31.2±2	211±13	1058±62

Table 3. Activation time constants of Kv7.5 in the presence of KCNE subunits. The voltage activation was determined by clamping the oocytes for 3 s from a holding potential of -50 mV to -30 mV, 0 mV and +60 mV, and followed by a constant pulse to -20 mV of 1 s duration. The current activated at different voltage test pulses was estimated by measuring the amplitude of corresponding tail currents at -20 mV. Time constants of activation were fit to the sum of three exponentials as described in the Materials and Methods. Values are the mean ± SEM of 10 to 15 oocytes. *, $p<0.05$; **, $p<0.01$; ***, $p<0.001$ vs. Kv7.5, Student's *t* test.

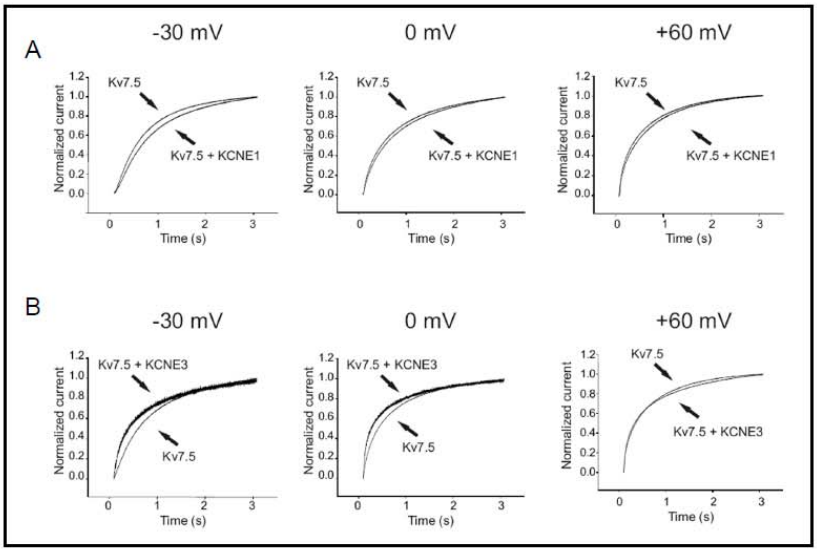

Fig. 4. KCNE1 and KCNE3 modulate Kv7.5 activation. Representative current traces from Kv.5-injected oocytes in the presence or absence of KCNE1 and KCNE3. Normalized current traces of experiments are the same as those used for Figure 2. Currents elicited by depolarizing pulses to -30 mV (left), 0 mV (center) and +60 mV (right) are shown. (A) KCNE1 slows Kv7.5 activation. (B) KCNE3 differentially shapes Kv7.5 activation. While KCNE3 accelerates activation at -30 mV and 0 mV, it slows activation at -60 mV.

τ3, and KCNE3 significantly raised the τ3 constant about 35%. In summary, KCNE1 and KCNE3 modulated the activation constants of Kv7.5. While KCNE1 tended to slow time constants, KCNE3 exerted a voltage-dependent differential modulation. This KCNE3-influenced pattern is probably the reason why Kv7.5 macroscopic currents behave similarly in the presence or absence of this subunit and why the half-maximal activation remained constant. Taking all together, our results would further support the discrete findings reported by Jentsch and coworkers [15].

We finally analyzed whether KCNE subunits modulated the deactivation time constant of Kv7.5 currents. Tail currents (see pulse protocol in Fig. 2) from -20 mV back to -50 mV (holding potential) were fitted to a single-exponential function. KCNE subunits exerted no modulation of the apparent deactivation of Kv7.5. Time constants of deactivation (in ms) were 181±9 for Kv7.5 alone and 227±22, 220±23, 216±18, 161±8 and 164±5 in the presence of KCNE1-5, respectively.

The biophysics of most ion channels has been characterized by functional expression in *Xenopus* oocytes. However, studies reveal discrepancies in channel properties between amphibian and mammalian expression systems suggesting that endogenous oocyte factors may regulate channel gating [13, 23, 29, 41, 42]. In fact, Abbott and co-workers demonstrated that oocytes may express some endogenous KCNE ancillary subunits [43]. Therefore, to further confirm our findings we co-expressed Kv7.5 and KCNE peptides in HEK-293 cells. Unlike in

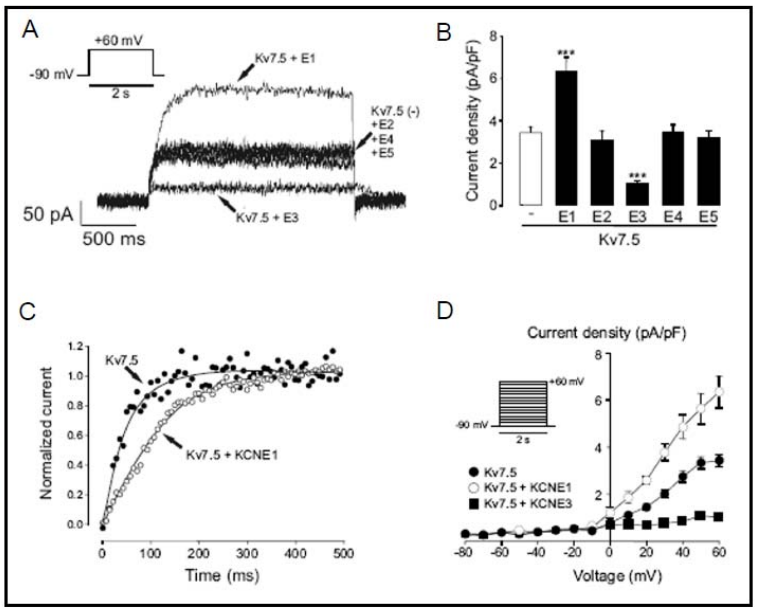

Fig. 5. KCNE1 and KCNE3 modulate Kv7.5 currents in HEK-293 cells. (A) Voltage-dependent K^+ currents were elicited by +60 mV depolarizing pulses in transiently transfected HEK-293 cells with Kv7.5 in the absence (-) or the presence of KCNE peptides. Representative traces are shown. (B) Current density of cells expressing either Kv7.5 (-) or Kv7.5 together with KCNE (E1-E5). Peak currents were measured at + 60 mV. Values are the mean ± SEM (n= 3-8). ***, $p<0.001$ vs. Kv7.5 alone (-) by Student's *t*-test. (C), Normalized traces, at +60 mV, of representative Kv7.5 currents in the absence (●) or the presence (○) of KCNE1. (D) I-V relationships from Kv7.5 currents recorded in HEK cells (n=4-8) in the absence (●) or presence of KCNE1 (○) and KCNE3 (■). Cells were clamped for 2 s from a holding potential of -90 mV to voltages between -80 to +60 mV in 10 mV steps. Current amplitudes were normalized to the cell capacitance.

oocytes, as previously demonstrated [8, 44], Kv7.5 conducted very low delayed-rectifier K^+ currents in mammalian cells (Fig. 5A), While KCNE1 increased the peak current density at +60 mV by 2-fold, KCNE3 inhibited the current by 75% (Fig. 5A and B). This result is in agreement with the effect of KCNE1 on Kv7.1, which is responsible for the cardiac I_{ks} current [25]. In addition, KCNE1 slowed the activation of Kv7.5 currents (Fig 5 C). Thus, τ for activation were 42±3 and 129±2 ms for Kv7.5 and Kv7.5/KCNE1 respectively ($p<0.001$, n=4-8) Again, the rest of KCNE subunits did not exert any effect. Unlike oocytes [14, 15], Kv7.5 currents in HEK cells showed no inward rectification at positive potentials [8] (Fig 5 D). However, the presence of KCNE1 clearly modulated the I/V curve (Fig 5 D). Overall our results in HEK cells further support those obtained in oocytes. The apparent discrepancy in the magnitude of current density and gating between *Xenopus* oocytes and the mammalian expression system could be explained by interactions with amphibian endogenous subunits [43]. This deserves further research.

Our results demonstrate that KCNE1 and KCNE3 modulate the gating of Kv7.5. These findings may be of physiological interest since both KCNE peptides and Kv7.5 are present in skeletal and vascular smooth muscle. While KCNE1 slowed activation and suppressed inward rectification, KCNE3 drastically inhibited the peak current amplitude. Unlike Kv7.4, KCNE1 exerts similar effects on Kv7.1 [31]. Skeletal muscle expresses Kv7.1 and Kv7.5, but not Kv7.4. It is tempting to speculate that KCNE1 would specifically partner with skeletal muscle Kv7 isoforms. In fact, proliferation increases Kv7.1 and Kv7.5 expression in myoblasts, and KCNE1 is up-regulated in atrial tumors and germ cell neoplastic growth [5, 11, 17]. Unlike activation or inward rectification, KCNE3 suppressed the Kv7.5 current amplitude. KCNE3 is a predominant skeletal muscle isoform that has been shown to be involved in periodic paralysis [16]. KCNE3 has drastic effects on Kv7.1 and inhibits other channels, such as Kv7.4 and the skeletal muscle isoforms of Kv2.1, Kv3.1 and Kv3.4 [31, 34, 40]. Therefore, this modulation should be taken into account when the role of Kv7.5 in skeletal muscle is contemplated.

Acknowledgements

This work was supported by the Ministerio Ciencia e Innovación (MICINN), Spain (BFU2005-00695, BFU2008-00431 to AF, and SAF2006-13450 to AV; and CSD2008-00005 to AF and AV). MR-F hold a fellowship from the Generalitat de Catalunya. A.E. was supported by a fellowship from the Basque Government. LS is a fellow from MICINN. NC is supported by the Juan de la Cierva program (MICINN). We thank the editorial assistance of American Journal Experts. NC, AV and AF contributed equally.

References

1 Hille B: Ion channels of excitable membranes. ed 3rd ed., Sunderland, Mass.; Great Britain, Sinauer, 2001.

2 Gutman GA, Chandy KG, Grissmer S, Lazdunski M, McKinnon D, Pardo LA, Robertson GA, Rudy B, Sanguinetti MC, Stuhmer W, Wang X: International Union of Pharmacology. LIII. Nomenclature and molecular relationships of voltage-gated potassium channels. Pharmacol Rev 2005;57:473-508.

3 Mackie AR, Byron KL: Cardiovascular KCNQ (Kv7) potassium channels: physiological regulators and new targets for therapeutic intervention. Mol Pharmacol 2008;74:1171-1179.

4 Miceli F, Soldovieri MV, Martire M, Taglialatela M: Molecular pharmacology and therapeutic potential of neuronal Kv7-modulating drugs. Curr Opin Pharmacol 2008;8:65-74.

5 Tsevi I, Vicente R, Grande M, Lopez-Iglesias C, Figueras A, Capella G, Condom E, Felipe A: KCNQ1/KCNE1 channels during germ-cell differentiation in the rat: expression associated with testis pathologies. J Cell Physiol 2005;202:400-410.

6 Wang HS, Pan Z, Shi W, Brown BS, Wymore RS, Cohen IS, Dixon JE, McKinnon D: KCNQ2 and KCNQ3 potassium channel subunits: molecular correlates of the M-channel. Science 1998;282:1890-1893.

7 Brueggemann LI, Moran CJ, Barakat JA, Yeh JZ, Cribbs LL, Byron KL: Vasopressin stimulates action potential firing by protein kinase C-dependent inhibition of KCNQ5 in A7r5 rat aortic smooth muscle cells. Am J Physiol Heart Circ Physiol 2007;292:H1352-1363.

8 Mani BK, Brueggemann LI, Cribbs LL, Byron KL: Opposite regulation of KCNQ5 and TRPC6 channels contributes to vasopressin-stimulated calcium spiking responses in A7r5 vascular smooth muscle cells. Cell Calcium 2009;45:400-411.

9 Yeung SY, Pucovsky V, Moffatt JD, Saldanha L, Schwake M, Ohya S, Greenwood IA: Molecular expression and pharmacological identification of a role for K(v)7 channels in murine vascular reactivity. Br J Pharmacol 2007;151:758-770.

10 Mackie AR, Brueggemann LI, Henderson KK, Shiels AJ, Cribbs LL, Scrogin KE, Byron KL: Vascular KCNQ potassium channels as novel targets for the control of mesenteric artery constriction by vasopressin, based on studies in single cells, pressurized arteries, and in vivo measurements of mesenteric vascular resistance. J Pharmacol Exp Ther 2008;325:475-483.

11 Roura-Ferrer M, Sole L, Martinez-Marmol R, Villalonga N, Felipe A: Skeletal muscle Kv7 (KCNQ) channels in myoblast differentiation and proliferation. Biochem Biophys Res Commun 2008;369:1094-1097.

12 Li Y, Um SY, McDonald TV: Voltage-gated potassium channels: regulation by accessory subunits. Neuroscientist 2006;12:199-210.

13 McCrossan ZA, Abbott GW: The MinK-related peptides. Neuropharmacology 2004;47:787-821.

14 Lerche C, Scherer CR, Seebohm G, Derst C, Wei AD, Busch AE, Steinmeyer K: Molecular cloning and functional expression of KCNQ5, a potassium channel subunit that may contribute to neuronal M-current diversity. J Biol Chem 2000;275:22395-22400.

15 Schroeder BC, Hechenberger M, Weinreich F, Kubisch C, Jentsch TJ: KCNQ5, a novel potassium channel broadly expressed in brain, mediates M-type currents. J Biol Chem 2000;275:24089-24095.

16 Abbott GW, Butler MH, Bendahhou S, Dalakas MC, Ptacek LJ, Goldstein SA: MiRP2 forms potassium channels in skeletal muscle with Kv3.4 and is associated with periodic paralysis. Cell 2001;104:217-231.

17 Felipe A, Knittle TJ, Doyle KL, Snyders DJ, Tamkun MM: Differential expression of Isk mRNAs in mouse tissue during development and pregnancy. Am J Physiol 1994;267:C700-705.

18 Villarroel A, Schwarz TL: Inhibition of the Kv4 (Shal) family of transient K+ currents by arachidonic acid. J Neurosci 1996;16:2522-2532.

19 Grunnet M, Rasmussen HB, Hay-Schmidt A, Rosenstierne M, Klaerke DA, Olesen SP, Jespersen T: KCNE4 is an inhibitory subunit to Kv1.1 and Kv1.3 potassium channels. Biophys J 2003;85:1525-1537.

20 Yus-Najera E, Munoz A, Salvador N, Jensen BS, Rasmussen HB, Defelipe J, Villarroel A: Localization of KCNQ5 in the normal and epileptic human temporal neocortex and hippocampal formation. Neuroscience 2003;120:353-364.

21 Lesage F, Attali B, Lazdunski M, Barhanin J: Developmental expression of voltage-sensitive K+ channels in mouse skeletal muscle and C2C12 cells. FEBS Lett 1992;310:162-166.

22 Piccini M, Vitelli F, Seri M, Galietta LJ, Moran O, Bulfone A, Banfi S, Pober B, Renieri A: KCNE1-like gene is deleted in AMME contiguous gene syndrome: identification and characterization of the human and mouse homologs. Genomics 1999;60:251-257.

23 Tapper AR, George AL, Jr.: MinK subdomains that mediate modulation of and association with KvLQT1. J Gen Physiol 2000;116:379-390.

24 Wang Q, Curran ME, Splawski I, Burn TC, Millholland JM, VanRaay TJ, Shen J, Timothy KW, Vincent GM, de Jager T, Schwartz PJ, Toubin JA, Moss AJ, Atkinson DL, Landes GM, Connors TD, Keating MT: Positional cloning of a novel potassium channel gene: KVLQT1 mutations cause cardiac arrhythmias. Nat Genet 1996;12:17-23.

25 Sanguinetti MC, Curran ME, Zou A, Shen J, Spector PS, Atkinson DL, Keating MT: Coassembly of K(V)LQT1 and minK (IsK) proteins to form cardiac I(Ks) potassium channel. Nature 1996;384:80-83.

26 Barhanin J, Lesage F, Guillemare E, Fink M, Lazdunski M, Romey G: K(V)LQT1 and lsK (minK) proteins associate to form the I(Ks) cardiac potassium current. Nature 1996;384:78-80.

27 Schroeder BC, Waldegger S, Fehr S, Bleich M, Warth R, Greger R, Jentsch TJ: A constitutively open potassium channel formed by KCNQ1 and KCNE3. Nature 2000;403:196-199.

28 Grunnet M, Jespersen T, Rasmussen HB, Ljungstrom T, Jorgensen NK, Olesen SP, Klaerke DA: KCNE4 is an inhibitory subunit to the KCNQ1 channel. J Physiol 2002;542:119-130.

29 Grunnet M, Olesen SP, Klaerke DA, Jespersen T: hKCNE4 inhibits the hKCNQ1 potassium current without affecting the activation kinetics. Biochem Biophys Res Commun 2005;328:1146-1153.

30 Biervert C, Schroeder BC, Kubisch C, Berkovic SF, Propping P, Jentsch TJ, Steinlein OK: A potassium channel mutation in neonatal human epilepsy. Science 1998;279:403-406.

31 Strutz-Seebohm N, Seebohm G, Fedorenko O, Baltaev R, Engel J, Knirsch M, Lang F: Functional coassembly of KCNQ4 with KCNE-beta-subunits in Xenopus oocytes. Cell Physiol Biochem 2006;18:57-66.

32 Wickenden AD, Zou A, Wagoner PK, Jegla T: Characterization of KCNQ5/Q3 potassium channels expressed in mammalian cells. Br J Pharmacol 2001;132:381-384.

33 de Castro MP, Aranega A, Franco D: Protein distribution of Kcnq1, Kcnh2, and Kcne3 potassium channel subunits during mouse embryonic development. Anat Rec A Discov Mol Cell Evol Biol 2006;288:304-315.

34 McCrossan ZA, Lewis A, Panaghie G, Jordan PN, Christini DJ, Lerner DJ, Abbott GW: MinK-related peptide 2 modulates Kv2.1 and Kv3.1 potassium channels in mammalian brain. J Neurosci 2003;23:8077-8091.

35 Pusch M, Magrassi R, Wollnik B, Conti F: Activation and inactivation of homomeric KvLQT1 potassium channels. Biophys J 1998;75:785-792.

36 Felipe A, Vicente R, Villalonga N, Roura-Ferrer M, Martinez-Marmol R, Sole L, Ferreres JC, Condom E: Potassium channels: new targets in cancer therapy. Cancer Detect Prev 2006;30:375-385.

37 Vicente R, Escalada A, Coma M, Fuster G, Sanchez-Tillo E, Lopez-Iglesias C, Soler C, Solsona C, Celada A, Felipe A: Differential voltage-dependent K+ channel responses during proliferation and activation in macrophages. J Biol Chem 2003;278:46307-46320.

38 Villalonga N, Martinez-Marmol R, Roura-Ferrer M, David M, Valenzuela C, Soler C, Felipe A: Cell cycle-dependent expression of Kv1.5 is involved in myoblast proliferation. Biochim Biophys Acta 2008;1783:728-736.

39 Abbott GW, Sesti F, Splawski I, Buck ME, Lehmann MH, Timothy KW, Keating MT, Goldstein SA: MiRP1 forms IKr potassium channels with HERG and is associated with cardiac arrhythmia. Cell 1999;97:175-187.

40 Lewis A, McCrossan ZA, Abbott GW: MinK, MiRP1, and MiRP2 diversify Kv3.1 and Kv3.2 potassium channel gating. J Biol Chem 2004;279:7884-7892.

41 Tinel N, Diochot S, Borsotto M, Lazdunski M, Barhanin J: KCNE2 confers background current characteristics to the cardiac KCNQ1 potassium channel. Embo J 2000;19:6326-6330.

42 Bendahhou S, Marionneau C, Haurogne K, Larroque MM, Derand R, Szuts V, Escande D, Demolombe S, Barhanin J: In vitro molecular interactions and distribution of KCNE family with KCNQ1 in the human heart. Cardiovasc Res 2005;67:529-538.

43 Gordon E, Roepke TK, Abbott GW: Endogenous KCNE subunits govern Kv2.1 K+ channel activation kinetics in Xenopus oocyte studies. Biophys J 2006;90:1223-1231.

44 Dupuis DS, Schroder RL, Jespersen T, Christensen JK, Christophersen P, Jensen BS, Olesen SP: Activation of KCNQ5 channels stably expressed in HEK293 cells by BMS-204352. Eur J Pharmacol 2002;437:129-137.

3.1.7. Resum de la contribució 3

Publicat en Muscle Nerve, 2012, 45:48-54.

Localització dels canals Kv7.5 (KCNQ5) als microdominis de la membrana plasmàtica

Meritxell Roura-Ferrer, Laura Solé, Anna Oliveras, Álvaro Villarroel, Nuria Comes, Antonio Felipe

Els canals Kv7.5 (KCNQ5) participen en les corrents de potassi tipus M en el cervell, s'expressen en múscul esquelètic i contribueixen al to de la musculatura vascular.

En el present treball es va co-expressar el canal Kv7.5 i les subunitats reguladores KCNE1-3 en cèl·lules HEK-293 i es va analitzar la seva associació mitjançant experiments d'electrofisiologia i co-immunoprecipitació. També es va analitzar els seu tràfic utilitzant la microscòpia confocal, i es va examinar la localització dels complexes oligomerics en microdominis de membrana rics en esfingolípids i colesterol aïllant els *lipid raft*. Posteriorment, es va avaluar la dinàmica de membrana dels complexes mitjançant la tecnologia de *Fluorescence Recovery After Photobleaching* (FRAP).

Hem pogut observar com Kv7.5 forma canals oligomèrics específicament amb KCNE1 i KCNE3. El percentatge de Kv7.5 que es localitza en microdominis de membrana rics en colesterol és molt baix. Malgrat això, quan es co-expressa Kv7.5 amb KCNE1 o KCNE3, s'observa com el canal deixa de localitzar-se en *lipid rafts*. També s'observa com l'associació amb Kv7.5 altera l'expressió de la subunitat KCNE3 en aquests microdominis.

Els nostres resultats indiquen que Kv7.5 contribueix a la regulació espacial de KCNE3. Aquest nou escenari podria ser important a la hora de determinar la rellevància fisiològica de possibles interaccions de KCNE3 en la musculatura i el sistema nerviós.

3.1.8. Report of the PhD student participation in the article

Informe de la participació de la doctoranda en l'article

Targeting of Kv7.5 (KCNQ5)/KCNE channels to surface microdomains of cell membranes.

Published Muscle and Nerve, **Impact Factor (2011): 2.37**

Laura Solé Codina performed the experiments and the data analysis related to the confocal co-localization experiments and the FRAP experiments.

Laura Solé Codina ha realitzat els experiments i l'anàlisi de les dades corresponents relatives als experiments de co-localització mitjançant microscopia confocal i els experiments de FRAP.

Thesis director

El director de la tesi

Dr. Antonio Felipe Campo

TARGETING OF Kv7.5 (KCNQ5)/KCNE CHANNELS TO SURFACE MICRODOMAINS OF CELL MEMBRANES

MERITXELL ROURA-FERRER, MD,[1,2] LAURA SOLÉ, MSc,[1] ANNA OLIVERAS, MSc,[1] ALVARO VILLARROEL, PhD,[2] NÚRIA COMES, PhD,[1] and ANTONIO FELIPE, PhD[1]

[1] Molecular Physiology Laboratory, Departament de Bioquímica i Biologia Molecular, Institut de Biomedicina (IBUB), Universitat de Barcelona, Avenida Diagonal 645, E-08028 Barcelona, Spain

[2] Unidad de Biofísica, Centro Mixto Consejo Superior de Investigaciones Científicas–Universidad del País Vasco/Euskal Herriko Unibertsitatea (UPV/EHU), Leioa, Spain

Accepted 5 July 2011

ABSTRACT: Background: Kv7.5 (KCNQ5) channels conduct M-type potassium currents in the brain, are expressed in skeletal muscle, and contribute to vascular muscle tone. Methods: We coexpressed Kv7.5 and KCNE1–3 peptides in HEK293 cells and then analyzed their association using electrophysiology and co-immunoprecipitation, assessed localization using confocal microscopy, examined targeting of the oligomeric channels to cholesterol-rich membrane surface microdomains using lipid raft isolation, and evaluated their membrane dynamics using fluorescence recovery after photobleaching (FRAP). Results: Kv7.5 forms oligomeric channels specifically with KCNE1 and KCNE3. The expression of Kv7.5 targeted to cholesterol-rich membrane surface microdomains was very low. Oligomeric Kv7.5/KCNE1 and Kv7.5/KCNE3 channels did not localize to lipid rafts. However, Kv7.5 association impaired KCNE3 expression in lipid raft microdomains. Conclusions: Our results indicate that Kv7.5 contributes to the spatial regulation of KCNE3. This new scenario could greatly assist in determining the physiological relevance of putative KCNE3 interactions in nerve and muscle.
Muscle Nerve **45:** 48–54, 2012

Voltage-dependent potassium channels (Kv) establish the resting membrane potential and modulate the duration of action potentials in nerve and muscle. Many Kv genes are expressed in excitable and non-excitable tissues, reflecting their wide participation in essential cellular processes.[1] The Kv7 (*KCNQ*) family encodes important K^+ neuronal currents, including the M current, produced by homomeric and heteromeric associations of different related isoforms.[2,3] The Kv7 family consists of five members (Kv7.1–Kv7.5), each encoded by single genes that generate slowly activating K^+-selective channels. Mutations in four genes (*KCNQ1–KCNQ4*) give rise to human genetic disorders, establishing the physiological relevance of this family.[2,3] In addition to their role in the nervous system, Kv7.1 and Kv.7.5 have been related to important muscle functions.[4,5] Kv7.1 was first identified in the heart and, when it is associated with the β-regulatory subunit KCNE1, it conducts the cardiac I_{ks} current.[6] Similarly, Kv7.5 is involved in the maintenance of vascular muscle tone.[5,7]

The diversity of Kv channels has been greatly increased by their assembly with regulatory subunits. The Kv7 family forms oligomeric channels in association with KCNE peptides, contributing to the functional diversity of K^+ currents.[8,9] The KCNE family is composed of five members (KCNE1–5).[8] These small, single-transmembrane peptides modulate gating, traffic, and surface expression of many Kv family members.[9–11] The physiological relevance of Kv7/KCNE is highlighted by KCNE mutations related to important human disorders such as cardiopathies and deafness.[8] Whereas Kv7.1/KCNE interactions have been studied widely, KCNE associations with Kv7.5 are comparatively unknown.

Kv7.1 and Kv7.5 are expressed in muscle and share regulation during myoblast proliferation.[12–14] Some KCNE subunits, which are also present in muscle, may modulate Kv7.1 and Kv7.5 currents and localization.[11,15,16] Specifically, we recently showed that KCNE1 and KCNE3 modulated Kv7.5 activity in both amphibian and mammalian expression systems.[15] In addition, KCNE subunits differentially influence Kv7.1 traffic and membrane surface localization in lipid raft microdomains.[16] Because KCNE mutations impair Kv7.1 traffic and activity,[17,18] the influence of KCNE subunits on Kv7.5 is of physiological interest.

In this study, we describe specific KCNE1 and KCNE3 associations with Kv7.5. Contrary to what is currently known about Kv7.1, Kv7.5 was barely detected in lipid rafts. Although oligomeric Kv7.5/KCNE associations did not alter Kv7.5 raft location, KCNE3 was targeted away from rafts in the presence of Kv7.5. This shift in KCNE3 location in the presence of Kv7.5 may have physiological consequences that have yet to be defined in nerve and muscle.

METHODS

Expression Plasmids. Human Kv7.5 cDNA in the pTPN vector was provided by T. Jentsch (Leibniz-Institut für Molekulare Pharmakologie and Max-Delbrück-Centrum für Molekulare Medizin, Berlin,

Abbreviations: CBD, caveolin-binding domain; CFP, cyan fluorescent protein; CSD, caveolin-scaffolding domain; DMEM, Dulbecco's modified Eagle's medium; EDTA, ethylene-diamine tetraacetic acid; EGTA, ethylene-glycol tetraacetic acid; FBS, fetal bovine serum; FRAP, fluorescence recovery after photobleaching; GFP, green fluorescent protein; Kv; voltage-dependent potassium channels; PBS, phosphate-buffered saline; ROI, region of interest; SDS-PAGE, sodium dodecylsulfate–polyacrylamide gel electrophoresis; YFP, yellow fluorescent protein

Key words: KCNE, Kv7.5, lipid rafts, potassium channels, regulatory subunits

Correspondence to: A. Felipe; e-mail: afelipe@ub.edu

© 2011 Wiley Periodicals, Inc.

Published online in Wiley Online Library (wileyonlinelibrary.com). DOI 10.1002/mus.22231

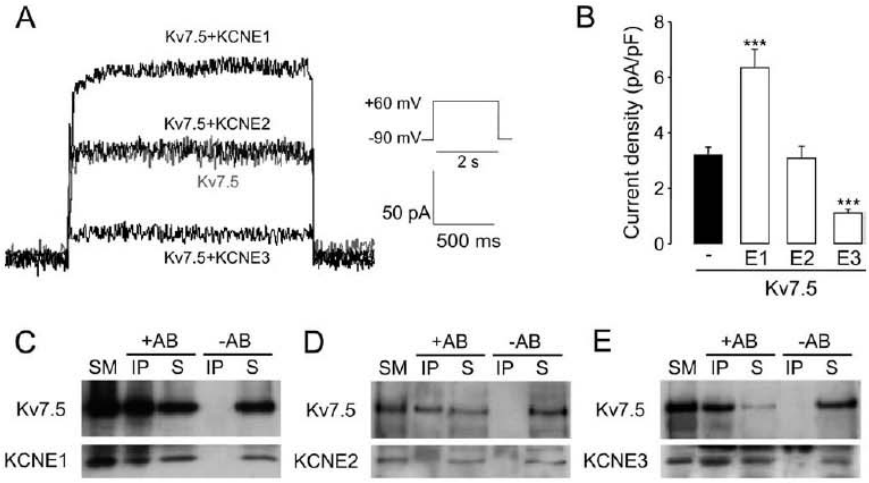

FIGURE 1. KCNE1 and KCNE3 associate with Kv7.5 to form oligomeric channels. (**A**) Voltage-dependent K^+ currents elicited by +60-mV depolarizing pulses in transiently transfected HEK293 cells with Kv7.5 in the absence (gray) or presence (black) of KCNE peptides. Representative traces are shown. (**B**) Current density of cells expressing either Kv7.5 alone (−) or Kv7.5 together with KCNEs (E1–E3). Peak currents measured at + 60 mV (mean ± SEM, $n = 4$–8). $^{***}P < 0.001$ vs. Kv7.5 alone (−). (**C–E**) KCNE1 and KCNE3, but not KCNE2, co-immunoprecipitate with Kv7.5. HEK cells transiently transfected with Kv7.5–CFP and KCNE1–3–HA. Top panels: Kv7.5 immunoprecipitation demonstrated by IP using anti-GFP antibody and immunoblotting against anti-Kv7.5. Bottom panels: KCNE co-immunoprecipitations demonstrated by IP using anti-GFP antibody and immunoblotting against anti-HA. (**C**) Kv7.5–CFP/KCNE1–HA. (**D**) Kv7.5–CFP/KCNE2–HA. (**E**) Kv7.5–CFP/KCNE3–HA. Labels: SM, starting material; IP, immunoprecipitated; S, immunoprecipitated supernatant; +AB, immunoprecipitation in the presence of GFP antibody; −AB, immunoprecipitation in the absence of antibody.

Germany) and subcloned in pCDNA3. Human KCNE1 and KCNE2 in pHA vectors were obtained from S. de la Luna (Centro de Regulación Genómica, Barcelona, Spain) and were subcloned into the pXOOM vector. Human KCNE3 in pXOOM was provided by J. Barhanin (Institut de Pharmacologie Moléculaire et Cellulaire, CNRS, and Université de Nice Sophia Antipolis, Valbonne Sophia Antipolis, France). To evaluate expression, proteins were also cloned into pEYFP and pECFP (Clontech). All constructs were verified by sequencing.

Cell Culture and Transient Transfection. HEK293 cells were grown in Dulbecco modified Eagle medium (DMEM) containing 10% fetal bovine serum (FBS) and supplemented with 10 U/ml penicillin/streptomycin. For confocal and electrophysiology studies, cells grown in polylysine-coated coverslips at nearly 80% confluence were transiently transfected using Metafectene Pro (Biontex). For microscopy, 24 hours after transfection, cells were washed in phosphate-buffered saline (PBS), fixed with 4% paraformaldehyde in PBS for 10 min, and mounted with Aqua Poly/Mount (Polysciences, Inc.).

Protein Extraction, Co-Immunoprecipitation, and Western Blot. At 24 h after transfection, cells were lysed in 1% Triton X-100, 50 mmol/L Tris (pH 7.2), 150 mmol/L NaCl, 1 mmol/L ethylenediamine tetraacetic acid (EDTA) supplemented with 1 μg/ml aprotinin, 1 μg/ml leupeptin, 1 μg/ml pepstatin, and 1 mM phenylmethylsulfonyl fluoride. Homogenates were centrifuged at 3000*g* for 10 min, and the supernatant was aliquoted and stored at −20°C.

For co-immunoprecipitation, samples were precleared with protein G–Sepharose beads with gentle mixing. The beads were removed by centrifugation at 1000*g* for 30 s at 4°C. The sample was incubated overnight with the desired antibody (4 ng/μg protein) at 4°C. Protein G–Sepharose (30 μl) was added to each sample for 4 h at 4°C. The beads were removed, washed four times in NGH buffer [50 mM HEPES, 150 mM NaCl, 1% Triton X-100, 10% glycerol (pH 7.2)] and resuspended in 70 μl of sodium dodecylsulfate (SDS) sample buffer.

Protein samples (50 μg) and immunoprecipitates were boiled in Laemmli SDS loading buffer and separated using 10% SDS–polyacrylimide gel electrophoresis (SDS-PAGE). Samples were transferred to nitrocellulose membranes (Immobilon-P; Millipore) and blocked in 5% dry milk with 0.05% Tween-20 in PBS before immunoreactions. Membranes were immunoblotted with antibodies against green fluorescent protein (GFP; 1:1000; Roche) or KCNQ5 (1:500; A. Villarroel). Anti–pan-caveolin antibody was used as a marker of lipid raft fractions (1:1000; BD Transduction Laboratories), and anti-clathrin antibody was used to characterize non-floating fractions (1:1000; Chemicon).

Lipid Raft Isolation. Low-density Triton-insoluble complexes were isolated as previously described[16]

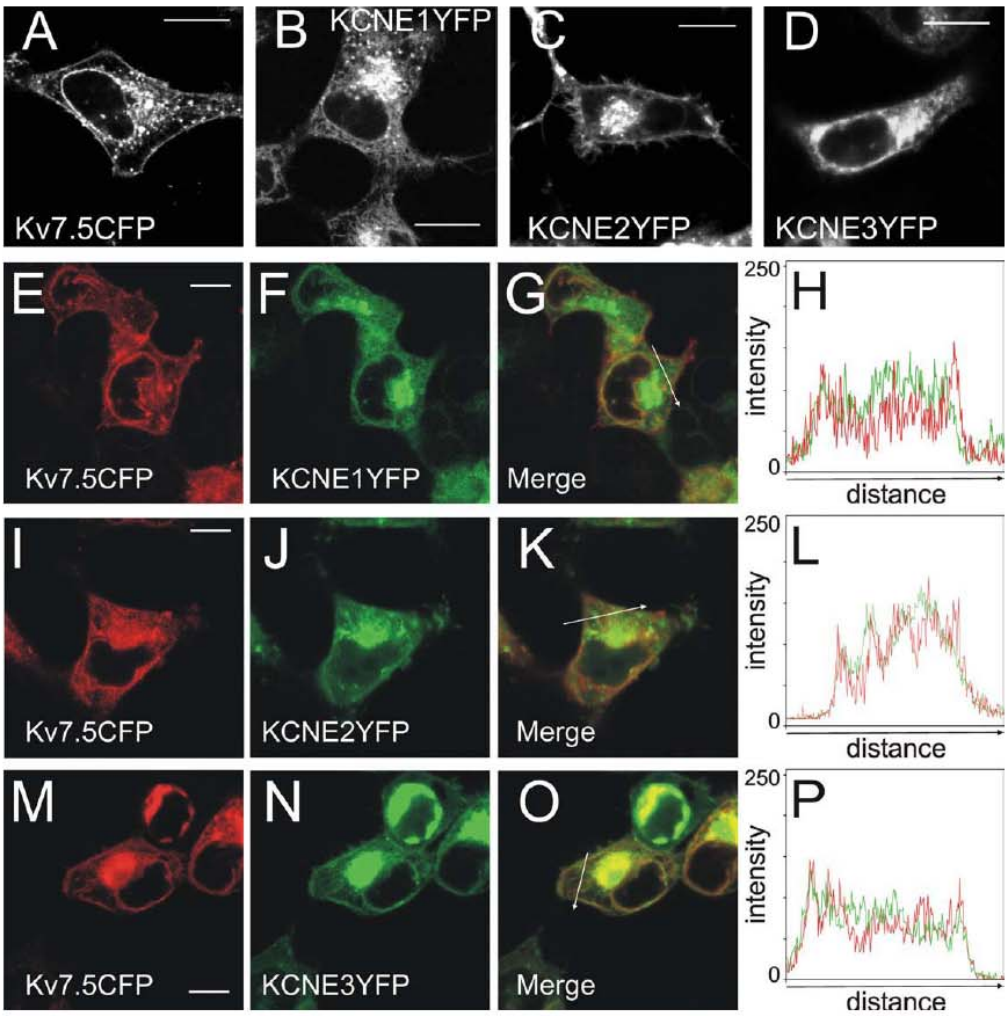

FIGURE 2. Kv7.5 colocalizes with KCNE1–3 subunits. HEK293 cells transiently transfected with Kv7.5–CFP (**A**) and KCNE1–3–YFP (**B–D**). (**E–P**) Cells double-transfected with Kv7.5–CFP and KCNE1–3–YFP. Red panels show Kv7.5–CFP (**E, I, M**). Green panels depict KCNE peptides (**F, J, N**). Merged panels show colocalization in yellow (**G, K, O**). (**H, L, P**) Histograms of pixel-by-pixel analysis of section indicated by arrows in the merged panels (**G**), (**K**), and (**O**), respectively. Red: Kv7.5; green: KCNEs. Bars = 10 μm. [Color figure can be viewed in the online issue, which is available at wileyonlinelibrary.com.]

from HEK cells transiently transfected with Kv7.5–cyan fluorescent protein (CFP) or double-transfected with Kv7.5–CFP/KCNEs–yellow fluorescent protein (YFP). Cells were homogenized in 1 ml of 1% Triton X-100, and sucrose was added to a final concentration of 40%. A 5–30% linear sucrose gradient was layered on top and centrifuged (39,000 rpm) for 20–22 h at 4°C in a rotor (SW41TI; Beckman). Gradient fractions (1 ml) were collected from the top, and a 50-μl sample was analyzed by Western blot.

Confocal Microscopy and FRAP. Fluorescence recovery after photobleaching (FRAP) experiments were performed 1 day after transfection at 37°C. Time series were taken with 20 scans before bleaching, which was accomplished by 20 iterations of bleaching with 100% laser power of the 514-nm line, followed by 100 scans every 0.36 s and 100 scans every second (2.5 min in total) of the bleached region with 6% laser power. In each cell, a circular region of interest (ROI) was bleached (n = 20 cells per group). Fluorescence intensity was normalized to the pre-bleach intensity and mobile fraction, and recovery time was calculated as previously described.[10,16] Data are expressed as mean ± SEM. Statistical analysis was performed using the Student t-test (GraphPad Prism).

For image processing, the percentage of colocalization was calculated using a pixel-by-pixel analysis of confocal images.

Electrophysiology. Kv7.5 and KCNE cDNAs were used at a 1:1 ratio.[15] Transiently transfected

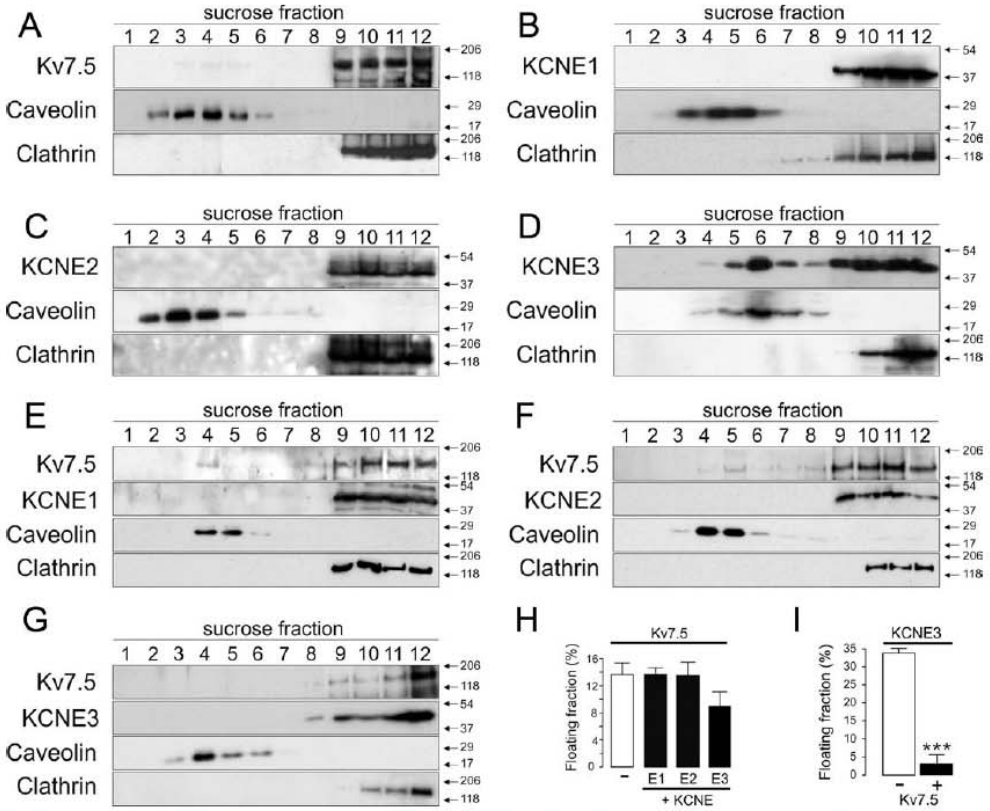

FIGURE 3. Kv7.5 and KCNE1–3 targeting to surface microdomains. Cells transfected with Kv7.5–CFP (**A**), KCNE1–YFP (**B**), KCNE2–YFP (**C**), or KCNE3–YFP (**D**). Sucrose density gradient fractions of HEK-transfected cells isolated and blotted against anti-GFP, caveolin, and clathrin. (**E–G**) HEK293 cells double-transfected with Kv7.5–CFP and KCNE1–3–YFP. (**E**) Sucrose density gradient fractions of Kv7.5/KCNE1. (**F**) Sucrose fractions of Kv7.5/KCNE2. (**G**) Fractions of Kv7.5/KCNE3. (**H**) Percentage of Kv7.5 relative abundance in floating fractions in the absence (−, white bar) and presence (+, black bars) of KCNE1–3. (**I**) Percentage of KCNE3 relative abundance in floating fractions in the absence (−, white bar) and presence (+, black bar) of Kv7.5. Values are expressed as mean ± SEM ($n = 4$). $^{***}P < 0.001$ vs. absence (−) of Kv7.5.

HEK293 cells grown on polylysine-coated coverslips were used 2–3 days after transfection. Whole-cell currents were measured with an Axopatch-1D (Axon Instruments) amplifier using the patch-clamp technique. The WinWCP Strathclyde Whole Cell Program, version 3.8.2 (John Dempster, University of Strathclyde, UK), was used for pulse generation, data acquisition, and subsequent analysis through an interface (1320A; Axon Digidata A/D). After achieving the whole-cell configurations, currents were recorded at 2–10 kHz and low-pass filtered at 1–2 kHz without leak subtraction. Series resistance compensation was always >70%. All experiments were performed at room temperature. Electrodes were fabricated from borosilicate glass capillaries (Harvard Apparatus) using a micropipette puller (P-97; Sutter Instruments) and fire polished. Electrode resistance was 2–4 MΩ when filled with a solution containing (in mM) 120 KCl, 5.37 $CaCl_2$, 2 $MgCl_2$, 10 ethylene-glycol tetraacetic acid (EGTA), 10 HEPES; and 2 adenosine triphosphate (ATP) (pH 7.2 by KOH). The extracellular solution contained (in mM) 140 NaCl, 4 KCl, 2 $CaCl_2$, 1 $MgCl_2$, and 10 HEPES (pH 7.4 by NaOH). The experimental junction potential was close to 0 mV, and therefore no corrections were applied. Cells were clamped at a holding potential of −90 mV. To evoke currents, cells were stimulated with 2000-ms square pulses at +60 mV. Traces were fitted with SigmaPlot, version 10.0 (SPSS, Inc.). Current density (pA/pF) at +60 mV is expressed as mean ± SEM. Statistical analysis was performed using the Student *t*-test (GraphPad Prism).

RESULTS

Among all KCNE peptides (not shown), only KCNE1 and KCNE3 regulate Kv7.5 gating. Figure 1 confirms and extends previous data[15] showing that, although KCNE1 and KCNE3 increased and decreased Kv7.5 currents, respectively, KCNE2 did not exert any effect (Fig. 1A and B). The putative association of KCNE1 and KCNE3, but not KCNE2, with Kv7.5 was further supported by co-immunoprecipitation (Fig. 1C–E). Our data

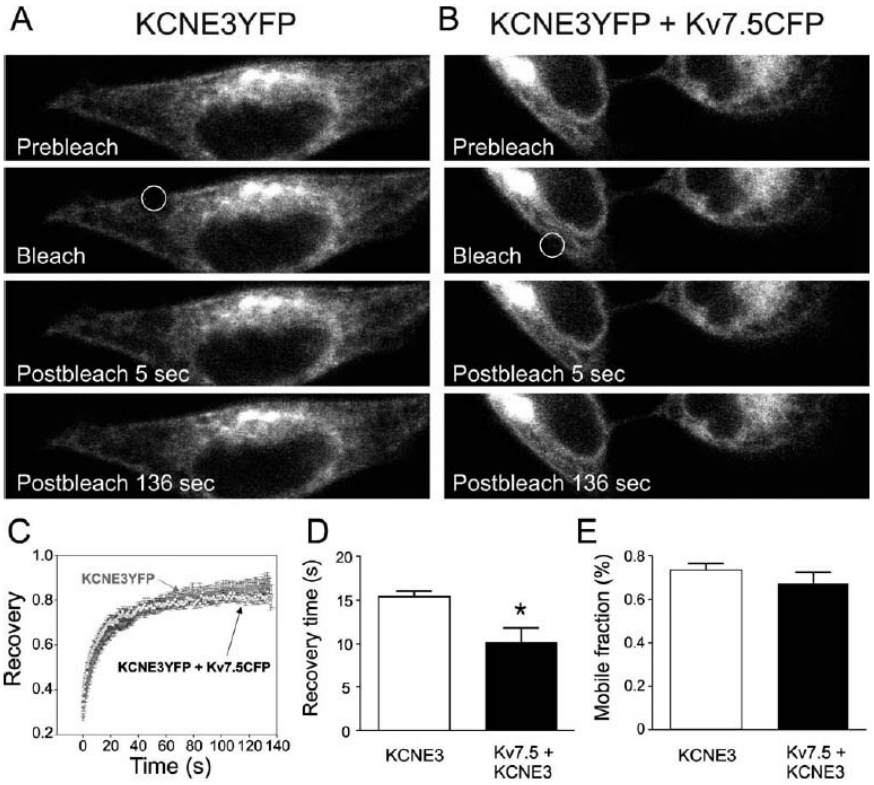

FIGURE 4. FRAP of KCNE3 and Kv7.5/KCNE3. Representative images of the KCNE3–YFP intensities at different time-points. Circles indicate regions of interest. (**A**) KCNE3. (**B**) Kv7.5/KCNE3. (**C**) Graphs of the average intensity from KCNE3 (gray circles) and Kv7.5/KCNE3 (white circles) ($n = 20$). (**D**) Recovery time was calculated as the time constant ($t_{1/2}$) of KCNE3 in the absence (white bar) or presence (black bar) of Kv7.5 (*$P < 0.05$ vs. absence of Kv7.5). (**E**) Mobile fraction as a percentage of KCNE3 in the absence (white bar) and presence (black bar) of Kv7.5. Values expressed as mean ± SEM ($n = 20$).

suggest that only KCNE1 and KCNE3 can interact with Kv7.5 to form oligomeric complexes in nerve and muscle.

Next, we further characterized the phenotype of this interaction by studying the traffic of Kv7.5 in the presence and absence of KCNE1–3. Kv7.5 and KCNE2 stained more cell surface than KCNE1 and KCNE3 (Fig. 2A–D). When Kv7.5 was coexpressed with all three KCNE regulatory peptides, Kv7.5 colocalized with KCNEs (65 ± 5%, 62 ± 9%, and 74 ± 3% for KCNE1, KCNE2, and KCNE3, respectively) whether they associated or not (Fig. 2E–P).

The membrane surface localization of ion channels attracts considerable attention.[16] Therefore, we first studied the targeting of individually expressed Kv7.5 and KCNE1–3 subunits to lipid raft microdomains. Kv7.5 alone is barely detected in low-buoyant sucrose fractions (Fig. 3A). In addition, KCNE1 and KCNE2 alone localize to out-of-raft microdomains (Fig. 3B and C). However, KCNE3 alone targeted to floating sucrose fractions (Fig. 3D). Although the coexpression of Kv7.5 with KCNE1–3 generated no apparent changes in the lipid raft localization of Kv7.5, KCNE1, and KCNE2, it displaced KCNE3 (Fig. 3E–G). Whereas the amount of Kv7.5 protein in rafts was not significantly modified (Fig. 3H), the abundance of KCNE3 peptide was reduced in the presence of Kv7.5 (Fig. 3I). This was further confirmed by FRAP (Fig. 4). Although the presence of KCNE3 did not change the recovery time or the mobile fraction of Kv7.5 (not shown), the recovery time of KCNE3 decreased in the presence of Kv7.5 (15.3 ± 0.7 s vs. 10.2 ± 1.6 s; $P < 0.05$; $n = 20$).

DISCUSSION

Kv7.5 was the last cloned and least characterized member of the Kv7 family.[12,14] It was isolated from brain, but its expression in skeletal muscle is abundant.[12–15] Although Kv7.5 and heteromeric Kv7.5/Kv7.3 channels contribute to the M current in the brain, no such current has been isolated in muscle.[12,14] Similar to Kv7.1/KCNE1 oligomers, this could indicate that KCNE peptides interact with Kv7.5 and increase the diversity of K^+ currents.[15] We demonstrated that only KCNE1 and KCNE3 regulate Kv7.5 channels. The modulation of

KCNE1 and KCNE3 peptides on Kv7 channels is quite variable. Whereas KCNE1 increases the activity of Kv7.1, Kv7.4, and Kv7.5, the effects are the opposite for Kv7.2/Kv7.3 currents.[6,19,20] The effects of KCNE3 on Kv7 channels are also diverse. KCNE3 association generates a rapidly activating voltage-independent Kv7.1 channel.[8,11,21] However, similar to Kv7.4, the presence of KCNE3 led to a decrease in Kv7.5 currents.[19]

We found that KCNE2 had better membrane targeting than KCNE1 and KCNE3.[16,22,23] There is no clear explanation for this trafficking. Although KCNE3 contains a canonical RXR (RSR, residues 81–83) endoplasmic reticulum retention signal, KCNE2 has a putative RR (residues 76–77) yet KCNE1 does not. Therefore, other, yet to be identified, molecular determinants must be involved. Once at the membrane surface, many ion channels target to lipid raft microdomains. These structures concentrate signaling molecules, and therefore the targeting of ion channels to raft domains has emerged as a novel mechanism of ion channel regulation.[24,25] Despite endocrine signals, such as β-adrenergic and nitric oxide synthase activation, known to regulate Kv7 channels localized in rafts,[26] only limited information about Kv7 and KCNEs is available. Low-buoyancy density fractions from cardiac and heterologous expression samples suggest that oligomeric Kv7.1/KCNE1 and Kv7.1/KCNE2 channels localize in lipid rafts.[16,27,28] However, unlike Kv7.1 and KCNE3, individually KCNE1 and KCNE2 peptides localize to out-of-raft microdomains.[16] Therefore, Kv7.1/KCNE1 and Kv7.1/KCNE2 oligomeric associations are responsible for targeting both regulatory peptides back to rafts. We found that, unlike Kv7.1, Kv7.5 was barely detected in cholesterol-enriched domains and, although the coexpression of Kv7.5 with KCNE1–3 generated no apparent changes in the lipid raft localization of Kv7.5, KCNE1, and KCNE2, the raft targeting of KCNE3 was impaired. Therefore, similar to what was observed with Kv7.1/KCNE3,[16] the association of Kv7.5 with KCNE3 triggered an out-of-raft displacement of the regulatory peptide. Taken together, our results suggest that Kv7.5 and Kv7.1 act as a modulator mechanism controlling the localization of KCNE3.

Our results were obtained by heterologous expression in HEK293 cells. Therefore, it is unknown to what extent the spatial regulation of Kv7.1/KCNE3 and Kv7.5/KCNE3 channels is physiologically relevant in muscle or nerve. However, because the targeting of ion channels to raft microdomains is crucial for cardiac function,[24,29] the localization of KCNE3 may be important for putative interactions with other channels, such as Kv2.1, Kv3.1, and Kv3.4, which are essential in muscle and brain.[30,31] Caveolae, specialized lipid rafts, contain caveolins as scaffolding proteins.[32] The deficiency of caveolins results in inherited human diseases.[24] Caveolins, which contain a caveolin-scaffolding domain (CSD) adjacent to the plasma membrane, interact with target proteins through caveolin-binding domains (CBDs; e.g., ΦXXXXΦXXΦ), which are rich in aromatic residues (Φ).[32] Unlike other KCNEs, KCNE3 has a putative, although backward, CBD located in the transmembrane segment (YILFVMFLF, residues 60–68), next to the TVG signature (amino acids 71–73) that interacts with Kv7 channels.[33] It is tempting to speculate that KCNE3 interacts with caveolin through this CBD, but Kv7.5 competing for the same region displaces the caveolin binding. In a previous report, however, we were unable to confirm an association between KCNE3 and caveolin-1.[16] The physiological relevance of the spatial regulation of ion channels in specific membrane surface microdomains remains unknown. Therefore, further studies to identify the molecular determinants of KCNE3 and, by extension, Kv7 and other KCNE proteins, are needed.

M.R.-F. and L.S. contributed equally to this work. The authors thank M. Calvo (Unitat de Microscòpia Confocal, Serveis Científico-tècnics, Facultat de Medicina, Universitat de Barcelona) for the confocal microscopy experiments. We also thank American Journal Experts for editorial assistance. This study was supported by the Ministerio de Ciencia e Innovación (MICINN), Spain (BFU2008-00431, BFU2011-23268, and CSD2008-00005 to A.F). M.R.-F. held a fellowship from the Generalitat de Catalunya. L.S. and A.O. are fellows from MICINN. N.C. is supported by the Juan de la Cierva program (MICINN).

REFERENCES

1. Hille B. Ion channels of excitable membranes. Sunderland, MA: Sinauer; 2001. 814 p.
2. Brown DA, Passmore GM. Neural KCNQ (Kv7) channels. Br J Pharmacol 2009;156:1185–1195.
3. Jentsch TJ. Neuronal KCNQ potassium channels: physiology and role in disease. Nat Rev Neurosci 2000;1:21–30.
4. Greenwood IA, Ohya S. New tricks for old dogs: KCNQ expression and role in smooth muscle. Br J Pharmacol 2009;156:1196–1203.
5. Mackie AR, Byron KL. Cardiovascular KCNQ (Kv7) potassium channels: physiological regulators and new targets for therapeutic intervention. Mol Pharmacol 2008;74:1171–1179.
6. Barhanin J, Lesage F, Guillemare E, Fink M, Lazdunski M, Romey G. K(V)LQT1 and lsK (minK) proteins associate to form the I (Ks) cardiac potassium current. Nature 1996;384:78–80.
7. Yeung SY, Pucovsky V, Moffatt JD, Saldanha L, Schwake M, Ohya S, et al. Molecular expression and pharmacological identification of a role for K(v)7 channels in murine vascular reactivity. Br J Pharmacol 2007;151:758–770.
8. Abbott GW, Goldstein SA. Potassium channel subunits encoded by the KCNE gene family: physiology and pathophysiology of the MinK-related peptides (MiRPs). Mol Interv 2001;1:95–107.
9. Li Y, Um SY, McDonald TV. Voltage-gated potassium channels: regulation by accessory subunits. Neuroscientist 2006;12:199–210.
10. Sole L, Roura-Ferrer M, Perez-Verdaguer M, Oliveras A, Calvo M, Fernandez-Fernandez JM, et al. KCNE4 suppresses Kv1.3 currents by modulating trafficking, surface expression and channel gating. J Cell Sci 2009;122:3738–3748.
11. McCrossan ZA, Abbott GW. The MinK-related peptides. Neuropharmacology 2004;47:787–821.
12. Lerche C, Scherer CR, Seebohm G, Derst C, Wei AD, Busch AE, et al. Molecular cloning and functional expression of KCNQ5, a potassium channel subunit that may contribute to neuronal M-current diversity. J Biol Chem 2000;275:22395–22400.

13. Roura-Ferrer M, Sole L, Martinez-Marmol R, Villalonga N, Felipe A. Skeletal muscle Kv7 (KCNQ) channels in myoblast differentiation and proliferation. Biochem Biophys Res Commun 2008;369: 1094–1097.
14. Schroeder BC, Hechenberger M, Weinreich F, Kubisch C, Jentsch TJ. KCNQ5, a novel potassium channel broadly expressed in brain, mediates M-type currents. J Biol Chem 2000;275:24089–24095.
15. Roura-Ferrer M, Etxebarria A, Sole L, Oliveras A, Comes N, Villarroel A, et al. Functional implications of KCNE subunit expression for the Kv7.5 (KCNQ5) channel. Cell Physiol Biochem 2009;24:325–334.
16. Roura-Ferrer M, Sole L, Oliveras A, Dahan R, Bielanska J, Villarroel A, et al. Impact of KCNE subunits on KCNQ1 (Kv7.1) channel membrane surface targeting. J Cell Physiol 2010;225:692–700.
17. Krumerman A, Gao X, Bian JS, Melman YF, Kagan A, McDonald TV. An LQT mutant minK alters KvLQT1 trafficking. Am J Physiol Cell Physiol 2004;286:C1453–1463.
18. Seebohm G, Strutz-Seebohm N, Ureche ON, Henrion U, Baltaev R, Mack AF, et al. Long QT syndrome-associated mutations in KCNQ1 and KCNE1 subunits disrupt normal endosomal recycling of IKs channels. Circ Res 2008;103:1451–1457.
19. Strutz-Seebohm N, Seebohm G, Fedorenko O, Baltaev R, Engel J, Knirsch M, et al. Functional coassembly of KCNQ4 with KCNE-beta-subunits in *Xenopus* oocytes. Cell Physiol Biochem 2006;18:57–66.
20. Yang WP, Levesque PC, Little WA, Conder ML, Ramakrishnan P, Neubauer MG, et al. Functional expression of two KvLQT1-related potassium channels responsible for an inherited idiopathic epilepsy. J Biol Chem 1998;273:19419–19423.
21. Robbins J. KCNQ potassium channels: physiology, pathophysiology, and pharmacology. Pharmacol Ther 2001;90:1–19.
22. Chandrasekhar KD, Bas T, Kobertz WR. KCNE1 subunits require co-assembly with K+ channels for efficient trafficking and cell surface expression. J Biol Chem 2006;281:40015–40023.
23. Um SY, McDonald TV. Differential association between HERG and KCNE1 or KCNE2. PLoS One 2007;2:e933.
24. Maguy A, Hebert TE, Nattel S. Involvement of lipid rafts and caveolae in cardiac ion channel function. Cardiovasc Res 2006;69:798–807.
25. Martens JR, O'Connell K, Tamkun M. Targeting of ion channels to membrane microdomains: localization of KV channels to lipid rafts. Trends Pharmacol Sci 2004;25:16–21.
26. Callera GE, Montezano AC, Yogi A, Tostes RC, Touyz RM. Vascular signaling through cholesterol-rich domains: implications in hypertension. Curr Opin Nephrol Hypertens 2007;16:90–104.
27. Balijepalli RC, Delisle BP, Balijepalli SY, Foell JD, Slind JK, Kamp TJ, et al. Kv11.1 (ERG1) K+ channels localize in cholesterol and sphingolipid enriched membranes and are modulated by membrane cholesterol. Channels (Austin) 2007;1:263–272.
28. Nakamura H, Kurokawa J, Bai CX, Asada K, Xu J, Oren RV, et al. Progesterone regulates cardiac repolarization through a nongenomic pathway: an in vitro patch-clamp and computational modeling study. Circulation 2007;116:2913–2922.
29. O'Connell KM, Martens JR, Tamkun MM. Localization of ion channels to lipid raft domains within the cardiovascular system. Trends Cardiovasc Med 2004;14:37–42.
30. Abbott GW, Butler MH, Bendahhou S, Dalakas MC, Ptacek LJ, Goldstein SA. MiRP2 forms potassium channels in skeletal muscle with Kv3.4 and is associated with periodic paralysis. Cell 2001;104: 217–231.
31. McCrossan ZA, Lewis A, Panaghie G, Jordan PN, Christini DJ, Lerner DJ, et al. MinK-related peptide 2 modulates Kv2.1 and Kv3.1 potassium channels in mammalian brain. J Neurosci 2003;23:8077–8091.
32. Couet J, Li S, Okamoto T, Ikezu T, Lisanti MP. Identification of peptide and protein ligands for the caveolin-scaffolding domain. Implications for the interaction of caveolin with caveolae-associated proteins. J Biol Chem 1997;272:6525–6533.
33. Bett GC, Morales MJ, Beahm DL, Duffey ME, Rasmusson RL. Ancillary subunits and stimulation frequency determine the potency of chromanol 293B block of the KCNQ1 potassium channel. J Physiol 2006;576:755–767.

3.2. Block 2:

KCNE4 modulation of Kv1.3

3.2.1. Resum de la contribució 4

Publicat en J Cell Sci, 2009,122:3738-48.

KCNE4 suprimeix les corrents de Kv1.3 modulant el tràfic, l'expressió en superfície i la cinètica del canal.

Laura Solé, Meritxell Roura-Ferrer, Mireia Pérez-Verdaguer, Anna Oliveras, Maria Calvo, José Manuel Fernández-Fernández, Antonio Felipe

Els canals de potassi dependents de voltatge (Kv) juguen un paper molt important en l'activació i proliferació leucocitària. S'ha descrit com els canals Kv poden ser homo- o hetero-oligomers. La composició del canal modula la seva expressió a superfície i és un exemple dels mecanismes que existeixen per a regular l'activitat dels canals. La interacció dels Kv amb subunitats reguladores incrementa la variabilitat per a respondre de manera diferent enfront a canvis en el potencial de membrana. En aquest treball, demostrem com KCNE4, però no KCNE2, funciona com a parella inhibidora del canal Kv1.3 en leucòcits. El tràfic, la localització i l'activitat del canal Kv1.3 són alterats per la presència de KCNE4. Demostrem com KCNE4 disminueix la densitat de corrent, alenteix l'activació, accelera la inactivació i augmenta la inactivació cumulativa del canal. A més a més, KCNE4 reté el canal Kv1.3 en el reticle endoplasmàtic i dificulta la localització del canal als microdominis de membrana *lipid rafts*. KCNE4 s'associa amb Kv1.3 en el reticle endoplasmàtic i disminueix el nombre de canals presents a la superfície cel·lular, fet que fa disminuir la excitabilitat cel·lular. Kv1.3 i KCNE4 són regulats de manera diferencial enfront l'activació o immunosupressió de macròfags. Així per exemple, l'activació induïda per lipopolisacàrid augmenta tant els nivells de mARN de Kv1.3 com KCNE4, mentre que el tractament amb dexametasona genera una disminució en Kv1.3, sense afectar als nivells de KCNE4. La composició del canalosoma determina la activitat i afecta l'expressió en superfície i localització dels canals en la membrana. Per aquest motiu, creiem que l'associació amb KCNE4 pot jugar un paper principal en el control de la resposta immunològica. Els nostres resultats indiquen que les subunitats reguladores podrien esdevenir noves dianes per a la immunomodulació.

3.2.2. Report of the PhD student participation in the article

Informe de la participació de la doctoranda en l'article

KCNE4 suppresses Kv1.3 currents by modulating trafficking, surface expression and channel gating.

Published in Journal of Cell Science, **Impact Factor (2009): 6.14**

Laura Solé Codina performed all the experiments of this paper except electrophysiological recordings and the Kv1.3 mRNA analysis expression in macrophages.

Laura Solé Codina ha realitzat tots els experiments d'aquest article excepte els experiments d'electrofisiologia i l'anàlisi de l'expressió de mRNA Kv1.3 en macròfags.

Thesis director

El director de la tesi

Dr. Antonio Felipe Campo

3738 Research Article

KCNE4 suppresses Kv1.3 currents by modulating trafficking, surface expression and channel gating

Laura Solé[1], Meritxell Roura-Ferrer[*,1], Mireia Pérez-Verdaguer[1], Anna Oliveras[1], Maria Calvo[2], José Manuel Fernández-Fernández[3] and Antonio Felipe[1,‡]

[1]Molecular Physiology Laboratory, Departament de Bioquímica i Biologia Molecular, Institut de Biomedicina (IBUB), Universitat de Barcelona, Avda. Diagonal 645, 08028 Barcelona, Spain
[2]Departament de Biologia Cel·lular, Institut d'Investigacions Biomèdiques August Pi i Sunyer, Universitat de Barcelona, 08036 Barcelona, Spain
[3]Laboratory of Molecular Physiology and Channelopathies, Departament de Ciències Experimentals i de la Salut, Universitat Pompeu Fabra, Dr Aiguader 88, 08003, Barcelona, Spain
*Present address: Unidad de Biofísica, CSIC-UPV/EHU, Universidad del País Vasco, Barrio Sarriena s/n, 48940 Leioa, Spain
‡Author for correspondence (afelipe@ub.edu)

Accepted 9 August 2009
Journal of Cell Science 122, 3738-3748 Published by The Company of Biologists 2009
doi:10.1242/jcs.056689

Summary

Voltage-dependent potassium channels (Kv) play a crucial role in the activation and proliferation of leukocytes. Kv channels are either homo- or hetero-oligomers. This composition modulates their surface expression and serves as a mechanism for regulating channel activity. Kv channel interaction with accessory subunits provides mechanisms for channels to respond to stimuli beyond changes in membrane potential. Here, we demonstrate that KCNE4 (potassium voltage-gated channel subfamily E member 4), but not KCNE2, functions as an inhibitory Kv1.3 partner in leukocytes. Kv1.3 trafficking, targeting and activity are altered by the presence of KCNE4. KCNE4 decreases current density, slows activation, accelerates inactivation, increases cumulative inactivation, retains Kv1.3 in the ER and impairs channel targeting to lipid raft microdomains. KCNE4 associates with Kv1.3 in the ER and decreases the number of Kv1.3 channels at the cell surface, which diminishes cell excitability. Kv1.3 and KCNE4 are differentially regulated upon activation or immunosuppression in macrophages. Thus, lipopolysaccharide-induced activation increases Kv1.3 and KCNE4 mRNA, whereas dexamethasone triggers a decrease in Kv1.3 with no changes in KCNE4. The channelosome composition determines the activity and affects surface expression and membrane localization. Therefore, KCNE4 association might play a crucial role in controlling immunological responses. Our results indicate that KCNE ancillary subunits could be new targets for immunomodulation.

Key words: KCNE regulatory subunits, Kv1.3, Leukocytes, Trafficking, Channelosome, Surface expression

Introduction

Voltage-dependent potassium channels (Kvs) play a crucial role in excitable cells by determining resting membrane potential and controlling action potentials (Hille, 2001). In addition, they are also involved in the immune system response. The activation and proliferation of leukocytes occurs via regulation of transmembrane ion fluxes, and increasing evidence indicates that some signaling occurs through K^+ channels. Thus, changes in the membrane potential are among the earliest events that occur upon stimulation of leukocytes, and K^+ channels underlie the Ca^{2+} signal involved in activation (Lewis and Cahalan, 1995; Cahalan et al., 2001; Panyi et al., 2004a).

The Kv1.3 channel (also known as KCNA3) is involved in the maintenance of the resting membrane potential in cells involved in the immune system, and several studies point to this protein as an excellent target for immunomodulation (Chandy et al., 2004; Beeton et al., 2005). Altered Kv1.3 expression is associated with autoimmune diseases such as multiple sclerosis, rheumatoid arthritis, psoriasis and type I diabetes, and Kv1.3-based therapies are effective in experimental models (Chandy et al., 2004; Beeton and Chandy, 2005; Beeton et al., 2006; Wulff and Pennington, 2007). In leukocytes, which express a restricted voltage-dependent K^+ current phenotype, Kv1.3 is considered the major channel. However, we previously demonstrated that Kv1.3-Kv1.5 heteromeric channels contribute to the major K^+ current in the myeloid lineage (Vicente et al., 2006; Villalonga et al., 2007). In this scenario, the oligomeric structure of the Kv1.3 channelosome when associated with other partners could be involved a wide variety of physiological activities and immunological functions. Assigning specific K^+ channel clones to native currents is often difficult as this complexity is enhanced by the presence of ancillary subunits. The interaction of Kv channels with Kvβ modulatory subunits provides a mechanism for channels to respond to a variety of stimuli beyond changes in membrane potential (Martens et al., 1999; Li et al., 2006).

In addition to Kvβ regulatory subunits, KCNE peptides, which have been widely studied in association with Kv7.1 and Kv11.1 cardiac channels, contribute to the functional diversity of K^+ currents (McCrossan and Abbott, 2004). These interactions have been shown to be important in genetic disorders such as long QT syndrome, which are linked to KCNE mutations (Abbott and Goldstein, 2001; Abbott and Goldstein, 2002). The *KCNE* gene family comprises five known members, *KCNE1* to *KCNE5*. KCNE peptides can assemble promiscuously, yielding a wide variety of biophysically distinct channels (McCrossan and Abbott, 2004). Thus, cardiac Kv1.5 coimmunoprecipitates with KCNE1 and KCNE2 and the absence of *kcne2* gene modifies the slow component of the delayed rectifying K^+ current (I_{Kslow}) in the heart (Melman et al., 2004; Roepke et al., 2008). In addition, KCNE3 alters the gating of Kv3.4 and reduces Kv2.1 and Kv3.1 currents in the brain and skeletal muscle (Abbott et al., 2001; McCrossan et al., 2003;

Lewis et al., 2004). Finally, KCNE4 inhibits Kv1.1 and Kv1.3 currents (Grunnet et al., 2003). However, there is no evidence of their physical association, and contradictory results (Deschenes and Tomaselli, 2002; McCrossan et al., 2009) have raised doubts about the specificity of these modulatory actions without further analysis.

Several lines of evidence indicate that post-translational events are involved in leukocyte Kv1.3 regulation. Recently, there has been much interest in channel targeting to the membrane that defines the protein microenvironment. Membrane microdomains (lipid rafts) rich in cholesterol and sphingolipids function as platforms on which signal transduction pathways interface. Multiple Kv channels have affinities for lipid rafts and different isoforms are targeted to distinct lipid microdomains (Martens et al., 2004; Maguy et al., 2006). In this context, Kv1.3 is targeted to raft domains involved in immunological synapses in T-cells (Panyi et al., 2004b), but the association of Kv1.3 and Kv1.5 in macrophages alters trafficking and targeting. However, pro-inflammatory activation targets Kv1.3 back to lipid rafts (Martinez-Marmol et al., 2008; Vicente et al., 2008). These determinants affect the expression and functional properties of the channels and contribute to the diversity of K^+ channels in leukocytes. Because KCNE peptides control gating and the surface expression of channels, we aimed to investigate whether KCNE4 associates with Kv1.3 to control channel expression. KCNE4, but not KCNE2, acts as a dominant negative Kv1.3 partner. Kv1.3 trafficking, targeting and activity are dramatically altered by the presence of KCNE4. Our results demonstrate, for the first time, that members of the Kv1 family (*Shaker*) associate with KCNE peptides, altering their surface expression and trafficking. Different K^+ channel subunit compositions could lead to specific alteration in cellular excitability, thus determining specific cell responses. Therefore, the identification of the components of the channelosome and their regulation are essential for their possible use as therapeutic targets. The present report points to KCNE ancillary subunits as new targets in immunomodulation.

Results

KCNE4 modifies Kv1.3 gating and trafficking

HEK293 cells transfected with Kv1.3-YFP exhibited outward K^+ currents at depolarizing potentials (Fig. 1A). The presence of KCNE4-CFP inhibited the peak current density. In addition, macroscopic currents suggested that KCNE4, but not KCNE2, modified the activation and inactivation kinetics. Unlike KCNE2, KCNE4 decreased the current density at all depolarized voltages by more than 50% (Fig. 1B). However, the threshold for activation was similar (–30 mV). Fig. 1C shows that KCNE4 slowed the activation time constant (τ) in all depolarized pulses. No currents were observed when depolarized pulses were applied to KCNE4- and KCNE2-transfected HEK293 cells (not shown).

Kv1.3 exhibits defined characteristics such as cumulative inactivation and C-type inactivation (Grissmer et al., 1990; Grissmer et al., 1994). KCNE4 increased the percentage and rate of cumulative inactivation of Kv1.3 (Fig. 1D). Kv1.3 exhibited 40% cumulative inactivation, but this value increased to 75% in the presence of KCNE4. In addition, cumulative inactivation, in the presence of KCNE4, occurred quickly and reached a plateau within the first 3 seconds (Fig. 1E). As expected from Fig. 1A, C-type inactivation was accelerated by KCNE4 (Fig. 1F). The effects of KCNE4 were specific because no changes were observed in the presence of KCNE2 (not shown).

Although KCNE4 inhibited Kv1.3 currents, changes in gating are not indicative of physiological interactions (Deschenes and Tomaselli, 2002; McCrossan et al., 2009). Therefore, we analyzed whether KCNE4 associates with Kv1.3. Fig. 2 demonstrates that KCNE4, but not KCNE2, retained Kv1.3 intracellularly. As we previously described (Vicente et al., 2008), Kv1.3 was targeted to the cell surface (Fig. 2A). Although KCNE2 distribution was similar to that of Kv1.3 (Fig. 2B), KCNE4 showed intracellular retention

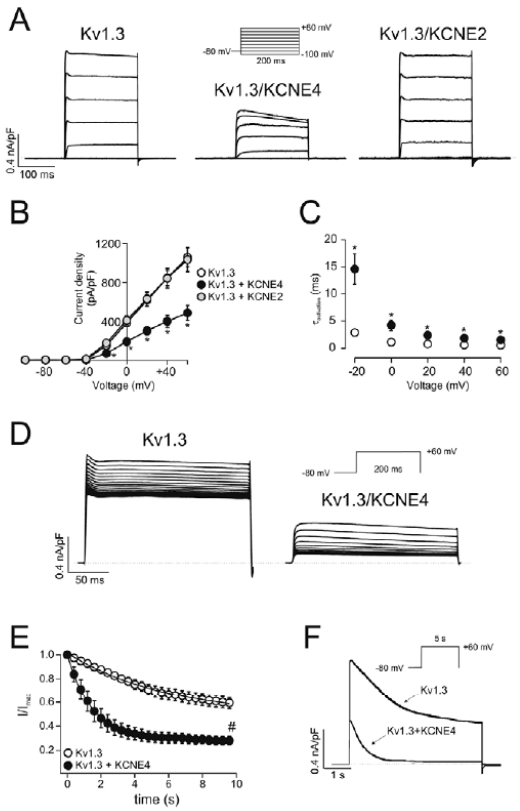

Fig. 1. KCNE4 modifies the gating of Kv1.3. (A) Representative current traces obtained from HEK293 cells expressing Kv1.3 alone (left), Kv1.3-KCNE4 (center) and Kv1.3-KCNE2 (right). (B) Current density (p*A*/p*F*) plotted against voltage (mV). Cells were clamped at –80 mV and current traces were elicited by 200 millisecond voltage steps to potentials ranging from –100 mV to +60 mV in 20-mV increments. White circles, Kv1.3 (n=13); black circles, Kv1.3-KCNE4 channels (n=8); gray circles, Kv1.3-KCNE2 (n=6). *P<0.01 (vs Kv1.3). (C) Time constant for activation ($\tau_{activation}$) at the indicated voltages, illustrating that activation time constants were slower for Kv1.3-KCNE4 channels. *P<0.01. White circles, Kv1.3 (n=13); black circles, Kv1.3-KCNE4 (n=8). (D) Representative traces for cumulative inactivation of outward K^+ currents through Kv1.3 (left) or Kv1.3-KCNE4 (right) channels. Currents were elicited by a train of 25× 200 millisecond depolarizing pulses to +60 mV once every 400 milliseconds. (E) Cumulative inactivation of Kv1.3 (white circles, n=10) and Kv1.3-KCNE4 (black circles, n=5) channels. The ratio of the peak current amplitude during each pulse, relative to that during the 1st pulse (I/I_{max}), is plotted against the time every pulse was applied. #P<0.001. (F) Representative traces illustrating inactivation kinetics of Kv1.3 and Kv1.3-KCNE4 channels, in response to a 5 seconds depolarizing pulse to +60 mV. Time constant for inactivation ($\tau_{inactivation}$), obtained after fitting the data to a single exponential, were (in seconds): for K_V1.3 channels, 1.12±0.2 (n=10); for K_V1.3-KCNE4 channels, 0.54±0.08 (n=6; P<0.05).

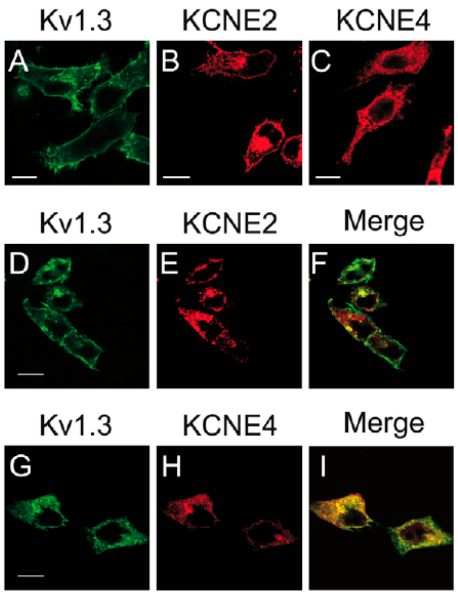

Fig. 2. Kv1.3 colocalizes with KCNE4. HEK293 cells were transiently transfected with Kv1.3-YFP (A), KCNE2 (B) or KCNE4 (C). Note that whereas Kv1.3 and KCNE2 have a robust surface membrane distribution, KCNE4 shows more intracellular retention. (D-I) Coexpression of Kv1.3 (D,G) with either KCNE2 (E) or KCNE4 (H). (F,I) Merged images of Kv1.3 and KCNE2, and Kv1.3 and KCNE4, respectively. Unlike KCNE2, KCNE4 triggers Kv1.3 intracellular retention. Scale bars: 10 μm.

(Fig. 2C). Kv1.3, co-expressed with KCNE2, remained at the cell surface with minor colocalization (Fig. 2D-F). By contrast, when co-expressed with KCNE4, Kv1.3 localization changed and both proteins colocalized within intracellular compartments (Fig. 2G-I). Our results suggest an interaction between Kv1.3 and KCNE4, which alters channel localization.

Most KCNE ancillary subunits improve the membrane localization of their Kv partners (Li et al., 2006). However, we found a dominant negative effect. Therefore, we studied Kv1.3 surface membrane expression in the presence of KCNE4. Fig. 3 demonstrates that KCNE4, but not KCNE2, impairs Kv1.3 targeting to the plasma membrane, thereby diminishing the amount of protein at the surface. Indeed, Kv1.3 mostly colocalized with the plasma membrane marker WGA (Fig. 3A-D). The analysis in Fig. 3D, derived from the section indicated by a white arrow in Fig. 3C, indicated that both proteins mostly share the same location. KCNE peptides are targeted to the cell surface with different efficiencies (Um and McDonald, 2007; Jiang et al., 2009). In this context, KCNE2 (Fig. 3I-L), but not KCNE4 (Fig. 3E-H), colocalized with WGA. When KCNE4 was co-transfected with Kv1.3 (Fig. 3M-P), KCNE4-induced Kv1.3 intracellular retention impaired Kv1.3-WGA colocalization (Fig. 3U). In addition, Kv1.3 and KCNE4 did not colocalize at the cell surface. In contrast, KCNE2 did not modify Kv.1.3 colocalization with WGA at the plasma membrane (Fig. 3Q-T,V). By using ImageJ software for a pixel-by-pixel analysis we found that 60% less KCNE4 was expressed at the cell surface than Kv1.3 and KCNE2. Unlike KCNE2, KCNE4 impaired Kv1.3 surface expression by 40% (Fig. 3W). KCNE4-CFP intracellular retention was not due to the fusion with CFP because KCNE4-HA showed a similar behavior (not shown). We further analyzed the amount of Kv1.3 at the cell surface by biotinylation in the presence of KCNE4. Fig. 4 shows that Kv1.3 is detected at the membrane as early as 4 hours following transfection. However, Kv1.3-KCNE4 and KCNE4 were detected after 12 and 24 hours, respectively. Therefore, KCNE4 delayed Kv1.3 reaching the cell surface (Fig. 4A). In addition, the amount of Kv1.3-KCNE4 at the membrane was tenfold less than Kv1.3 (Fig. 4B).

We have described that Kv1.3 exits the endoplasmic reticulum (ER) efficiently, which allows rapid sorting into Golgi vesicles designated for plasma membrane targeting. However, heteromeric association with Kv1.5 impairs Kv1.3 trafficking and increases ER retention (Vicente et al., 2008). Therefore, we wanted to study whether KCNE4-induced Kv1.3 retention was also associated with ER retention. Kv1.3 did not colocalize with an ER marker (Fig. 5A-C). However, KCNE4 was mostly targeted to this compartment (Fig. 5D-F). Thus, KCNE4 functions to retain Kv1.3 within the ER (Fig. 5G-J).

Oligomeric assembly of Kv1.3 and KCNE4

Although electrophysiological and confocal studies suggested an interaction between Kv1.3 and KCNE4, no physical association has been demonstrated. To this end, we designed a series of co-immunoprecipitation studies with differently tagged Kv1.3 and KCNE4 proteins. Fig. 6 demonstrates that KCNE4 forms a stable oligomer with Kv1.3. By co-transfecting KCNE4-CFP (~50 kDa) and Kv1.3-HA (~70 kDa) we found that Kv1.3 associated with KCNE4 (Fig. 6A,B). By contrast, no interaction was observed with KCNE2 (Fig. 6C). Thus, immunoprecipitation with an anti-Kv1.3 antibody against Kv1.3-YFP (~100 kDa) did not reveal an apparent KCNE2-CFP signal (~45 kDa). To unequivocally demonstrate that KCNE4 interacts physically with Kv1.3 we performed FRET experiments (Fig. 6D-G). As shown in Fig. 6H, FRET analysis revealed that a homomeric association between Kv1.3-YFP and Kv1.3-CFP gave a FRET signal greater than 20%. In this context, the oligomeric association of KCNE4-Kv1.3 resulted in ~15% significant FRET.

KCNE modulates Kv surface expression but the cellular compartment where this association takes place is uncertain. However, Kvβ ancillary subunits form stable complexes with Kv1 channels in the ER (Nagaya and Papazian, 1997). Therefore, we next analyzed whether KCNE4 and Kv1.3 associate in this compartment. Brefeldin A (BFA) is an inhibitor of protein transport from the ER to the Golgi apparatus. The incubation of Kv1.3-KCNE4 HEK293 cells with BFA demonstrated that both proteins showed ER localization, which is upstream of the Golgi network and subsequent membrane targeting. Our results suggest that Kv1.3 and KCNE4 interact early in the secretory pathway in the ER, similar to what has been described with classical Kvβ (Nagaya and Papazian, 1997). In addition, FRET experiments on living cells (Fig. 6G) further supported the molecular proximity of Kv1.3 and KCNE4 within the ER.

KCNE4 modifies Kv1.3 membrane surface targeting

The localization of Kv channels in specific locations at the plasma membrane leads to precise signaling and spatial compartmentalization. The composition of raft microdomains is crucial for Kv1.3 activity, thereby modulating immune responses. Kv1.3 localizes in lipid raft microdomains and cell activation

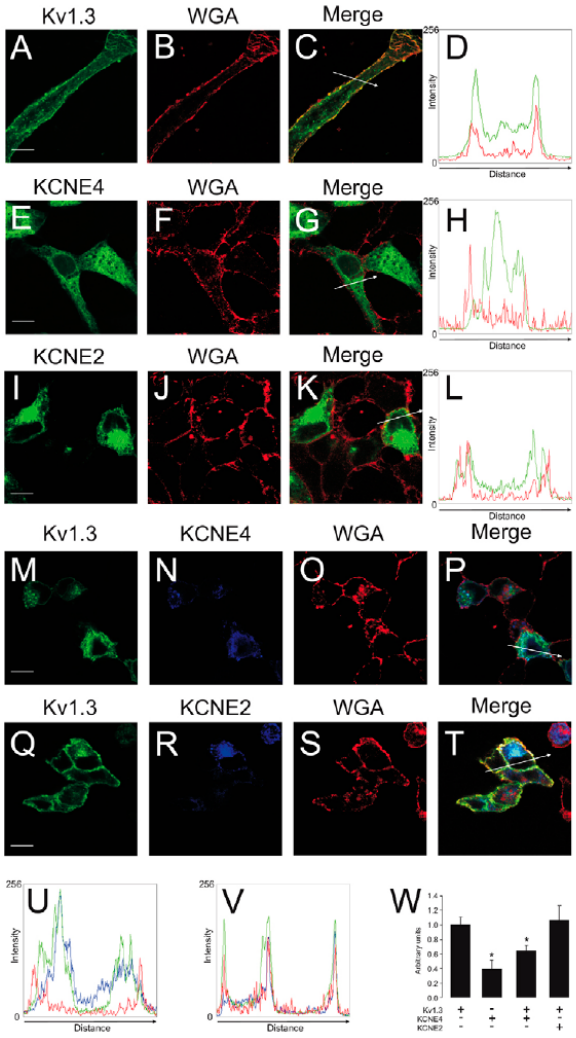

Fig. 3. KCNE4 impairs Kv1.3 targeting to the plasma membrane. Confocal images demonstrating that the presence of KCNE4 mistargets Kv1.3 surface expression, as analyzed by WGA overlay. (A-D) Kv1.3 shows membrane surface expression. (A) Kv1.3, (B) WGA, (C) merged image and (D) histogram of the pixel by pixel analysis of the section indicated by the arrow in C. Green, Kv1.3; red, WGA. (E-H) KCNE4 does not colocalize with WGA. (E) KCNE4, (F) WGA, (G) merged image and (H) histogram of the pixel by pixel analysis of the section indicated by the arrow in G. (I-L) KCNE2 shows strong colocalization with WGA. (I) KCNE2, (J) WGA, (K) merged image and (L) histogram of the pixel by pixel analysis of the section indicated by the arrow in K. (M-P) Coexpression of Kv1.3 and KCNE4. (M) Kv1.3, (N) KCNE4, (O) WGA and (P) merged image. Unlike in C, no Kv1.3 and WGA colocalization is observed. By contrast, massive Kv1.3 and KCNE4 colocalization is apparent (cyan). (Q-T) Coexpression of Kv1.3 and KCNE2. (Q) Kv1.3, (R) KCNE2, (S) WGA and (T) merged image. Unlike in P, Kv1.3 and WGA colocalize (yellow). Little triple colocalization (in white) is observed. (U,V) Histogram of the pixel by pixel analysis of the section indicated by the arrows in P and T, respectively. Green, Kv1.3; blue, KCNE2 or KCNE4; red, WGA. Although the presence of KCNE2 does not mistarget Kv1.3 to the surface (V), KCNE4 affects Kv1.3 and WGA colocalization (U). (W) Analysis of the relative expression of Kv1.3, KCNE4, Kv1.3-KCNE4 and Kv1.3-KCNE2. Pixel by pixel intensities from confocal images were analyzed using ImageJ software and compared with the relative intensity of Kv1.3 at the plasma membrane (determined by colocalization with WGA). Values are the mean ± s.e.m. of at least 20 cells. *P<0.05 vs Kv1.3 (Student's t-test). Scale bars: 10 µm.

concentrates Kv1.3 in lipid rafts near to signaling molecules (Panyi et al., 2004b). However, Kv1.3 targeting is impaired by oligomerization with Kv1.5 (Martinez-Marmol et al., 2008; Vicente et al., 2008). In addition, the association of Kv1.5 with the Kvβ2.1 regulatory subunit impairs channel targeting to rafts (Martinez-Marmol et al., 2008). With this in mind, we analyzed whether KCNE4 modifies Kv1.3 targeting to these domains. Although limited, Kv1.3-KCNE4 complexes reached the membrane surface (Fig. 4). Fig. 7 demonstrates that KCNE4 impaired Kv1.3 localization in lipid rafts. Although Kv1.3 targeted to rafts, KCNE4 did not localize to these domains (Fig. 7A,B). In Kv1.3-KCNE4 cells, Kv1.3 did not colocalize with caveolin, demonstrating that KCNE4 association mistargets Kv1.3 location (Fig. 7C). In addition, confocal microscopy experiments using FITC-labeled cholera toxin β subunit (CTXβ), which is a marker for rafts, further supports this result (Fig. 7D). In Kv1.3-KCNE4 cells the toxin did not colocalize with the hetero-oligomer (upper cell), in Kv1.3 cells, CTXβ colocalized with the channel (lower cell).

To further investigate whether Kv1.3 homo- and Kv1.3-KCNE4 hetero-oligomers target to different membrane surface microdomains, we performed FRAP experiments (Fig. 8). Fluorescence recovery within membrane regions was monitored until a steady state was achieved. Mobile fractions were similar (63±1% and 65±1% for Kv1.3 and Kv1.3-KCNE4, respectively) but the time constant ($t_{1/2}$) of the Kv1.3-KCNE4 hetero-oligomer exhibited greater lateral mobility (24±2.1 seconds and 13±1.7 seconds for Kv1.3 and Kv1.3-KCNE4, respectively, P<0.001). Our results indicate that KCNE4 association targets Kv1.3 to different membrane domains with higher mobility.

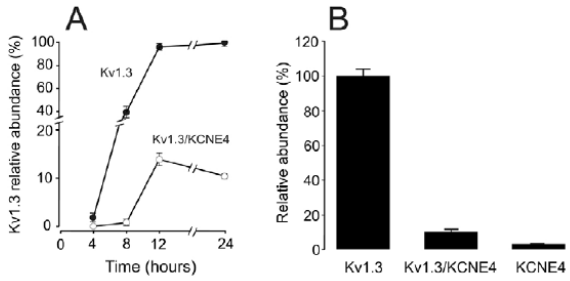

Fig. 4. KCNE4 delays and diminishes the expression of Kv1.3 at the cell surface. (A) HEK293 cells were transiently transfected with Kv1.3-YFP, KCNE4-CFP and Kv1.3-YFP/KCNE4-CFP. After transfection, cells were labeled with biotin at different times and processed as described in Materials and Methods. Western blot analysis was performed with and anti-GFP antibody. Values are means ± s.e.m. (n=4) of the percentage of the biotinylated surface protein relative to the maximal expression of Kv1.3. black symbols, Kv1.3; white symbols, Kv1.3-KCNE4. (B) Relative abundance (%) of biotinylated proteins compared with Kv1.3 after 24 hours of transfection. Values are means ± s.e.m. (n=4) of the percentage of the biotinylated surface protein relative to the expression of Kv1.3 24 hours post-transfection. Note that Kv1.3-KCNE4 is about 10 times less abundant than Kv1.3 alone.

Macrophages express Kv1.3 and KCNE4

Our results thus far indicate important physiological significance. Kv1.3 is involved in macrophage physiology and the expression of Kv1.3 and putative partners, such as Kv1.5 and Kvβ subunits, is under extensive regulation (Vicente et al., 2005; Vicente et al., 2006). In addition, Kv channels in leukocytes are considered pharmacological targets (Wulff et al., 2003; Beeton and Chandy, 2005) and the composition of the channel complex could impair potential therapies (Villalonga et al., 2007). Therefore, differential regulation of Kv1.3 and KCNE4 could modify the subunit composition of the channel, altering their biophysical and physiological properties. KCNE4 and Kv1.3 mRNAs were expressed in RAW 264.7 macrophages (Fig. 9A). This coexpression is a general characteristic of leukocytes because Jurkat T cells also share this phenotype (not shown). Unfortunately, unlike Kv1.3, we were not able to detect KCNE4 in macrophages by western blot with commercially available antibodies (not shown). Similarly, immunocytochemistry studies with anti-Kv1.3 and anti-KCNE4 antibodies were unsuccessful. However, because RAW cells have Kv1.3 and KCNE4 intracellular processing and trafficking programs, we transfected these cells with Kv1.3-YFP and KCNE4-CFP. In general, cells were poorly transfected, but confocal microscopy analysis of double-transfected RAW cells demonstrated that KCNE4 colocalizes with Kv1.3 in macrophages (Fig. 9B,C). In addition, although Kv1.3 is targeted to the plasma membrane (Fig. 9B), the presence of KCNE4 impaired Kv1.3 targeting (Fig. 9C).

Our data suggest that KCNE4 functions as a Kv1.3 negative modulatory subunit. Therefore, the regulation of KCNE4 might affect channelosome composition triggering important physiological consequences. For this reason, we analyzed the regulation of KCNE4 and Kv1.3 upon activation and immunosuppression in macrophages. Lipopolysaccharide, which activates macrophages and regulates Kv (Vicente et al., 2003), increased Kv1.3 and KCNE4 mRNA expression up to three- and 12-fold, respectively (Fig. 9D). By contrast, the addition of dexamethasone (DEX) for 24 hours decreased Kv1.3 by 50% with no effects on KCNE4.

Discussion

This study demonstrates that Kv1.3 and KCNE4 form oligomeric structures and suggests that KCNE4 might act as an inhibiting ancillary subunit for the Kv channel in macrophages. Furthermore, our data show that their association leads to biophysically distinct channels. The present report also demonstrates, for the first time, that KCNE peptides associate with members of the Kv1 (Shaker) family and alters channel surface expression and trafficking. This association further increases the number of possible oligomeric combinations of the Kv channelosome in leukocytes. Thus, similar to nervous tissue and muscles, it is difficult to assign currents to specific channels in the immune system.

Electrophysiological studies suggested that lymphocytes express several Kv channels (n-, n'- and l-type). Kv1.3 was associated with the n-type channel whereas the l-type was attributed to Kv3.1 (Grissmer et al., 1990; Grissmer et al., 1992). However, the protein responsible for the n'-type is largely unknown, although other channels, such as Kv1.1, Kv1.2, Kv1.5 and Kv1.6, have been described in immune-system cells (Freedman et al., 1995; Jou et al., 1998; Liu et al., 2002; Vicente et al., 2003; Mullen et al., 2006). Therefore, currents might be accounted for by a variety of hybrid forms and heteromeric formation of K^+ channels has been suggested as mechanisms to increase channel functional diversity (Manganas and Trimmer,

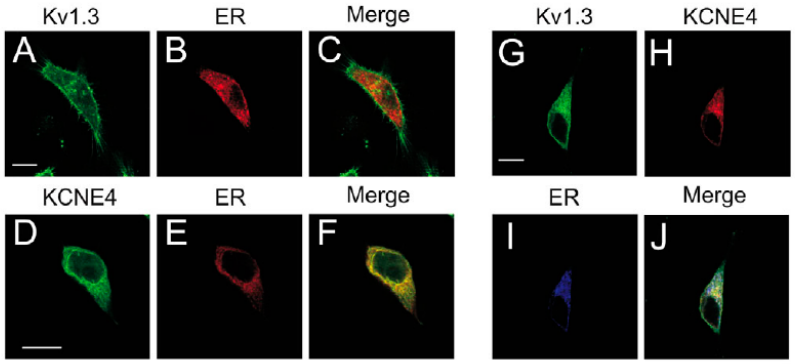

Fig. 5. KCNE4 retains Kv1.3 at the endoplasmic reticulum. Kv1.3-YFP and KCNE4-CFP have distinct cellular distributions. HEK293 cells were transiently transfected with Kv1.3-YFP , KCNE4-CFP , Kv1.3-YFP/KCNE4-CFP and DsRed-ER marker. (A-C) Kv1.3 does not colocalize with the ER. (D-F) KCNE4 shows strong ER colocalization. (A,D) Kv1.3 and KCNE4 respectively; (B,E) DsRed-ER marker; (C,F) merged image of Kv1.3- and KCNE4-transfected cells respectively. Yellow indicated colocalization. (G-J) Coexpression of Kv1.3, KCNE4 and DsRed-ER marker. (G) Kv1.3; (H) KCNE4; (I) DsRed-ER marker; (J) merged image. White color indicates triple colocalization. Scale bars: 10 μm.

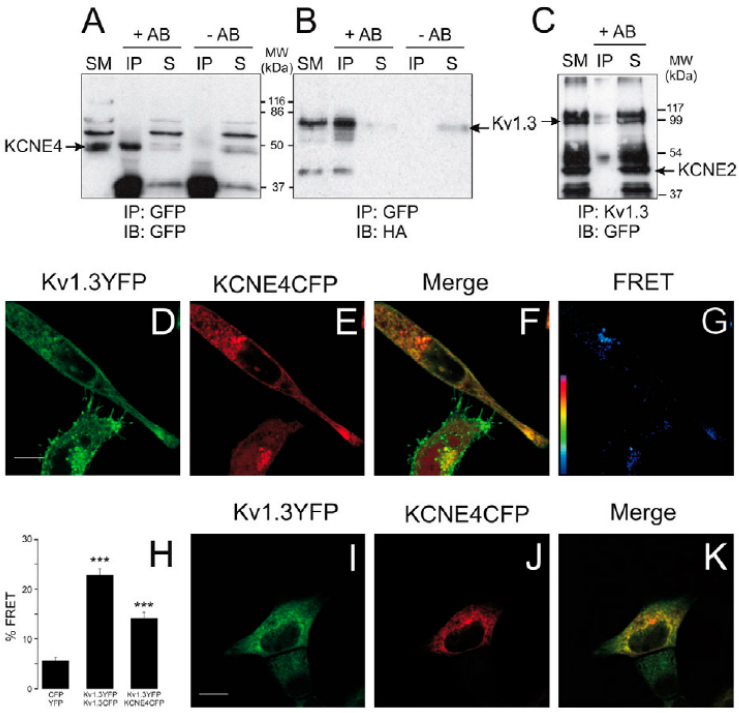

Fig. 6. KCNE4 associates with Kv1.3. KCNE4, but not KCNE2, and forms stable complexes with Kv1.3. (A,B) HEK293 cells were transiently transfected with Kv1.3-HA and KCNE4-CFP. Cells were lysed and total cell extracts were immunoprecipitated with anti-GFP antibody. (A) Western blot against GFP demonstrating that KCNE4-CFP immunoprecipitates. (B) Western blot against HA demonstrating that Kv1.3-HA co-immunoprecipitates with KCNE4-CFP. (C) KCNE2 does not interact with Kv1.3. HEK293 cells were transiently transfected with Kv1.3-YFP and KCNE2-CFP. Cells were lysed and total cell extracts were immunoprecipitated with anti-Kv1.3 antibody. Western blot against GFP demonstrates that Kv1.3 does not co-immunoprecipitate with KCNE2. SM, starting material; IP, immunoprecipitate; S, immunoprecipitate supernatant; +AB, immunoprecipitation in the presence of antibody; –AB, immunoprecipitation in the absence of antibody. (D-H) Representative fluorescence resonance energy transfer (FRET) experiment. Panels show fluorescence signal of Kv1.3-YFP and KCNE4-CFP. (D) Kv1.3; (E) KCNE4; (F) merged image; (G) FRET channel. FRET shows the YFP fluorescence intensity after CFP excitation. (H) Histogram shows FRET efficiency of different combinations of proteins. Negative control was performed with cells expressing CFP and YFP. Positive control was performed using cells expressing Kv1.3-CFP and Kv1.3-YFP. ***P<0.001 vs CFP/YFP (n=10, Student's t-test). (I-K) Kv1.3 and KCNE4 associate in the ER. HEK293 cells were doubly transfected with Kv1.3-YFP (green) and KCNE4-CFP (red) and brefeldin A was added to the culture. (I) Kv1.3; (J) KCNE4; (K) Merged image shows colocalization (yellow). Scale bars: 10 µm.

2000; Vicente et al., 2006). This complexity might be further increased by the presence of auxiliary subunits, such as Kvβ, which confers rapid inactivation, alters current amplitude and gating, and promotes Kv cell surface expression (Manganas and Trimmer, 2000). In fact, Kv1.3 is able to assemble with Kvβ subunits to form functional Kv channels, increasing the variety of electrical responses in leukocytes. The expression of Kv1.3 together with Kvβ subunits modifies the rate of inactivation and the amplitude of the K^+ current (McCormack et al., 1999). Although Kvβ1 peptides accelerate the rate of inactivation, Kvβ2 mostly facilitates surface expression (Martens et al., 1999; Manganas and Trimmer, 2000). Surprisingly, KCNE4 controls both fast inactivation and plasma membrane expression.

KCNE regulatory subunits have been primarily studied in the heart but their activity in the brain and in many other tissues is being increasingly recognized (McCrossan and Abbott, 2004). KCNE peptides associate with Kv7.1 and Kv11.1 channels generating cardiac I_{ks} (slowly activating delayed rectifier K^+) and I_{kr} (rapid delayed rectifier K^+) currents (Barhanin et al., 1996; Abbott et al., 1999). However, KCNE shows more promiscuity than previously thought. For example, KCNE3 in association with Kv3.4 sets resting membrane potential in skeletal muscle cells

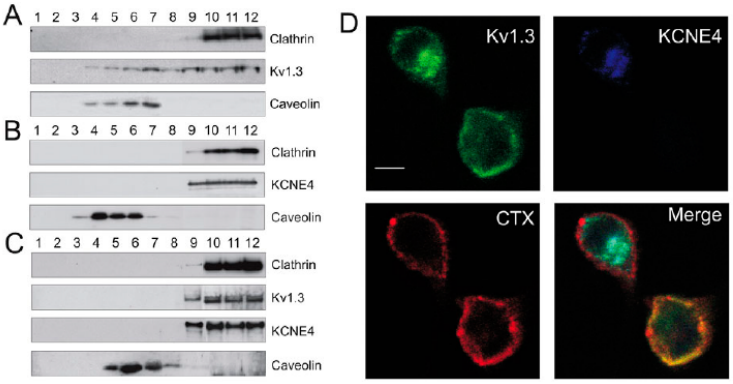

Fig. 7. KCNE4 impairs Kv1.3 localization in lipid rafts. Unlike KCNE4 and Kv1.3-KCNE4 hetero-oligomers, Kv1.3 channels target to lipid rafts. (A-C) Detergent-based isolation of lipid rafts. Sucrose density gradient centrifugation of 1% Triton-X-100-solubilized extracts from cells, transfected with Kv1.3 (A), KCNE4 (B) or doubly-transfected with Kv1.3 and KCNE4 (C) were analyzed by western blot. Caveolin indicates low-buoyancy rafts, but clathrin is found in non-floating fractions. Lane numbers denote different fractions from the top (1) to the bottom (12) of the sucrose density gradient. (D) KCNE4 association impairs Kv1.3 colocalization with FITC-labeled cholera toxin β subunit (CTXβ). Green, Kv1.3; blue, KCNE4; red, CTXβ; merged image, yellow represents colocalization between Kv1.3 and CTXβ in a KCNE4-negative cell (bottom cell). Top cell is a KCNE4-positive cell that shows no colocalization between Kv1.3 and CTXβ. Cyan represents Kv1.3-KCNE4 colocalization. Scale bar: 5 µm.

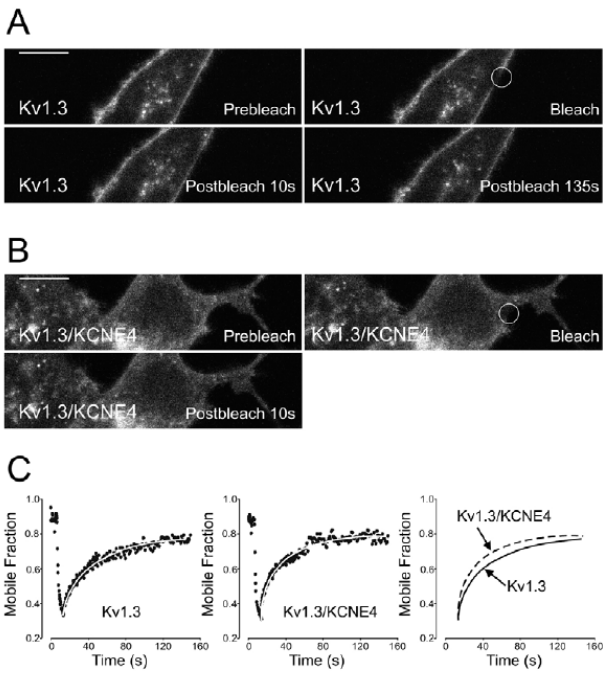

Fig. 8. Fluorescence recovery after photobleaching (FRAP) of Kv1.3 and Kv1.3-KCNE4. FRAP experiments monitored YFP intensity after 20 iterations of bleaching with 100% laser power. Representative images of Kv1.3-YFP at different times. Circles indicate regions of interest. (A) Kv1.3; (B) Kv1.3-KCNE4. Scale bars: 10 µm. (C) Graphs of the average (n=10) intensity from Kv1.3 and Kv1.3-KCNE4. Right, Kv1.3; center, Kv1.3-KCNE4; left, the regression analysis of the data (white lines from Kv1.3 and Kv1.3-KCNE4 panels) for comparison. Solid line, Kv1.3; Dashed line, Kv1.3-KCNE4.

(Abbott et al., 2001). In addition, KCNE1 and KCNE2 form stable complexes with Kv2.1 in the heart and brain (McCrossan et al., 2009). Few studies have demonstrated the existence of KCNE in leukocytes. KCNE1 was cloned from T-cells (Attali et al., 1992) and the KCNE3 and KCNE4 have been detected in leukocytes (Grunnet et al., 2003; Lundquist et al., 2006). We have found that KCNE4 is present in macrophages and T-cells (not shown). In addition, similarly to Kv1.3, lipopolysaccharide-induced activation increases KCNE4; and in cells treated with DEX, Kv1.3 is downregulated but KCNE4 remains constant. This behavior is in agreement with a putative negative regulatory action of KCNE4. Whereas pro-inflammatory agents, such as lipopolysaccharides, activate leukocytes (Vicente et al., 2003), prolonged insult triggers cell death by apoptosis (Detre et al., 2006). In this context, Kv1.3 seems to play a dual role. The channel is involved in the initiation of the signaling, but it also contributes to programmed cell death (Panyi et al., 2004a; Szabo et al., 2008). Sustained Kv1.3 induction would be downregulated by an increase in KCNE4 and the formation of Kv1.3-KCNE4 oligomers. In this scenario, lower expression, or repression, of Kv1.3 makes the cell resistant to apoptosis (Szabo et al., 2008). Therefore, the formation of Kv1.3-KCNE4 complexes would fine-tune the cell response. However, under an immunosuppressant insult, such as DEX, the dominant-negative effect of KCNE4 will have no physiological relevance.

KCNE4 specifically decreases Kv1.3 currents concomitantly with a reduction in channel surface expression and traffic. In addition, activation, C-type inactivation and cumulative inactivation are altered by KCNE4. Apart from cardiac Kv7.1 and Kv11.1, a number of different channels are affected by KCNE peptides (McCrossan and Abbott, 2004). For instance, KCNE1 slows Kv3.1 and Kv3.2 activation and KCNE3 increases the activation time constants of Kv2.1, Kv3.1 and Kv3.2 (McCrossan et al., 2003; Lewis et al., 2004). In addition, KCNE3 also modulates Kv3.4 current without a significant effect on either Kv1.4 or Kv4.1 (Abbott et al., 2001). Grunnet et al. demonstrated that among all KCNE peptides, only KCNE4 is able to modify Kv1.3 currents (Grunnet et al., 2003). Unlike other KCNE members, KCNE4 could act as a repressor ancillary subunit because unrelated channels such as Kv7.1 and the calcium and voltage-gated $K_{Ca}1.1$ channel (BK) are also inhibited by KCNE4 (Grunnet et al., 2002; Levy et al., 2008). It is important to point out that unlike other KCNE proteins, KCNE4 possesses a larger C-terminal intracellular domain (McCrossan and Abbott, 2004; Rocheleau et al., 2006). It is tempting to speculate that this bulky domain is involved in these processes but this hypothesis warrants further research. However, the inhibitory property of KCNE4 on selected channels, such as Kv7.1, seems to be very efficient as well as specific because Kv7.2 to Kv7.5 and Kv11.1 channels are unaffected (Grunnet et al., 2002).

To what extent electrophysiological changes have functional relevance is not known. As previously described, most ancillary subunit modulation might not be physiologically relevant (Deschenes and Tomaselli, 2002). Our results suggest that this is not the case for Kv1.3 and KCNE4 in leukocytes. Changes in trafficking and surface expression in macrophages further support Kv1.3-KCNE4 oligomeric channels, and Kv1.3 spatial regulation points towards a specific and physiological interaction. Other KCNE interactions with Kv1 members (Shaker) have been documented. Thus, KCNE1 and KCNE2 associate with Kv1.5, and experiments with *kcne2* null mice suggest that associations with Kv1.5 and Kv4.2, but not with Kv1.4 and Kv4.3, recapitulate cardiac I_{Kslow} and $I_{to,f}$ (transient outward fast) currents (Melman et al., 2004; Roepke et al., 2008).

KCNE peptides also control the surface expression of K^+ channels (McCrossan and Abbott, 2004). In addition, specific

Journal of Cell Science

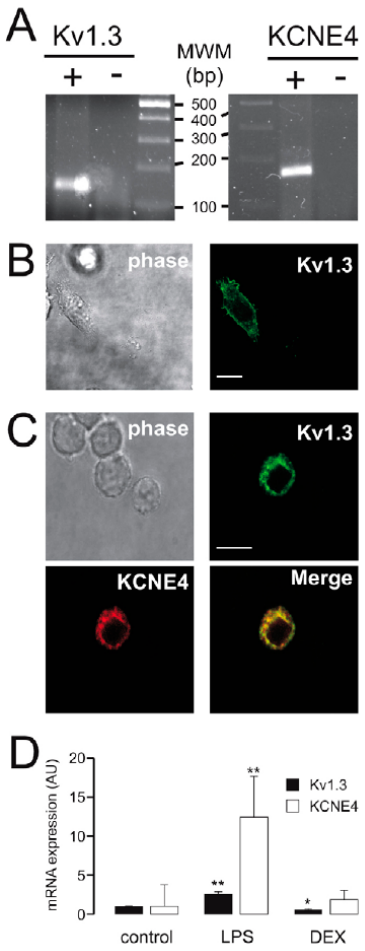

Fig. 9. RAW 264.7 macrophages express Kv1.3 and KCNE4. (A) Kv1.3 and KCNE4 mRNA expression analyzed by RT-PCR. Total RNA was extracted from RAW macrophages and PCR reactions were performed in the presence (+) or the absence (–) of the retrotranscriptase reaction. (B,C) KCNE4 impairs Kv1.3 targeting to the macrophage membrane and increases intracellular retention. (B) Kv1.3 expression. Right, phase image of a RAW macrophage. Left, confocal imaging of Kv1.3-YFP in the same cell. (C) Kv1.3-KCNE4 expression. Upper left, phase image of RAW macrophages; upper right, a cell expressing Kv1.3-YFP; lower left, KCNE4-CFP expression in the same cell; lower right, merged image showing colocalization in yellow. Note that in macrophages that expressed both proteins, Kv1.3 was mostly intracellular. Scale bar, 10 µm. (D) Kv1.3 and KCNE4 are differentially regulated upon activation and immunosuppression. Cells were incubated for 24 hours in the presence or the absence of lipopolysaccharides (LPS) and DEX. Samples were collected and Kv1.3 and KCNE4 mRNA expression was analyzed by real-time PCR. Black bars, Kv1.3; white bars, KCNE4. Values are the means + s.e.m. of the relative mRNA expression (n=4). Significant differences were found in the presence of lipopolysaccharides (Kv1.3: *P<0.05 and **P<0.01 vs control and KCNE4: **P<0.01 vs control; Student's t-test) and DEX (Kv1.3: *P<0.05 vs control, Student's t-test). Relative mRNA was calculated using standard curves, and fold variation in arbitrary units (AU) were normalized to the relative quantity (RQ) of 18S as follows: (Kv1.3 or KCNE4 RQ at 24 hours/18S RQ at 24 hours)/(Kv1.3 or KCNE4 RQ at control/18S RQ at control).

associations are crucial for KCNE1 expression at the plasma membrane (Chandrasekhar et al., 2006). In fact, KCNE1 shows greater ER retention than KCNE2 and this determines Kv11.1 association (Um and McDonald, 2007). KCNE4 also shows more ER retention than KCNE2. Although KCNE4 and KCNE2 share an intracellular RR motif, KCNE4 possess multiple arginine and lysine-based ER retention signals (Sharma et al., 1999; Michelsen et al., 2005; Zuzarte et al., 2009). KCNE4 does not modify surface expression of Kv7.1 and Kv1.1(Grunnet et al., 2002; Grunnet et al., 2003). However, both channels exhibit less surface expression than Kv1.3. In addition, the cellular compartment where KCNE associates with K^+ channels is controversial. Although some studies demonstrate that, unlike Kvβ subunits, this interaction takes place at the membrane (Grunnet et al., 2002), others indicate an association in the ER (Krumerman et al., 2004; Chandrasekhar et al., 2006). Our results indicate that, similar to Kvβ, KCNE4 associates with Kv1.3 in the ER.

Besides trafficking, lipid raft sublocalization regulates ion channels by compartmentalizing signaling components. Kv1.3 targets to different rafts upon activation and apoptosis in lymphocytes (Szabo et al., 2004; Vicente et al., 2008). Disruption of these domains alters channel activity and raft association seems to be dynamic because the interaction with other subunits, such as Kv1.5, impairs this localization (Vicente et al., 2008). However, scaffolding proteins, such as membrane associated guanylate kinases (MAGUK) and caveolins, improve Kv1.5 channel association with raft domains (Folco et al., 2004). Unlike scaffolding proteins, Kvβ2.1 regulatory subunit mistargets Kv1.5 channels to lipid rafts (Martinez-Marmol et al., 2008). Similarly, KCNE4 act as a repressor ancillary subunit. Kv1.3 localizes in rafts but this is strongly dependent on associations with KCNE4. Because Kv1.3 activity is regulated by the composition of the lipid raft (Szabo et al., 2004), different membrane platform locations must be contemplated as an important regulatory mechanism of Kv1.3 in leukocyte physiology. The channelosome composition is a determinant in shaping the repertoire of Kv1.3 channels present at the plasma membrane of leukocytes. This composition affects the expression and functional properties of the channels and contributes to the diversity of K^+ channels in leukocytes. This data will be critical for further determination of the molecular composition of individual Kv currents and the physiological relevance of these α-β interactions. Investigation of the mechanisms involved in the regulation of potassium ion conduction is, therefore, essential for understanding potassium channel function in the immune response to infection and inflammation. Macrophages turn the immune response toward inflammation or tolerance. These cells, which also act as antigen-presenting cells, modify the cytokine milieu and the intensity of T-lymphocyte signaling. In response to different growth factors and cytokines, macrophages can proliferate, become activated or differentiate. These cells have a key function at inflammatory loci, where they remain until inflammation disappears. However, the persistence of activated macrophages at inflammatory loci is associated with a wide range of inflammatory diseases. The negative KCNE4 effect on Kv1.3 could be interpreted in this life-time scenario.

In summary, Kv1.3 trafficking, targeting and activity are dramatically modified by the presence of KCNE4. The association of Kv1.3 and KCNE4, which are coexpressed in the immune system, could play a crucial role in controlling the immunological response. Therefore, our results further the understanding of how K^+ channels are involved in leukocyte physiology and indicate that KCNE4 could be a novel pharmacological target in the immune system.

Materials and Methods

Expression plasmids

rKv1.3 in pRcCMV was provided by Todd C. Holmes (New York University, New York, NY). mKCNE4 in pSGEM was from Michael Sanguinetti (University of Utah, Salt Lake City, UT). hKCNE2 in pHA was obtained from Susana de la Luna (CRG, Barcelona, Spain). Kv1.3, KCNE4 and KCNE2 were subcloned into pEYFP-C1 (Kv1.3) and pECFP-N1 (KCNE2 and KCNE4; Clontech). Constructs were verified by sequencing. rKv1.3, externally tagged with HA between S3 and S4, was from Donald B. Arnold (University of Southern California, Los Angeles, CA). piRES-EGFP-hKCNE4-HA was obtained from Alfred L. George (Vanderbilt University, Nashville, TN). The endoplasmic reticulum marker, pDsRed-ER, was obtained from Clontech.

Cell culture and transient transfections

HEK293 cells were grown on poly-lysine-coated coverslips in DMEM containing 10% fetal bovine serum (FBS). Transient transfection was performed using MetafectenePro (Biontex) at nearly 80% confluence. Twenty-four hours after transfection, cells were washed in PBS (phosphate-buffered saline), fixed and mounted with Aqua Poly/Mount from Polysciences. In some experiments, Kv1.3–KCNE4-transfected cells were treated with 2.5 μg/ml brefeldin A (BFA) for 12 hours.

RAW 264.7 macrophages were cultured in RPMI culture medium containing 5% FBS supplemented with 10 IU/ml penicillin and streptomycin, and 2 mM L-glutamine. Cells, grown in 100-mm tissue culture dishes, were incubated with lipopolysaccharides (100 ng/ml) and DEX (1 μM; Sigma) for 24 hours. In some experiments, RAW cells were transfected with Kv1.3-YFP and KCNE4-CFP and processed as above.

RNA isolation, RT-PCR analysis and real-time PCR

Total RNA from RAW 264.7 macrophages was isolated using Nucleospin RNAII (Machery-Nagel). RNA was treated with DNase I and cDNA synthesis was performed using transcriptor reverse transcriptase (Roche) with a random hexanucleotide and oligo(dT) according to the manufacturer's instructions.

Real-time PCR was performed using a LightCycler machine (Roche) with LightCycler FastStart DNA Master^{PLUS} SYBR Green I (Roche), according to the manufacturer's instructions. PCR primers were: Kv1.3, F: 5′-AGTATATG-GTGATCGAAGAGG-3′, R: 5′-AGTGAATATCTTCTTGATGTT-3′ (136 bp); KCNE4, F: 5′-CCTGACAGAGAAGAGAAACA-3′, R: 5′-TGAACAGCACA-TACCCCAG-3′ (139 bp). The reactions were performed under the following conditions: 95°C for 5 seconds, 55°C for 8 seconds, and 72°C for 9 seconds, proceeded by 10 minutes at 95°C and followed by 10 minutes at 95°C. Melting curves were performed to verify the specificity of the product and 18S (AN: X00686), F: 5′-CGCAGAATTCCCACTCCCGACCC-3′, R: 5′-CCCAAGCTCCAACTACGAGC-3′ (212 bp), was included as an internal reference, as previously described (Villalonga et al., 2007). Results were analyzed with Light Cycler software 3.5 (Roche). For each primer set, a standard curve was made and the slope factor calculated. Values were normalized to the corresponding 18S. The corresponding real-time PCR efficiency (E) of one cycle in the exponential phase was calculated according to the equation: $E=10^{(-1/\text{slope})}$.

Protein extraction, co-immunoprecipitation and western blotting

Cells were washed twice in cold PBS and lysed on ice with lysis solution (1% Triton X-100, 10% glycerol, 50 mM Hepes pH 7.2, 150 mM NaCl) supplemented with 1 μg/ml aprotinin, 1 μg/ml leupeptin, 1 μg/ml pepstatin and 1 mM phenylmethylsulfonyl fluoride as protease inhibitors. Homogenates were centrifuged at 3000 *g* for 10 minutes and the supernatant was divided into aliquots and stored at –20°C. Protein content was determined using the Bio-Rad Protein Assay (Bio-Rad).

For co-immunoprecipitation, samples were precleared with 25 μl of protein G-Sepharose beads, for 2 hours at 4°C with gentle mixing. The beads were then removed by centrifugation at 1000 *g* for 30 seconds at 4°C. The sample was then incubated overnight with the desired antibody (4 ng/μg protein) at 4°C with gently mixing. 30 μl of protein-G-Sepharose was added to each sample for 4 h at 4°C. The beads were removed by centrifugation at 1000 *g* for 30 seconds at 4°C, washed four times in PBS, and resuspended in 70 μl of SDS sample buffer.

Protein samples (50 μg) and immunoprecipitates were boiled in Laemmli SDS loading buffer and separated on 10% SDS-PAGE. Next, they were transferred to nitrocellulose membranes (Immobilon-P; Millipore) and blocked in 0.2% Tween-20-PBS supplemented with 5% dry milk, before immunoreaction. Filters were immunoblotted with antibodies against Kv1.3 (1/200, Alomone), HA (1/200, Sigma) and GFP (1/1000, Roche). Anti-pan-caveolin antibody, which recognizes caveolin 1, 2 and 3 was used as a marker of lipid raft fractions (1/1000; BD Transduction) and anti-clathrin antibody was used to characterize non-floating fractions (1/1000, Chemicon).

Raft isolation

Low density, Triton-insoluble complexes were isolated as previously described (Martens et al., 2000) from HEK293 cells transiently transfected with either Kv1.3-YFP or double transfected with Kv1.3-YFP and KCNE4-CFP. Cells were homogenized in 1 ml of 1% Triton X-100, and sucrose was added to a final concentration of 40%. A 5-30% linear sucrose gradient was layered on top and further centrifuged (260,000 *g*) for 20-22 hours at 4°C in a Beckman SW41 rotor. Gradient fractions (1 ml) were collected from the top and analyzed by western blotting.

Confocal microscopy, FRET and FRAP

Staining with FITC-labeled cholera toxin β subunit (CTXβ) for lipid raft microdomains and wheat germ agglutinin (WGA)-Texas red (Invitrogen) for the plasma membrane was performed under non-permeabilized conditions. Cells were washed with PBS at 4°C and stained with FITC-CTXβ or WGA for 30 minutes at 4°C. Subsequently, cells were washed and fixed with 4% paraformaldehyde in PBS for 6 minutes.

Fluorescence resonance energy transfer (FRET) sensitized emission was used to measure the molecular proximity between Kv1.3 and KCNE4. A Leica TCS SL laser scanning confocal spectral microscope (Leica Microsystems) equipped with an argon laser, 63× oil immersion objective lens (NA 1.32) and a double dichroic filter (458/514 nm) was used. CFP was used as the donor fluorochrome paired with YFP, as the acceptor fluorochrome. To measure FRET, three images were acquired in the same order in all experiments through (1) the CFP channel (absorption 458 nm; emission 465–510 nm), (2) the FRET channel (absorption 458 nm; emission 525–600 nm) and (3) the YFP channel (absorption 514 nm; emission 525–600 nm). The background values were subtracted from the image values before performing FRET calculations. Control and experimental images were taken under the same photomultiplier gain conditions, offset and pinhole aperture. In order to calculate and eliminate non-FRET components from the FRET channel, images of cells transfected with either CFP or YFP alone were taken under the same conditions as for the experiments. The fraction of cross-over of CFP (A) and YFP (B) fluorescence was calculated for the different experimental conditions. Corrected FRET (FRET^C) was calculated on a pixel-by-pixel basis for the entire image using the equation: $\text{FRET}^C=\text{FRET}–(A\times\text{CFP})–(B\times\text{YFP})$, where FRET, CFP and YFP are the values for the background-subtracted images of cells expressing CFP and YFP acquired through the FRET, CFP and YFP channels, respectively. Mean FRET^C values were calculated from mean fluorescence intensities for each selected region of interest (ROI) according to the above equation, and normalized (FRET^N) values for membrane regions were calculated according to the following equation: $\text{FRET}^N=\text{FRET}^C/\text{YFP}$. All calculations were performed using the FRET sensitized emission wizard from Leica Confocal Software and Microsoft Excel. FRET values were expressed as the mean ± s.e.m. of n>15 cells for each group.

Fluorescence recovery after photobleaching (FRAP) experiments were performed 1 day after transfection at room temperature. Dishes were replaced every 2 hours. Time series were taken with 20 scans before bleaching, which was accomplished by 20 iterations of bleaching with 100% laser power of the 514 nm line followed by 100 scans every 0.36 seconds and 100 scans every second (2.5 minutes in total) of the bleached region with 6% laser power. In each cell, a circular ROI of 6.57 μm^2 was bleached. Experiments were performed with n>15 cells per group. Fluorescence intensity was normalized to the prebleach intensity. Any loss of fluorescence during the recording was corrected with unbleached regions of the cell. The mobile fraction (F_M) was calculated according to the following equation: $F_M=(F_\infty–F_i)/(F_0–F_i)$, where F_∞ is the fluorescence at the end of the steady state, F_i is the fluorescence intensity post-bleaching and F_0 is the fluorescence of the ROI previous to the bleaching.

Values were fitted to a non-linear regression equation, $F(t)=F_M\ [1-\exp(-t/t_{1/2})]$, where F is the fluorescence intensity, F_M is the mobile fraction and $t_{1/2}$ is the time constant. Data are given as mean ± s.e.m. Statistical analysis was performed using Student's t-test (GraphPad Prism).

Cells were examined with a 63× oil immersion objective on a Leica TCS SL laser scanning confocal microscope. All offline image analysis was done using Leica confocal and Image J software and Sigmaplot.

Biotinylation of cell surface proteins

Cell surface biotinylation was carried out with the Pierce Cell Surface Protein Isolation Kit (Pierce) following manufacturer's instructions. HEK293 cells were transfected with Kv1.3-YFP, KCNE4-CFP or both constructs and their temporal presence at the surface was analyzed by western blotting. At the desired times after transfection, cell surface proteins were labeled with sulfosuccinimidyl-2-(biotinamido)ethyl-1,3-dithiopropionate (Sulfo-NHS-SS-biotin; Pierce). Briefly, cells were washed with ice-cold PBS twice, and Sulfo-NHS-SS-biotin was added and incubated at 4°C with constant rotation for 30 minutes. Excess biotin was quenched with quenching solution. Cells were treated with lysis buffer and centrifuged at 10,000 *g* for 2 minutes at 4°C. Clear supernatant was reacted with immobilized NeutrAvidin gel slurry in columns (Pierce) to isolate surface proteins. Columns were washed and protein eluted in sample buffer containing DTT. Surface proteins were resolved on a SDS-PAGE gel and the samples were analyzed by western blotting using a monoclonal anti-GFP antibody (Roche). Western blot bands were quantified using Phoretix (Nonlinear Dynamics). Data are expressed as the optical density (%) of the biotinylated protein relative to the maximal expression of Kv1.3. Filters were also immunoblotted with β-actin monoclonal antibody (Sigma) as control.

Electrophysiology

Whole-cell currents were measured with a D-6100 Darmstadt amplifier (List Medical) using the patch clamp technique. Currents were low-pass filtered at 1 kHz. Series resistance compensation was always above 70%. The pClamp8 software (Axon

Instruments) was used for pulse generation and data acquired using an Axon Digidata A/D interface and subsequent analysis. Electrodes were fabricated from borosilicate glass capillaries (Clark Electromedical Instruments) using a Flaming-Brown (P-87) micropipette puller (Sutter Instruments) and fire polished. Pipettes had a resistance of 2-3 MΩ when filled with a solution containing (in mM): 144 KCl, 0.2 $CaCl_2$, 1.2 $MgCl_2$, 10 Hepes, 0.5 EGTA (pH 7.35 and 302 mosmoles/l). The extracellular solution contained (in mM): 150 NaCl, 4 KCl, 2 $CaCl_2$, 1 $MgCl_2$, 10 Hepes (pH 7.4 and 310 mosmoles/l). Cells were clamped to a holding potential of –80 mV. To evoke voltage-gated currents, all cells were stimulated with 200-millisecond square pulses ranging from –100 to +60 mV in 20 mV steps. All recordings were routinely subtracted for leak currents. To calculate inactivation time constants (τ), cells were held at –80 mV and a +60 mV pulse potential of 5 seconds was applied. Inactivation adjustment was calculated from the peak of the current at 60 mV to the steady-state inactivation, and traces were fitted with Sigma Plot (SPSS, Chicago, IL). To analyze cumulative inactivation, currents were elicited by a train of 25 depolarizing voltage steps of 200 milliseconds to +60 mV once every 400 milliseconds.

This study was supported by the Ministerio de Ciencia e Innovación (MICINN), Spain (BFU2005-00695, BFU2008-00431 and CSD2008-00005 to A.F. and SAF2006-13893-C02-02 to J.M.F.-F.). L.S. holds fellowships from the MICINN and 'Fundación La Caixa'. The FI program of the Generalitat de Catalunya supported M.R.-F. and M.P.-V. We thank American Journal Experts for editorial assistance.

References

Abbott, G. W. and Goldstein, S. A. (2001). Potassium channel subunits encoded by the KCNE gene family: physiology and pathophysiology of the MinK-related peptides (MiRPs). *Mol. Interv.* **1**, 95-107.

Abbott, G. W. and Goldstein, S. A. (2002). Disease-associated mutations in KCNE potassium channel subunits (MiRPs) reveal promiscuous disruption of multiple currents and conservation of mechanism. *FASEB J.* **16**, 390-400.

Abbott, G. W., Sesti, F., Splawski, I., Buck, M. E., Lehmann, M. H., Timothy, K. W., Keating, M. T. and Goldstein, S. A. (1999). MiRP1 forms IKr potassium channels with HERG and is associated with cardiac arrhythmia. *Cell* **97**, 175-187.

Abbott, G. W., Butler, M. H., Bendahhou, S., Dalakas, M. C., Ptacek, L. J. and Goldstein, S. A. (2001). MiRP2 forms potassium channels in skeletal muscle with Kv3.4 and is associated with periodic paralysis. *Cell* **104**, 217-231.

Attali, B., Romey, G., Honore, E., Schmid-Alliana, A., Mattei, M. G., Lesage, F., Ricard, P., Barhanin, J. and Lazdunski, M. (1992). Cloning, functional expression, and regulation of two K+ channels in human T lymphocytes. *J. Biol. Chem.* **267**, 8650-8657.

Barhanin, J., Lesage, F., Guillemare, E., Fink, M., Lazdunski, M. and Romey, G. (1996). K(V)LQT1 and lsK (minK) proteins associate to form the I(Ks) cardiac potassium current. *Nature* **384**, 78-80.

Beeton, C. and Chandy, K. G. (2005). Potassium channels, memory T cells, and multiple sclerosis. *Neuroscientist* **11**, 550-562.

Beeton, C., Pennington, M. W., Wulff, H., Singh, S., Nugent, D., Crossley, G., Khaytin, I., Calabresi, P. A., Chen, C. Y., Gutman, G. A. et al. (2005). Targeting effector memory T cells with a selective peptide inhibitor of Kv1.3 channels for therapy of autoimmune diseases. *Mol. Pharmacol.* **67**, 1369-1381.

Beeton, C., Wulff, H., Standifer, N. E., Azam, P., Mullen, K. M., Pennington, M. W., Kolski-Andreaco, A., Wei, E., Grino, A., Counts, D. R. et al. (2006). Kv1.3 channels are a therapeutic target for T cell-mediated autoimmune diseases. *Proc. Natl. Acad. Sci. USA* **103**, 17414-17419.

Cahalan, M. D., Wulff, H. and Chandy, K. G. (2001). Molecular properties and physiological roles of ion channels in the immune system. *J. Clin. Immunol.* **21**, 235-252.

Chandrasekhar, K. D., Bas, T. and Kobertz, W. R. (2006). KCNE1 subunits require co-assembly with K+ channels for efficient trafficking and cell surface expression. *J. Biol. Chem.* **281**, 40015-40023.

Chandy, K. G., Wulff, H., Beeton, C., Pennington, M., Gutman, G. A. and Cahalan, M. D. (2004). K+ channels as targets for specific immunomodulation. *Trends Pharmacol. Sci.* **25**, 280-289.

Deschenes, I. and Tomaselli, G. F. (2002). Modulation of Kv4.3 current by accessory subunits. *FEBS Lett.* **528**, 183-188.

Detre, C., Kiss, E., Varga, Z., Ludanyi, K., Paszty, K., Enyedi, A., Kovesdi, D., Panyi, G., Rajnavolgyi, E. and Matko, J. (2006). Death or survival: membrane ceramide controls the fate and activation of antigen-specific T-cells depending on signal strength and duration. *Cell Signal.* **18**, 294-306.

Folco, E. J., Liu, G. X. and Koren, G. (2004). Caveolin-3 and SAP97 form a scaffolding protein complex that regulates the voltage-gated potassium channel Kv1.5. *Am. J. Physiol. Heart Circ. Physiol.* **287**, H681-H690.

Freedman, B. D., Fleischmann, B. K., Punt, J. A., Gaulton, G., Hashimoto, Y. and Kotlikoff, M. I. (1995). Identification of Kv1.1 expression by murine CD4-CD8- thymocytes: a role for voltage-dependent K+ channels in murine thymocyte development. *J. Biol. Chem.* **270**, 22406-22411.

Grissmer, S., Dethlefs, B., Wasmuth, J. J., Goldin, A. L., Gutman, G. A., Cahalan, M. D. and Chandy, K. G. (1990). Expression and chromosomal localization of a lymphocyte K+ channel gene. *Proc. Natl. Acad. Sci. USA* **87**, 9411-9415.

Grissmer, S., Ghanshani, S., Dethlefs, B., McPherson, J. D., Wasmuth, J. J., Gutman, G. A., Cahalan, M. D. and Chandy, K. G. (1992). The Shaw-related potassium channel gene, Kv3.1, on human chromosome 11, encodes the type l K+ channel in T cells. *J. Biol. Chem.* **267**, 20971-20979.

Grissmer, S., Nguyen, A. N., Aiyar, J., Hanson, D. C., Mather, R. J., Gutman, G. A., Karmilowicz, M. J., Auperin, D. D. and Chandy, K. G. (1994). Pharmacological characterization of five cloned voltage-gated K+ channels, types Kv1.1, 1.2, 1.3, 1.5, and 3.1, stably expressed in mammalian cell lines. *Mol. Pharmacol.* **45**, 1227-1234.

Grunnet, M., Jespersen, T., Rasmussen, H. B., Ljungstrom, T., Jorgensen, N. K., Olesen, S. P. and Klaerke, D. A. (2002). KCNE4 is an inhibitory subunit to the KCNQ1 channel. *J. Physiol.* **542**, 119-130.

Grunnet, M., Rasmussen, H. B., Hay-Schmidt, A., Rosenstierne, M., Klaerke, D. A., Olesen, S. P. and Jespersen, T. (2003). KCNE4 is an inhibitory subunit to Kv1.1 and Kv1.3 potassium channels. *Biophys. J.* **85**, 1525-1537.

Hille, B. (2001). *Ion Channels of Excitable Membranes*. Sunderland, MA: Sinauer.

Jiang, M., Xu, X., Wang, Y., Toyoda, F., Liu, X. S., Zhang, M., Robinson, R. B. and Tseng, G. N. (2009). Dynamic partnership between KCNQ1 and KCNE1 and influence on cardiac IKS current amplitude by KCNE2. *J. Biol. Chem.* **284**, 16452-16462.

Jou, I., Pyo, H., Chung, S., Jung, S. Y., Gwag, B. J. and Joe, E. H. (1998). Expression of Kv1.5 K+ channels in activated microglia in vivo. *Glia* **24**, 408-414.

Krumerman, A., Gao, X., Bian, J. S., Melman, Y. F., Kagan, A. and McDonald, T. V. (2004). An LQT mutant minK alters KvLQT1 trafficking. *Am. J. Physiol. Cell Physiol.* **286**, C1453-C1463.

Levy, D. I., Wanderling, S., Biemesderfer, D. and Goldstein, S. A. (2008). MiRP3 acts as an accessory subunit with the BK potassium channel. *Am. J. Physiol. Renal Physiol.* **295**, F380-F387.

Lewis, A., McCrossan, Z. A. and Abbott, G. W. (2004). MinK, MiRP1, and MiRP2 diversify Kv3.1 and Kv3.2 potassium channel gating. *J. Biol. Chem.* **279**, 7884-7892.

Lewis, R. S. and Cahalan, M. D. (1995). Potassium and calcium channels in lymphocytes. *Annu. Rev. Immunol.* **13**, 623-653.

Li, Y., Um, S. Y. and McDonald, T. V. (2006). Voltage-gated potassium channels: regulation by accessory subunits. *Neuroscientist* **12**, 199-210.

Liu, Q. H., Fleischmann, B. K., Hondowicz, B., Maier, C. C., Turka, L. A., Yui, K., Kotlikoff, M. I., Wells, A. D. and Freedman, B. D. (2002). Modulation of Kv channel expression and function by TCR and costimulatory signals during peripheral CD4(+) lymphocyte differentiation. *J. Exp. Med.* **196**, 897-909.

Lundquist, A. L., Turner, C. L., Ballester, L. Y. and George, A. L., Jr (2006). Expression and transcriptional control of human KCNE genes. *Genomics* **87**, 119-128.

Maguy, A., Hebert, T. E. and Nattel, S. (2006). Involvement of lipid rafts and caveolae in cardiac ion channel function. *Cardiovasc. Res.* **69**, 798-807.

Manganas, L. N. and Trimmer, J. S. (2000). Subunit composition determines Kv1 potassium channel surface expression. *J. Biol. Chem.* **275**, 29685-29693.

Martens, J. R., Kwak, Y. G. and Tamkun, M. M. (1999). Modulation of Kv channel alpha/beta subunit interactions. *Trends Cardiovasc. Med.* **9**, 253-258.

Martens, J. R., Navarro-Polanco, R., Coppock, E. A., Nishiyama, A., Parshley, L., Grobaski, T. D. and Tamkun, M. M. (2000). Differential targeting of Shaker-like potassium channels to lipid rafts. *J. Biol. Chem.* **275**, 7443-7446.

Martens, J. R., O'Connell, K. and Tamkun, M. (2004). Targeting of ion channels to membrane microdomains: localization of KV channels to lipid rafts. *Trends Pharmacol. Sci.* **25**, 16-21.

Martinez-Marmol, R., Villalonga, N., Sole, L., Vicente, R., Tamkun, M. M., Soler, C. and Felipe, A. (2008). Multiple Kv1.5 targeting to membrane surface microdomains. *J. Cell Physiol.* **217**, 667-673.

McCormack, T., McCormack, K., Nadal, M. S., Vieira, E., Ozaita, A. and Rudy, B. (1999). The effects of Shaker beta-subunits on the human lymphocyte K+ channel Kv1.3. *J. Biol. Chem.* **274**, 20123-20126.

McCrossan, Z. A. and Abbott, G. W. (2004). The MinK-related peptides. *Neuropharmacology* **47**, 787-821.

McCrossan, Z. A., Lewis, A., Panaghie, G., Jordan, P. N., Christini, D. J., Lerner, D. J. and Abbott, G. W. (2003). MinK-related peptide 2 modulates Kv2.1 and Kv3.1 potassium channels in mammalian brain. *J. Neurosci.* **23**, 8077-8091.

McCrossan, Z. A., Roepke, T. K., Lewis, A., Panaghie, G. and Abbott, G. W. (2009). Regulation of the Kv2.1 potassium channel by MinK and MiRP1. *J. Membr. Biol.* **228**, 1-14.

Melman, Y. F., Um, S. Y., Krumerman, A., Kagan, A. and McDonald, T. V. (2004). KCNE1 binds to the KCNQ1 pore to regulate potassium channel activity. *Neuron* **42**, 927-937.

Michelsen, K., Yuan, H. and Schwappach, B. (2005). Hide and run. Arginine-based endoplasmic-reticulum-sorting motifs in the assembly of heteromultimeric membrane proteins. *EMBO Rep.* **6**, 717-722.

Mullen, K. M., Rozycka, M., Rus, H., Hu, L., Cudrici, C., Zafranskaia, E., Pennington, M. W., Johns, D. C., Judge, S. I. and Calabresi, P. A. (2006). Potassium channels Kv1.3 and Kv1.5 are expressed on blood-derived dendritic cells in the central nervous system. *Ann. Neurol.* **60**, 118-127.

Nagaya, N. and Papazian, D. M. (1997). Potassium channel alpha and beta subunits assemble in the endoplasmic reticulum. *J. Biol. Chem.* **272**, 3022-3027.

Panyi, G., Varga, Z. and Gaspar, R. (2004a). Ion channels and lymphocyte activation. *Immunol. Lett.* **92**, 55-66.

Panyi, G., Vamosi, G., Bacso, Z., Bagdany, M., Bodnar, A., Varga, Z., Gaspar, R., Matyus, L. and Damjanovich, S. (2004b). Kv1.3 potassium channels are localized in the immunological synapse formed between cytotoxic and target cells. *Proc. Natl. Acad. Sci. USA* **101**, 1285-1290.

Rocheleau, J. M., Gage, S. D. and Kobertz, W. R. (2006). Secondary structure of a KCNE cytoplasmic domain. *J. Gen. Physiol.* **128**, 721-729.

Roepke, T. K., Kontogeorgis, A., Ovanez, C., Xu, X., Young, J. B., Purtell, K., Goldstein, P. A., Christini, D. J., Peters, N. S., Akar, F. G. et al. (2008). Targeted deletion of kcne2 impairs ventricular repolarization via disruption of I(K,slow1) and I(to,f). *FASEB J.* **22**, 3648-3660.

Sharma, N., Crane, A., Clement, J. P. t., Gonzalez, G., Babenko, A. P., Bryan, J. and Aguilar-Bryan, L. (1999). The C terminus of SUR1 is required for trafficking of KATP channels. *J. Biol. Chem.* **274**, 20628-20632.

Szabo, I., Adams, C. and Gulbins, E. (2004). Ion channels and membrane rafts in apoptosis. *Pflugers Arch.* **448**, 304-312.

Szabo, I., Bock, J., Grassme, H., Soddemann, M., Wilker, B., Lang, F., Zoratti, M. and Gulbins, E. (2008). Mitochondrial potassium channel Kv1.3 mediates Bax-induced apoptosis in lymphocytes. *Proc. Natl. Acad. Sci. USA* **105**, 14861-14866.

Um, S. Y. and McDonald, T. V. (2007). Differential association between HERG and KCNE1 or KCNE2. *PLoS ONE* **2**, e933.

Vicente, R., Escalada, A., Coma, M., Fuster, G., Sanchez-Tillo, E., Lopez-Iglesias, C., Soler, C., Solsona, C., Celada, A. and Felipe, A. (2003). Differential voltage-dependent K+ channel responses during proliferation and activation in macrophages. *J. Biol. Chem.* **278**, 46307-46320.

Vicente, R., Escalada, A., Soler, C., Grande, M., Celada, A., Tamkun, M. M., Solsona, C. and Felipe, A. (2005). Pattern of Kv beta subunit expression in macrophages depends upon proliferation and the mode of activation. *J. Immunol.* **174**, 4736-4744.

Vicente, R., Escalada, A., Villalonga, N., Texido, L., Roura-Ferrer, M., Martin-Satue, M., Lopez-Iglesias, C., Soler, C., Solsona, C., Tamkun, M. M. et al. (2006). Association of Kv1.5 and Kv1.3 contributes to the major voltage-dependent K+ channel in macrophages. *J. Biol. Chem.* **281**, 37675-37685.

Vicente, R., Villalonga, N., Calvo, M., Escalada, A., Solsona, C., Soler, C., Tamkun, M. M. and Felipe, A. (2008). Kv1.5 association modifies Kv1.3 traffic and membrane localization. *J. Biol. Chem.* **283**, 8756-8764.

Villalonga, N., Escalada, A., Vicente, R., Sanchez-Tillo, E., Celada, A., Solsona, C. and Felipe, A. (2007). Kv1.3/Kv1.5 heteromeric channels compromise pharmacological responses in macrophages. *Biochem. Biophys. Res. Commun.* **352**, 913-918.

Wulff, H. and Pennington, M. (2007). Targeting effector memory T-cells with Kv1.3 blockers. *Curr. Opin. Drug Discov. Devel.* **10**, 438-445.

Wulff, H., Beeton, C. and Chandy, K. G. (2003). Potassium channels as therapeutic targets for autoimmune disorders. *Curr. Opin. Drug Discov. Devel.* **6**, 640-647.

Zuzarte, M., Heusser, K., Renigunta, V., Schlichthorl, G., Rinne, S., Wischmeyer, E., Daut, J., Schwappach, B. and Preisig-Muller, R. (2009). Intracellular traffic of the K+ channels TASK-1 and TASK-3: role of N- and C-terminal sorting signals and interaction with 14-3-3 proteins. *J. Physiol.* **587**, 929-952.

Journal of Cell Science

AVÍS IMPORTANT

El text dels apartats 3.2.4 a 3.2.9 ha estat retirat seguint instruccions de l'autora de la tesi, en existir participació d'empreses, existir conveni de confidencialitat o existeix la possibilitat de generar patents

AVISO IMPORTANTE

El texto de los apartados 3.2.4 a 3.2.9 ha sido retirado siguiendo instrucciones de la autora, al existir participación de empresas, convenio de confidencialidad o la posibilidad de generar patentes.

IMPORTANT NOTICE

The text of sections from 3.2.4 to 3.2.9 has been withdrawn on the instructions of the author, as there is participation of undertakings, confidentiality agreement or the ability to generate patent

3.3. Block 3:

KCNE regulation in leukocytes

3.3.1. Resum de la contribució 7

Publicat a Commun Integr Biol, 2010, 3:166-8.

Existeix un paper fisiològic per a les subunitats KCNE en el sistema immunitari?

Laura Solé i Antonio Felipe

L'estudi de la modulació dels canals per subunitats reguladores ha atret considerablement l'atenció de molts investigadors. Existeixen evidències que indiquen un paper fonamental per a les proteïnes accessòries en el canalosoma. Així per exemple, aquestes subunitats reguladores són necessàries per tal de recapitular els corrents iònics registrats *in vivo* i també per tal d'entendre el paper fisiològic dels canals iònics. Els KCNEs són una família de subunitats reguladores que interaccionen amb un gran rang de canals. Prèviament, hem caracteritzat, per primer cop, la interacció entre KCNE4 i el canal de potassi dependent de voltatge Kv1.3. La associació amb KCNE4, el qual altera les propietats biofísiques, tràfic i localització de membrana del canal Kv1.3, funciona com un mecanisme dominant negatiu endogen. Degut a que ambdues proteïnes s'expressen en el sistema immunitari, els canals Kv1.3/KCNE4 podrien contribuir a regular de manera precisa la resposta immunitària. Per tant, els nostres resultats assenyalen a KCNE4 com a una nova diana per a la immunomodulació. KCNE4 però no és el únic KCNE que s'expressa en leucòcits. Tots els KCNEs (KCNE1-5) hi estan presents i alguns membres mostren una modulació de la seva expressió durant la proliferació i càncer. En resum, les subunitats reguladores KCNE s'expressen en el sistema immunitari. A més a més, alguns canals de potassi dependents de voltatge, que podrien interaccionar amb els KCNEs, també s'hi expressen. Per tant, les subunitats KCNE poden jugar un paper encara per descobrir en la fisiologia del sistema immunitari.

3.3.2. Report of the PhD student participation in the article

Informe de la participació de la doctoranda en l'article

Does a physiological role for KCNE subunits exist in the immune system?

Published in Communicative and Integrative Biology

Laura Solé Codina performed all the recompilation of the data and wrote this communication.

Laura Solé Codina va realitzar la recopil·lació de totes les dades incloses en aquest article i va escriure aquesta comunicació.

Thesis director

El director de la tesi

Dr. Antonio Felipe Campo

Communicative & Integrative Biology 3:2, 166-168; March/April 2010; © 2010 Landes Bioscience

Does a physiological role for KCNE subunits exist in the immune system?

Laura Solé and Antonio Felipe*

Molecular Physiology Laboratory; Departament de Bioquímica i Biologia Molecular; Institut de Biomedicina; Universitat de Barcelona; Barcelona, Spain

Key words: voltage-dependent potassium channels, KCNE4, $K_V1.3$, leukocytes, regulatory subunits

Submitted: 11/10/09

Accepted: 11/10/09

Previously published online: www.landesbioscience.com/journals/cib/article/10602

*Correspondence to: Antonio Felipe; Email: afelipe@ub.edu

Addendum to: Solé L, Roura-Ferrer M, Pérez-Verdaguer M, Oliveras A, Calvo M, Fernández-Fernández JM, Felipe A. KCNE4 suppresses $K_V1.3$ currents by modulating trafficking, surface expression and channel gating. J Cell Sci 2009; 122:3738–48; PMID: 19773357; DOI:10.1242/jcs.056689.

The study of channel modulation by regulatory subunits has attracted considerable attention. Evidence indicates a pivotal role for accessory proteins in the channelosome. For instance, these regulatory subunits are necessary to recapitulate in vivo ion currents and to further understand the physiological role of ion channels. KCNEs are a family of regulatory subunits that interact with a wide range of channels. We have described for the first time a molecular interaction between KCNE4 and the voltage-dependent potassium channel $K_V1.3$. The association of KCNE4, which alters the biophysical properties, trafficking and membrane localization of $K_V1.3$, functions as an endogenous dominant-negative mechanism. Since both proteins are expressed in the immune system, $K_V1.3$/KCNE4 channels may contribute to the fine-tuning of the immune response. Therefore, our results point to KCNE4 as a novel target for immunomodulation. KCNE4 is not the only KCNE which is expressed in leukocytes. All KCNEs (KCNE1-5) are present, and some members demonstrate modulation during proliferation and cancer. In summary, regulatory KCNE subunits are expressed in the immune system. In addition, several voltage-dependent K^+ channels, which could interact with KCNEs, are also detected. Therefore, KCNE subunits may play a yet undiscovered role in the physiology of the immune system.

KCNEs are a group of regulatory subunits composed of 5 members (KCNE1-5). KCNE peptides are small single spanning membrane proteins (<20 KDa) which modulate a large number of voltage-dependent K^+ channels.[1] The most well characterized interaction occurs with KCNQ1 ($K_V7.1$) channels.[2-4] $K_V7.1$/KCNE1 channels recapitulate the cardiac I_{ks} current.[5] Several KCNE1 mutations, which trigger severe cardiac channelopathies, demonstrate the pivotal function of KCNE1 on cardiovascular physiology.[6-8] The implication of that the remaining KCNE peptides may contribute to the modulation of I_{ks} is now under intense investigation.[9-13] Besides $K_V7.1$, KCNE members associate with other K^+ channels. Thus, $K_V11.1$ in association with KCNE2 conducts the cardiac I_{kr} current.[14]

Although many KCNE subunits share tissue expression with Shaker K^+ channels (K_V1) channels, KCNE interactions with K_V1 channels have attracted little research.[1] Early in 1992, $K_V1.3$ and KCNE1 were simultaneously cloned in human Jurkat T-cells.[15] Ten years later, Grunnet et al. (2003) described that KCNE4 modulates $K_V1.1$ and $K_V1.3$ channels and their heteromeric forms. However, while $K_V1.1$ and $K_V1.3$ biophysics were affected, $K_V1.1$ membrane surface targeting was not altered.[16] Later, Melman et al. (2004) described that KCNE1 co-immunoprecipitated with $K_V1.5$, but no further research was undertaken.[17] Recently, Abbot et al. (2008) demonstrated that *kcne2*$^{-/-}$ mice exhibit altered cardiac I_{kslow}, identified an interaction between $K_V1.5$ and KCNE2 in murine ventricles and suggested a functional role for KCNE2 in promoting $K_V1.5$ surface expression.[18]

In this context, our recent contribution unequivocally demonstrates molecular interactions between KCNE4 and $K_V1.3$,

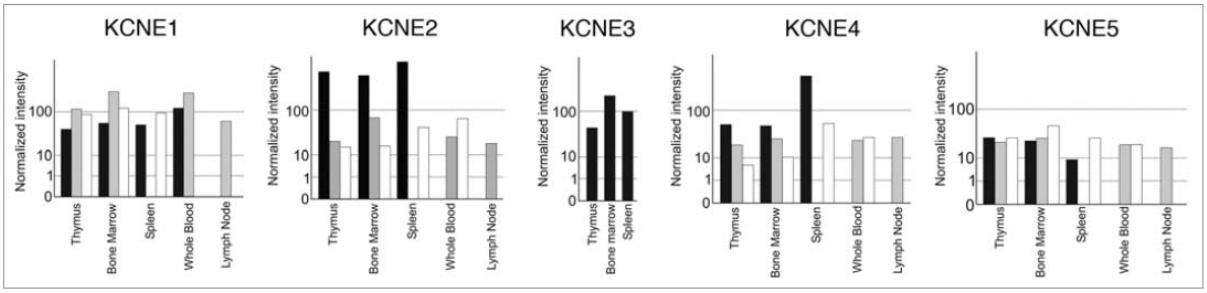

Figure 1. Human KCNE expression in healthy and cancer tissues. Affymetrix GeneChips HG-U95A-E (GeneNote, http://bioinfo2.weizmann.ac.il/cgi-bin/genenote/home_page.pl) and HG-U133A (GNF, (http://biogps.gnf.org) normalized as described in GeneCard (http://www.genecards.org). Black columns: healthy tissue (GeneNote); Grey columns: healthy tissues (GNF); White columns: cancer samples (GNF).

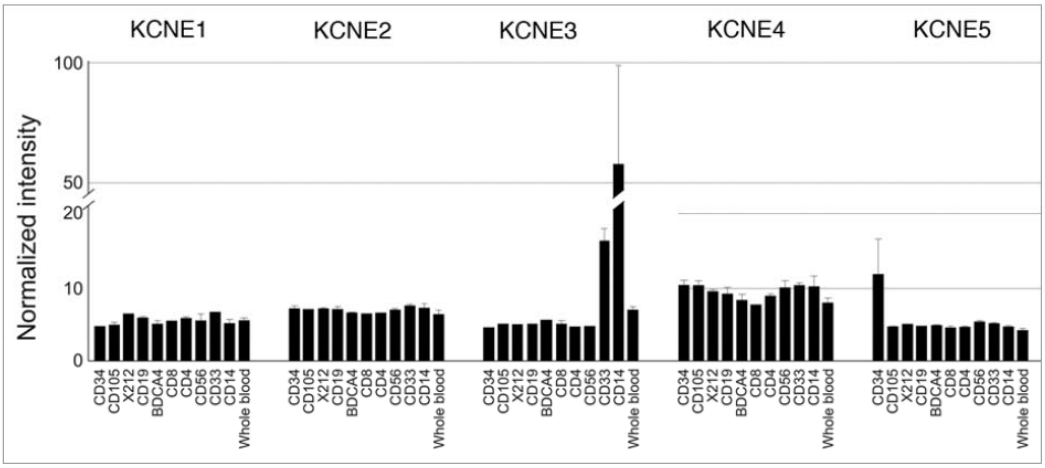

Figure 2. KCNE expression in human leukocytic cell lines. Array data from GNF BioGPS (http://biogps.gnf.org) normalized according to Su et al.[31] Legend: CD34, bone marrow CD34⁺ progenitors; CD105, endothelial; X212, B lymphoblasts; CD19, B cells; BDCA4, dendritic cells; CD8, CD8⁺ T-cells; CD4, CD4⁺ T-cells; CD56, NK cells; CD33, myeloid; CD14, monocytes.

which impairs the trafficking and localization of these channels.[19] KCNE4 acts as an endogenous dominant-negative regulatory subunit. Further inhibitory mechanisms by KCNE4 have been observed. Grunnet et al. (2002) describe that KCNE4 abrogates $K_V7.1$ currents.[20] Later, George and coworkers (2008) postulate that KCNE4 could form part of a $K_V7.1$/KCNE1 heterocomplex, responsible for downregulating the I_{ks} current.[10] Furthermore, KCNE4 also inhibits the calcium-activated K^+ channel ($K_{Ca}1.1$)[21] and oligomeric $K_V4.2$ + KChIP2 channels.[22]

Although limited, the immunitary system has a defined repertoire of K^+ channel genes. Leukocytes express, $K_V1.3$, $K_V1.5$ and several $K_V\beta$ regulatory subunits.[23-25] We have demonstrated that $K_V1.3$ and $K_V1.5$ form heteromeric complexes to fine-tune the immunitary response.[23,26] The evidence that KCNE4 is also implicated,[19] the presence of KCNE1 in lymphocytes,[15] and its putative association to $K_V1.5$,[17] suggest an unidentified role for KCNE peptides in immunitary system physiology.

In fact, our recent study is not the first to describe the presence of the KCNEs in the immunitary system. KCNE1 was cloned in T-lymphocytes.[15] Grunnet et al. (2003) found KCNE4 mRNA in lymphocytes.[16] In addition, KCNEs mRNA expression has also been investigated in thymus.[10,27] Here we recapitulate the information available about the expression of KCNE1-5 in different tissue arrays, all derived from the immune system. To that end, data from tissues and tumors, cell lines and cancer cell lines are shown in Figures 1, 2 and 3, respectively. All KCNE1-5 members have been detected in myeloid and lymphoid lineages. It is noteworthy that while KCNE1 expression increases in some cancers, KCNE2 and KCNE4 decrease. Similarly, KCNE1 induction has also been detected in germinal tumors.[28] We have previously described the importance of $K_V1.3$ during activation and proliferation of macrophages.[25,26] Although both processes augment $K_V1.3$, the channel seems to play a dual role. Prolonged signaling during activation triggers apoptosis.[29,30] Additionally, highly proliferative cells exhibit lower KCNE4 expression

than their counterparts do (Fig. 1). During an insult, $K_V1.3$ is activated and sustained activation triggers cell death. The persistence of activated macrophages during inflammation leads to disease. In this scenario, KCNE4 would exert an inhibitory effect not needed in proliferation. Accordingly, it is worth noting that during proliferation, most cells become resistant to apoptosis.

Evidence demonstrates that KCNE subunits are present in the immune system and may interact with K_V1 channels. Therefore, we suggest that KCNE subunits may play a yet undiscovered role in the immune system via associations with leukocyte K^+ channels. These new interactions situate KCNE, specifically KCNE4, as novel targets for immunomodulation. Further research should be undertaken to shed some light on this new issue.

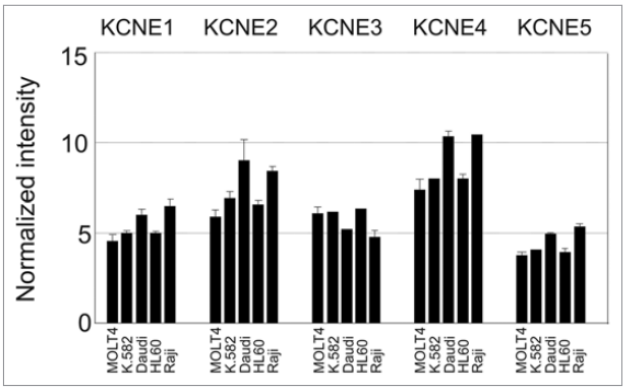

Figure 3. KCNE expression in different human leukemia and lymphoma cell lines. Array data from GNF BioGPS (http://biogps.gnf.org) normalized according to Su et al.[31] Legend: MOLT4, Lymphoblastic Leukemia; K.582, Chronic Myelogenous Leukemia; Daudi, Burkitt's Lymphoma; HL60, Promyelocytic Leukemia; Raji, Burkitt's Lymphoma.

Acknowledgements

The authors thank to all present and past members of the molecular physiology laboratory. Supported by the Ministerio de Ciencia e Innovación (MICINN), Spain (BFU2008-00431 and CSD2008-00005). L.S. is a fellow from MICINN.

References

1. McCrossan ZA, Abbott GW. The MinK-related peptides. Neuropharmacology 2004; 47:787-821.
2. Haitin Y, Wiener R, Shaham D, Peretz A, Cohen EB, Shamgar L, et al. Intracellular domains interactions and gated motions of I(KS) potassium channel subunits. EMBO J 2009; 28:1994-2005.
3. Chen J, Zheng R, Melman YF, McDonald TV. Functional interactions between KCNE1 C-terminus and the KCNQ1 channel. PLoS One 2009; 4:5143.
4. Kang C, Tian C, Sonnichsen FD, Smith JA, Meiler J, George AL Jr, et al. Structure of KCNE1 and implications for how it modulates the KCNQ1 potassium channel. Biochemistry 2008; 47:7999-8006.
5. Barhanin J, Lesage F, Guillemare E, Fink M, Lazdunski M, Romey G. K(V)LQT1 and lsK (minK) proteins associate to form the I(Ks) cardiac potassium current. Nature 1996; 384:78-80.
6. Schulze-Bahr E, Wang Q, Wedekind H, Haverkamp W, Chen Q, Sun Y, et al. KCNE1 mutations cause jervell and Lange-Nielsen syndrome. Nat Genet 1997; 17:267-8.
7. Splawski I, Tristani-Firouzi M, Lehmann MH, Sanguinetti MC, Keating MT. Mutations in the hminK gene cause long QT syndrome and suppress IKs function. Nat Genet 1997; 17:338-40.
8. Chiang CE, Roden DM. The long QT syndromes: genetic basis and clinical implications. J Am Coll Cardiol 2000; 36:1-12.
9. Lundquist AL, Manderfield LJ, Vanoye CG, Rogers CS, Donahue BS, Chang PA, et al. Expression of multiple KCNE genes in human heart may enable variable modulation of I(Ks). J Mol Cell Cardiol 2005; 38:277-87.
10. Manderfield LJ, George AL Jr. KCNE4 can co-associate with the I(Ks) (KCNQ1-KCNE1) channel complex. Febs J 2008; 275:1336-49.
11. Tseng GN. The phenotype of a KCNQ1 mutation depends on its KCNE partners: is the cardiac slow delayed rectifier (IKs) channel more than a KCNQ1/KCNE1 complex? Heart Rhythm 2007; 4:1542-3.
12. Morin TJ, Kobertz WR. A derivatized scorpion toxin reveals the functional output of heteromeric KCNQ1-KCNE K^+ channel complexes. ACS Chem Biol 2007; 2:469-73.
13. Bendahhou S, Marionneau C, Haurogne K, Larroque MM, Derand R, Szuts V, et al. In vitro molecular interactions and distribution of KCNE family with KCNQ1 in the human heart. Cardiovasc Res 2005; 67:529-38.
14. Abbott GW, Sesti F, Splawski I, Buck ME, Lehmann MH, Timothy KW, et al. MiRP1 forms IKr potassium channels with HERG and is associated with cardiac arrhythmia. Cell 1999; 97:175-87.
15. Attali B, Romey G, Honore E, Schmid-Alliana A, Mattei MG, Lesage F, et al. Cloning, functional expression, and regulation of two K^+ channels in human T lymphocytes. J Biol Chem 1992; 267:8650-7.
16. Grunnet M, Rasmussen HB, Hay-Schmidt A, Rosenstierne M, Klaerke DA, Olesen SP, Jespersen T. KCNE4 is an inhibitory subunit to $K_V1.1$ and $K_V1.3$ potassium channels. Biophys J 2003; 85:1525-37.
17. Melman YF, Um SY, Krumerman A, Kagan A, McDonald TV. KCNE1 binds to the KCNQ1 pore to regulate potassium channel activity. Neuron 2004; 42:927-37.
18. Roepke TK, Kontogeorgis A, Ovanez C, Xu X, Young JB, Purtell K, et al. Targeted deletion of kcne2 impairs ventricular repolarization via disruption of I(K,slow1) and I(to,f). Faseb J 2008; 22:3648-60.
19. Sole L, Roura-Ferrer M, Perez-Verdaguer M, Oliveras A, Calvo M, Fernandez-Fernandez JM, Felipe A. KCNE4 suppresses $K_V1.3$ currents by modulating trafficking, surface expression and channel gating. J Cell Sci 2009; 122:3738-48.
20. Grunnet M, Jespersen T, Rasmussen HB, Ljungstrom T, Jorgensen NK, Olesen SP, Klaerke DA. KCNE4 is an inhibitory subunit to the KCNQ1 channel. J Physiol 2002; 542:119-30.
21. Levy DI, Wanderling S, Biemesderfer D, Goldstein SA. MiRP3 acts as an accessory subunit with the BK potassium channel. Am J Physiol Renal Physiol 2008; 295:380-7.
22. Radicke S, Cotella D, Graf EM, Banse U, Jost N, Varro A, et al. Functional modulation of the transient outward current Ito by KCNE beta-subunits and regional distribution in human non-failing and failing hearts. Cardiovasc Res 2006; 71:695-703.
23. Vicente R, Escalada A, Villalonga N, Texido L, Roura-Ferrer M, Martin-Satue M, et al. Association of $K_V1.5$ and $K_V1.3$ contributes to the major voltage-dependent K^+ channel in macrophages. J Biol Chem 2006; 281:37675-85.
24. Vicente R, Escalada A, Soler C, Grande M, Celada A, Tamkun MM, et al. Pattern of K_V beta subunit expression in macrophages depends upon proliferation and the mode of activation. J Immunol 2005; 174:4736-44.
25. Vicente R, Escalada A, Coma M, Fuster G, Sanchez-Tillo E, Lopez-Iglesias C, et al. Differential voltage-dependent K^+ channel responses during proliferation and activation in macrophages. J Biol Chem 2003; 278:46307-20.
26. Villalonga N, Escalada A, Vicente R, Sanchez-Tillo E, Celada A, Solsona C, Felipe A. $K_V1.3/K_V1.5$ heteromeric channels compromise pharmacological responses in macrophages. Biochem Biophys Res Commun 2007; 352:913-8.
27. Lundquist AL, Turner CL, Ballester LY, George AL Jr. Expression and transcriptional control of human KCNE genes. Genomics 2006; 87:119-28.
28. Tsevi I, Vicente R, Grande M, Lopez-Iglesias C, Figueras A, Capella G, et al. KCNQ1/KCNE1 channels during germ-cell differentiation in the rat: expression associated with testis pathologies. J Cell Physiol 2005; 202:400-10.
29. Detre C, Kiss E, Varga Z, Ludanyi K, Paszty K, Enyedi A, et al. Death or survival: membrane ceramide controls the fate and activation of antigen-specific T-cells depending on signal strength and duration. Cell Signal 2006; 18:294-306.
30. Szabo I, Adams C, Gulbins E. Ion channels and membrane rafts in apoptosis. Pflugers Arch 2004; 448:304-12.
31. Su AI, Wiltshire T, Batalov S, Lapp H, Ching KA, Block D, et al. A gene atlas of the mouse and human protein-encoding transcriptomes. Proc Natl Acad Sci USA 2004; 101:6062-7.

3.3.4. Resum de la contribució 8

Publicat a Channels, 2013, 7:85-96.

L'expressió gènica dels KCNEs depèn de la proliferació i la manera d'activació dels leucòcits.

Laura Solé, Albert Vallejo-Gracia, Sara R. Roig, Antonio Serrano-Albarràs, Laura Marruecos, Joan Manils, Diana Gómez, Concepció Soler i Antonio Felipe.

Els canals de potassi dependents de voltatge (Kv) estan regulats de manera molt precisa durant la resposta immunitària. Tot i que els leucòcits expressen un repertori limitat de canals Kv, el seu paper fisiològic encara és motiu d'intenses investigacions. Un canal Kv funcional es un complex oligomèric format per subunitats formadores del porus i subunitats reguladores. La família de gens KCNE es un grup relativament nou de subunitats moduladores del sistema immunitari dels canals Kv. En aquest treball, hem caracteritzat l'expressió gènica dels KCNEs(1-5) en els leucòcits i investigat la seva regulació durant la proliferació leucocitària i davant diferents tipus d'activació. S'ha analitzat l'expressió dels KCNEs en macròfags murins derivats del moll de l'ós (BMDMs), limfòcits T humans (Jurkat), i cèl·lules B humanes (Raji). Els KCNEs (1-5) s'expressen en les tres línies leucocitàries. La majoria de mARNs dels KCNEs presenten una regulació depenent del cicle cel·lular i són regulats de manera diferencial sota diferents estímuls. Els nostres resultats suggereixen un nou i encara per descobrir paper fisiològic de les subunitats KCNE en el sistema immunitari. Les múltiples associacions d'aquestes subunitats reguladores amb els canals Kv podrien donar lloc a una gran varietat de canals funcionals diferents, tant a nivell biofísic com farmacològic, que podrien regular de manera precisa la resposta immunològica.

3.3.5. Report of the PhD student participation in the article

Informe de la participació de la doctoranda en l'article

KCNE gene expression is dependent on the proliferation and mode of activation of leukocytes

Published in Channels, **Impact Factor (2012): 2.14**

Laura Solé Codina performed all the cDNA synthesis and the KCNEs RT-PCR experiments in BMDC and the RT-PCR analysis corresponding of KCNE4 of Raji and Jurkat cell lines.

Laura Solé Codina va realitzar la síntesi de cDNA i els experiments de RT PCR de BMDC de tots els KCNEs i les RT PCRs corresponents a KCNE4 en cèl·lules Raji i Jurkat.

Thesis director

El director de la tesi

Dr. Antonio Felipe Campo

RESEARCH PAPER

Channels 7:2, 1–12; March/April 2013; © 2013 Landes Bioscience

KCNE gene expression is dependent on the proliferation and mode of activation of leukocytes

Laura Solé,[1] Albert Vallejo-Gracia,[1] Sara R. Roig,[1] Antonio Serrano-Albarrás,[1] Laura Marruecos,[2] Joan Manils,[2] Diana Gómez,[2] Concepció Soler[2] and Antonio Felipe[1,*]

[1]Molecular Physiology Laboratory; Departament de Bioquímica i Biologia Molecular; Institut de Biomedicina; Universitat de Barcelona; Barcelona, Spain; [2]Departament de Patologia i Terapèutica Experimental; Facultat de Medicina; Campus de Bellvitge; Universitat de Barcelona; L'Hospitalet de Llobregat; Barcelona, Spain

Keywords: voltage-dependent potassium channels, gene expression, macrophages, lymphocytes, cell-cycle, activation, regulatory subunits

Voltage-dependent K^+ (Kv) channels are tightly regulated during the immune system response. Leukocytes have a limited repertoire of Kv channels, whose physiological role is under intense investigation. A functional Kv channel is an oligomeric complex composed of pore-forming and ancillary subunits. The KCNE gene family is a novel group of modulatory Kv channel elements in leukocytes. Here, we characterized the gene expression of KCNEs (1–5) in leukocytes and investigated their regulation during leukocyte proliferation and mode of activation. Murine bone-marrow-derived macrophages, human Jurkat T-lymphocytes and human Raji B-cells were analyzed. KCNEs (1–5) are expressed in all leukocytes lineages. Most KCNE mRNAs show cell cycle-dependent regulation and are differentially regulated under specific insults. Our results further suggest a new and yet undefined physiological role for KCNE subunits in the immune system. Putative associations of these ancillary proteins with Kv channels would yield a wide variety of biophysically and pharmacologically distinct channels that fine-tune the immunological response.

Introduction

Voltage-dependent potassium (Kv) channels play an important role in determining resting membrane potential and controlling action potentials in nerves and muscles.[1] In addition, Kv channels control the proliferation and activation of macrophages and lymphocytes.[2,3] Leukocytes have a limited repertoire of Kv channels, which include Kv1.3, Kv1.5 and Kv11.1, which are major determinants of cell physiology.[4] While Kv1.3 is ubiquitous in the immune system, Kv1.5 functions primarily in mononuclear phagocytes and Kv11.1 in lymphoblastoid proliferative cells.[5-8] In addition, other Kv channels play minor roles and have also been detected in specific cell subtypes.[9,10] Many Kv channels can assemble promiscuously, yielding a wide variety of biophysically and pharmacologically distinct channels. Therefore, native currents are not necessarily recapitulated through the activity of a single subunit. Furthermore, the presence of regulatory subunits enhances this complexity.[11]

Kvβ regulatory subunits might modulate Kv1.3 and Kv1.5 channels.[11-13] These ancillary peptides are expressed in lymphocytes and macrophages and can form heteromeric structures.[12,13] Different *Kv*β genes, namely *Kv*β*1, Kv*β*2* and *Kv*β*3*, generate Kvβ proteins that are differentially regulated through leukocyte proliferation and activation.[11] The association of different Kvβ subunits with Kv1.3 and Kv1.5 channels generates distinct functional Kv channel complexes that fine-tune the cellular response.[11-13] There has been a massive effort by the research community to characterize Kv channels; however, there are few studies concerning regulatory subunits in leukocytes.[11-13] The recent identification of novel modulatory proteins has attracted much attention.

KCNEs are a group of regulatory subunits composed of 5 members (KCNE1–5).[14] KCNE peptides are single-span membrane proteins that modulate many Kv channels. Characterized interactions, such as Kv7.1 (KCNQ1)/KCNE1 and Kv11.1 (hERG)/KCNE2 channels, recapitulate the cardiac I_{ks} and I_{kr} currents, respectively.[14] Several KCNE mutations trigger severe cardiac channelopathies and demonstrate the pivotal role of these ancillary peptides in cardiovascular physiology. The implication of KCNE3–5 peptides in cardiac physiology is under intense investigation.[15] Although many KCNE subunits share tissue expression with Kv1 channels, their interactions need to be defined. Thus, Kv1.3 and KCNE1 were simultaneously cloned in human Jurkat T-cells.[16] It was shown that KCNE4 modulates Kv1.1 and Kv1.3 channels and their heteromeric forms.[17] Furthermore, an interaction between KCNE2 with Kv1.5 and Kv1.3 in murine ventricles and choroid plexus epithelium has been proposed.[18,19]

*Correspondence to: Antonio Felipe; Email: afelipe@ub.edu
Submitted: 10/05/12; Revised: 12/13/12; Accepted: 12/13/12
http://dx.doi.org/10.4161/chan.23258

Scarce information is available concerning the role of KCNE peptides in leukocytes. We recently demonstrated that KCNE4 associates with Kv1.3, suppressing K^+ currents through modulations in trafficking, surface expression and channel gating.[20] Although few preliminary screenings support a KCNE variable phenotype, there have been no KCNE regulation studies involving the immune system.[21] Therefore, the aim of the present work was to identify the presence of KCNE regulatory subunits in leukocytes and further characterize their expression during leukocyte proliferation and activation. We demonstrate that macrophages and T- and B- lymphocytes express KCNE subunits. In addition, the expression of many KCNE proteins is cell cycle dependent, and distinct cell-specific insults differentially regulate KCNE expression. In summary, leukocytes express KCNE regulatory subunits, and their expression varies with proliferation and activation; therefore, we suggest that the heteromeric Kv channel structure might be variable.

Results

Regulation of KCNE modulatory subunits through MCSF-dependent proliferation and LPS- and IFNγ-induced activation in macrophages. Macrophages perform critical functions in the immune system, acting as regulators of homeostasis and effector cells in infection, wounding, and tumor growth. In response to different growth factors and cytokines, macrophages proliferate and become activated or differentiated.[22] We used BMDM as a cell model that mimics the physiological schedule within the body. Mature cells might proliferate or become activated after the application of specific stimuli, such as M-CSF, which is a specific growth factor for this cell type.[22] After incubation of BMDMs for 18–24 h in the absence of MCSF, cell growth was terminated (> 98%) and the cells became quiescent.[3,22] The addition of M-CSF (1200 U/ml) triggered macrophage proliferation and an increase of the outward K^+ currents (**Fig. 1A and Fig. S1**).[3,12,22] Although BMDMs expressed all five KCNE subunits, different cell cycle-dependent patterns were observed (**Fig. 1B–G**). KCNE2, KCNE4 and KCNE5 notably increased at 6 h during the early phases (G1/S) of the cell cycle (**Fig. 1C, E and F**). In contrast, KCNE3 exhibited the opposite behavior (**Fig. 1D**), and KCNE1 levels remained constant throughout the cell cycle (**Fig. 1B**). Therefore, proliferation generated major differences in the KCNE phenotype (**Fig. 1G**).

The incubation of bone marrow macrophages with LPS and IFN-γ inhibits cell proliferation.[22,23] However, while LPS triggers apoptosis, IFN-γ protects the cells from programmed cell death.[23,24] **Figure 2** shows that after 24 h of IFN-γ-induced activation (300 U/ml), confirmed by iNOS abundance (**Fig. 2A**),[25] the expression of the KCNE subunits was relatively stable. Moreover, a gradual decrease of KCNE3 expression was also observed (**Fig. 2D**), while the other KCNEs experienced only minor changes in expression (**Fig. 2B–F**). Similar to proliferation, KCNE4 and KCNE5 were the most abundant subunits, and KCNE3 was the least abundant subunit (**Fig. 2G**).

The addition of 100 ng/ml LPS to proliferating macrophages elevated K^+ currents (**Fig. S1**), induced the expression of iNOS (**Fig. 3A**), blocks the cell cycle at the G1/S boundary and induces apoptosis.[23] Under this treatment, the expression of not only KCNE3 but also KCNE4 and apparently, but not significantly, KCNE2 was also reduced (**Fig. 3B-F**). However, the KCNE phenotype in LPS-treated macrophages was similar to that observed with IFN-γ. Thus, KCNE4 and KCNE5 were the most abundant subunits, whereas KCNE3 was least abundant (**Fig. 3G**).

KCNE regulatory subunits during the proliferation and LPS- and PMA-induced activation of Raji B-lymphocytes. Human B-lymphocytes express Kv1.3 and Kv11.1 channels that might be associated with KCNE subunits.[4] Raji B-lymphocytes are a lymphoblast-like cell line derived from Burkitt's B-cell lymphoma. Although neoplastic proliferation increases the expression of Kv1.3 and Kv11.1, no information is available concerning the KCNE subunits.[8] Unlike macrophages, activated B cells undergo proliferation and differentiation into memory and plasma cells. We first analyzed the expression of KCNE subunits in resting Raji B-lymphocytes. The abundance of KCNE subunits in B-cells starved for 24 h indicated that the expression of KCNE1 and KCNE4 was extremely low (**Fig. 4G**). FBS-dependent proliferation triggered the differential regulation of KCNEs subunits (**Fig. 4A–F**). While KCNE2, KCNE3 and, to a lesser extent, KCNE4 showed decreased expression after 24 h, the expression of KCNE1 and KCNE5 remained constant (**Fig. 4B–F**). However, the KCNE profile in B-cells throughout the cell cycle progression was mostly stable and after 24 h, the KCNE phenotype was recovered to that observed at the initial stage (**Fig. 4G**).

Raji B-lymphocytes, incubated with LPS (100 μg/ml), became activated as confirmed by the expression of TNFα (**Fig. 5A**).[26] However, after 24 h of LPS-induced activation, no major changes in the KCNE profile were observed (**Fig. 5B–G**). In addition, 10 nM PMA activation, which also elevated TNFα expression (**Fig. 6A**),[27] did not trigger apparent changes in KCNE expression (**Fig. 6B–F**). As a consequence, and similar to the results obtained with LPS-induced activation, no major differences in the KCNE profile were observed (**Fig. 6G**).

KCNE regulatory subunits during the proliferation and PMA/PHA-induced activation of Jurkat T-lymphocytes. Human T-lymphocytes expressing a limited repertoire of Kv1 channels, which include Kv1.1, Kv1.4, Kv1.6 and Kv1.3.[9,28] Kv1.3 and KCNE1, were isolated simultaneously in Jurkat T-cells, and KCNE4 regulates Kv1.1 and Kv1.3.[16,17,20] Although we observed the expression of all KCNE transcripts in Jurkat T-cells, surprisingly, KCNE1 was, by far, the less abundant KCNE subunit in Jurkat cells (**Fig. 7G**). Unlike KCNE1, KCNE3 and KCNE5, FBS-dependent proliferation (**Fig. 7A**) triggered a cell cycle-dependent increase of KCNE2 and KCNE4 expression (**Fig. 7B-F**). Compared with the relative abundance among KCNE subunits under FBS-dependent proliferation, the higher increase corresponded with KCNE4 expression. However, the KCNE profile experienced minor changes (**Fig. 7G**).

The combination of PHA (5 μg/ml) and PMA (80 nM) triggers an important activation of Jurkat T-cells[28] reflected by the massive production of IL-2 (**Fig. 8A**). Under these circumstances, an important remodeling of KCNE mRNA expression

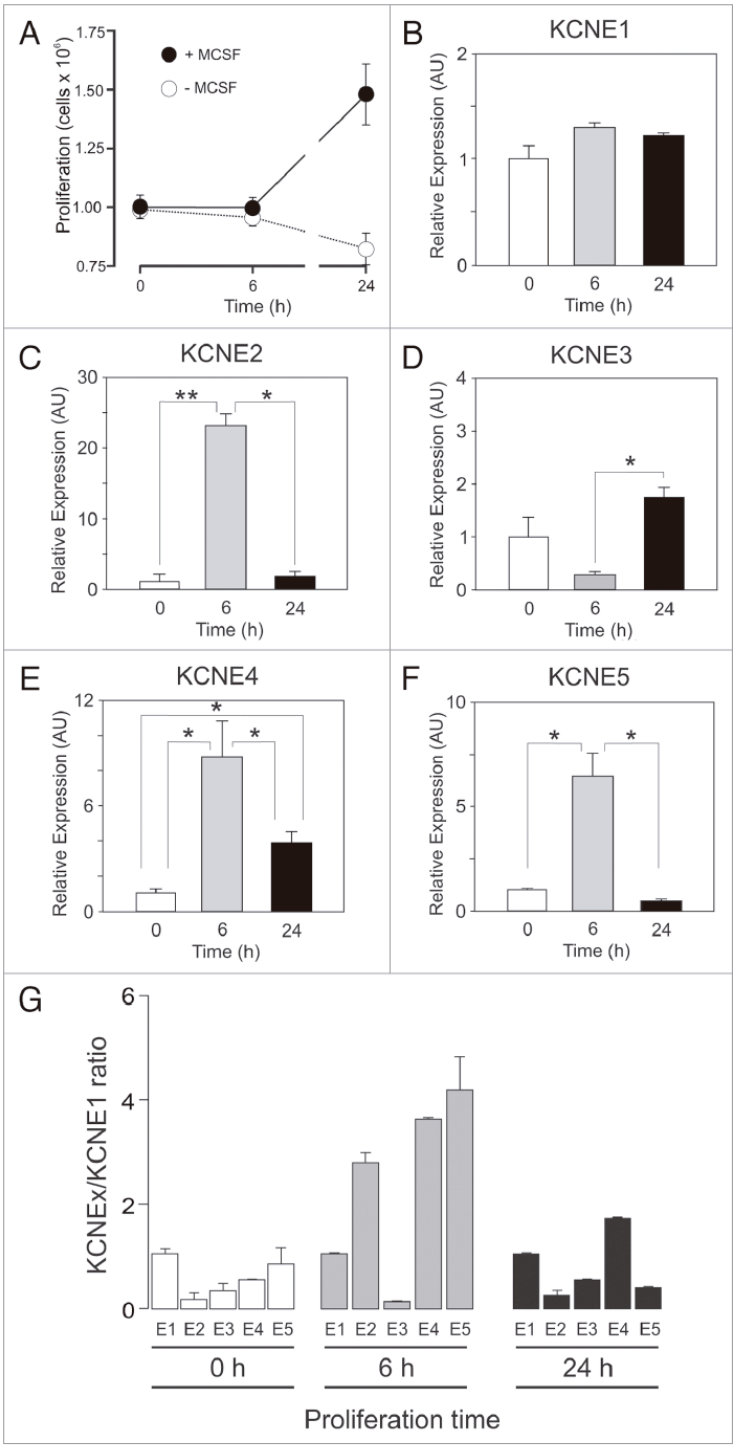

Figure 1. Expression and regulation of KCNE (1–5) mRNA in MCSF-dependent BMDM proliferation. G_0-arrested BMDMs were incubated in the presence of 1200 U/ml MCSF, and the mRNA was isolated simultaneously after the indicated times of treatment. Real-time PCR was performed as described in the Materials and Methods. (**A**) MCSF-dependent proliferation of BMDM. The values are given as the mean ± SEM and represent cell number of four independent experiments each performed in triplicate. ●, + MCSF; ○, - MCSF. (**B–F**) Relative mRNA expression, in arbitrary units (AU), of KCNE1–5. (**B**) KCNE1; (**C**) KCNE2; (**D**) KCNE3; (**E**) KCNE4; (**F**) KCNE5. The values are given as the mean ± SEM ($n = 3–6$). *, $p < 0.05$; **, $p < 0.01$ (Student's t test). (**G**) KCNEx/KCNE1 ratio. The relative expression of each KCNE and the KCNEx/KCNE1 ratio was calculated using the KCNE specific real-time PCR efficiency. See Materials and Methods for details. White bars, 0 h; gray bars, 6 h; black bars, 24 h of MCSF-dependent proliferation.

was observed (Fig. 8B–G). Again, KCNE1, the less abundant subunit, remained constant (Fig. 8B and G). However, the KCNE4 mRNA expression, which was initially low, showed an increase under PHA/PMA incubation (Fig. 8E and G). Moreover, the expression of KCNE5 and, to a lesser extent, KCNE3 steadily increased (Fig. 8D and F). In contrast, KCNE2 expression was significantly decreased (Fig. 8C). Our results demonstrated that the expression of KCNE4 was, by far, the major regulated under PMA/PHA-induced activation (Fig. 8G).

Discussion

Kv channels are involved in maintaining resting membrane potential and participate in the immune system response.[2,5] In nerve and muscle cells, native K^+ currents are not recapitulated through single-channel genes. Therefore, the hetero-oligomerization of related Kv subunits and their association with regulatory peptides to form functional channelosomes is crucial for cell physiology.[12,29] Leukocytes have a limited Kv repertoire that remains elusive. Kv channels in the immune system might be formed through associations between Kv products and auxiliary subunits, which enormously increase the K^+ current phenotype and fine-tune the immunological response.[12] Thus, Kv1.3 and Kv1.5, and Kv11.1 channels have been implicated as important targets in leukocyte physiology.[5,7,8,30] In addition, Kv1.1, Kv1.2, Kv1.6, Kv3.1 and Kv7.1 have also been detected in

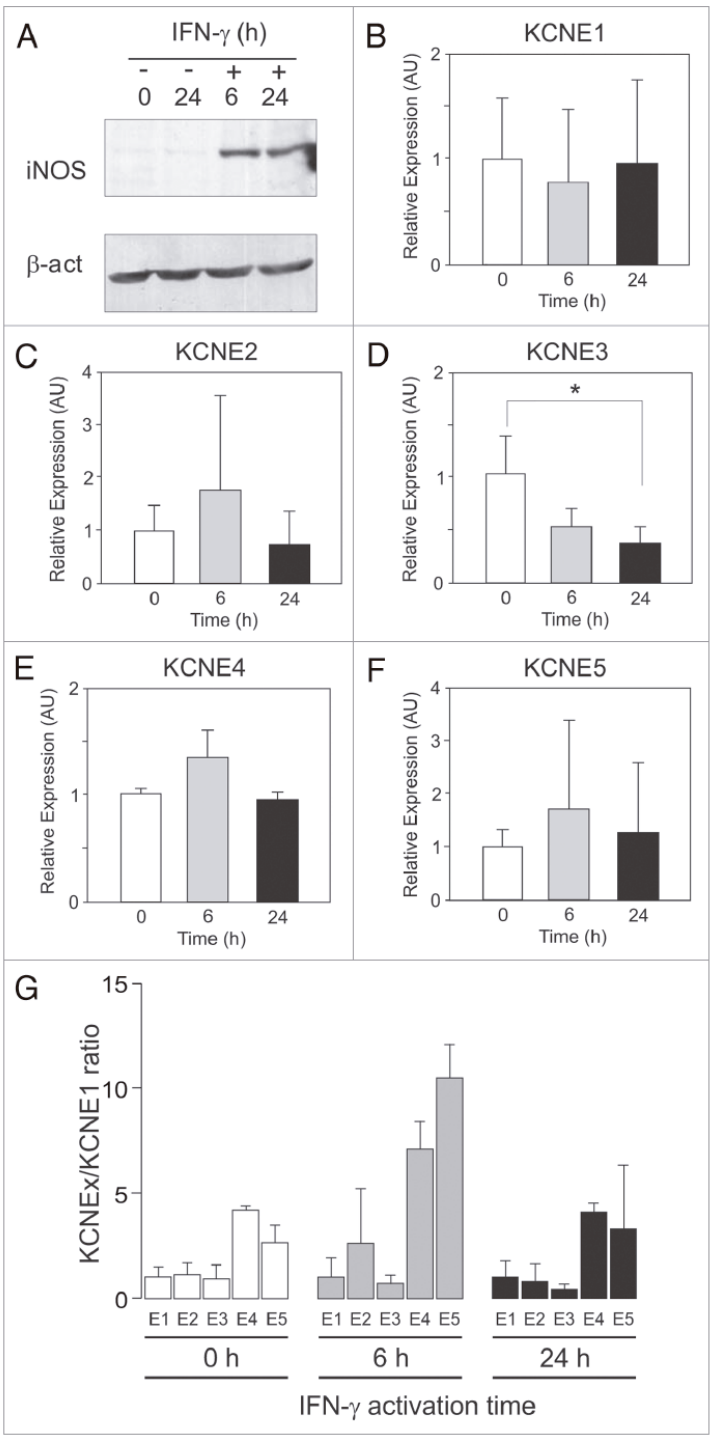

Figure 2. Expression and regulation of KCNE (1–5) mRNA in IFN-γ-activated BMDMs. BMDMs were incubated in the presence of IFN-γ (300 U/ml), and the mRNA was isolated simultaneously after the indicated times of treatment. Real-time PCR was performed as described in Materials and Methods. (**A**) Representative western blot of iNOS expression. Cells were incubated in the presence (+) or the absence (-) of IFN-γ and proteins were isolated at different times. β-actin was used as loading and transfer control. (**B–F**) Relative mRNA expression, in arbitrary units (AU), of KCNE1–5. (**B**) KCNE1; (**C**) KCNE2; (**D**) KCNE3; (**E**) KCNE4; (**F**) KCNE5. The values are given as the mean ± SEM (n = 3–6). *, $p < 0.05$ (ANOVA and post-hoc Tukey's test). (**G**) KCNEx/KCNE1 ratio. The relative expression of each KCNE and the KCNEx/KCNE1 ratio was calculated using the KCNE specific real-time PCR efficiency. See Materials and Methods for details. White bars, 0 h; gray bars, 6 h; black bars, 24 h in the presence of IFN-γ.

specific leukocytes.[7,10,31] The oligomerization of several of these subunits might contribute to the diversity of K^+ currents, but the participation of modulatory subunits must also be considered. Regulatory Kv subunits are primarily distributed into three main groups: (1) the Kvβ subunit gene family, with three major gene products, *Kvβ1*, *Kvβ2* and *Kvβ3*;[11] (2) the KCNE family, which comprises five different members (KCNE1–5);[14] and (3) the potassium channel-interacting (KChip) and potassium channel-accessory (KChap) proteins, which form an heterogeneous group of peptides.[32,33] While the last group is primarily considered as a collection of chaperones, which almost exclusively modulate the level of channel surface expression, the former groups also control kinetics. There is a considerable amount of data concerning the Kvβ interaction with Kv channels and the identification of these subunits in leukocytes. However, the presence and the regulation of KCNE subunits in the immune system have not been thoroughly addressed, although sound evidence indicates that KCNE peptides might modulate leukocytic Kv channels.[21]

The present work is the first to systematically analyze the expression of KCNE1–5 mRNA in differentiated leukocytes, such as macrophages and B- and T-lymphocytes. Although all leukocytes expressed KCNE1–5, the mRNA abundance varied among the cell lineage. Preliminary and heterogeneous affymetrix gene chip studies have previously addressed this issue leading to controversial interpretations as discussed below (see Supplemental Online Information for details). In this context, our study paves the way for further

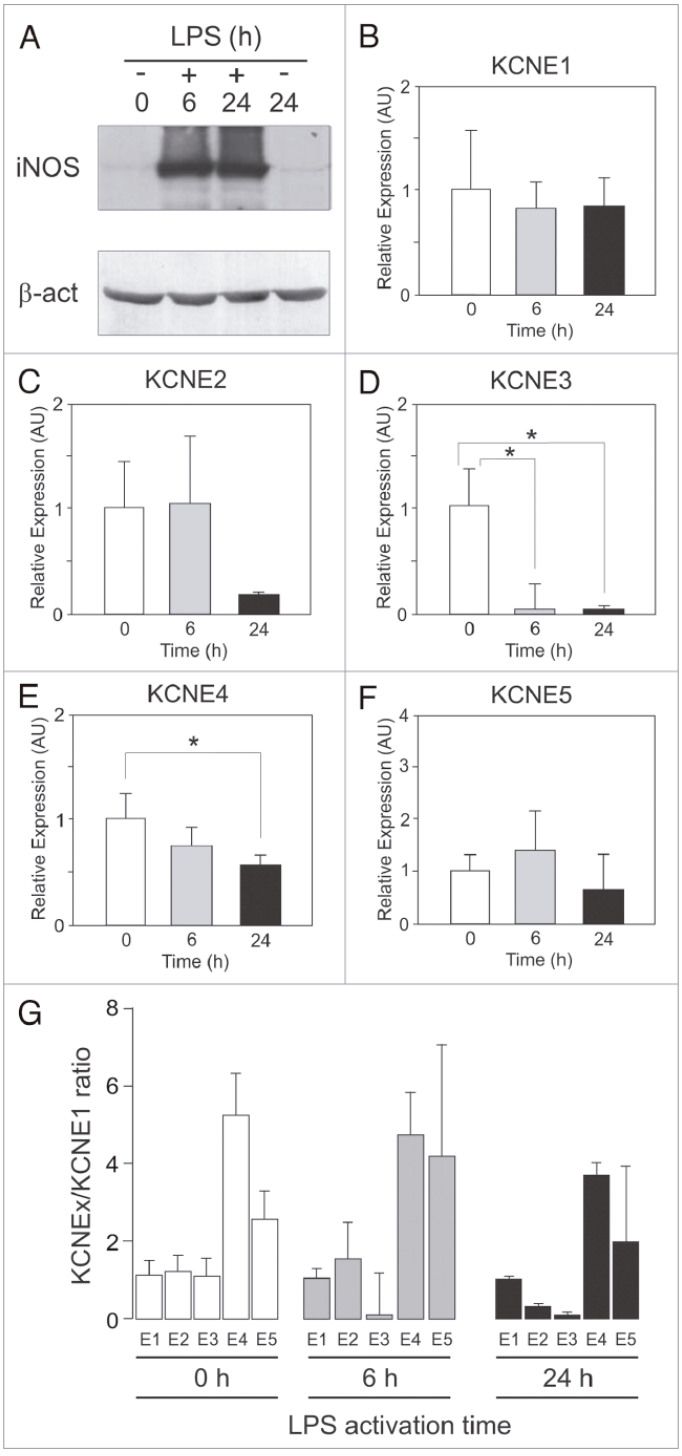

Figure 3. Expression and regulation of KCNE (1–5) mRNA in LPS-activated BMDMs. BMDMs were incubated in the presence of LPS (100 ng/ml), and the mRNA was isolated simultaneously after the indicated times of treatment. Real-time PCR was performed as described in Materials and Methods. (**A**) Representative western blot of iNOS expression. Cells were incubated in the presence (+) or the absence (-) of LPS and proteins were isolated at different times. β-actin was used as loading and transfer control. (**B–F**) Relative mRNA expression, in arbitrary units (AU), of KCNE1–5. (**B**) KCNE1; (**C**) KCNE2; (**D**) KCNE3; (**E**) KCNE4; (**F**) KCNE5. Values are the mean ± SEM (n = 3–6). *, $p < 0.05$ in KCNE3 (Student's t test). *, $p < 0.05$ in KCNE4 (ANOVA and post-hoc Tukey's test). (**G**) KCNEx/KCNE1 ratio. The relative expression of each KCNE and the KCNEx/KCNE1 ratio was calculated using the KCNE specific real-time PCR efficiency. See Materials and Methods for details. White bars, 0 h; gray bars, 6 h; black bars, 24 h in the presence of LPS.

research. However, our work relies on the KCNE gene expression and possible post-transcriptional modifications should be contemplated for future research.

Because Kv channels play crucial roles in the immune response, we further studied KCNE mRNA regulation upon leukocyte proliferation and activation. A few studies have documented the expression of KCNE subunits in the immune system, but show contradictory results. In 1992, Attali and coworkers isolated KCNE1 from Jurkat T-cells, but reported no changes upon activation.[16] Chouabe et al. (1997) confirmed the expression of KCNE1 in peripheral blood leukocytes but observed no expression in the spleen and thymus.[34] The results of these pioneering studies have led to controversial debates concerning which cell lineage expresses KCNE1, and what state of differentiation/maturation/activation is required to detect KCNE1 expression. Here, we further confirmed that KCNE1 expression, which is scarcely detected, remained almost consistent upon proliferation or under various insults in macrophages and B and T-lymphocytes. Our results are consistent with those of Lunquist et al. (2006) who demonstrated that the KCNE1 mRNA is the least abundant subunit in thymus, spleen and peripheral leukocytes.[35] However, the array data from different sources support contradictory results, arguing that there is similar mRNA expression among the KCNEs, with no changes in neoplastic growth between the lineages (GeneChips from GeneNote, http://bioinfo2.weizmann.ac.il/cgi-bin/genenote/home_page.pl and GNF BioGPS, http://biogps.gnf.org, see supplemental material for extended information). This could be characteristic of the immune system because the upregulation of KCNE1 has been previously shown under neoplastic growth in other tissues.[36,37] Similar differential tissue-specific

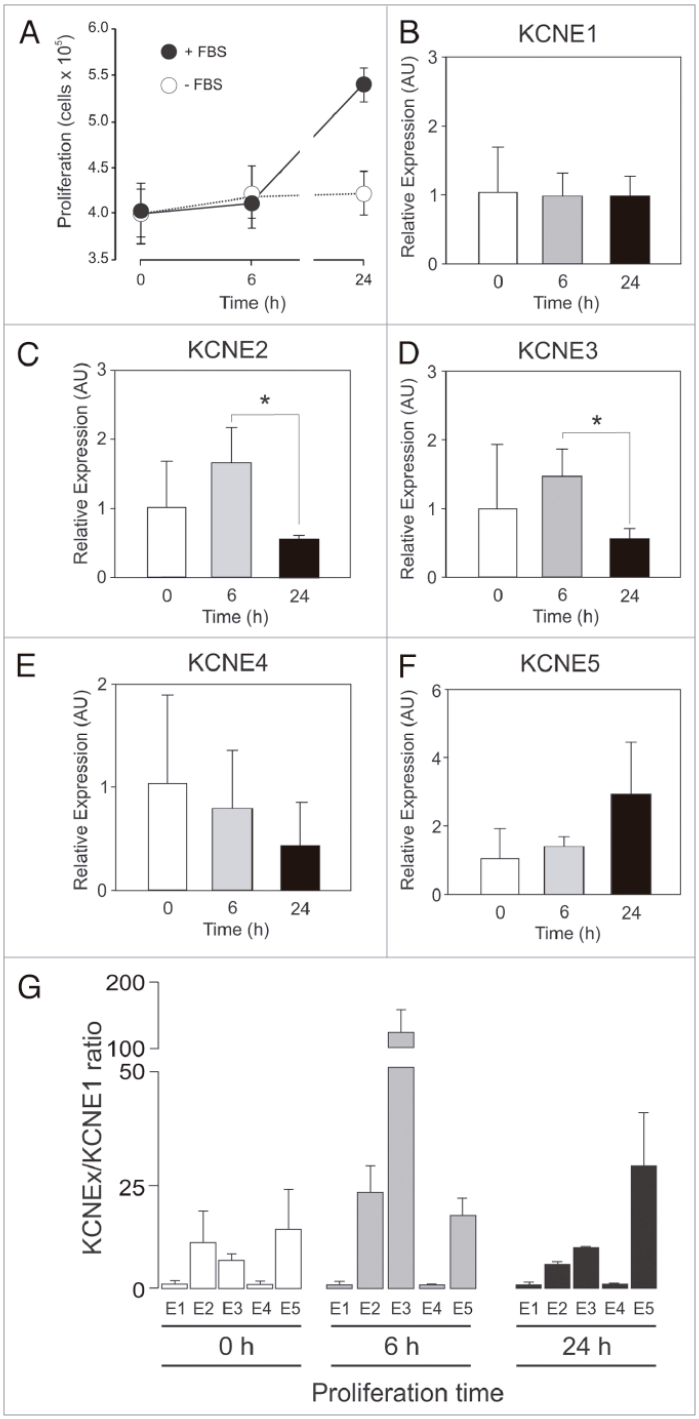

Figure 4. Expression and regulation of KCNE (1–5) mRNA in FBS-dependent Raji B-lymphocytes proliferation. G_0-arrested B-cells were incubated in the presence of FBS, and the mRNA was isolated simultaneously after the indicated times of treatment. Real-time PCR was performed as described in Materials and Methods. (**A**) FBS-dependent proliferation of Raji B-cells. The values are given as the mean ± SEM and represent cell number of four independent experiments each performed in triplicate. ●, + FBS; ○, - FBS. (**B–F**) Relative mRNA expression, in arbitrary units (AU), of KCNE1–5. (**B**) KCNE1; (**C**) KCNE2; (**D**) KCNE3; (**E**) KCNE4; (**F**) KCNE5. The values are given as the mean ± SEM (n = 3–6). *, $p < 0.05$ (Student's t test). (**G**) KCNEx/KCNE1 ratio. The relative expression of each KCNE and the KCNEx/KCNE1 ratio was calculated using the KCNE specific real-time PCR efficiency. See Materials and Methods for details. White bars, 0 h; gray bars, 6 h; black bars, 24 h of FBS-dependent proliferation.

responses have also been demonstrated with Kv1.3 and Kv1.5 in macrophages and muscle cells.[3,38]

Are there other KCNEs expressed in the immune system? The expression of other KCNEs has not been thoroughly examined in leukocytes. The expression of KCNE2 in leukocytes and tissues from the immune system is limited.[35] We observed that MCSF and FBS induce a notable cell cycle-dependent upregulation of KCNE2 mRNA. However, affymetrix GeneChip studies show that KCNE2 mRNA abundance is similar between cancerous and healthy thymus, bone marrow and whole blood specimens. In contrast, activation triggers the downregulation of KCNEs in Jurkat T-cells, but other insults failed in macrophages or Raji B-cells. The results obtained from array data from experiments performed in different leukocytic, human leukemia and lymphoma cell lines suggest that KCNE2 expression is quite stable (see supplemental material for GeneChip information). Changes during the cell cycle and/or differentiation might explain these differences. In fact, in most cases, we report that the upregulation of KCNE2 was transient and returned to basal levels during late phases of the cell cycle.

The expression of KCNE3 presents an interesting debate. While Abbott et al. (2001) reported no expression of KCNE3 in thymus, spleen and human leukocytes[39] Lundquist et al. (2006) observed the abundant expression of KCNE3 in the same tissues.[35] Other evidence also indicates a disparity among cell lines. For instance, array data from GNF BioGPS has shown that KCNE3 might be prominent in cells of a myeloid origin (see supplemental material for GeneChip information). Our data do not

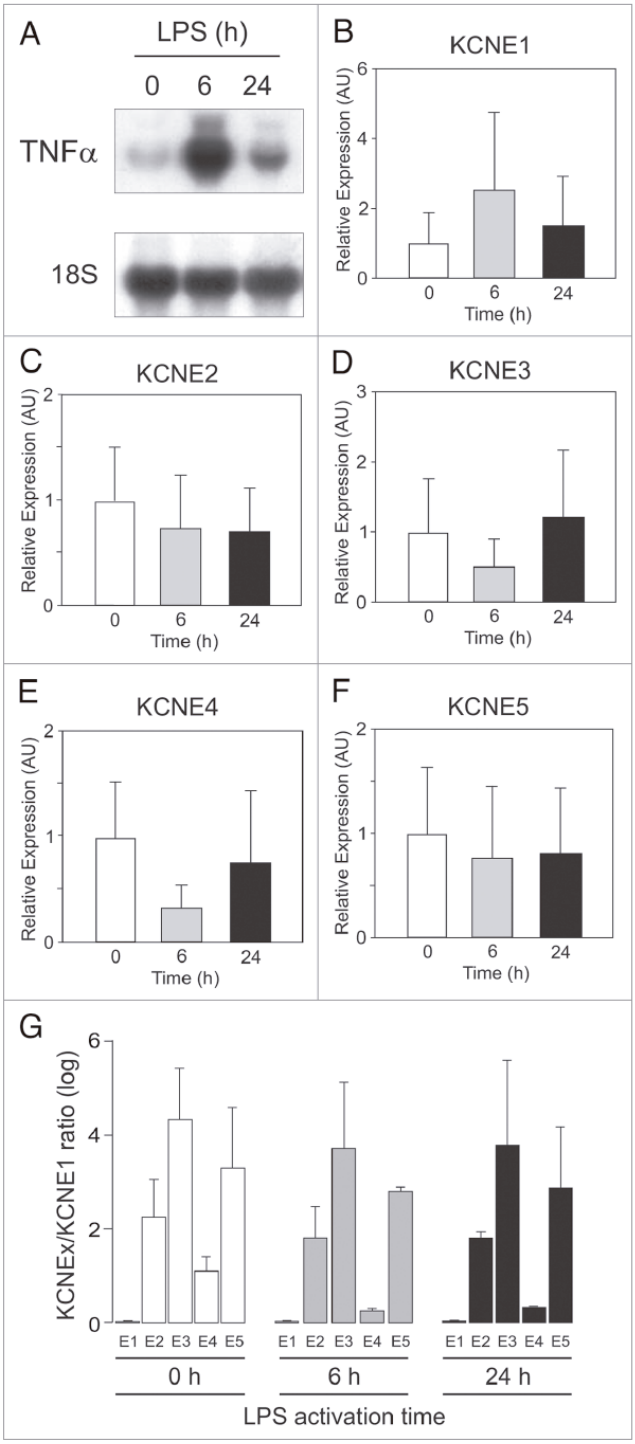

Figure 5. Expression and regulation of KCNE (1–5) mRNA in LPS-activated Raji B-lymphocytes. B-cells were incubated in the presence of LPS (100 μg/ml), and the mRNA was isolated simultaneously after the indicated times of treatment. Real-time PCR was performed as described in Materials and Methods. (**A**) TNFα mRNA expression. Ribosomal 18S RNA was used as control. (**B–F**) Relative mRNA expression, in arbitrary units (AU), of KCNE1–5. (**B**) KCNE1; (**C**) KCNE2; (**D**) KCNE3; (**E**) KCNE4; (**F**) KCNE5. The values are given as the mean ± SEM (n = 3–6). (**G**) KCNEx/KCNE1 ratio. The relative expression of each KCNE and the KCNEx/KCNE1 ratio was calculated using the KCNE specific real-time PCR efficiency. See Materials and Methods for details. White bars, 0 h; gray bars, 6 h; black bars, 24 h in the presence of LPS.

support the results obtained from the last study because KCNE3 expression was low in macrophages. However, KCNE3 mRNA suffers differential regulation between proliferation and activation with a remarkable downregulation under LPS and IFN-γ incubation. Furthermore, we did observe notable KCNE3 mRNA expression in human B and T-lymphocytes, with minor regulation upon proliferation or activation.

Grunnet et al. (2003) documented the consistent expression of KCNE4 in activated T-lymphocytes.[17] KCNE4 expression is relatively abundant in the immune system (see supplemental material for GeneChip information). Although most studies show that KCNE4 mRNA levels are slightly higher than other KCNEs in the spleen, multiple native leukocytes and several leukemia and lymphoma cell lines show little expression in peripheral leukocytes.[35] Our data support the idea that the mRNA levels of KCNE4 are quite abundant, and experienced interesting regulation. We have previously reported that while KCNE4 expression increased in LPS-activated Raw 264.7 macrophages, the immunosuppressant dexamethasone triggered no changes.[20] In the present work, we further documented the cell cycle-dependent upregulation of KCNE4 in BMDM, whereas the levels of mRNA remained constant or decreased upon IFN-γ and LPS incubation, respectively. Unlike in Raw cells, the presence of LPS and IFN-γ inhibits proliferation in BMDMs.[22,23] IFN-γ and LPS arrests cells at the G1/S boundary, but only LPS induces apoptosis.[23,24] Thus, Kv1.3, a documented target of KCNE4-dependent negative regulation, potentially plays a dual role in proliferation and apoptosis.[40] Therefore, it is tempting to speculate that the Kv1.3 activity should be conserved during proliferation and apoptosis in BMDMs. We observed similar regulation in T-lymphocytes but not in B-cells, where KCNE4 mRNA levels remained consistent.

Finally, KCNE5 is the less documented KCNE.[35] The results of affymetrix GeneChip studies (see supplemental material for GeneChip information) have demonstrated that KCNE5 is present in cells and healthy and cancerous tissues from the immune system. However, no KCNE5 regulation has been documented. We observed the cell cycle-dependent regulation of KCNE5 in BMDMs and

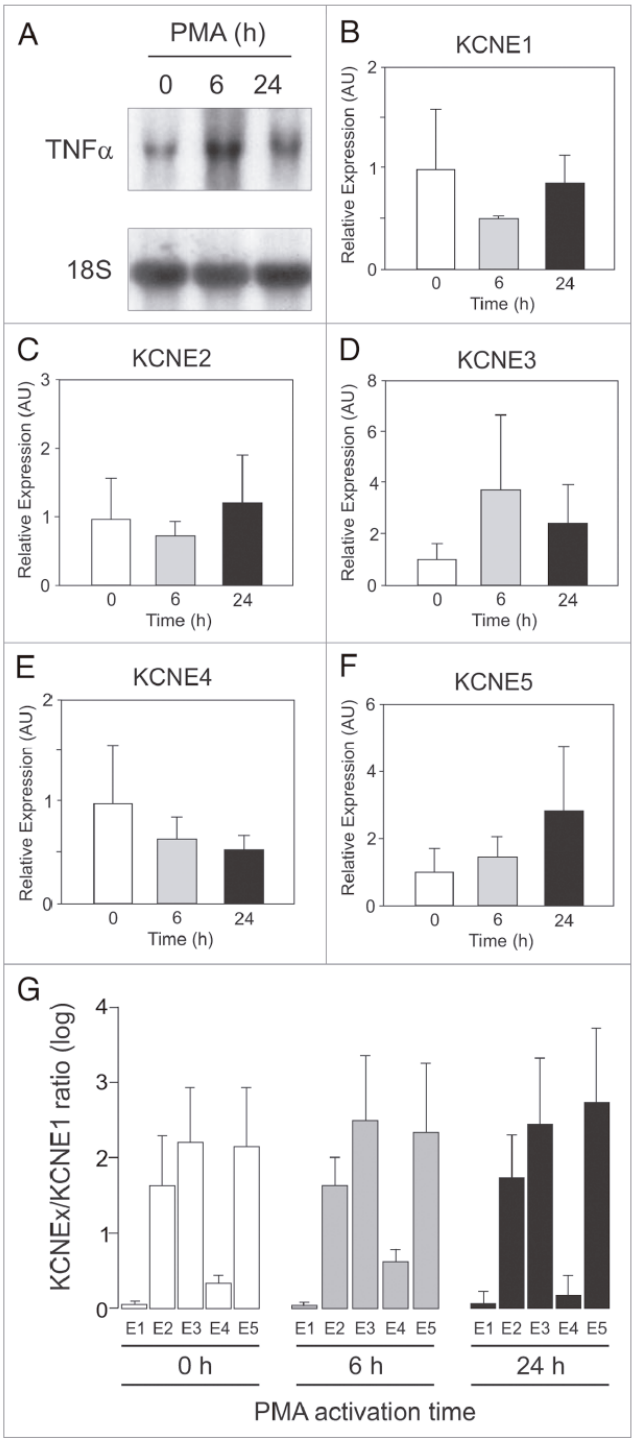

Figure 6. Expression and regulation of KCNE (1–5) mRNA in PMA-activated Raji B-lymphocytes. B-cells were incubated in the presence of 10 nM PMA and mRNA was isolated simultaneously after the indicated times of treatment. Real-time PCR was performed as described in Materials and Methods. (**A**) TNFα mRNA expression. Ribosomal 18S RNA was used as control. (**B–F**) Relative mRNA expression, in arbitrary units (AU), of KCNE1–5. (**B**) KCNE1; (**C**) KCNE2; (**D**) KCNE3; (**E**) KCNE4; (**F**) KCNE5. The values are given as the mean ± SEM (n = 3–6). (**G**) KCNEx/KCNE1 ratio. The relative expression of each KCNE and the KCNEx/KCNE1 ratio was calculated using the KCNE specific real-time PCR efficiency. See Materials and Methods for details. White bars, 0 h; gray bars, 6 h; black bars, 24 h in the presence of PMA.

a steady increase in activated T-lymphocytes. In general, our results would support quite notable levels of KCNE5 mRNA in leukocytes consistent with the highest levels detected in thymus and myeloid cells (see supplemental material for GeneChip information).[35]

In summary, our work systematically addresses, for the first time, the mRNA expression of the five KCNE subunits in leukocytes. These newly identified auxiliary leukocytic channel subunits might exert regulatory actions, such as the regulation of Kv gating, traffic and localization. This field is in its infancy and these data serve as a useful roadmap to inform future studies and represents a step toward understanding the role of these regulatory subunits in leukocyte physiology.

Materials and Methods

Animals, cell culture and proliferation assays. Murine bone marrow-derived macrophages (BMDM) from 6- to 10-wk-old BALB/c (Charles River laboratories) were used. The cells were isolated and cultured as described elsewhere.[3,22] Briefly, animals were sacrificed by cervical dislocation, and the adherent tissue was removed to dissect both femurs. The ends of bones were cut off, and the marrow tissue was flushed using irrigation with medium. The marrow plugs were passed through a 25-gauge needle for dispersion. The cells were cultured in DMEM containing 20% FBS and 30% L-929 fibroblast (L-cell) conditioned media as a source of macrophage colony-stimulating factor (MCSF). The macrophages were obtained as a homogeneous population of adherent cells after 7 d of culture and maintained at 37°C in a humidified incubator under 5% CO_2. For the experiments, the cells were cultured with tissue culture differentiation medium (DMEM, 20% FBS, 30% L-cell medium) or arrested at G_0 using M-CSF deprivation in DMEM supplemented with 10% FBS for at least 18 h. The G_0-arrested cells were further incubated in the absence or the presence of recombinant murine M-CSF (1200 U/ml), with or without lipopolysaccharide (LPS, 100 ng/ml, Sigma-Aldrich) and with or without IFN-γ (300 U/ml, Preprotech). The ethics committee from the University of Barcelona approved all methods for animal

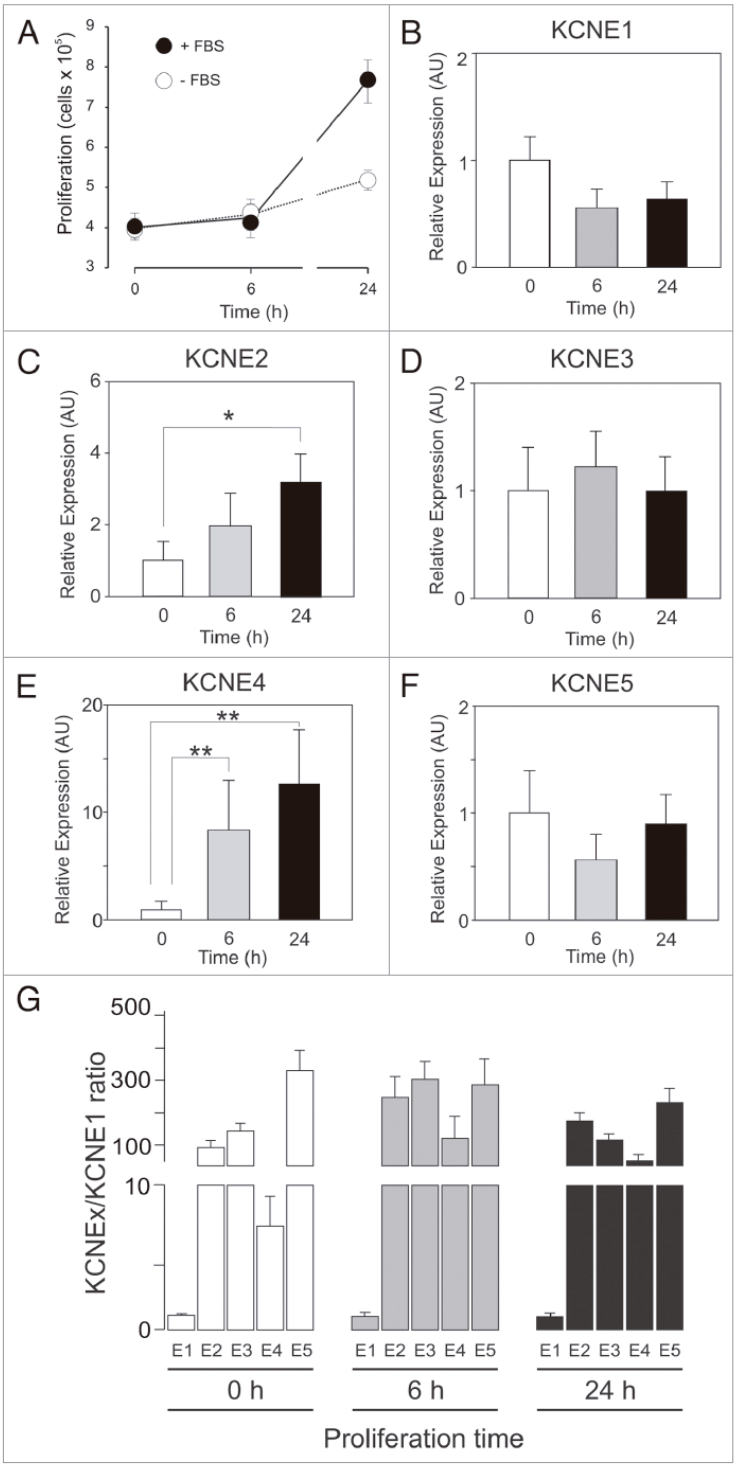

Figure 7. Expression and regulation of KCNE (1–5) mRNA in FBS-dependent Jurkat T-lymphocyte proliferation. G_0-arrested T-cells were incubated in the presence of FBS, and the mRNA was isolated simultaneously after the indicated times of treatment. Real-time PCR was performed as described in Materials and Methods. (**A**) FBS-dependent proliferation of Jurkat T-cells. The values are given as the mean ± SEM and represent cell number of four independent experiments each performed in triplicate. ●, + FBS; ○, - FBS. (**B–F**) Relative mRNA expression, in arbitrary units (AU), of KCNE1–5. (**B**) KCNE1; (**C**) KCNE2; (**D**) KCNE3; (**E**) KCNE4; (**F**) KCNE5. The values are given as the mean ± SEM (n = 3–6). *, $p < 0.05$; **, $p < 0.01$ (ANOVA and post-hoc Tukey's test). (**G**) KCNEx/KCNE1 ratio. The relative expression of each KCNE and the KCNEx/KCNE1 ratio was calculated using the KCNE specific real-time PCR efficiency. See Materials and Methods for details. White bars, 0 h; gray bars, 6 h; black bars, 24 h of FBS-dependent proliferation.

care and handling, and the experiments were conducted in accordance with EU regulations.

Raji human B lymphocytes and Jurkat human T-lymphocytes were routinely cultured in RPMI culture media containing 10% FBS and supplemented with 10 U/mL penicillin and streptomycin. In proliferation experiments, the Raji B-cells and Jurkat T-cells were incubated for 24 h in RPMI media without FBS supplemented with 0.02% BSA (G_0-arrested cells) prior to culture in regular RPMI supplemented with 10% FBS. While 10 nM phorbol ester (PMA, Sigma-Aldrich) and LPS (100 μg/ml) were used to activate B-lymphocytes, the Jurkat T-cells were stimulated with 5 μg/ml of phytohematogglutinin (PHA, Sigma-Aldrich) supplemented with 80 nM of PMA. Control cells treated with DMSO, the vehicle for PMA, were used to discard possible non-specific side effects.

Proliferation was investigated by analyzing the cell number and viability. A Countess™ automated cell counter (Invitrogen) was used for cell counting and viability analyzed by means of tripan blue exclusion. Viabilities higher than 85 ± 15% were used in all groups.

RNA isolation, RT-PCR analysis and real-time PCR. Cells cultured in 100-mm tissue culture dishes were incubated for a 24 h test period before harvesting, with agents added 6 h or 24 h before harvesting or with no agents added ("0 h," see Fig. S2). Total RNA from BMDM, Raji B-cells and Jurkat T-cells was isolated using the Nucleospin RNA II kit (Invitrogen), which contains DNase I. PCR controls were performed in the absence of reverse transcriptase. cDNA synthesis was performed using Transcriptor Reverse

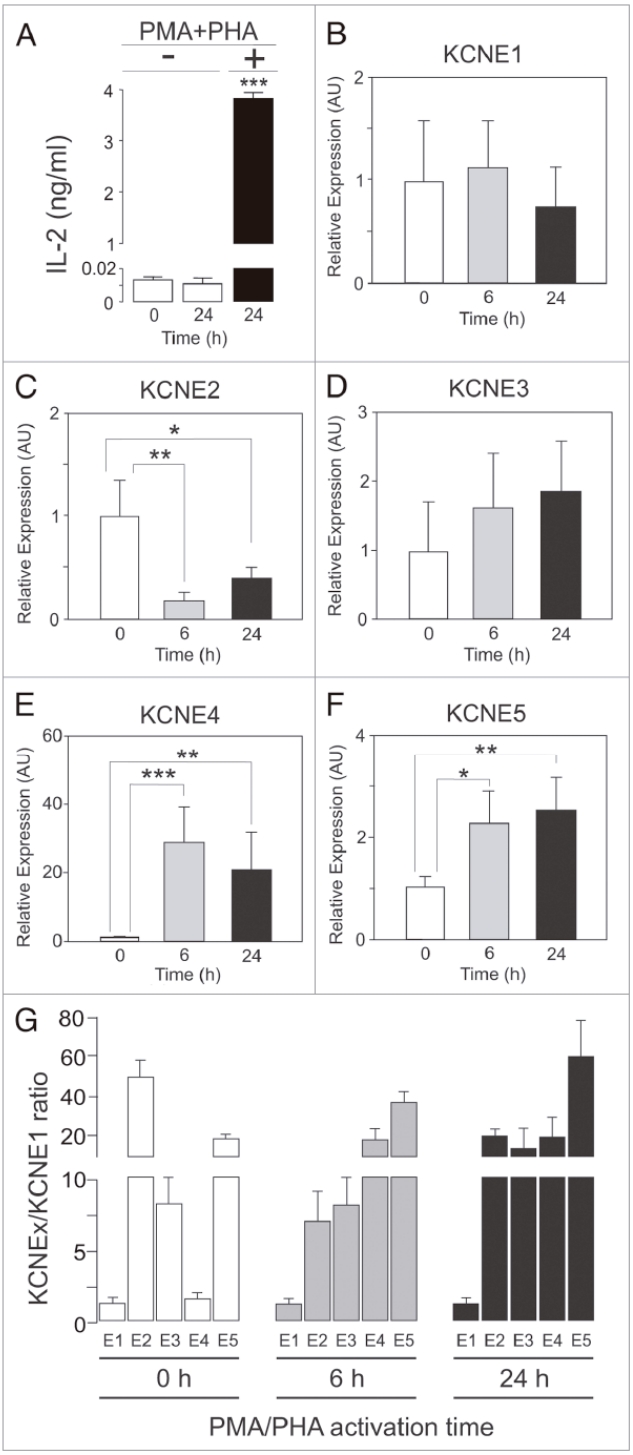

Figure 8. Expression and regulation of KCNE (1–5) mRNA in PMA/PHA-activated Jurkat T-lymphocytes. T-cells were incubated in the presence of PMA/PHA (80 nM/5 µg/ml), and mRNA was isolated simultaneously after the indicated times of treatment. Real-time PCR was performed as described in Materials and Methods. (**A**) IL-2 production (ng/ml) of control (-) and PMA/PHA-stimulated Jurkat T lymphocytes (+). ***, $p < 0.001$ vs. non treated (-). Open bars, absence of PMA/PHA; closed bar, presence of PMA/PHA. Values are mean ± SEM (n = 4). (**B–F**) Relative mRNA expression, in arbitrary units (AU), of KCNE1–5. (**B**) KCNE1; (**C**) KCNE2; (**D**) KCNE3; (**E**) KCNE4; (**F**) KCNE5. The values are given as the mean ± SEM (n = 3–6). *, $p < 0.05$; **, $p < 0.01$; ***, $p < 0.001$ (Student's t test). (**G**) KCNEx/KCNE1 ratio. The relative expression of each KCNE and the KCNEx/KCNE1 ratio was calculated using the KCNE specific real-time PCR efficiency. See Materials and Methods for details. White bars, 0 h; gray bars, 6 h; black bars, 24 h in the presence of PMA/PHA.

Transcriptase (Roche) with a random hexanucleotide and oligo(dT) primers according to the manufacturer's instructions. Real-time PCR was performed using a thermocycler (Applied Biosystems) and the LightCycler FastStart DNA Master^{PLUS} SYBR Green I kit (Roche) according to the manufacturer's instructions. The PCR primer sequences, gene accession numbers, annealing conditions and amplicon lengths for each KCNE are listed in Table 1. The reactions were performed under the following conditions: an initial incubation at 95°C for 10 min followed by cycling at 95°C for 5 sec, specific annealing at T°C for 8 sec, and 72°C for 6–9 sec, and a final incubation at 95°C for 10 min. Melting curves were performed to verify the specificity of the product, and ribosomal 18S RNA was included as an internal reference as previously described.[3,12] The results were analyzed using commercial software (Applied Biosystems). For each primer set, a standard curve was generated, and the slope factor was calculated. The values were normalized to the corresponding 18S RNA. The corresponding real-time PCR efficiency (E) of one cycle in the exponential phase was calculated according to the equation $E = 10^{(-1/slope)}$. The normalized KCNEx/KCNE1 ratio was calculated taking into account the primer pair efficiencies as follows: Ratio = $(1+E)^{\Delta Ct\,(KCNEx)} / (1+E)^{\Delta Ct\,(KCNE1)}$, where Ct signifies the threshold cycle.[41]

Northern blot analysis. Up to 20 µg of total RNA was fractionated by electrophoresis through a 1% agarose, 3% formaldehyde gel in 20 mm MOPS and 1 mm EDTA, pH 7.4. Application of equal amounts of RNA to each lane was confirmed by the addition of ethidium bromide to the samples before electrophoresis. RNA was transferred overnight to an Immobilon filter (Amersham Pharmacia Biotech) by capillary action in 20 × SSC (SSC, 3 min NaCl, 300 mm sodium citrate, pH 7.0). RNA was cross-linked to the filter by irradiation with UV light. Filters were hybridized with hTNF-α and rat 18 S rRNA cDNA probes. Filters were washed once for 30 min at 65°C in 3 × SSC and 1% lauryl sulfate, once in 1 × SSC and 1% lauryl sulfate, and once with 0.2 × SSC and 1% lauryl sulfate before autoradiography.

Table 1. PCR primers, accession numbers, annealing conditions and amplicon lengths for each KCNE

	Sequence	Accession number	Annealing (°C)	Amplicon (bp)
Mouse KCNE1	F: 5'-TGA CAG CAA GCA GGA GGC GCT-3' R: 5'-GAC ATA GCA AGC TCT GAA GC-3'	NM_008424	58	210
Mouse KCNE2	F: 5'-GTC ATC CTG TAC CTC ATG GT-3' R: 5'-TTC TCA TGG ATG GTG GCC TT-3'	NM_134110	60	194
Mouse KCNE3	F: 5'-CGT AAT GAC AAC TCC TAC ATG-3' R: 5'-TAC ACA TGA TAG GGG TCA CT-3'	NM_020574	67	127
Mouse KCNE4	F: 5'- TCC AGC AGC CCC CTC GAG TC-3' R: 5'-AGG CTG GAC TTC TTC TCC CG-3'	NM_021342	60	158
Mouse KCNE5	F: 5'-ACC CCT ACC CCG CAT ATC CAA-3' R: 5'-TTG GAC GTG CTG GAT TCT GTT-3'	NM_021487	55	106
Human KCNE1	F: 5'-TGT GCC TGG GAA GTT TGA G-3' R: 5'-GGG AAC CAC TGA CAG TCT ATC-3'	NM_000219	70	634
Human KCNE2	F: 5'-ACG CCA GCA AGA AGG TTC A-3' R: 5'-CTT GCT CAG CTG TTG TGT TC-3'	NM_172201	60	183
Human KCNE3	F: 5'-GCT AAT ACA TGC AAT GTG GC-3' R: 5'-TTC AAT GGG TAC TTC CAG G-3'	NM_005472	55	137
Human KCNE4*	Quantitect primer assay from Qiagen Ref QT00046676	NM_080671	55	105
Human KCNE5	F: 5'-CCT ACC CCG CAC ATC CAA CTG CAC-3' R: 5'-TTG GAC GTG TTG GAT TCA GTT CC-3'	NM_012282	62	104
18S	F: 5'-CGC AGA ATT CCC ACT CCC GAC CC-3' R: 5'-CCC AAG ATC CAA CTA CGA GC-3'	NR_003286 Human NR_003278 Mouse	55	210

F, forward; R, reverse. For hKCNE4 a validated Quantitect primer assay from Qiagen (Ref QT00046676) was used with no available primer sequences.

Western blot analysis. Cell extracts for western blot analysis were obtained after washing the cells twice in cold phosphate-buffered saline followed by lysis in 1% Nonidet P-40, 10% glycerol, 50 mm HEPES, pH 7.5, and 150 mm NaCl, supplemented with a protease inhibitor mixture consisting of 1 μg/ml aprotinin, 1 μg/ml leupeptin, 86 μg/ml iodoacetamide, and 1 mm phenylmethylsulfonyl fluoride. Protein was determined following the Bradford technique (Bio-Rad). Protein samples (20 μg) were incubated for 6 min at 95°C prior to 10% SDS-PAGE. Proteins were transferred onto filters (Immobilon-P, Millipore), which were then blocked in a 5% dry milk-supplemented 0.2% Tween 20, phosphate-buffered saline prior to immunoreaction. To monitor the expression of iNOS, a commercial rabbit antibody against mouse iNOS (M-19, Santa Cruz Biotechnology) was used. As a loading and transfer control for this technique, a mouse anti-mouse β-actin antibody (Sigma) was used.

IL-2 production measurements. IL-2 production in Jurkat T-lymphocytes was measured with an ELISA kit (eBioscience), following the manufacturer's instructions. Cells were centrifuged at 1200 rpm for 4 min, and the supernatant was used to quantify the IL-2 concentration. Reactions were performed in 96-well plates coated with the capture antibody. After blocking, standards and samples were incubated with Detection Antibody followed by HRP-Streptavidin. H_3PO_4 (1M) was used as stop solution. Plates were read at 450 nm.

Statistics. The values are expressed as the mean ± SEM of 3–6 experiments performed in triplicate. The significance of the differences was established using Student's t test or one-way ANOVA followed by a post-hoc Tukey's test (GraphPad, PRISM 5.0) where indicated. The decision to perform one-way ANOVA analysis was considered when significance was not observed using Student's t test. A value of $p < 0.05$ was considered significant. Due to the mathematical transformation, the statistical significance of the normalized KCNEx/KCNE1 ratio was considered irrelevant. The data should be considered qualitatively illustrative rather than a quantitative value.

Disclosure of Potential Conflicts of Interest

No potential conflicts of interest were disclosed.

Acknowledgments

Supported by the Ministerio de Economia y Competitividad (MINECO), Spain (BFU2011–23268 and CSD2008–00005 to A.F., BFU2010–15674 to C.S.). L.S., A.V.G., S.R.R. and D.G. hold fellowships from the MINECO. J.M. was an APIF fellow (Universitat de Barcelona). L.S. and A.V.G. contributed equally. C.S. and A.F. contributed equally.

Supplemental Materials

Supplemental materials may be found here:
www.landesbioscience.com/journals/chan/article/23258/

References

1. Hille B. Ion channels of excitable membranes. Sunderland, Mass.; [Great Britain]: Sinauer, 2001.
2. Conforti L. The ion channel network in T lymphocytes, a target for immunotherapy. Clin Immunol 2012; 142:105-6; PMID:22189042; http://dx.doi.org/10.1016/j.clim.2011.11.009.
3. Vicente R, Escalada A, Coma M, Fuster G, Sánchez-Tilló E, López-Iglesias C, et al. Differential voltage-dependent K^+ channel responses during proliferation and activation in macrophages. J Biol Chem 2003; 278:46307-20; PMID:12923194; http://dx.doi.org/10.1074/jbc.M304388200.
4. Chandy KG, Wulff H, Beeton C, Pennington M, Gutman GA, Cahalan MDK. K+ channels as targets for specific immunomodulation. Trends Pharmacol Sci 2004; 25:280-9; PMID:15120495; http://dx.doi.org/10.1016/j.tips.2004.03.010.
5. Cahalan MD, Chandy KG. The functional network of ion channels in T lymphocytes. Immunol Rev 2009; 231:59-87; PMID:19754890; http://dx.doi.org/10.1111/j.1600-065X.2009.00816.x.
6. Vicente R, Villalonga N, Calvo M, Escalada A, Solsona C, Soler C, et al. Kv1.5 association modifies Kv1.3 traffic and membrane localization. J Biol Chem 2008; 283:8756-64; PMID:18218624; http://dx.doi.org/10.1074/jbc.M708223200.
7. Pillozzi S, Brizzi MF, Balzi M, Crociani O, Cherubini A, Guasti L, et al. HERG potassium channels are constitutively expressed in primary human acute myeloid leukemias and regulate cell proliferation of normal and leukemic hemopoietic progenitors. Leukemia 2002; 16:1791-8; PMID:12200695; http://dx.doi.org/10.1038/sj.leu.2402572.
8. Smith GA, Tsui HW, Newell EW, Jiang X, Zhu XP, Tsui FW, et al. Functional up-regulation of HERG K^+ channels in neoplastic hematopoietic cells. J Biol Chem 2002; 277:18528-34; PMID:11893742; http://dx.doi.org/10.1074/jbc.M200592200.
9. Liu QH, Fleischmann BK, Hondowicz B, Maier CC, Turka LA, Yui K, et al. Modulation of Kv channel expression and function by TCR and costimulatory signals during peripheral CD4(+) lymphocyte differentiation. J Exp Med 2002; 196:897-909; PMID:12370252; http://dx.doi.org/10.1084/jem.20020381.
10. Grissmer S, Ghanshani S, Dethlefs B, McPherson JD, Wasmuth JJ, Gutman GA, et al. The Shaw-related potassium channel gene, Kv3.1, on human chromosome 11, encodes the type I K^+ channel in T cells. J Biol Chem 1992; 267:20971-9; PMID:1400413.
11. Martens JR, Kwak YG, Tamkun MM. Modulation of Kv channel alpha/beta subunit interactions. Trends Cardiovasc Med 1999; 9:253-8; PMID:11094335; http://dx.doi.org/10.1016/S1050-1738(00)00037-2.
12. Vicente R, Escalada A, Soler C, Grande M, Celada A, Tamkun MM, et al. Pattern of Kv beta subunit expression in macrophages depends upon proliferation and the mode of activation. J Immunol 2005; 174:4736-44; PMID:15814698.
13. McCormack T, McCormack K, Nadal MS, Vieira E, Ozaita A, Rudy B. The effects of Shaker beta-subunits on the human lymphocyte K^+ channel Kv1.3. J Biol Chem 1999; 274:20123-6; PMID:10400624; http://dx.doi.org/10.1074/jbc.274.29.20123.
14. McCrossan ZA, Abbott GW. The MinK-related peptides. Neuropharmacology 2004; 47:787-821; PMID:15527815; http://dx.doi.org/10.1016/j.neuropharm.2004.06.018.
15. Bendahhou S, Marionneau C, Haurogne K, Larroque MM, Derand R, Szuts V, et al. In vitro molecular interactions and distribution of KCNE family with KCNQ1 in the human heart. Cardiovasc Res 2005; 67:529-38; PMID:16039274; http://dx.doi.org/10.1016/j.cardiores.2005.02.014.
16. Attali B, Romey G, Honoré E, Schmid-Alliana A, Mattéi MG, Lesage F, et al. Cloning, functional expression, and regulation of two K^+ channels in human T lymphocytes. J Biol Chem 1992; 267:8650-7; PMID:1373731.
17. Grunnet M, Rasmussen HB, Hay-Schmidt A, Rosenstierne M, Klaerke DA, Olesen SP, et al. KCNE4 is an inhibitory subunit to Kv1.1 and Kv1.3 potassium channels. Biophys J 2003; 85:1525-37; PMID:12944270; http://dx.doi.org/10.1016/S0006-3495(03)74585-8.
18. Roepke TK, Kanda VA, Purtell K, King EC, Lerner DJ, Abbott GW. KCNE2 forms potassium channels with KCNA3 and KCNQ1 in the choroid plexus epithelium. FASEB J 2011; 25:4264-73; PMID:21859894; http://dx.doi.org/10.1096/fj.11-187609.
19. Roepke TK, Kontogeorgis A, Ovanez C, Xu X, Young JB, Purtell K, et al. Targeted deletion of kcne2 impairs ventricular repolarization via disruption of I(K,slow1) and I(to,f). FASEB J 2008; 22:3648-60; PMID:18603586; http://dx.doi.org/10.1096/fj.08-110171.
20. Solé L, Roura-Ferrer M, Pérez-Verdaguer M, Oliveras A, Calvo M, Fernández-Fernández JM, et al. KCNE4 suppresses Kv1.3 currents by modulating trafficking, surface expression and channel gating. J Cell Sci 2009; 122:3738-48; PMID:19773357; http://dx.doi.org/10.1242/jcs.056689.
21. Solé L, Felipe A. Does a physiological role for KCNE subunits exist in the immune system? Commun Integr Biol 2010; 3:166-8; PMID:20585512; http://dx.doi.org/10.4161/cib.3.2.10602.
22. Soler C, García-Manteiga J, Valdés R, Xaus J, Comalada M, Casado FJ, et al. Macrophages require different nucleoside transport systems for proliferation and activation. FASEB J 2001; 15:1979-88; PMID:11532978; http://dx.doi.org/10.1096/fj.01-0022com.
23. Soler C, Valdés R, Garcia-Manteiga J, Xaus J, Comalada M, Casado FJ, et al. Lipopolysaccharide-induced apoptosis of macrophages determines the up-regulation of concentrative nucleoside transporters Cnt1 and Cnt2 through tumor necrosis factor-alpha-dependent and -independent mechanisms. J Biol Chem 2001; 276:30043-9; PMID:11346649; http://dx.doi.org/10.1074/jbc.M101807200.
24. Xaus J, Cardó M, Valledor AF, Soler C, Lloberas J, Celada A. Interferon gamma induces the expression of $p21^{waf-1}$ and arrests macrophage cell cycle, preventing induction of apoptosis. Immunity 1999; 11:103-13; PMID:10435583; http://dx.doi.org/10.1016/S1074-7613(00)80085-0.
25. Soler C, Felipe A, García-Manteiga J, Serra M, Guillén-Gómez E, Casado FJ, et al. Interferon-gamma regulates nucleoside transport systems in macrophages through signal transduction and activator of transduction factor 1 (STAT1)-dependent and -independent signalling pathways. Biochem J 2003; 375:777-83; PMID:12868960; http://dx.doi.org/10.1042/BJ20030260.
26. Soler C, Felipe A, Mata JF, Casado FJ, Celada A, Pastor-Anglada M. Regulation of nucleoside transport by lipopolysaccharide, phorbol esters, and tumor necrosis factor-alpha in human B-lymphocytes. J Biol Chem 1998; 273:26939-45; PMID:9756942; http://dx.doi.org/10.1074/jbc.273.41.26939.
27. Soler C, Felipe A, Casado FJ, Celada A, Pastor-Anglada M. Nitric oxide regulates nucleoside transport in activated B lymphocytes. J Leukoc Biol 2000; 67:345-9; PMID:10733094.
28. Villalonga N, David M, Bielanska J, González T, Parra D, Soler C, et al. Immunomodulatory effects of diclofenac in leukocytes through the targeting of Kv1.3 voltage-dependent potassium channels. Biochem Pharmacol 2010; 80:858-66; PMID:20488163; http://dx.doi.org/10.1016/j.bcp.2010.05.012.
29. David M, Macías A, Moreno C, Prieto A, Martínez-Mármol R, Vicente R, et al. Protein kinase C (PKC) activity regulates functional effects of Kvβ1.3 subunit on KV1.5 channels: identification of a cardiac Kv1.5 channelosome. J Biol Chem 2012; 287:21416-28; PMID:22547057; http://dx.doi.org/10.1074/jbc.M111.328278.
30. Felipe A, Soler C, Comes N. Kv1.5 in the immune system: the good, the bad, or the ugly? Front Physiol 2010; 1:152; PMID:21423392; http://dx.doi.org/10.3389/fphys.2010.00152.
31. Saferali A, Grundberg E, Berlivet S, Beauchemin H, Morcos L, Polychronakos C, et al. Cell culture-induced aberrant methylation of the imprinted IG DMR in human lymphoblastoid cell lines. Epigenetics 2010; 5:50-60; PMID:20026906; http://dx.doi.org/10.4161/epi.5.1.10436.
32. Norris AJ, Foeger NC, Nerbonne JM. Neuronal voltage-gated K^+ (Kv) channels function in macromolecular complexes. Neurosci Lett 2010; 486:73-7; PMID:20813163; http://dx.doi.org/10.1016/j.neulet.2010.08.067.
33. Pourrier M, Schram G, Nattel S. Properties, expression and potential roles of cardiac K^+ channel accessory subunits: MinK, MiRPs, KChIP, and KChAP. J Membr Biol 2003; 194:141-52; PMID:14502427; http://dx.doi.org/10.1007/s00232-003-2034-8.
34. Chouabe C, Neyroud N, Guicheney P, Lazdunski M, Romey G, Barhanin J. Properties of KvLQT1 K^+ channel mutations in Romano-Ward and Jervell and Lange-Nielsen inherited cardiac arrhythmias. EMBO J 1997; 16:5472-9; PMID:9312006; http://dx.doi.org/10.1093/emboj/16.17.5472.
35. Lundquist AL, Turner CL, Ballester LY, George AL Jr. Expression and transcriptional control of human KCNE genes. Genomics 2006; 87:119-28; PMID:16303284; http://dx.doi.org/10.1016/j.ygeno.2005.09.004.
36. Tsevi I, Vicente R, Grande M, López-Iglesias C, Figueras A, Capellà G, et al. KCNQ1/KCNE1 channels during germ-cell differentiation in the rat: expression associated with testis pathologies. J Cell Physiol 2005; 202:400-10; PMID:15389592; http://dx.doi.org/10.1002/jcp.20132.
37. Felipe A, Knittle TJ, Doyle KL, Snyders DJ, Tamkun MM. Differential expression of Isk mRNAs in mouse tissue during development and pregnancy. Am J Physiol 1994; 267:C700-5; PMID:7943198.
38. Villalonga N, Martínez-Mármol R, Roura-Ferrer M, David M, Valenzuela C, Soler C, et al. Cell cycle-dependent expression of Kv1.5 is involved in myoblast proliferation. Biochim Biophys Acta 2008; 1783:728-36; PMID:18230363.
39. Abbott GW, Butler MH, Bendahhou S, Dalakas MC, Ptacek LJ, Goldstein SA. MiRP2 forms potassium channels in skeletal muscle with Kv3.4 and is associated with periodic paralysis. Cell 2001; 104:217-31; PMID:11207363; http://dx.doi.org/10.1016/S0092-8674(01)00207-0.
40. Gulbins E, Sassi N, Grassmè H, Zoratti M, Szabò I. Role of Kv1.3 mitochondrial potassium channel in apoptotic signalling in lymphocytes. Biochim Biophys Acta 2010; 1797:1251-9; PMID:20114030.
41. Villalonga N, Escalada A, Vicente R, Sánchez-Tilló E, Celada A, Solsona C, et al. Kv1.3/Kv1.5 heteromeric channels compromise pharmacological responses in macrophages. Biochem Biophys Res Commun 2007; 352:913-8; PMID:17157812; http://dx.doi.org/10.1016/j.bbrc.2006.11.120.

3.3.7. Resum de la contribució 9

Article en preparació

Expressió de Kv1.3 i KCNE4 en limfòcits T

Laura Solé i Antonio Felipe

Els leucòcits expressen un repertori limitat de canals de potassi, els quals estan implicats en processos claus com són la proliferació i l'activació del sistema immunitari. Els principals canals de potassi que s'expressen en limfòcits T son Kv1.3 i K_{Ca}3.1. A més a més, l'expressió de subunitats reguladores incrementa encara més la diversitat fisiològica dels canals de potassi. Prèviament, hem demostrat com, de manera similar a Kv1.3, el patró d'expressió de mRNA dels KCNEs es veu modulat durant la proliferació i l'activació dels limfòcits T. A més a més, hem demostrat com Kv1.3 interacciona amb KCNE4 en sistemes d'expressió heteròloga i comparteixen també l'expressió en macròfags. Degut al paper crucial que juga Kv1.3 en la fisiologia dels limfòcits T, i que KCNE4 és una subunitat reguladora amb un marcat efecte dominant negatiu sobre Kv1.3, el principal objectiu d'aquest estudi era el d'analitzar si Kv1.3 i KCNE4 co-localitzaven en limfòcits T humans (Jurkat). Els nostres resultats demostren com Kv1.3 i KCNE4 co-localitzen en limfòcits T. Immunohistoquímiques d'"*Induced Patching*" a més a més confirmen l'existència de complexes Kv1.3-KCNE4, tal i com demostra la redistribució que pateix KCNE4, presentant un patró molt similar al que presenta Kv1.3, quan s'aplica un marcatge *d'inducing patching* contra Kv1.3.. Aquests resultats confirmen l'expressió de KCNE4 en cèl·lules T Jurkat, i a més a més, donen suport a al significat fisiològic del complex funcional Kv1.3.-KCNE4

3.3.8. Report of the PhD student participation in the article

Informe de la participació de la doctoranda en l'article

Kv1.3 and KCNE4 expression in T-lymphocytes.

In preparation / En preparació

Laura Solé Codina performed all the experiments and the data analysis corresponding to this article.

Laura Solé Codina ha realitzat íntegrament tots els experiments i anàlisis dels resultats corresponents a aquest article.

Thesis director

El director de la tesi

Dr. Antonio Felipe Campo

3.3.9. Contribution 9: Kv1.3 and KCNE4 expression in T-lymphocytes

Laura Solé and Antonio Felipe

Molecular Physiology Laboratory, Departament de Bioquímica i Biologia Molecular, Institut de Biomedicina (IBUB), Universitat de Barcelona, Avda. Diagonal 643, 08028 Barcelona, Spain

ABSTRACT

Leukocytes express a limited repertoire of potassium channels, which are involved in the proliferation and activation of the immune system. The main potassium channels expressed in T-lymphocytes are Kv1.3 and K_{Ca}3.1. In addition, lymphocytic regulatory subunits further raise the physiological diversity of the potassium channels. We have previously reported that, similar to Kv1.3, KCNE mRNA expression pattern is modulated during proliferation and activation of T-lymphocytes. In addition, Kv1.3 interacts with KCNE4 in heterologous expression systems and share expression in macrophages. Because Kv1.3 is crucial in T-lymphocyte physiology and KCNE4 is an important Kv1.3-dominant negative regulatory subunit, the aim of this study was to analyze whether of Kv1.3 and KCNE4 co-localyzed in human Jurkat T-cells. We found that Kv1.3 and KCNE4 co-localized in T-cells. Induced patching immunocytochemistry further confirmed the existence of Kv1.3-KCNE4 complexes due KCNE4 distribution rearranged in a similar way than Kv1.3 under Kv1.3-Induced patching labeling. These results confirm the expression of KCNE4 in Jurkat T-cells which further supports the physiological significance of the Kv1.3-KCNE4 functional complex.

INTRODUCTION

Potassium channels are involved in the regulation of proliferation and activation of immune cells (Cahalan and Chandy 1997; Panyi et al. 2004). Several potassium channels determine the membrane potential of leukocytes, thereby playing a crucial role in cellular excitability. Changes in the membrane potential are among the earliest events during the immune system response and ion channels underlie the calcium signal involved in leukocyte responses. Leukocytes express a limited repertoire of potassium channels (Cahalan and Chandy 2009). The main potassium channels expressed in T-lymphocytes are Kv1.3 and K_{Ca}3.1. In addition, the presence of Kv1.1, Kv1.2 and Kv1.6 in mouse T-cells have also been reported (Liu et al. 2002). T-lymphocytes also express regulatory subunits such as Kvβ1.1 and Kvβ2.1 (Autieri et al. 1997) and all the members of the KCNE family (Sole et al. 2013), which further raise the physiological diversity of the potassium channels in these cells. We have previously reported that, similar to Kv1.3, KCNE mRNA expression pattern is modulated during proliferation and activation of T-lymphocytes (Sole et al. 2013). In addition,

Kv1.3 interacts with KCNE4 in heterologous expression systems and share expression in macrophages (Sole et al. 2009). The aim of this study was to analyze the expression of Kv1.3 and KCNE4 in human Jurkat T-cells. We found that Kv1.3 and KCNE4 co-localized in Jurkat T-cells which further supports the physiological significance of the Kv1.3-KCNE4 functional complex.

MATERIALS AND METHODS

Cell culture. Jurkat T-cells were cultured in RPMI medium containing 10% FBS supplemented with penicillin (10.000U/ml), streptomycin (100 µg/ml) L-glutamine (2 mM) and HEPES (25 mM). Jurkat T-cells were grown in 25 or 75-cm^2 flasks. For immunocytochemistry experiments 2,5-3,5x10^6 cells/well were seed in a 12-multiwell dish (Cultek) in poly-L-lysine (Sigma) coated coverslips, with starving media (RPMI medium with L-glutamine (2 mM) and HEPES (25 mM). Twenty-four h after seeding, immunocitochemistries were performed.

Immunocitochemistry. Cells were washed twice quickly with 1x PBS without K^+ and fixed with 4% paraformaldehyde (PFA) (Sigma) in PBS-K^+ for 10 min at RT (room temperature). Then, cells were washed three times with PBS-K^+ for 5 min. Next, cells were permeabilized for 20 min with 0.1 % Triton X-100 PBS-K^+. After three washes with 0.05 % Triton X-100 PBS-K^+, cells where further incubated with the Blocking solution (5 % milk, 10 % goat serum in 0.05 % Triton X-100 PBS-K^+), for 1 h at RT. Next, cells were incubated with a dilution anti-KNCE4 (1/150, Proteintech) or anti-Kv1.3 extracellular (1/150, Alomone) antibody with 10 % goat serum in 0.05 % Triton X-100 PBS-K^+, for 1 h 45 min at RT. After that, cells were washed three times with 0.05 % Triton X-100 PBS-K^+, and then incubated with a dilution of the secondary antibody (1/150 of Cya5-goat-anti-rabbit of Alexa-568-goat-anti-rabbit, Molecular Probes) with 1 % BSA 0.05 % Triton X-100 PBS-K^+, for 45 min at RT. Finally, cells were washed tree times with PBS-K^+ for 5 min, and the coverslips were mounted on microscope slides (Acefesa) with a drop of the mounting media (Molecular Probes). Coverslips were let dry at RT at least one day before being observed at the microscope.

Induced patching immunocytochemistry (IPI) was also performed in order to increase the signal of the labeling. The protocol started with a quick wash of the cells with PBS-K^+, and incubated with the primary antibody (1/150 of rabbit-anti-Kv1.3 extracellular) diluted in DMEM media supplemented with 30 mM HEPES, for 1 h at 37ºC. Next, cells were washed twice quickly with PBS-K^+, and incubated with the secondary antibody (goat-anti-rabbit-Cya5, 1/150) diluted in DMEM media supplemented with 30 mM HEPES, for 1 h at 4 ºC. Then cells were washed thrice quickly and fixed with 4 % PFA for 10 min RT. Finally, cells were washed

three times with PBS-K^+ and mounted as described before. When an extra labeling was needed, a second round of labeling with primary and secondary antibodies was performed after the fixation protocol, following the indications described above.

Confocal imaging. Leica TCS SL laser scanning confocal spectral microscope (Leica Microsystems) equipped with an Argon and Helium-Neon lasers was used for imaging. All the experiments were done with a 63x oil-immersion objective lens (NA 1.32). Images were acquired sequentially: Alexa-568 image, Cya5 image and phase image. Alexa-568 was excited using the 543 nm line of the laser, and emission was collected using the variable band-pass filter set at 555-623 nm. Cya5 was excited using the 633 line of the laser and emission was collected using the variable band-pass filter set at 647-777 nm. All images from all the conditions were acquired with the same photomultiplier gain. All offline image processing was done using Image J software.

RESULTS AND DISCUSSION

In order to analyze the distribution of Kv1.3 and KCNE4 in Jurkat T-cells, immunocytochemistries under permeating conditions were performed. Kv1.3 and KCNE4 intracellular signal was detected (Fig. 1B and D, respectively). Exhaustive negative controls with primary (not shown) and secondary antibodies were also performed (Fig. 1C and 1D). Kv1.3 and KCNE4 distributed intracellular, further supporting what described before in HEK-293 and Raw 264.7 macrophages (Solé et al. 2009). Therefore, KCNE4 impairs Kv1.3 targeting to the cell surface in human T-cells.

To further demonstrate the shared phenotype, we performed induced-patching immunocytochemistries (IPI). In this technique the incubation with the primary and secondary antibody are performed on live cells under non permeating conditions. The binding of the primary antibody at the plasma membrane, cause a rearrangement of the membrane, which triggers aggregates of the target protein at the plasma membrane. Furthermore, whether this protein interacts with another protein both proteins should co-localize, sharing the same pattern.

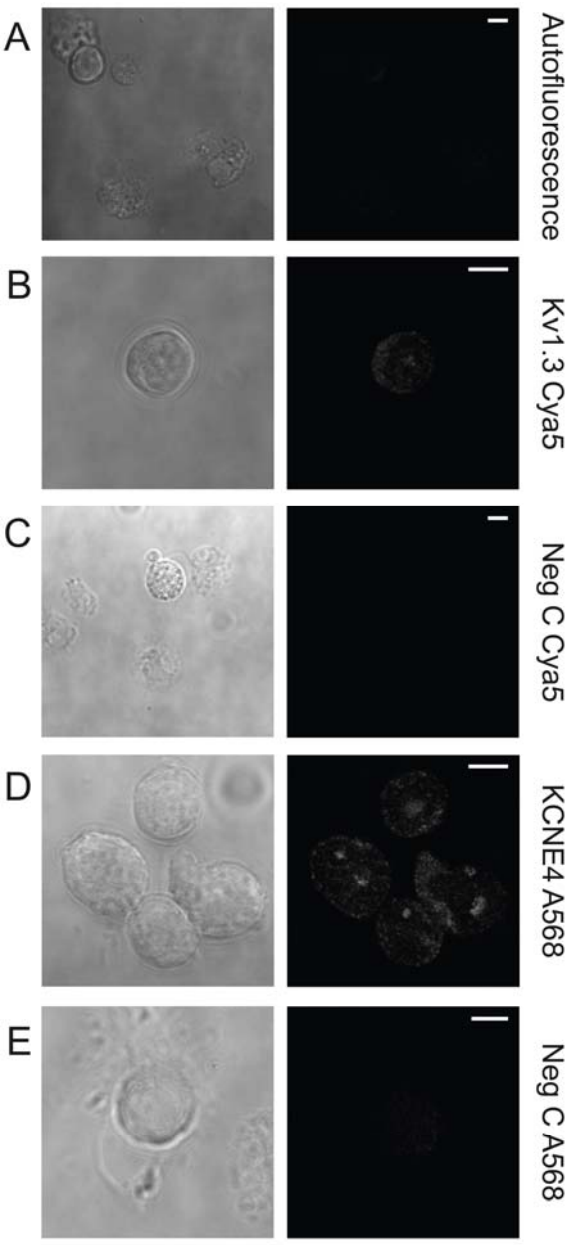

Fig. 1. *Expression of Kv1.3 and KCNE4 in human Jurkat T-lymphocytes.* A. Fixed Jurkat cells. Autofluorescence at 633 nm. B. Anti-Kv1.3-Cya5 labeling. C. Negative control, Secondary antibody goat-anti-RaCya5. D. Anti-KCNE4-Alexa568 labeling. E. Negative control, Secondary antibody goat-anti-RaAlexa568. Bars represent 5µm.

IPI was performed with anti-Kv1.3 extracellular antibody. Fig. 2A shows that Kv1.3, which mainly distributed uniformly throughout the cell (see Fig. 1), presented a patched distribution. Many aggregates of Kv1.3 are located at the cell surface. IPI was also performed with anti-KCNE4 antibody and the regulatory subunit presented a minor punctuated pattern (Fig. 2B).

When IPI against anti-Kv1.3 was performed prior a classical immunocytochemistry against KCNE4, cells presented an evident punctuated labeling. Kv1.3 rearranged around the membrane showing a punctuated pattern (Fig. 2C). Interestingly, KCNE4 labeling follows almost the same pattern than Kv1.3 (Fig 2C, bottom left), and in the bottom right image of the same panel, where yellow means co-localization between the channel and the regulatory subunit. To test whether this punctuated distribution of KCNE4 was caused by unspecific rearrangements during IPI, cells were incubated in the absence of the Kv1.3 antibody. In this case the rearrangement of the surface proteins was absent (Fig 2D). Our results show that IPI-Kv1.3 rearrangement causes also a change in the KCNE4 distribution thereby suggesting that both proteins form part of the same complex. These results would support results obtained in heterologous expression systems.

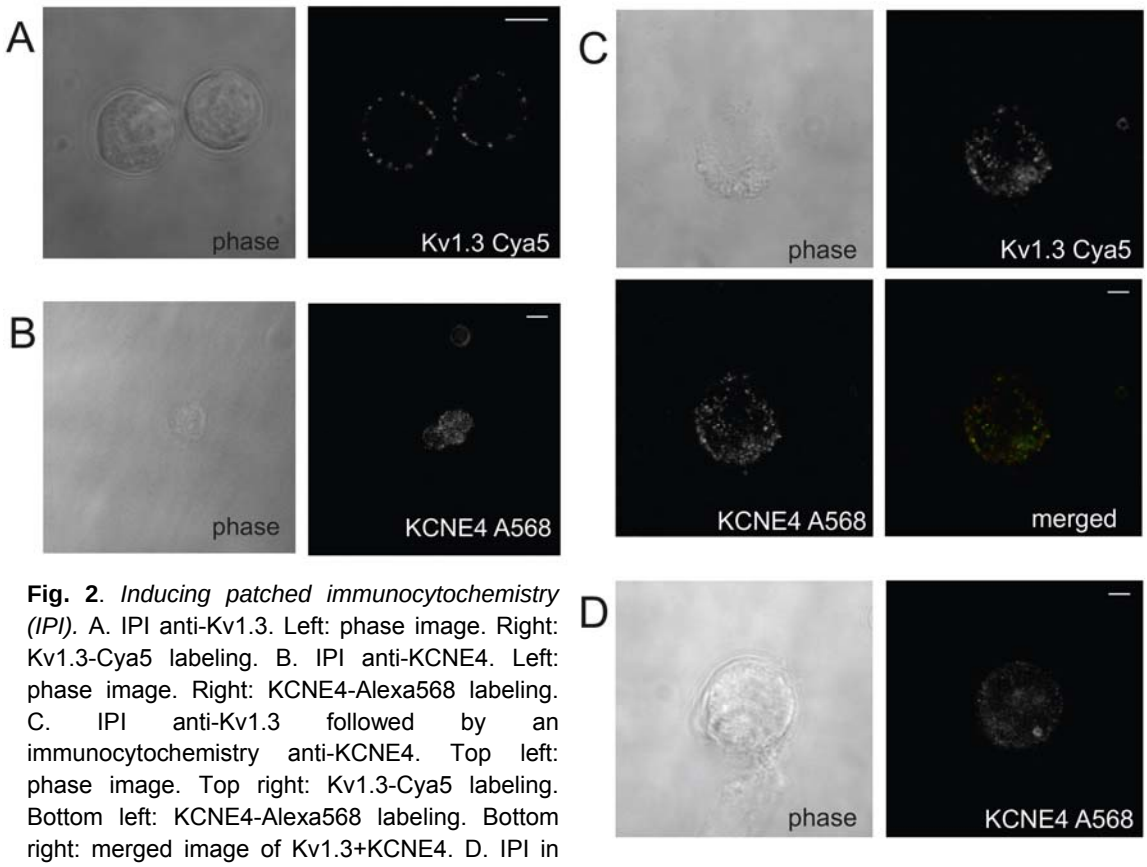

Fig. 2. *Inducing patched immunocytochemistry (IPI).* A. IPI anti-Kv1.3. Left: phase image. Right: Kv1.3-Cya5 labeling. B. IPI anti-KCNE4. Left: phase image. Right: KCNE4-Alexa568 labeling. C. IPI anti-Kv1.3 followed by an immunocytochemistry anti-KCNE4. Top left: phase image. Top right: Kv1.3-Cya5 labeling. Bottom left: KCNE4-Alexa568 labeling. Bottom right: merged image of Kv1.3+KCNE4. D. IPI in absence of Kv1.3 antibody, followed by an immunocytochemistry anti-KCNE4. Left: phase image. Right: KCNE4-Alexa568 labeling. Bars represent 5μm.

In HEK293 cells, KCNE4 inhibits Kv1.3 currents and alters traffic and targeting of Kv1.3 at the lipid rafts microdomains (Sole et al. 2009). Kv1.3 concentrates in the T-cell immunological synapse (Panyi et al. 2004), within lipid rafts, and it has been described that raft disruption impairs the immune response (Panyi et al. 2004; Nicolaou et al. 2007; Toth et al. 2009). In addition, immobilizing Kv1.3 channels at the immunological synapse increases the calcium signaling, raising the downstream signaling transduction pathways (Nicolaou et al. 2007; Nicolaou et al. 2009). Here we demonstrated Kv1.3 and KCNE4 expression in T-cells and analyzed their distribution. The role of KCNE4 in the Kv1.3 channelosome during the formation of the T-cell immunological synapse deserves further research.

We have previously reported that KCNE expression is regulated during T-cell activation and proliferation (Sole et al. 2013). For instance, while KCNE2 expression is decreased in PMA-PHA T-cells activation, KCNE4 and KCNE5 are increased, and KCNE4 levels are also raised during proliferation. In this context, Kvβ expression depends upon proliferation and activation in macrophages (Vicente et al. 2005). Furthermore, while quiescent naïve T_{CM} and T_{EM} cells exhibit a similar potassium channel expression pattern with 300 Kv1.3 and 10-20 $K_{Ca}3.1$ channels/cell upon activation, T_{CM} effector up-regulated the

$K_{Ca}3.1$ channels (x50fold) and T_{EM} effectors up-regulated Kv1.3 channels (x5fold) (Cahalan et al. 2001; Panyi et al. 2004). Therefore, regulation of auxiliary subunits may also have a role in this functional adaptation upon different insults.

Immune system is a very complex cellular network formed by a myriad of different cells such as B cells, macrophages, Dendritic Cells, Natural Killers, etc. Every type of cell and their differentiation state express different potassium channels. While microglia express Kv1.3, Kv1.5, $K_{Ca}2.2$, $K_{Ca}2.2$, $K_{Ca}2.3$, $K_{Ca}3.1$, $K_{ir}2.1$, Herg-like channels, and $K_{Ca}1.1$, macrophages express Kv1.3, Kv1.5, Kir2.1 and $K_{Ca}1.1$ (Beeton and Chandy 2005). Further research should be done in order to decipher the expression pattern of regulatory subunits in these cells, which could affect to the functional response. It is important to remark that not all the channels are modulated by the same regulatory subunits (i.e. KCNE4) and that heterotetramerization between Kv1.3 and Kv1.5, which happens in macrophages (Vicente et al. 2006; Villalonga et al. 2007), may affect to the KCNE4 association and modulation of the channels altering the physiological response of the cell. The fact that Kv1.3 and KCNE4 are expressed in immune cells paves the way for future research on the Kv1.3-KCNE4 interaction and its role in the immune system.

AKNOWLEDGEMENTS

Supported by the Ministerio de Economia y Competitividad (MINECO), Spain (BFU2011–23268 and CSD2008–00005 to A.F).

REFERENCES

Autieri, M. V., Belkowski, S. M., Constantinescu, C. S., Cohen, J. A. and Prystowsky, M. B. (1997). "*Lymphocyte-specific inducible expression of potassium channel beta subunits*." J Neuroimmunol 77(1): 8-16.

Beeton, C. and Chandy, K. G. (2005). "*Potassium channels, memory T cells, and multiple sclerosis*." Neuroscientist 11(6): 550-562.

Cahalan, M. D. and Chandy, K. G. (1997). "*Ion channels in the immune system as targets for immunosuppression*." Curr Opin Biotechnol 8(6): 749-756.

Cahalan, M. D. and Chandy, K. G. (2009). "*The functional network of ion channels in T lymphocytes*." Immunol Rev 231(1): 59-87.

Cahalan, M. D., Wulff, H. and Chandy, K. G. (2001). "*Molecular properties and physiological roles of ion channels in the immune system*." J Clin Immunol 21(4): 235-252.

Liu, Q. H., Fleischmann, B. K., Hondowicz, B., Maier, C. C., Turka, L. A., Yui, K., . . . Freedman, B. D. (2002). "*Modulation of Kv channel expression and function by TCR and costimulatory signals during peripheral CD4(+) lymphocyte differentiation*." J Exp Med 196(7): 897-909.

Nicolaou, S. A., Neumeier, L., Steckly, A., Kucher, V., Takimoto, K. and Conforti, L. (2009). "*Localization of Kv1.3 channels in the immunological synapse modulates the calcium response to antigen stimulation in T lymphocytes*." J Immunol 183(10): 6296-6302.

Nicolaou, S. A., Szigligeti, P., Neumeier, L., Lee, S. M., Duncan, H. J., Kant, S. K., . . . Conforti, L. (2007). "*Altered dynamics of Kv1.3 channel compartmentalization in the immunological synapse in systemic lupus erythematosus*." J Immunol 179(1): 346-356.

Panyi, G., Vamosi, G., Bacso, Z., Bagdany, M., Bodnar, A., Varga, Z., . . . Damjanovich, S. (2004). "*Kv1.3 potassium channels are localized in the immunological synapse formed between cytotoxic and target cells*." Proc Natl Acad Sci U S A 101(5): 1285-1290.

Panyi, G., Varga, Z. and Gaspar, R. (2004). "*Ion channels and lymphocyte activation*." Immunol Lett 92(1-2): 55-66.

Sole, L., Roura-Ferrer, M., Perez-Verdaguer, M., Oliveras, A., Calvo, M., Fernandez-Fernandez, J. M. and Felipe, A. (2009). "*KCNE4 suppresses Kv1.3 currents by modulating trafficking, surface expression and channel gating*." J Cell Sci 122(Pt 20): 3738-3748.

Sole, L., Vallejo-Gracia, A., Roig, S. R., Serrano-Albarras, A., Marruecos, L., Manils, J., . . . Felipe, A. (2013). "*KCNE gene expression is dependent on the proliferation and mode of activation of leukocytes*." Channels (Austin) 7(2): 85-96.

Toth, A., Szilagyi, O., Krasznai, Z., Panyi, G. and Hajdu, P. (2009). "*Functional consequences of Kv1.3 ion channel rearrangement into the immunological synapse*." Immunol Lett 125(1): 15-21.

Vicente, R., Escalada, A., Soler, C., Grande, M., Celada, A., Tamkun, M. M., . . . Felipe, A. (2005). "*Pattern of Kv beta subunit expression in macrophages depends upon proliferation and the mode of activation*." J Immunol 174(8): 4736-4744.

Vicente, R., Escalada, A., Villalonga, N., Texido, L., Roura-Ferrer, M., Martin-Satue, M., . . . Felipe, A. (2006). "*Association of Kv1.5 and Kv1.3 contributes to the major voltage-dependent K+ channel in macrophages*." J Biol Chem 281(49): 37675-37685.

Villalonga, N., Escalada, A., Vicente, R., Sanchez-Tillo, E., Celada, A., Solsona, C. and Felipe, A. (2007). "*Kv1.3/Kv1.5 heteromeric channels compromise pharmacological responses in macrophages*." Biochem Biophys Res Commun 352(4): 913-918.

4. Discussion

AVÍS IMPORTANT

El text d'aquest capítol ha estat retirat seguint instruccions de l'autora de la tesi, en existir participació d'empreses, existir conveni de confidencialitat o existeix la possibilitat de generar patents

AVISO IMPORTANTE

El texto de este capítulo ha sido retirado siguiendo instrucciones de la autora, al existir participación de empresas, convenio de confidencialidad o la posibilidad de generar patentes.

IMPORTANT NOTICE

The text of this chapter has been withdrawn on the instructions of the author, as there is participation of undertakings, confidentiality agreement or the ability to generate patent

5. Conclusions

AVÍS IMPORTANT

El text d'aquest capítol ha estat retirat seguint instruccions de l'autora de la tesi, en existir participació d'empreses, existir conveni de confidencialitat o existeix la possibilitat de generar patents

AVISO IMPORTANTE

El texto de este capítulo ha sido retirado siguiendo instrucciones de la autora, al existir participación de empresas, convenio de confidencialidad o la posibilidad de generar patentes.

IMPORTANT NOTICE

The text of this chapter has been withdrawn on the instructions of the author, as there is participation of undertakings, confidentiality agreement or the ability to generate patent

6. References

Abbott, G. W., Butler, M. H., Bendahhou, S., Dalakas, M. C., Ptacek, L. J. and Goldstein, S. A. (2001). "*MiRP2 forms potassium channels in skeletal muscle with Kv3.4 and is associated with periodic paralysis*." Cell 104(2): 217-231.

Abbott, G. W. and Goldstein, S. A. (1998). "*A superfamily of small potassium channel subunits: form and function of the MinK-related peptides (MiRPs)*." Q Rev Biophys 31(4): 357-398.

Abbott, G. W., Sesti, F., Splawski, I., Buck, M. E., Lehmann, M. H., Timothy, K. W., . . . Goldstein, S. A. (1999). "*MiRP1 forms IKr potassium channels with HERG and is associated with cardiac arrhythmia*." Cell 97(2): 175-187.

Abi-Char, J., Maguy, A., Coulombe, A., Balse, E., Ratajczak, P., Samuel, J. L., . . . Hatem, S. N. (2007). "*Membrane cholesterol modulates Kv1.5 potassium channel distribution and function in rat cardiomyocytes*." J Physiol 582(Pt 3): 1205-1217.

Abriel, H., Kamynina, E., Horisberger, J. D. and Staub, O. (2000). "*Regulation of the cardiac voltage-gated Na+ channel (H1) by the ubiquitin-protein ligase Nedd4*." FEBS Lett 466(2-3): 377-380.

Accili, E. A., Kiehn, J., Wible, B. A. and Brown, A. M. (1997). "*Interactions among inactivating and noninactivating Kvbeta subunits, and Kvalpha1.2, produce potassium currents with intermediate inactivation*." J Biol Chem 272(45): 28232-28236.

Aiyar, J., Rizzi, J. P., Gutman, G. A. and Chandy, K. G. (1996). "*The signature sequence of voltage-gated potassium channels projects into the external vestibule*." J Biol Chem 271(49): 31013-31016.

Albarwani, S., Nemetz, L. T., Madden, J. A., Tobin, A. A., England, S. K., Pratt, P. F. and Rusch, N. J. (2003). "*Voltage-gated K+ channels in rat small cerebral arteries: molecular identity of the functional channels*." J Physiol 551(Pt 3): 751-763.

Alioua, A., Lu, R., Kumar, Y., Eghbali, M., Kundu, P., Toro, L. and Stefani, E. (2008). "*Slo1 caveolin-binding motif, a mechanism of caveolin-1-Slo1 interaction regulating Slo1 surface expression*." J Biol Chem 283(8): 4808-4817.

An, W. F., Bowlby, M. R., Betty, M., Cao, J., Ling, H. P., Mendoza, G., . . . Rhodes, K. J. (2000). "*Modulation of A-type potassium channels by a family of calcium sensors*." Nature 403(6769): 553-556.

Anantharam, A., Lewis, A., Panaghie, G., Gordon, E., McCrossan, Z. A., Lerner, D. J. and Abbott, G. W. (2003). "*RNA interference reveals that endogenous Xenopus MinK-related peptides govern mammalian K+ channel function in oocyte expression studies*." J Biol Chem 278(14): 11739-11745.

Andersen, O. S. and Koeppe, R. E., 2nd (2007). "*Bilayer thickness and membrane protein function: an energetic perspective*." Annu Rev Biophys Biomol Struct 36: 107-130.

Anderson, R. G. (1998). "*The caveolae membrane system*." Annu Rev Biochem 67: 199-225.

Angelo, K., Jespersen, T., Grunnet, M., Nielsen, M. S., Klaerke, D. A. and Olesen, S. P. (2002). "*KCNE5 induces time- and voltage-dependent modulation of the KCNQ1 current*." Biophys J 83(4): 1997-2006.

Arkett, S. A., Dixon, J., Yang, J. N., Sakai, D. D., Minkin, C. and Sims, S. M. (1994). "*Mammalian osteoclasts express a transient potassium channel with properties of Kv1.3*." Receptors Channels 2(4): 281-293.

Arnestad, M., Crotti, L., Rognum, T. O., Insolia, R., Pedrazzini, M., Ferrandi, C., . . . Schwartz, P. J. (2007). "*Prevalence of long-QT syndrome gene variants in sudden infant death syndrome*." Circulation 115(3): 361-367.

Arrighi, I., Bloch-Faure, M., Grahammer, F., Bleich, M., Warth, R., Mengual, R., . . . Meneton, P. (2001). "*Altered potassium balance and aldosterone secretion in a mouse model of human congenital long QT syndrome*." Proc Natl Acad Sci U S A 98(15): 8792-8797.

Attali, B., Romey, G., Honore, E., Schmid-Alliana, A., Mattei, M. G., Lesage, F., . . . Lazdunski, M. (1992). "*Cloning, functional expression, and regulation of two K+ channels in human T lymphocytes*." J Biol Chem 267(12): 8650-8657.

Autieri, M. V., Belkowski, S. M., Constantinescu, C. S., Cohen, J. A. and Prystowsky, M. B. (1997). "*Lymphocyte-specific inducible expression of potassium channel beta subunits*." J Neuroimmunol 77(1): 8-16.

Bahring, R., Milligan, C. J., Vardanyan, V., Engeland, B., Young, B. A., Dannenberg, J., . . . Pongs, O. (2001). "*Coupling of voltage-dependent potassium channel inactivation and oxidoreductase active site of Kvbeta subunits*." J Biol Chem 276(25): 22923-22929.

Bal, M., Zhang, J., Zaika, O., Hernandez, C. C. and Shapiro, M. S. (2008). "*Homomeric and heteromeric assembly of KCNQ (Kv7) K+ channels assayed by total internal reflection fluorescence/fluorescence resonance energy transfer and patch clamp analysis*." J Biol Chem 283(45): 30668-30676.

Balasubramaniam, R., Grace, A. A., Saumarez, R. C., Vandenberg, J. I. and Huang, C. L. (2003). "*Electrogram prolongation and nifedipine-suppressible ventricular arrhythmias in mice following targeted disruption of KCNE1*." J Physiol 552(Pt 2): 535-546.

Balijepalli, R. C., Delisle, B. P., Balijepalli, S. Y., Foell, J. D., Slind, J. K., Kamp, T. J. and January, C. T. (2007). "*Kv11.1 (ERG1) K+ channels localize in cholesterol and sphingolipid enriched membranes and are modulated by membrane cholesterol*." Channels (Austin) 1(4): 263-272.

Balijepalli, R. C., Foell, J. D., Hall, D. D., Hell, J. W. and Kamp, T. J. (2006). "*Localization of cardiac L-type Ca(2+) channels to a caveolar macromolecular signaling complex is required for beta(2)-adrenergic regulation*." Proc Natl Acad Sci U S A 103(19): 7500-7505.

Balijepalli, R. C. and Kamp, T. J. (2008). "*Caveolae, ion channels and cardiac arrhythmias*." Prog Biophys Mol Biol 98(2-3): 149-160.

Barbuti, A., Gravante, B., Riolfo, M., Milanesi, R., Terragni, B. and DiFrancesco, D. (2004). "*Localization of pacemaker channels in lipid rafts regulates channel kinetics*." Circ Res 94(10): 1325-1331.

Barhanin, J., Lesage, F., Guillemare, E., Fink, M., Lazdunski, M. and Romey, G. (1996). "*K(V)LQT1 and lsK (minK) proteins associate to form the I(Ks) cardiac potassium current*." Nature 384(6604): 78-80.

Barros, F., Dominguez, P. and de la Pena, P. (2012). "*Cytoplasmic domains and voltage-dependent potassium channel gating*." Front Pharmacol 3: 49.

Barth, K., Weinhold, K., Guenther, A., Linge, A., Gereke, M. and Kasper, M. (2008). "*Characterization of the molecular interaction between caveolin-1 and the P2X receptors 4 and 7 in E10 mouse lung alveolar epithelial cells*." Int J Biochem Cell Biol 40(10): 2230-2239.

Barth, K., Weinhold, K., Guenther, A., Young, M. T., Schnittler, H. and Kasper, M. (2007). "*Caveolin-1 influences P2X7 receptor expression and localization in mouse lung alveolar epithelial cells*." FEBS J 274(12): 3021-3033.

Beeton, C. and Chandy, K. G. (2005). "*Potassium channels, memory T cells, and multiple sclerosis*." Neuroscientist 11(6): 550-562.

Beeton, C., Pennington, M. W. and Norton, R. S. (2011). "*Analogs of the sea anemone potassium channel blocker ShK for the treatment of autoimmune diseases*." Inflamm Allergy Drug Targets 10(5): 313-321.

Beeton, C., Pennington, M. W., Wulff, H., Singh, S., Nugent, D., Crossley, G., . . . Chandy, K. G. (2005). "*Targeting effector memory T cells with a selective peptide inhibitor of Kv1.3 channels for therapy of autoimmune diseases*." Mol Pharmacol 67(4): 1369-1381.

Beeton, C., Wulff, H., Barbaria, J., Clot-Faybesse, O., Pennington, M., Bernard, D., . . . Beraud, E. (2001). "*Selective blockade of T lymphocyte K(+) channels ameliorates experimental autoimmune encephalomyelitis, a model for multiple sclerosis*." Proc Natl Acad Sci U S A 98(24): 13942-13947.

Beeton, C., Wulff, H., Singh, S., Botsko, S., Crossley, G., Gutman, G. A., . . . Chandy, K. G. (2003). "*A novel fluorescent toxin to detect and investigate Kv1.3 channel up-regulation in chronically activated T lymphocytes*." J Biol Chem 278(11): 9928-9937.

Bendahhou, S., Marionneau, C., Haurogne, K., Larroque, M. M., Derand, R., Szuts, V., . . . Barhanin, J. (2005). "*In vitro molecular interactions and distribution of KCNE family with KCNQ1 in the human heart*." Cardiovasc Res 67(3): 529-538.

Beraud, E. and Chandy, K. G. (2011). "*Therapeutic potential of peptide toxins that target ion channels*." Inflamm Allergy Drug Targets 10(5): 322-342.

Bianchi, L., Shen, Z., Dennis, A. T., Priori, S. G., Napolitano, C., Ronchetti, E., . . . Brown, A. M. (1999). "*Cellular dysfunction of LQT5-minK mutants: abnormalities of IKs, IKr and trafficking in long QT syndrome*." Hum Mol Genet 8(8): 1499-1507.

Bielanska, J., Hernandez-Losa, J., Moline, T., Somoza, R., Cajal, S. R., Condom, E., . . . Felipe, A. (2012). "*Increased voltage-dependent K(+) channel Kv1.3 and Kv1.5 expression correlates with leiomyosarcoma aggressiveness*." Oncol Lett 4(2): 227-230.

Bielanska, J., Hernandez-Losa, J., Moline, T., Somoza, R., Ramon y Cajal, S., Condom, E., . . . Felipe, A. (2012). "*Differential expression of Kv1.3 and Kv1.5 voltage-dependent K+ channels in human skeletal muscle sarcomas*." Cancer Invest 30(3): 203-208.

Bielanska, J., Hernandez-Losa, J., Perez-Verdaguer, M., Moline, T., Somoza, R., Ramon, Y. C. S., . . . Felipe, A. (2009). "*Voltage-dependent potassium channels Kv1.3 and Kv1.5 in human cancer*." Curr Cancer Drug Targets 9(8): 904-914.

Blunck, R., Cordero-Morales, J. F., Cuello, L. G., Perozo, E. and Bezanilla, F. (2006). "*Detection of the opening of the bundle crossing in KcsA with fluorescence lifetime spectroscopy reveals the existence of two gates for ion conduction*." J Gen Physiol 128(5): 569-581.

Bock, J., Szabo, I., Gamper, N., Adams, C. and Gulbins, E. (2003). "*Ceramide inhibits the potassium channel Kv1.3 by the formation of membrane platforms*." Biochem Biophys Res Commun 305(4): 890-897.

Bock, J., Szabo, I., Jekle, A. and Gulbins, E. (2002). "*Actinomycin D-induced apoptosis involves the potassium channel Kv1.3*." Biochem Biophys Res Commun 295(2): 526-531.

Boehmer, C., Laufer, J., Jeyaraj, S., Klaus, F., Lindner, R., Lang, F. and Palmada, M. (2008). "*Modulation of the voltage-gated potassium channel Kv1.5 by the SGK1 protein kinase involves inhibition of channel ubiquitination*." Cell Physiol Biochem 22(5-6): 591-600.

Bokil, N. J., Baisden, J. M., Radford, D. J. and Summers, K. M. (2010). "*Molecular genetics of long QT syndrome*." Mol Genet Metab 101(1): 1-8.

Borjesson, S. I. and Elinder, F. (2008). "*Structure, function, and modification of the voltage sensor in voltage-gated ion channels*." Cell Biochem Biophys 52(3): 149-174.

Bowlby, M. R., Fadool, D. A., Holmes, T. C. and Levitan, I. B. (1997). "*Modulation of the Kv1.3 potassium channel by receptor tyrosine kinases*." J Gen Physiol 110(5): 601-610.

Braakman, I. and Bulleid, N. J. (2011). "*Protein folding and modification in the mammalian endoplasmic reticulum*." Annu Rev Biochem 80: 71-99.

Brainard, A. M., Korovkina, V. P. and England, S. K. (2009). "*Disruption of the maxi-K-caveolin-1 interaction alters current expression in human myometrial cells*." Reprod Biol Endocrinol 7: 131.

Brandt, M. C., Endres-Becker, J., Zagidullin, N., Motloch, L. J., Er, F., Rottlaender, D., . . . Hoppe, U. C. (2009). "*Effects of KCNE2 on HCN isoforms: distinct modulation of membrane expression and single channel properties*." Am J Physiol Heart Circ Physiol 297(1): H355-363.

Brown, D. A. and London, E. (1998). "*Structure and origin of ordered lipid domains in biological membranes*." J Membr Biol 164(2): 103-114.

Brown, D. A. and Rose, J. K. (1992). "*Sorting of GPI-anchored proteins to glycolipid-enriched membrane subdomains during transport to the apical cell surface*." Cell 68(3): 533-544.

Brueggemann, L. I., Moran, C. J., Barakat, J. A., Yeh, J. Z., Cribbs, L. L. and Byron, K. L. (2007). "*Vasopressin stimulates action potential firing by protein kinase C-dependent inhibition of KCNQ5 in A7r5 rat aortic smooth muscle cells*." Am J Physiol Heart Circ Physiol 292(3): H1352-1363.

Cahalan, M. D. and Chandy, K. G. (2009). "*The functional network of ion channels in T lymphocytes*." Immunol Rev 231(1): 59-87.

Cahalan, M. D., Chandy, K. G., DeCoursey, T. E. and Gupta, S. (1985). "*A voltage-gated potassium channel in human T lymphocytes*." J Physiol 358: 197-237.

Cahalan, M. D., Wulff, H. and Chandy, K. G. (2001). "*Molecular properties and physiological roles of ion channels in the immune system*." J Clin Immunol 21(4): 235-252.

Cai, Y. C. and Douglass, J. (1993). "*In vivo and in vitro phosphorylation of the T lymphocyte type n (Kv1.3) potassium channel*." J Biol Chem 268(31): 23720-23727.

Cai, Y. C., Osborne, P. B., North, R. A., Dooley, D. C. and Douglass, J. (1992). "*Characterization and functional expression of genomic DNA encoding the human lymphocyte type n potassium channel*." DNA Cell Biol 11(2): 163-172.

Calaghan, S. and White, E. (2006). "*Caveolae modulate excitation-contraction coupling and beta2-adrenergic signalling in adult rat ventricular myocytes*." Cardiovasc Res 69(4): 816-824.

Campbell, C. A., Della Santina, C. C., Meyer, N. C., Smith, N. B., Myrie, O. A., Stone, E. M., . . . Smith, R. J. (2010). "*Polymorphisms in KCNE1 or KCNE3 are not associated with Meniere disease in the Caucasian population*." Am J Med Genet A 152A(1): 67-74.

Casimiro, M. C., Knollmann, B. C., Ebert, S. N., Vary, J. C., Jr., Greene, A. E., Franz, M. R., . . . Pfeifer, K. (2001). "*Targeted disruption of the Kcnq1 gene produces a mouse model of Jervell and Lange-Nielsen Syndrome*." Proc Natl Acad Sci U S A 98(5): 2526-2531.

Ciampa, E. J. (2011). "*Investigating the function of KCNE4 in cardiac physiology.* ." PhD thesis.

Ciampa, E. J., Welch, R. C., Vanoye, C. G. and George, A. L., Jr. (2011). "*KCNE4 juxtamembrane region is required for interaction with calmodulin and for functional suppression of KCNQ1*." J Biol Chem 286(6): 4141-4149.

Clancy, S. M., Chen, B., Bertaso, F., Mamet, J. and Jegla, T. (2009). "*KCNE1 and KCNE3 beta-subunits regulate membrane surface expression of Kv12.2 K(+) channels in vitro and form a tripartite complex in vivo*." PLoS One 4(7): e6330.

Coleman, S. K., Newcombe, J., Pryke, J. and Dolly, J. O. (1999). "*Subunit composition of Kv1 channels in human CNS*." J Neurochem 73(2): 849-858.

Couet, J., Li, S., Okamoto, T., Ikezu, T. and Lisanti, M. P. (1997). "*Identification of peptide and protein ligands for the caveolin-scaffolding domain. Implications for the interaction of caveolin with caveolae-associated proteins*." J Biol Chem 272(10): 6525-6533.

Cox, R. H., Folander, K. and Swanson, R. (2001). "*Differential expression of voltage-gated K(+) channel genes in arteries from spontaneously hypertensive and Wistar-Kyoto rats*." Hypertension 37(5): 1315-1322.

Cui, J., Kline, R. P., Pennefather, P. and Cohen, I. S. (1994). "*Gating of IsK expressed in Xenopus oocytes depends on the amount of mRNA injected*." J Gen Physiol 104(1): 87-105.

Cushman, S. J., Nanao, M. H., Jahng, A. W., DeRubeis, D., Choe, S. and Pfaffinger, P. J. (2000). "*Voltage dependent activation of potassium channels is coupled to T1 domain structure*." Nat Struct Biol 7(5): 403-407.

Chadha, P. S., Zunke, F., Davis, A. J., Jepps, T. A., Linders, J. T., Schwake, M., . . . Greenwood, I. A. (2012). "*Pharmacological dissection of K(v)7.1 channels in systemic and pulmonary arteries*." Br J Pharmacol 166(4): 1377-1387.

Chan, P. J., Osteen, J. D., Xiong, D., Bohnen, M. S., Doshi, D., Sampson, K. J., . . . Kass, R. S. (2012). "*Characterization of KCNQ1 atrial fibrillation mutations reveals distinct dependence on KCNE1*." J Gen Physiol 139(2): 135-144.

Chanda, B., Asamoah, O. K. and Bezanilla, F. (2004). "*Coupling interactions between voltage sensors of the sodium channel as revealed by site-specific measurements*." J Gen Physiol 123(3): 217-230.

Chanda, B., Asamoah, O. K., Blunck, R., Roux, B. and Bezanilla, F. (2005). "*Gating charge displacement in voltage-gated ion channels involves limited transmembrane movement*." Nature 436(7052): 852-856.

Chandrasekhar, K. D., Bas, T. and Kobertz, W. R. (2006). "*KCNE1 subunits require co-assembly with K+ channels for efficient trafficking and cell surface expression*." J Biol Chem 281(52): 40015-40023.

Chang, M. C., Khanna, R. and Schlichter, L. C. (2001). "*Regulation of Kv1.3 channels in activated human T lymphocytes by Ca(2+)-dependent pathways*." Cell Physiol Biochem 11(3): 123-134.

Chen, H., Kim, L. A., Rajan, S., Xu, S. and Goldstein, S. A. (2003). "*Charybdotoxin binding in the I(Ks) pore demonstrates two MinK subunits in each channel complex*." Neuron 40(1): 15-23.

Chen, J., Mitcheson, J. S., Tristani-Firouzi, M., Lin, M. and Sanguinetti, M. C. (2001). "*The S4-S5 linker couples voltage sensing and activation of pacemaker channels*." Proc Natl Acad Sci U S A 98(20): 11277-11282.

Chen, J., Zheng, R., Melman, Y. F. and McDonald, T. V. (2009). "*Functional interactions between KCNE1 C-terminus and the KCNQ1 channel*." PLoS One 4(4): e5143.

Chen, L. and Kass, R. S. (2006). "*Dual roles of the A kinase-anchoring protein Yotiao in the modulation of a cardiac potassium channel: a passive adaptor versus an active regulator*." Eur J Cell Biol 85(7): 623-626.

Cheng, Y. M. and Claydon, T. W. (2012). "*Voltage-dependent gating of HERG potassium channels*." Front Pharmacol 3: 83.

Chi, V., Pennington, M. W., Norton, R. S., Tarcha, E. J., Londono, L. M., Sims-Fahey, B., . . . Chandy, K. G. (2012). "*Development of a sea anemone toxin as an immunomodulator for therapy of autoimmune diseases*." Toxicon 59(4): 529-546.

Choi, E. and Abbott, G. W. (2007). "*The MiRP2-Kv3.4 potassium channel: muscling in on Alzheimer's disease*." Mol Pharmacol 72(3): 499-501.

Chouabe, C., Neyroud, N., Richard, P., Denjoy, I., Hainque, B., Romey, G., . . . Barhanin, J. (2000). "*Novel mutations in KvLQT1 that affect Iks activation through interactions with Isk*." Cardiovasc Res 45(4): 971-980.

Christie, M. J., North, R. A., Osborne, P. B., Douglass, J. and Adelman, J. P. (1990). "*Heteropolymeric potassium channels expressed in Xenopus oocytes from cloned subunits*." Neuron 4(3): 405-411.

Chung, D. Y., Chan, P. J., Bankston, J. R., Yang, L., Liu, G., Marx, S. O., . . . Kass, R. S. (2009). "*Location of KCNE1 relative to KCNQ1 in the I(KS) potassium channel by disulfide cross-linking of substituted cysteines*." Proc Natl Acad Sci U S A 106(3): 743-748.

Dalby-Brown, W., Jessen, C., Hougaard, C., Jensen, M. L., Jacobsen, T. A., Nielsen, K. S., . . . Jorgensen, S. (2013). "*Characterization of a novel high-potency positive modulator of K(v)7 channels*." Eur J Pharmacol 709(1-3): 52-63.

Darby, P. J., Kwan, C. Y. and Daniel, E. E. (2000). "*Caveolae from canine airway smooth muscle contain the necessary components for a role in Ca(2+) handling*." Am J Physiol Lung Cell Mol Physiol 279(6): L1226-1235.

Dart, C. (2010). "*Lipid microdomains and the regulation of ion channel function*." J Physiol 588(Pt 17): 3169-3178.

David, J. P., Andersen, M. N., Olesen, S. P., Rasmussen, H. B. and Schmitt, N. (2013). "*Trafficking of the IKs -complex in MDCK cells: site of subunit assembly and determinants of polarized localization*." Traffic 14(4): 399-411.

Davies, A. M., Batchelor, T. J., Eardley, I. and Beech, D. J. (2002). "*Potassium channel KV alpha1 subunit expression and function in human detrusor muscle*." J Urol 167(4): 1881-1886.

Decher, N., Bundis, F., Vajna, R. and Steinmeyer, K. (2003). "*KCNE2 modulates current amplitudes and activation kinetics of HCN4: influence of KCNE family members on HCN4 currents*." Pflugers Arch 446(6): 633-640.

Decher, N., Pirard, B., Bundis, F., Peukert, S., Baringhaus, K. H., Busch, A. E., . . . Sanguinetti, M. C. (2004). "*Molecular basis for Kv1.5 channel block: conservation of drug binding sites among voltage-gated K+ channels*." J Biol Chem 279(1): 394-400.

Dedek, K. and Waldegger, S. (2001). "*Colocalization of KCNQ1/KCNE channel subunits in the mouse gastrointestinal tract*." Pflugers Arch 442(6): 896-902.

del Camino, D., Holmgren, M., Liu, Y. and Yellen, G. (2000). "*Blocker protection in the pore of a voltage-gated K+ channel and its structural implications*." Nature 403(6767): 321-325.

del Camino, D. and Yellen, G. (2001). "*Tight steric closure at the intracellular activation gate of a voltage-gated K(+) channel*." Neuron 32(4): 649-656.

Delpon, E., Cordeiro, J. M., Nunez, L., Thomsen, P. E., Guerchicoff, A., Pollevick, G. D., . . . Antzelevitch, C. (2008). "*Functional effects of KCNE3 mutation and its role in the development of Brugada syndrome*." Circ Arrhythm Electrophysiol 1(3): 209-218.

Delling, M., Wischmeyer, E., Dityatev, A., Sytnyk, V., Veh, R. W., Karschin, A. and Schachner, M. (2002). "*The neural cell adhesion molecule regulates cell-surface delivery of G-protein-activated inwardly rectifying potassium channels via lipid rafts*." J Neurosci 22(16): 7154-7164.

Demolombe, S., Franco, D., de Boer, P., Kuperschmidt, S., Roden, D., Pereon, Y., . . . Escande, D. (2001). "*Differential expression of KvLQT1 and its regulator IsK in mouse epithelia*." Am J Physiol Cell Physiol 280(2): C359-372.

Dias Da Silva, M. R., Cerutti, J. M., Arnaldi, L. A. and Maciel, R. M. (2002). "*A mutation in the KCNE3 potassium channel gene is associated with susceptibility to thyrotoxic hypokalemic periodic paralysis*." J Clin Endocrinol Metab 87(11): 4881-4884.

Ding, S. and Horn, R. (2002). "*Tail end of the s6 segment: role in permeation in shaker potassium channels*." J Gen Physiol 120(1): 87-97.

Doi, K., Sato, T., Kuramasu, T., Hibino, H., Kitahara, T., Horii, A., . . . Kubo, T. (2005). "*Meniere's disease is associated with single nucleotide polymorphisms in the human potassium channel genes, KCNE1 and KCNE3*." ORL J Otorhinolaryngol Relat Spec 67(5): 289-293.

Donger, C., Denjoy, I., Berthet, M., Neyroud, N., Cruaud, C., Bennaceur, M., . . . Guicheney, P. (1997). "*KVLQT1 C-terminal missense mutation causes a forme fruste long-QT syndrome*." Circulation 96(9): 2778-2781.

Dougherty, K. and Covarrubias, M. (2006). "*A dipeptidyl aminopeptidase-like protein remodels gating charge dynamics in Kv4.2 channels*." J Gen Physiol 128(6): 745-753.

Doyle, D. A., Morais Cabral, J., Pfuetzner, R. A., Kuo, A., Gulbis, J. M., Cohen, S. L., . . . MacKinnon, R. (1998). "*The structure of the potassium channel: molecular basis of K+ conduction and selectivity*." Science 280(5360): 69-77.

Du, Y. M., Zhang, X. X., Tu, D. N., Zhao, N., Liu, Y. J., Xiao, H., . . . Liao, Y. H. (2010). "*Molecular determinants of Kv1.5 channel block by diphenyl phosphine oxide-1*." J Mol Cell Cardiol 48(6): 1111-1120.

Duggal, P., Vesely, M. R., Wattanasirichaigoon, D., Villafane, J., Kaushik, V. and Beggs, A. H. (1998). "*Mutation of the gene for IsK associated with both Jervell and Lange-Nielsen and Romano-Ward forms of Long-QT syndrome*." Circulation 97(2): 142-146.

Dupuis, D. S., Schroder, R. L., Jespersen, T., Christensen, J. K., Christophersen, P., Jensen, B. S. and Olesen, S. P. (2002). "*Activation of KCNQ5 channels stably expressed in HEK293 cells by BMS-204352*." Eur J Pharmacol 437(3): 129-137.

Durell, S. R., Hao, Y. and Guy, H. R. (1998). "*Structural models of the transmembrane region of voltage-gated and other K+ channels in open, closed, and inactivated conformations*." J Struct Biol 121(2): 263-284.

Ehrlich, J. R., Zicha, S., Coutu, P., Hebert, T. E. and Nattel, S. (2005). "*Atrial fibrillation-associated minK38G/S polymorphism modulates delayed rectifier current and membrane localization*." Cardiovasc Res 67(3): 520-528.

Ekberg, J., Schuetz, F., Boase, N. A., Conroy, S. J., Manning, J., Kumar, S., . . . Adams, D. J. (2007). "*Regulation of the voltage-gated K(+) channels KCNQ2/3 and KCNQ3/5 by ubiquitination. Novel role for Nedd4-2*." J Biol Chem 282(16): 12135-12142.

Eldstrom, J., Choi, W. S., Steele, D. F. and Fedida, D. (2003). "*SAP97 increases Kv1.5 currents through an indirect N-terminal mechanism*." FEBS Lett 547(1-3): 205-211.

Eldstrom, J., Van Wagoner, D. R., Moore, E. D. and Fedida, D. (2006). "*Localization of Kv1.5 channels in rat and canine myocyte sarcolemma*." FEBS Lett 580(26): 6039-6046.

Epshtein, Y., Chopra, A. P., Rosenhouse-Dantsker, A., Kowalsky, G. B., Logothetis, D. E. and Levitan, I. (2009). "*Identification of a C-terminus domain critical for the sensitivity of Kir2.1 to cholesterol*." Proc Natl Acad Sci U S A 106(19): 8055-8060.

Fadool, D. A., Holmes, T. C., Berman, K., Dagan, D. and Levitan, I. B. (1997). "*Tyrosine phosphorylation modulates current amplitude and kinetics of a neuronal voltage-gated potassium channel*." J Neurophysiol 78(3): 1563-1573.

Fadool, D. A., Tucker, K., Perkins, R., Fasciani, G., Thompson, R. N., Parsons, A. D., . . . Kaczmarek, L. K. (2004). "*Kv1.3 channel gene-targeted deletion produces "Super-Smeller Mice" with altered glomeruli, interacting scaffolding proteins, and biophysics*." Neuron 41(3): 389-404.

Fanger, C. M., Ghanshani, S., Logsdon, N. J., Rauer, H., Kalman, K., Zhou, J., . . . Aiyar, J. (1999). "*Calmodulin mediates calcium-dependent activation of the intermediate conductance KCa channel, IKCa1*." J Biol Chem 274(9): 5746-5754.

Fatini, C., Sticchi, E., Marcucci, R., Verdiani, V., Nozzoli, C., Vassallo, C., . . . Gensini, G. F. (2010). "*S38G single-nucleotide polymorphism at the KCNE1 locus is associated with heart failure*." Heart Rhythm 7(3): 363-367.

Fedida, D., Wible, B., Wang, Z., Fermini, B., Faust, F., Nattel, S. and Brown, A. M. (1993). "*Identity of a novel delayed rectifier current from human heart with a cloned K+ channel current*." Circ Res 73(1): 210-216.

Feng, J., Wible, B., Li, G. R., Wang, Z. and Nattel, S. (1997). "*Antisense oligodeoxynucleotides directed against Kv1.5 mRNA specifically inhibit ultrarapid delayed rectifier K+ current in cultured adult human atrial myocytes*." Circ Res 80(4): 572-579.

Fergus, D. J., Martens, J. R. and England, S. K. (2003). "*Kv channel subunits that contribute to voltage-gated K+ current in renal vascular smooth muscle*." Pflugers Arch 445(6): 697-704.

Folco, E. J., Liu, G. X. and Koren, G. (2004). "*Caveolin-3 and SAP97 form a scaffolding protein complex that regulates the voltage-gated potassium channel Kv1.5*." Am J Physiol Heart Circ Physiol 287(2): H681-690.

Fordyce, C. B., Jagasia, R., Zhu, X. and Schlichter, L. C. (2005). "*Microglia Kv1.3 channels contribute to their ability to kill neurons*." J Neurosci 25(31): 7139-7149.

Franqueza, L., Lin, M., Shen, J., Splawski, I., Keating, M. T. and Sanguinetti, M. C. (1999). "*Long QT syndrome-associated mutations in the S4-S5 linker of KvLQT1 potassium channels modify gating and interaction with minK subunits*." J Biol Chem 274(30): 21063-21070.

Freidin, M. B., Bragina, E., Fedorova, O. S., Deev, I. A., Kulikov, E. S., Ogorodova, L. M. and Puzyrev, V. P. (2011). "*[Genome-wide association study of allergic diseases in Russians of Western Siberia]*." Mol Biol (Mosk) 45(3): 464-472.

Frohlich, H., Boini, K. M., Seebohm, G., Strutz-Seebohm, N., Ureche, O. N., Foller, M., . . . Lang, F. (2011). "*Hypothyroidism of gene-targeted mice lacking Kcnq1*." Pflugers Arch 461(1): 45-52.

Gage, S. D. and Kobertz, W. R. (2004). "*KCNE3 truncation mutants reveal a bipartite modulation of KCNQ1 K+ channels*." J Gen Physiol 124(6): 759-771.

Gamper, N., Li, Y. and Shapiro, M. S. (2005). "*Structural requirements for differential sensitivity of KCNQ K+ channels to modulation by Ca2+/calmodulin*." Mol Biol Cell 16(8): 3538-3551.

Gamper, N. and Shapiro, M. S. (2003). "*Calmodulin mediates Ca2+-dependent modulation of M-type K+ channels*." J Gen Physiol 122(1): 17-31.

Gamper, N., Stockand, J. D. and Shapiro, M. S. (2003). "*Subunit-specific modulation of KCNQ potassium channels by Src tyrosine kinase*." J Neurosci 23(1): 84-95.

Garcia-Calvo, M., Leonard, R. J., Novick, J., Stevens, S. P., Schmalhofer, W., Kaczorowski, G. J. and Garcia, M. L. (1993). "*Purification, characterization, and biosynthesis of margatoxin, a component of Centruroides margaritatus venom that selectively inhibits voltage-dependent potassium channels*." J Biol Chem 268(25): 18866-18874.

Garg, V., Jiao, J. and Hu, K. (2009). "*Regulation of ATP-sensitive K+ channels by caveolin-enriched microdomains in cardiac myocytes*." Cardiovasc Res 82(1): 51-58.

Gilling, M., Rasmussen, H. B., Calloe, K., Sequeira, A. F., Baretto, M., Oliveira, G., . . . Tommerup, N. (2013). "*Dysfunction of the Heteromeric KV7.3/KV7.5 Potassium Channel is Associated with Autism Spectrum Disorders*." Front Genet 4: 54.

Gocke, A. R., Lebson, L. A., Grishkan, I. V., Hu, L., Nguyen, H. M., Whartenby, K. A., . . . Calabresi, P. A. (2012). "*Kv1.3 deletion biases T cells toward an immunoregulatory phenotype and renders mice resistant to autoimmune encephalomyelitis*." J Immunol 188(12): 5877-5886.

Gordon, E., Panaghie, G., Deng, L., Bee, K. J., Roepke, T. K., Krogh-Madsen, T., . . . Abbott, G. W. (2008). "*A KCNE2 mutation in a patient with cardiac arrhythmia induced by auditory stimuli and serum electrolyte imbalance*." Cardiovasc Res 77(1): 98-106.

Gordon, E., Roepke, T. K. and Abbott, G. W. (2006). "*Endogenous KCNE subunits govern Kv2.1 K+ channel activation kinetics in Xenopus oocyte studies*." Biophys J 90(4): 1223-1231.

Grahammer, F., Herling, A. W., Lang, H. J., Schmitt-Graff, A., Wittekindt, O. H., Nitschke, R., . . . Warth, R. (2001). "*The cardiac K+ channel KCNQ1 is essential for gastric acid secretion*." Gastroenterology 120(6): 1363-1371.

Greenwood, I. A. and Ohya, S. (2009). "*New tricks for old dogs: KCNQ expression and role in smooth muscle*." Br J Pharmacol 156(8): 1196-1203.

Grissmer, S., Dethlefs, B., Wasmuth, J. J., Goldin, A. L., Gutman, G. A., Cahalan, M. D. and Chandy, K. G. (1990). "*Expression and chromosomal localization of a lymphocyte K+ channel gene*." Proc Natl Acad Sci U S A 87(23): 9411-9415.

Grissmer, S., Nguyen, A. N., Aiyar, J., Hanson, D. C., Mather, R. J., Gutman, G. A., . . . Chandy, K. G. (1994). "*Pharmacological characterization of five cloned voltage-gated K+ channels, types Kv1.1, 1.2, 1.3, 1.5, and 3.1, stably expressed in mammalian cell lines*." Mol Pharmacol 45(6): 1227-1234.

Grunnet, M., Jespersen, T., Rasmussen, H. B., Ljungstrom, T., Jorgensen, N. K., Olesen, S. P. and Klaerke, D. A. (2002). "*KCNE4 is an inhibitory subunit to the KCNQ1 channel*." J Physiol 542(Pt 1): 119-130.

Grunnet, M., Olesen, S. P., Klaerke, D. A. and Jespersen, T. (2005). "*hKCNE4 inhibits the hKCNQ1 potassium current without affecting the activation kinetics*." Biochem Biophys Res Commun 328(4): 1146-1153.

Grunnet, M., Rasmussen, H. B., Hay-Schmidt, A., Rosenstierne, M., Klaerke, D. A., Olesen, S. P. and Jespersen, T. (2003). "*KCNE4 is an inhibitory subunit to Kv1.1 and Kv1.3 potassium channels*." Biophys J 85(3): 1525-1537.

Grupe, A., Schroter, K. H., Ruppersberg, J. P., Stocker, M., Drewes, T., Beckh, S. and Pongs, O. (1990). "*Cloning and expression of a human voltage-gated potassium channel. A novel member of the RCK potassium channel family*." EMBO J 9(6): 1749-1756.

Guirland, C. and Zheng, J. Q. (2007). "*Membrane lipid rafts and their role in axon guidance*." Adv Exp Med Biol 621: 144-155.

Gulbins, E., Sassi, N., Grassme, H., Zoratti, M. and Szabo, I. (2010). "*Role of Kv1.3 mitochondrial potassium channel in apoptotic signalling in lymphocytes*." Biochim Biophys Acta 1797(6-7): 1251-1259.

Gulbis, J. M., Zhou, M., Mann, S. and MacKinnon, R. (2000). "*Structure of the cytoplasmic beta subunit-T1 assembly of voltage-dependent K+ channels*." Science 289(5476): 123-127.

Gutman, G. A., Chandy, K. G., Adelman, J. P., Aiyar, J., Bayliss, D. A., Clapham, D. E., . . . Wymore, R. S. (2003). "*International Union of Pharmacology. XLI. Compendium of voltage-gated ion channels: potassium channels*." Pharmacol Rev 55(4): 583-586.

Haitin, Y. and Attali, B. (2008). "*The C-terminus of Kv7 channels: a multifunctional module*." J Physiol 586(7): 1803-1810.

Haitin, Y., Wiener, R., Shaham, D., Peretz, A., Cohen, E. B., Shamgar, L., . . . Attali, B. (2009). "*Intracellular domains interactions and gated motions of I(KS) potassium channel subunits*." EMBO J 28(14): 1994-2005.

Hanzal-Bayer, M. F. and Hancock, J. F. (2007). "*Lipid rafts and membrane traffic*." FEBS Lett 581(11): 2098-2104.

Harder, T. and Simons, K. (1997). "*Caveolae, DIGs, and the dynamics of sphingolipid-cholesterol microdomains*." Curr Opin Cell Biol 9(4): 534-542.

Harvey, A. L. (2001). "*Twenty years of dendrotoxins*." Toxicon 39(1): 15-26.

Heginbotham, L., Lu, Z., Abramson, T. and MacKinnon, R. (1994). "*Mutations in the K+ channel signature sequence*." Biophys J 66(4): 1061-1067.

Heinemann, S., Rettig, J., Scott, V., Parcej, D. N., Lorra, C., Dolly, J. and Pongs, O. (1994). "*The inactivation behaviour of voltage-gated K-channels may be determined by association of alpha- and beta-subunits*." J Physiol Paris 88(3): 173-180.

Heinemann, S. H., Rettig, J., Graack, H. R. and Pongs, O. (1996). "*Functional characterization of Kv channel beta-subunits from rat brain*." J Physiol 493 (Pt 3): 625-633.

Heitzmann, D., Grahammer, F., von Hahn, T., Schmitt-Graff, A., Romeo, E., Nitschke, R., . . . Warth, R. (2004). "*Heteromeric KCNE2/KCNQ1 potassium channels in the luminal membrane of gastric parietal cells*." J Physiol 561(Pt 2): 547-557.

Herreros, J., Ng, T. and Schiavo, G. (2001). "*Lipid rafts act as specialized domains for tetanus toxin binding and internalization into neurons*." Mol Biol Cell 12(10): 2947-2960.

Hibino, H. and Kurachi, Y. (2007). "*Distinct detergent-resistant membrane microdomains (lipid rafts) respectively harvest K(+) and water transport systems in brain astroglia*." Eur J Neurosci 26(9): 2539-2555.

Higashida, H., Hoshi, N., Zhang, J. S., Yokoyama, S., Hashii, M., Jin, D., . . . Robbins, J. (2005). "*Protein kinase C bound with A-kinase anchoring protein is involved in muscarinic receptor-activated modulation of M-type KCNQ potassium channels*." Neurosci Res 51(3): 231-234.

Hill, W. G., Butterworth, M. B., Wang, H., Edinger, R. S., Lebowitz, J., Peters, K. W., . . . Johnson, J. P. (2007). "*The epithelial sodium channel (ENaC) traffics to apical membrane in lipid rafts in mouse cortical collecting duct cells*." J Biol Chem 282(52): 37402-37411.

Hirota, Y., Kurata, Y., Kato, M., Notsu, T., Koshida, S., Inoue, T., . . . Hisatome, I. (2008). "*Functional stabilization of Kv1.5 protein by Hsp70 in mammalian cell lines*." Biochem Biophys Res Commun 372(3): 469-474.

Holmes, T. C., Fadool, D. A., Ren, R. and Levitan, I. B. (1996). "*Association of Src tyrosine kinase with a human potassium channel mediated by SH3 domain*." Science 274(5295): 2089-2091.

Holmgren, M., Smith, P. L. and Yellen, G. (1997). "*Trapping of organic blockers by closing of voltage-dependent K+ channels: evidence for a trap door mechanism of activation gating*." J Gen Physiol 109(5): 527-535.

Hong, Z., Smith, A. J., Archer, S. L., Wu, X. C., Nelson, D. P., Peterson, D., . . . Weir, E. K. (2005). "*Pergolide is an inhibitor of voltage-gated potassium channels, including Kv1.5, and causes pulmonary vasoconstriction*." Circulation 112(10): 1494-1499.

Hoppe, U. C., Marban, E. and Johns, D. C. (2001). "*Distinct gene-specific mechanisms of arrhythmia revealed by cardiac gene transfer of two long QT disease genes, HERG and KCNE1*." Proc Natl Acad Sci U S A 98(9): 5335-5340.

Hoshi, T., Zagotta, W. N. and Aldrich, R. W. (1990). "*Biophysical and molecular mechanisms of Shaker potassium channel inactivation*." Science 250(4980): 533-538.

Howard, R. J., Clark, K. A., Holton, J. M. and Minor, D. L., Jr. (2007). "*Structural insight into KCNQ (Kv7) channel assembly and channelopathy*." Neuron 53(5): 663-675.

Hu, H., Vervaeke, K. and Storm, J. F. (2007). "*M-channels (Kv7/KCNQ channels) that regulate synaptic integration, excitability, and spike pattern of CA1 pyramidal cells are located in the perisomatic region*." J Neurosci 27(8): 1853-1867.

Hugnot, J. P., Salinas, M., Lesage, F., Guillemare, E., de Weille, J., Heurteaux, C., . . . Lazdunski, M. (1996). "*Kv8.1, a new neuronal potassium channel subunit with specific inhibitory properties towards Shab and Shaw channels*." EMBO J 15(13): 3322-3331.

Imbrici, P., D'Adamo, M. C., Grottesi, A., Biscarini, A. and Pessia, M. (2011). "*Episodic ataxia type 1 mutations affect fast inactivation of K+ channels by a reduction in either subunit surface expression or affinity for inactivation domain*." Am J Physiol Cell Physiol 300(6): C1314-1322.

Isbrandt, D., Friederich, P., Solth, A., Haverkamp, W., Ebneth, A., Borggrefe, M., . . . Schulze-Bahr, E. (2002). "*Identification and functional characterization of a novel KCNE2 (MiRP1) mutation that alters HERG channel kinetics*." J Mol Med (Berl) 80(8): 524-532.

Jacob, A., Hurley, I. R., Goodwin, L. O., Cooper, G. W. and Benoff, S. (2000). "*Molecular characterization of a voltage-gated potassium channel expressed in rat testis*." Mol Hum Reprod 6(4): 303-313.

Jenkinson, D. H. (2006). "*Potassium channels--multiplicity and challenges*." Br J Pharmacol 147 Suppl 1: S63-71.

Jensen, H. S., Grunnet, M. and Olesen, S. P. (2007). "*Inactivation as a new regulatory mechanism for neuronal Kv7 channels*." Biophys J 92(8): 2747-2756.

Jerng, H. H., Kunjilwar, K. and Pfaffinger, P. J. (2005). "*Multiprotein assembly of Kv4.2, KChIP3 and DPP10 produces ternary channel complexes with ISA-like properties*." J Physiol 568(Pt 3): 767-788.

Jervell, A. and Lange-Nielsen, F. (1957). "*Congenital deaf-mutism, functional heart disease with prolongation of the Q-T interval and sudden death*." Am Heart J 54(1): 59-68.

Jiang, M., Tseng-Crank, J. and Tseng, G. N. (1997). "*Suppression of slow delayed rectifier current by a truncated isoform of KvLQT1 cloned from normal human heart*." J Biol Chem 272(39): 24109-24112.

Jiang, M., Xu, X., Wang, Y., Toyoda, F., Liu, X. S., Zhang, M., . . . Tseng, G. N. (2009). "*Dynamic partnership between KCNQ1 and KCNE1 and influence on cardiac IKs current amplitude by KCNE2*." J Biol Chem 284(24): 16452-16462.

Jiang, Y., Lee, A., Chen, J., Cadene, M., Chait, B. T. and MacKinnon, R. (2002). "*Crystal structure and mechanism of a calcium-gated potassium channel*." Nature 417(6888): 515-522.

Jiang, Y., Lee, A., Chen, J., Ruta, V., Cadene, M., Chait, B. T. and MacKinnon, R. (2003). "*X-ray structure of a voltage-dependent K+ channel*." Nature 423(6935): 33-41.

Jiao, J., Garg, V., Yang, B., Elton, T. S. and Hu, K. (2008). "*Protein kinase C-epsilon induces caveolin-dependent internalization of vascular adenosine 5'-triphosphate-sensitive K+ channels*." Hypertension 52(3): 499-506.

Jindal, H. K., Folco, E. J., Liu, G. X. and Koren, G. (2008). "*Posttranslational modification of voltage-dependent potassium channel Kv1.5: COOH-terminal palmitoylation modulates its biological properties*." Am J Physiol Heart Circ Physiol 294(5): H2012-2021.

Kaab, S., Crawford, D. C., Sinner, M. F., Behr, E. R., Kannankeril, P. J., Wilde, A. A., . . . Roden, D. M. (2012). "*A large candidate gene survey identifies the KCNE1 D85N polymorphism as a possible modulator of drug-induced torsades de pointes*." Circ Cardiovasc Genet 5(1): 91-99.

Kanda, V. A. and Abbott, G. W. (2012). "*KCNE Regulation of K(+) Channel Trafficking - a Sisyphean Task?*" Front Physiol 3: 231.

Kanda, V. A., Lewis, A., Xu, X. and Abbott, G. W. (2011). "*KCNE1 and KCNE2 inhibit forward trafficking of homomeric N-type voltage-gated potassium channels*." Biophys J 101(6): 1354-1363.

Kanda, V. A., Lewis, A., Xu, X. and Abbott, G. W. (2011). "*KCNE1 and KCNE2 provide a checkpoint governing voltage-gated potassium channel alpha-subunit composition*." Biophys J 101(6): 1364-1375.

Kang, C., Tian, C., Sonnichsen, F. D., Smith, J. A., Meiler, J., George, A. L., Jr., . . . Sanders, C. R. (2008). "*Structure of KCNE1 and implications for how it modulates the KCNQ1 potassium channel*." Biochemistry 47(31): 7999-8006.

Keynes, R. D. and Elinder, F. (1999). "*The screw-helical voltage gating of ion channels*." Proc Biol Sci 266(1421): 843-852.

Khanna, R., Roy, L., Zhu, X. and Schlichter, L. C. (2001). "*K+ channels and the microglial respiratory burst*." Am J Physiol Cell Physiol 280(4): C796-806.

Kim, E., Niethammer, M., Rothschild, A., Jan, Y. N. and Sheng, M. (1995). "*Clustering of Shaker-type K+ channels by interaction with a family of membrane-associated guanylate kinases*." Nature 378(6552): 85-88.

Kim, E. and Sheng, M. (1996). "*Differential K+ channel clustering activity of PSD-95 and SAP97, two related membrane-associated putative guanylate kinases*." Neuropharmacology 35(7): 993-1000.

Kim, L. A., Furst, J., Gutierrez, D., Butler, M. H., Xu, S., Goldstein, S. A. and Grigorieff, N. (2004). "*Three-dimensional structure of I(to); Kv4.2-KChIP2 ion channels by electron microscopy at 21 Angstrom resolution*." Neuron 41(4): 513-519.

Kim, S. J. and Greger, R. (1999). "*Voltage-dependent, slowly activating K+ current (I(Ks)) and its augmentation by carbachol in rat pancreatic acini*." Pflugers Arch 438(5): 604-611.

King, C. H. and Scherer, S. S. (2012). "*Kv7.5 is the primary Kv7 subunit expressed in C-fibers*." J Comp Neurol 520(9): 1940-1950.

Koch, R. O., Wanner, S. G., Koschak, A., Hanner, M., Schwarzer, C., Kaczorowski, G. J., . . . Knaus, H. G. (1997). "*Complex subunit assembly of neuronal voltage-gated K+ channels. Basis for high-affinity toxin interactions and pharmacology*." J Biol Chem 272(44): 27577-27581.

Koni, P. A., Khanna, R., Chang, M. C., Tang, M. D., Kaczmarek, L. K., Schlichter, L. C. and Flavella, R. A. (2003). "*Compensatory anion currents in Kv1.3 channel-deficient thymocytes*." J Biol Chem 278(41): 39443-39451.

Kowalski, M. P. and Pier, G. B. (2004). "*Localization of cystic fibrosis transmembrane conductance regulator to lipid rafts of epithelial cells is required for Pseudomonas aeruginosa-induced cellular activation*." J Immunol 172(1): 418-425.

Krumerman, A., Gao, X., Bian, J. S., Melman, Y. F., Kagan, A. and McDonald, T. V. (2004). "*An LQT mutant minK alters KvLQT1 trafficking*." Am J Physiol Cell Physiol 286(6): C1453-1463.

Kues, W. A. and Wunder, F. (1992). "*Heterogeneous Expression Patterns of Mammalian Potassium Channel Genes in Developing and Adult Rat Brain*." Eur J Neurosci 4(12): 1296-1308.

Kunzelmann, K., Hubner, M., Schreiber, R., Levy-Holzman, R., Garty, H., Bleich, M., . . . Greger, R. (2001). "*Cloning and function of the rat colonic epithelial K+ channel KVLQT1*." J Membr Biol 179(2): 155-164.

Kupershmidt, S., Yang, T., Chanthaphaychith, S., Wang, Z., Towbin, J. A. and Roden, D. M. (2002). "*Defective human Ether-a-go-go-related gene trafficking linked to an endoplasmic reticulum retention signal in the C terminus*." J Biol Chem 277(30): 27442-27448.

Kurokawa, J., Abriel, H. and Kass, R. S. (2001). "*Molecular basis of the delayed rectifier current I(ks)in heart*." J Mol Cell Cardiol 33(5): 873-882.

Kurokawa, J., Chen, L. and Kass, R. S. (2003). "*Requirement of subunit expression for cAMP-mediated regulation of a heart potassium channel*." Proc Natl Acad Sci U S A 100(4): 2122-2127.

Kurokawa, J., Motoike, H. K. and Kass, R. S. (2001). "*TEA(+)-sensitive KCNQ1 constructs reveal pore-independent access to KCNE1 in assembled I(Ks) channels*." J Gen Physiol 117(1): 43-52.

Kuryshev, Y. A., Gudz, T. I., Brown, A. M. and Wible, B. A. (2000). "*KChAP as a chaperone for specific K(+) channels*." Am J Physiol Cell Physiol 278(5): C931-941.

Kuryshev, Y. A., Wible, B. A., Gudz, T. I., Ramirez, A. N. and Brown, A. M. (2001). "*KChAP/Kvbeta1.2 interactions and their effects on cardiac Kv channel expression*." Am J Physiol Cell Physiol 281(1): C290-299.

Kwiatek, A. M., Minshall, R. D., Cool, D. R., Skidgel, R. A., Malik, A. B. and Tiruppathi, C. (2006). "*Caveolin-1 regulates store-operated Ca2+ influx by binding of its scaffolding domain to transient receptor potential channel-1 in endothelial cells*." Mol Pharmacol 70(4): 1174-1183.

Labro, A. J., Raes, A. L., Grottesi, A., Van Hoorick, D., Sansom, M. S. and Snyders, D. J. (2008). "*Kv channel gating requires a compatible S4-S5 linker and bottom part of S6, constrained by non-interacting residues*." J Gen Physiol 132(6): 667-680.

Lanigan, M. D., Kalman, K., Lefievre, Y., Pennington, M. W., Chandy, K. G. and Norton, R. S. (2002). "*Mutating a critical lysine in ShK toxin alters its binding configuration in the pore-vestibule region of the voltage-gated potassium channel, Kv1.3*." Biochemistry 41(40): 11963-11971.

Larsson, H. P., Baker, O. S., Dhillon, D. S. and Isacoff, E. Y. (1996). "*Transmembrane movement of the shaker K+ channel S4*." Neuron 16(2): 387-397.

Leanza, L., Zoratti, M., Gulbins, E. and Szabo, I. (2012). "*Induction of apoptosis in macrophages via Kv1.3 and Kv1.5 potassium channels*." Curr Med Chem 19(31): 5394-5404.

Leblanc, N. (2010). "*Kv3.4, a key signalling molecule controlling the cell cycle and proliferation of human arterial smooth muscle cells*." Cardiovasc Res 86(3): 351-352.

Lee, I. H., Campbell, C. R., Song, S. H., Day, M. L., Kumar, S., Cook, D. I. and Dinudom, A. (2009). "*The activity of the epithelial sodium channels is regulated by caveolin-1 via a Nedd4-2-dependent mechanism*." J Biol Chem 284(19): 12663-12669.

Lee, M. P., Hu, R. J., Johnson, L. A. and Feinberg, A. P. (1997). "*Human KVLQT1 gene shows tissue-specific imprinting and encompasses Beckwith-Wiedemann syndrome chromosomal rearrangements*." Nat Genet 15(2): 181-185.

Lee, M. P., Ravenel, J. D., Hu, R. J., Lustig, L. R., Tomaselli, G., Berger, R. D., . . . Feinberg, A. P. (2000). "*Targeted disruption of the Kvlqt1 gene causes deafness and gastric hyperplasia in mice*." J Clin Invest 106(12): 1447-1455.

Leicher, T., Bahring, R., Isbrandt, D. and Pongs, O. (1998). "*Coexpression of the KCNA3B gene product with Kv1.5 leads to a novel A-type potassium channel*." J Biol Chem 273(52): 35095-35101.

Lerche, C., Scherer, C. R., Seebohm, G., Derst, C., Wei, A. D., Busch, A. E. and Steinmeyer, K. (2000). "*Molecular cloning and functional expression of KCNQ5, a potassium channel subunit that may contribute to neuronal M-current diversity*." J Biol Chem 275(29): 22395-22400.

Lerche, C., Seebohm, G., Wagner, C. I., Scherer, C. R., Dehmelt, L., Abitbol, I., . . . Busch, A. E. (2000). "*Molecular impact of MinK on the enantiospecific block of I(Ks) by chromanols*." Br J Pharmacol 131(8): 1503-1506.

Levitan, E. S. and Takimoto, K. (1998). "*Dynamic regulation of K+ channel gene expression in differentiated cells*." J Neurobiol 37(1): 60-68.

Levy, D. I., Cepaitis, E., Wanderling, S., Toth, P. T., Archer, S. L. and Goldstein, S. A. (2010). "*The membrane protein MiRP3 regulates Kv4.2 channels in a KChIP-dependent manner*." J Physiol 588(Pt 14): 2657-2668.

Levy, D. I., Wanderling, S., Biemesderfer, D. and Goldstein, S. A. (2008). "*MiRP3 acts as an accessory subunit with the BK potassium channel*." Am J Physiol Renal Physiol 295(2): F380-387.

Lewis, A., McCrossan, Z. A. and Abbott, G. W. (2004). "*MinK, MiRP1, and MiRP2 diversify Kv3.1 and Kv3.2 potassium channel gating*." J Biol Chem 279(9): 7884-7892.

Li, D., Takimoto, K. and Levitan, E. S. (2000). "*Surface expression of Kv1 channels is governed by a C-terminal motif*." J Biol Chem 275(16): 11597-11602.

Li, G. R., Feng, J., Wang, Z., Fermini, B. and Nattel, S. (1996). "*Adrenergic modulation of ultrarapid delayed rectifier K+ current in human atrial myocytes*." Circ Res 78(5): 903-915.

Li, H., Guo, W., Mellor, R. L. and Nerbonne, J. M. (2005). "*KChIP2 modulates the cell surface expression of Kv 1.5-encoded K(+) channels*." J Mol Cell Cardiol 39(1): 121-132.

Li, M., Jan, Y. N. and Jan, L. Y. (1992). "*Specification of subunit assembly by the hydrophilic amino-terminal domain of the Shaker potassium channel*." Science 257(5074): 1225-1230.

Li, Y., Gamper, N., Hilgemann, D. W. and Shapiro, M. S. (2005). "*Regulation of Kv7 (KCNQ) K+ channel open probability by phosphatidylinositol 4,5-bisphosphate*." J Neurosci 25(43): 9825-9835.

Li, Y., Gamper, N. and Shapiro, M. S. (2004). "*Single-channel analysis of KCNQ K+ channels reveals the mechanism of augmentation by a cysteine-modifying reagent*." J Neurosci 24(22): 5079-5090.

Li, Y., Um, S. Y. and McDonald, T. V. (2006). "*Voltage-gated potassium channels: regulation by accessory subunits*." Neuroscientist 12(3): 199-210.

Li, Y., Zaydman, M. A., Wu, D., Shi, J., Guan, M., Virgin-Downey, B. and Cui, J. (2011). "*KCNE1 enhances phosphatidylinositol 4,5-bisphosphate (PIP2) sensitivity of IKs to modulate channel activity*." Proc Natl Acad Sci U S A 108(22): 9095-9100.

Liang, C., Li, X., Xu, Y., Chen, Q., Wu, Y., Wang, W., . . . Qiu, M. (2013). "*KCNE1 rs1805127 Polymorphism Increases the Risk of Atrial Fibrillation: A Meta-Analysis of 10 Studies*." PLoS One 8(7): e68690.

Liao, T., Wang, L., Halm, S. T., Lu, L., Fyffe, R. E. and Halm, D. R. (2005). "*K+ channel KVLQT1 located in the basolateral membrane of distal colonic epithelium is not essential for activating Cl- secretion*." Am J Physiol Cell Physiol 289(3): C564-575.

Liman, E. R., Hess, P., Weaver, F. and Koren, G. (1991). "*Voltage-sensing residues in the S4 region of a mammalian K+ channel*." Nature 353(6346): 752-756.

Liu, C., Zhao, Q., Su, T., Tang, S., Lv, G., Liu, H., . . . Cheng, J. (2013). "*Postmortem molecular analysis of KCNQ1, KCNH2, KCNE1 and KCNE2 genes in sudden unexplained nocturnal death syndrome in the Chinese Han population*." Forensic Sci Int 231(1-3): 82-87.

Liu, J., Deng, J. X., Pan, B. X. and Huang, Q. B. (2006). "*[KCNE2 modulates the function of Kv4.3 channel]*." Nan Fang Yi Ke Da Xue Xue Bao 26(12): 1754-1756.

Liu, W. J., Wang, H. T., Chen, W. W., Deng, J. X., Jiang, Y. and Liu, J. (2008). "*Co-expression of KCNE2 and KChIP2c modulates the electrophysiological properties of Kv4.2 current in COS-7 cells*." Acta Pharmacol Sin 29(6): 653-660.

Liu, X. S., Zhang, M., Jiang, M., Wu, D. M. and Tseng, G. N. (2007). "*Probing the interaction between KCNE2 and KCNQ1 in their transmembrane regions*." J Membr Biol 216(2-3): 117-127.

Logothetis, D. E., Movahedi, S., Satler, C., Lindpaintner, K. and Nadal-Ginard, B. (1992). "*Incremental reductions of positive charge within the S4 region of a voltage-gated K+ channel result in corresponding decreases in gating charge*." Neuron 8(3): 531-540.

Long, S. B., Campbell, E. B. and Mackinnon, R. (2005). "*Crystal structure of a mammalian voltage-dependent Shaker family K+ channel*." Science 309(5736): 897-903.

Long, S. B., Campbell, E. B. and Mackinnon, R. (2005). "*Voltage sensor of Kv1.2: structural basis of electromechanical coupling*." Science 309(5736): 903-908.

Long, S. B., Tao, X., Campbell, E. B. and MacKinnon, R. (2007). "*Atomic structure of a voltage-dependent K+ channel in a lipid membrane-like environment*." Nature 450(7168): 376-382.

Loussouarn, G., Baro, I. and Escande, D. (2006). "*KCNQ1 K+ channel-mediated cardiac channelopathies*." Methods Mol Biol 337: 167-183.

Loussouarn, G., Park, K. H., Bellocq, C., Baro, I., Charpentier, F. and Escande, D. (2003). "*Phosphatidylinositol-4,5-bisphosphate, PIP2, controls KCNQ1/KCNE1 voltage-gated potassium channels: a functional homology between voltage-gated and inward rectifier K+ channels*." EMBO J 22(20): 5412-5421.

Lu, J., Robinson, J. M., Edwards, D. and Deutsch, C. (2001). "*T1-T1 interactions occur in ER membranes while nascent Kv peptides are still attached to ribosomes*." Biochemistry 40(37): 10934-10946.

Lu, S., Das, P., Fadool, D. A. and Kaczmarek, L. K. (2010). "*The slack sodium-activated potassium channel provides a major outward current in olfactory neurons of Kv1.3-/- super-smeller mice*." J Neurophysiol 103(6): 3311-3319.

Lu, Z., Klem, A. M. and Ramu, Y. (2002). "*Coupling between voltage sensors and activation gate in voltage-gated K+ channels*." J Gen Physiol 120(5): 663-676.

Lundby, A. and Olesen, S. P. (2006). "*KCNE3 is an inhibitory subunit of the Kv4.3 potassium channel*." Biochem Biophys Res Commun 346(3): 958-967.

Lundby, A., Ravn, L. S., Svendsen, J. H., Hauns, S., Olesen, S. P. and Schmitt, N. (2008). "*KCNE3 mutation V17M identified in a patient with lone atrial fibrillation*." Cell Physiol Biochem 21(1-3): 47-54.

Lundquist, A. L., Manderfield, L. J., Vanoye, C. G., Rogers, C. S., Donahue, B. S., Chang, P. A., . . . George, A. L., Jr. (2005). "*Expression of multiple KCNE genes in human heart may enable variable modulation of I(Ks)*." J Mol Cell Cardiol 38(2): 277-287.

Lundquist, A. L., Turner, C. L., Ballester, L. Y. and George, A. L., Jr. (2006). "*Expression and transcriptional control of human KCNE genes*." Genomics 87(1): 119-128.

Ma, D., Zerangue, N., Lin, Y. F., Collins, A., Yu, M., Jan, Y. N. and Jan, L. Y. (2001). "*Role of ER export signals in controlling surface potassium channel numbers*." Science 291(5502): 316-319.

Ma, K. J., Li, N., Teng, S. Y., Zhang, Y. H., Sun, Q., Gu, D. F. and Pu, J. L. (2007). "*Modulation of KCNQ1 current by atrial fibrillation-associated KCNE4 (145E/D) gene polymorphism*." Chin Med J (Engl) 120(2): 150-154.

MacKinnon, R. (1991). "*Determination of the subunit stoichiometry of a voltage-activated potassium channel*." Nature 350(6315): 232-235.

MacKinnon, R. (2003). "*Potassium channels*." FEBS Lett 555(1): 62-65.

MacKinnon, R., Reinhart, P. H. and White, M. M. (1988). "*Charybdotoxin block of Shaker K+ channels suggests that different types of K+ channels share common structural features*." Neuron 1(10): 997-1001.

MacVinish, L. J., Guo, Y., Dixon, A. K., Murrell-Lagnado, R. D. and Cuthbert, A. W. (2001). "*Xe991 reveals differences in K(+) channels regulating chloride secretion in murine airway and colonic epithelium*." Mol Pharmacol 60(4): 753-760.

Mall, M., Wissner, A., Schreiber, R., Kuehr, J., Seydewitz, H. H., Brandis, M., . . . Kunzelmann, K. (2000). "*Role of K(V)LQT1 in cyclic adenosine monophosphate-mediated Cl(-) secretion in human airway epithelia*." Am J Respir Cell Mol Biol 23(3): 283-289.

Manderfield, L. J., Daniels, M. A., Vanoye, C. G. and George, A. L., Jr. (2009). "*KCNE4 domains required for inhibition of KCNQ1*." J Physiol 587(Pt 2): 303-314.

Manderfield, L. J. and George, A. L., Jr. (2008). "*KCNE4 can co-associate with the I(Ks) (KCNQ1-KCNE1) channel complex*." FEBS J 275(6): 1336-1349.

Manganas, L. N. and Trimmer, J. S. (2000). "*Subunit composition determines Kv1 potassium channel surface expression*." J Biol Chem 275(38): 29685-29693.

Manganas, L. N. and Trimmer, J. S. (2004). "*Calnexin regulates mammalian Kv1 channel trafficking*." Biochem Biophys Res Commun 322(2): 577-584.

Manganas, L. N., Wang, Q., Scannevin, R. H., Antonucci, D. E., Rhodes, K. J. and Trimmer, J. S. (2001). "*Identification of a trafficking determinant localized to the Kv1 potassium channel pore*." Proc Natl Acad Sci U S A 98(24): 14055-14059.

Marcus, D. C. and Shen, Z. (1994). "*Slowly activating voltage-dependent K+ conductance is apical pathway for K+ secretion in vestibular dark cells*." Am J Physiol 267(3 Pt 1): C857-864.

Martens, J. R., Navarro-Polanco, R., Coppock, E. A., Nishiyama, A., Parshley, L., Grobaski, T. D. and Tamkun, M. M. (2000). "*Differential targeting of Shaker-like potassium channels to lipid rafts*." J Biol Chem 275(11): 7443-7446.

Martens, J. R., O'Connell, K. and Tamkun, M. (2004). "*Targeting of ion channels to membrane microdomains: localization of KV channels to lipid rafts*." Trends Pharmacol Sci 25(1): 16-21.

Martens, J. R., Sakamoto, N., Sullivan, S. A., Grobaski, T. D. and Tamkun, M. M. (2001). "*Isoform-specific localization of voltage-gated K+ channels to distinct lipid raft populations. Targeting of Kv1.5 to caveolae*." J Biol Chem 276(11): 8409-8414.

Martínez-Mármol, R. (2010). "*Determinantes moleculares implicados en la función de los canales iónicos dependientes de voltaje.*" PhD thesis.

Martínez-Mármol, R., Pérez-Verdaguer, M., Roig, S. R., Vallejo-Gracia, A., Gotsi, P., Serrano-Albarrás, A., . . . Felipe, A. (2013). "*A non-canonical di-acidic signal at the C-terminal of Kv1.3 determines anterograde trafficking and surface expression*." Journal Cell Science in press.

Martinez-Marmol, R., Villalonga, N., Sole, L., Vicente, R., Tamkun, M. M., Soler, C. and Felipe, A. (2008). "*Multiple Kv1.5 targeting to membrane surface microdomains*." J Cell Physiol 217(3): 667-673.

Martínez-Pinna, J. (2012). "*Novel regulatoin of Kv1.3 channel inactivation by intracellular calcium*." Proceedings of Acta Physiologica 206(Supplement 693).

Marx, S. O., Kurokawa, J., Reiken, S., Motoike, H., D'Armiento, J., Marks, A. R. and Kass, R. S. (2002). "*Requirement of a macromolecular signaling complex for beta adrenergic receptor modulation of the KCNQ1-KCNE1 potassium channel*." Science 295(5554): 496-499.

Mays, D. J., Foose, J. M., Philipson, L. H. and Tamkun, M. M. (1995). "*Localization of the Kv1.5 K+ channel protein in explanted cardiac tissue*." J Clin Invest 96(1): 282-292.

Mazhari, R., Greenstein, J. L., Winslow, R. L., Marban, E. and Nuss, H. B. (2001). "*Molecular interactions between two long-QT syndrome gene products, HERG and KCNE2, rationalized by in vitro and in silico analysis*." Circ Res 89(1): 33-38.

McCallum, L. A., Greenwood, I. A. and Tribe, R. M. (2009). "*Expression and function of K(v)7 channels in murine myometrium throughout oestrous cycle*." Pflugers Arch 457(5): 1111-1120.

McCormack, T., McCormack, K., Nadal, M. S., Vieira, E., Ozaita, A. and Rudy, B. (1999). "*The effects of Shaker beta-subunits on the human lymphocyte K+ channel Kv1.3*." J Biol Chem 274(29): 20123-20126.

McCrossan, Z. A. and Abbott, G. W. (2004). "*The MinK-related peptides*." Neuropharmacology 47(6): 787-821.

McCrossan, Z. A., Lewis, A., Panaghie, G., Jordan, P. N., Christini, D. J., Lerner, D. J. and Abbott, G. W. (2003). "*MinK-related peptide 2 modulates Kv2.1 and Kv3.1 potassium channels in mammalian brain*." J Neurosci 23(22): 8077-8091.

McCrossan, Z. A., Roepke, T. K., Lewis, A., Panaghie, G. and Abbott, G. W. (2009). "*Regulation of the Kv2.1 potassium channel by MinK and MiRP1*." J Membr Biol 228(1): 1-14.

McDonald, T. V., Yu, Z., Ming, Z., Palma, E., Meyers, M. B., Wang, K. W., . . . Fishman, G. I. (1997). "*A minK-HERG complex regulates the cardiac potassium current I(Kr)*." Nature 388(6639): 289-292.

McIntosh, P., Southan, A. P., Akhtar, S., Sidera, C., Ushkaryov, Y., Dolly, J. O. and Robertson, B. (1997). "*Modification of rat brain Kv1.4 channel gating by association with accessory Kvbeta1.1 and beta2.1 subunits*." Pflugers Arch 435(1): 43-54.

Melman, Y. F., Domenech, A., de la Luna, S. and McDonald, T. V. (2001). "*Structural determinants of KvLQT1 control by the KCNE family of proteins*." J Biol Chem 276(9): 6439-6444.

Melman, Y. F., Krumerman, A. and McDonald, T. V. (2002). "*A single transmembrane site in the KCNE-encoded proteins controls the specificity of KvLQT1 channel gating*." J Biol Chem 277(28): 25187-25194.

Melman, Y. F., Krummerman, A. and McDonald, T. V. (2002). "*KCNE regulation of KvLQT1 channels: structure-function correlates*." Trends Cardiovasc Med 12(4): 182-187.

Melman, Y. F., Um, S. Y., Krumerman, A., Kagan, A. and McDonald, T. V. (2004). "*KCNE1 binds to the KCNQ1 pore to regulate potassium channel activity*." Neuron 42(6): 927-937.

Miao, S., Bao, J., Garcia, M. L., Goulet, J. L., Hong, X. J., Kaczorowski, G. J., . . . Rupprecht, K. M. (2003). "*Benzamide derivatives as blockers of Kv1.3 ion channel*." Bioorg Med Chem Lett 13(6): 1161-1164.

Miguel-Velado, E., Moreno-Dominguez, A., Colinas, O., Cidad, P., Heras, M., Perez-Garcia, M. T. and Lopez-Lopez, J. R. (2005). "*Contribution of Kv channels to phenotypic remodeling of human uterine artery smooth muscle cells*." Circ Res 97(12): 1280-1287.

Miguel-Velado, E., Perez-Carretero, F. D., Colinas, O., Cidad, P., Heras, M., Lopez-Lopez, J. R. and Perez-Garcia, M. T. (2010). "*Cell cycle-dependent expression of Kv3.4 channels modulates proliferation of human uterine artery smooth muscle cells*." Cardiovasc Res 86(3): 383-391.

Miller, C., Moczydlowski, E., Latorre, R. and Phillips, M. (1985). "*Charybdotoxin, a protein inhibitor of single Ca2+-activated K+ channels from mammalian skeletal muscle*." Nature 313(6000): 316-318.

Minor, D. L., Lin, Y. F., Mobley, B. C., Avelar, A., Jan, Y. N., Jan, L. Y. and Berger, J. M. (2000). "*The polar T1 interface is linked to conformational changes that open the voltage-gated potassium channel*." Cell 102(5): 657-670.

Misonou, H., Mohapatra, D. P., Park, E. W., Leung, V., Zhen, D., Misonou, K., . . . Trimmer, J. S. (2004). "*Regulation of ion channel localization and phosphorylation by neuronal activity*." Nat Neurosci 7(7): 711-718.

Misonou, H. and Trimmer, J. S. (2004). "*Determinants of voltage-gated potassium channel surface expression and localization in Mammalian neurons*." Crit Rev Biochem Mol Biol 39(3): 125-145.

Morales, M. J., Castellino, R. C., Crews, A. L., Rasmusson, R. L. and Strauss, H. C. (1995). "*A novel beta subunit increases rate of inactivation of specific voltage-gated potassium channel alpha subunits*." J Biol Chem 270(11): 6272-6277.

Morin, T. J. and Kobertz, W. R. (2007). "*A derivatized scorpion toxin reveals the functional output of heteromeric KCNQ1-KCNE K+ channel complexes*." ACS Chem Biol 2(7): 469-473.

Morin, T. J. and Kobertz, W. R. (2008). "*Counting membrane-embedded KCNE beta-subunits in functioning K+ channel complexes*." Proc Natl Acad Sci U S A 105(5): 1478-1482.

Mourre, C., Chernova, M. N., Martin-Eauclaire, M. F., Bessone, R., Jacquet, G., Gola, M., . . . Crest, M. (1999). "*Distribution in rat brain of binding sites of kaliotoxin, a blocker of Kv1.1 and Kv1.3 alpha-subunits*." J Pharmacol Exp Ther 291(3): 943-952.

Mullen, K. M., Rozycka, M., Rus, H., Hu, L., Cudrici, C., Zafranskaia, E., . . . Calabresi, P. A. (2006). "*Potassium channels Kv1.3 and Kv1.5 are expressed on blood-derived dendritic cells in the central nervous system*." Ann Neurol 60(1): 118-127.

Nadal, M. S., Ozaita, A., Amarillo, Y., Vega-Saenz de Miera, E., Ma, Y., Mo, W., . . . Rudy, B. (2003). "*The CD26-related dipeptidyl aminopeptidase-like protein DPPX is a critical component of neuronal A-type K+ channels*." Neuron 37(3): 449-461.

Nagaya, N. and Papazian, D. M. (1997). "*Potassium channel alpha and beta subunits assemble in the endoplasmic reticulum*." J Biol Chem 272(5): 3022-3027.

Nakajima, T., Wu, J., Kaneko, Y., Ashihara, T., Ohno, S., Irie, T., . . . Horie, M. (2012). "*KCNE3 T4A as the genetic basis of Brugada-pattern electrocardiogram*." Circ J 76(12): 2763-2772.

Nakajo, K., Nishino, A., Okamura, Y. and Kubo, Y. (2011). "*KCNQ1 subdomains involved in KCNE modulation revealed by an invertebrate KCNQ1 orthologue*." J Gen Physiol 138(5): 521-535.

Nakajo, K., Ulbrich, M. H., Kubo, Y. and Isacoff, E. Y. (2010). "*Stoichiometry of the KCNQ1 - KCNE1 ion channel complex*." Proc Natl Acad Sci U S A 107(44): 18862-18867.

Nattel, S., Yue, L. and Wang, Z. (1999). "*Cardiac ultrarapid delayed rectifiers: a novel potassium current family o f functional similarity and molecular diversity*." Cell Physiol Biochem 9(4-5): 217-226.

Nerbonne, J. M. and Kass, R. S. (2005). "*Molecular physiology of cardiac repolarization*." Physiol Rev 85(4): 1205-1253.

Nesti, E., Everill, B. and Morielli, A. D. (2004). "*Endocytosis as a mechanism for tyrosine kinase-dependent suppression of a voltage-gated potassium channel*." Mol Biol Cell 15(9): 4073-4088.

Neyroud, N., Tesson, F., Denjoy, I., Leibovici, M., Donger, C., Barhanin, J., . . . Guicheney, P. (1997). "*A novel mutation in the potassium channel gene KVLQT1 causes the Jervell and Lange-Nielsen cardioauditory syndrome*." Nat Genet 15(2): 186-189.

Ng, F. L., Davis, A. J., Jepps, T. A., Harhun, M. I., Yeung, S. Y., Wan, A., . . . Greenwood, I. A. (2011). "*Expression and function of the K+ channel KCNQ genes in human arteries*." Br J Pharmacol 162(1): 42-53.

Nicolaou, S. A., Neumeier, L., Steckly, A., Kucher, V., Takimoto, K. and Conforti, L. (2009). "*Localization of Kv1.3 channels in the immunological synapse modulates the calcium response to antigen stimulation in T lymphocytes*." J Immunol 183(10): 6296-6302.

Nicolaou, S. A., Neumeier, L., Takimoto, K., Lee, S. M., Duncan, H. J., Kant, S. K., . . . Conforti, L. (2010). "*Differential calcium signaling and Kv1.3 trafficking to the immunological synapse in systemic lupus erythematosus*." Cell Calcium 47(1): 19-28.

Nicolaou, S. A., Szigligeti, P., Neumeier, L., Lee, S. M., Duncan, H. J., Kant, S. K., . . . Conforti, L. (2007). "*Altered dynamics of Kv1.3 channel compartmentalization in the immunological synapse in systemic lupus erythematosus*." J Immunol 179(1): 346-356.

Nicolas, M., Dememes, D., Martin, A., Kupershmidt, S. and Barhanin, J. (2001). "*KCNQ1/KCNE1 potassium channels in mammalian vestibular dark cells*." Hear Res 153(1-2): 132-145.

Nitabach, M. N., Llamas, D. A., Thompson, I. J., Collins, K. A. and Holmes, T. C. (2002). "*Phosphorylation-dependent and phosphorylation-independent modes of modulation of shaker family voltage-gated potassium channels by SRC family protein tyrosine kinases*." J Neurosci 22(18): 7913-7922.

Noma, K., Kimura, K., Minatohara, K., Nakashima, H., Nagao, Y., Mizoguchi, A. and Fujiyoshi, Y. (2009). "*Triple N-glycosylation in the long S5-P loop regulates the activation and trafficking of the Kv12.2 potassium channel*." J Biol Chem 284(48): 33139-33150.

O'Connell, K. M., Martens, J. R. and Tamkun, M. M. (2004). "*Localization of ion channels to lipid Raft domains within the cardiovascular system*." Trends Cardiovasc Med 14(2): 37-42.

O'Connell, K. M., Rolig, A. S., Whitesell, J. D. and Tamkun, M. M. (2006). "*Kv2.1 potassium channels are retained within dynamic cell surface microdomains that are defined by a perimeter fence*." J Neurosci 26(38): 9609-9618.

Ohno, S., Toyoda, F., Zankov, D. P., Yoshida, H., Makiyama, T., Tsuji, K., . . . Horie, M. (2009). "*Novel KCNE3 mutation reduces repolarizing potassium current and associated with long QT syndrome*." Hum Mutat 30(4): 557-563.

Ohno, S., Zankov, D. P., Ding, W. G., Itoh, H., Makiyama, T., Doi, T., . . . Horie, M. (2011). "*KCNE5 (KCNE1L) variants are novel modulators of Brugada syndrome and idiopathic ventricular fibrillation*." Circ Arrhythm Electrophysiol 4(3): 352-361.

Ohno, S., Zankov, D. P., Yoshida, H., Tsuji, K., Makiyama, T., Itoh, H., . . . Horie, M. (2007). "*N- and C-terminal KCNE1 mutations cause distinct phenotypes of long QT syndrome*." Heart Rhythm 4(3): 332-340.

Ohya, S., Asakura, K., Muraki, K., Watanabe, M. and Imaizumi, Y. (2002). "*Molecular and functional characterization of ERG, KCNQ, and KCNE subtypes in rat stomach smooth muscle*." Am J Physiol Gastrointest Liver Physiol 282(2): G277-287.

Olesen, M. S., Bentzen, B. H., Nielsen, J. B., Steffensen, A. B., David, J. P., Jabbari, J., . . . Schmitt, N. (2012). "*Mutations in the potassium channel subunit KCNE1 are associated with early-onset familial atrial fibrillation*." BMC Med Genet 13: 24.

Osteen, J. D., Gonzalez, C., Sampson, K. J., Iyer, V., Rebolledo, S., Larsson, H. P. and Kass, R. S. (2010). "*KCNE1 alters the voltage sensor movements necessary to open the KCNQ1 channel gate*." Proc Natl Acad Sci U S A 107(52): 22710-22715.

Palade, G. (1975). "*Intracellular aspects of the process of protein synthesis*." Science 189(4206): 867.

Panaghie, G., Tai, K. K. and Abbott, G. W. (2006). "*Interaction of KCNE subunits with the KCNQ1 K+ channel pore*." J Physiol 570(Pt 3): 455-467.

Pani, B., Ong, H. L., Brazer, S. C., Liu, X., Rauser, K., Singh, B. B. and Ambudkar, I. S. (2009). "*Activation of TRPC1 by STIM1 in ER-PM microdomains involves release of the channel from its scaffold caveolin-1*." Proc Natl Acad Sci U S A 106(47): 20087-20092.

Pannaccione, A., Boscia, F., Scorziello, A., Adornetto, A., Castaldo, P., Sirabella, R., . . . Annunziato, L. (2007). "*Up-regulation and increased activity of KV3.4 channels and their accessory subunit MinK-related peptide 2 induced by amyloid peptide are involved in apoptotic neuronal death*." Mol Pharmacol 72(3): 665-673.

Pannasch, U., Farber, K., Nolte, C., Blonski, M., Yan Chiu, S., Messing, A. and Kettenmann, H. (2006). "*The potassium channels Kv1.5 and Kv1.3 modulate distinct functions of microglia*." Mol Cell Neurosci 33(4): 401-411.

Panyi, G., Vamosi, G., Bacso, Z., Bagdany, M., Bodnar, A., Varga, Z., . . . Damjanovich, S. (2004). "*Kv1.3 potassium channels are localized in the immunological synapse formed between cytotoxic and target cells*." Proc Natl Acad Sci U S A 101(5): 1285-1290.

Papazian, D. M. (1999). "*Potassium channels: some assembly required*." Neuron 23(1): 7-10.

Papazian, D. M., Shao, X. M., Seoh, S. A., Mock, A. F., Huang, Y. and Wainstock, D. H. (1995). "*Electrostatic interactions of S4 voltage sensor in Shaker K+ channel*." Neuron 14(6): 1293-1301.

Papazian, D. M., Silverman, W. R., Lin, M. C., Tiwari-Woodruff, S. K. and Tang, C. Y. (2002). "*Structural organization of the voltage sensor in voltage-dependent potassium channels*." Novartis Found Symp 245: 178-190; discussion 190-172, 261-174.

Park, K. H., Piron, J., Dahimene, S., Merot, J., Baro, I., Escande, D. and Loussouarn, G. (2005). "*Impaired KCNQ1-KCNE1 and phosphatidylinositol-4,5-bisphosphate interaction underlies the long QT syndrome*." Circ Res 96(7): 730-739.

Park, S. A., Lee, Y. C., Ma, T. Z., Park, J. A., Han, M. K., Lee, H. H., . . . Kwak, Y. G. (2006). "*hKv1.5 channels play a pivotal role in the functions of human alveolar macrophages*." Biochem Biophys Res Commun 346(2): 567-571.

Parton, R. G., Way, M., Zorzi, N. and Stang, E. (1997). "*Caveolin-3 associates with developing T-tubules during muscle differentiation*." J Cell Biol 136(1): 137-154.

Passmore, G. M., Selyanko, A. A., Mistry, M., Al-Qatari, M., Marsh, S. J., Matthews, E. A., . . . Brown, D. A. (2003). "*KCNQ/M currents in sensory neurons: significance for pain therapy*." J Neurosci 23(18): 7227-7236.

Patel, H. H., Murray, F. and Insel, P. A. (2008). "*Caveolae as organizers of pharmacologically relevant signal transduction molecules*." Annu Rev Pharmacol Toxicol 48: 359-391.

Paulussen, A. D., Gilissen, R. A., Armstrong, M., Doevendans, P. A., Verhasselt, P., Smeets, H. J., . . . Aerssens, J. (2004). "*Genetic variations of KCNQ1, KCNH2, SCN5A, KCNE1, and KCNE2 in drug-induced long QT syndrome patients*." J Mol Med (Berl) 82(3): 182-188.

Payet, M. D. and Dupuis, G. (1992). "*Dual regulation of the n type K+ channel in Jurkat T lymphocytes by protein kinases A and C*." J Biol Chem 267(26): 18270-18273.

Pennington, M. W., Mahnir, V. M., Krafte, D. S., Zaydenberg, I., Byrnes, M. E., Khaytin, I., . . . Kem, W. R. (1996). "*Identification of three separate binding sites on SHK toxin, a potent inhibitor of voltage-dependent potassium channels in human T-lymphocytes and rat brain*." Biochem Biophys Res Commun 219(3): 696-701.

Peter, M., Jr., Varga, Z., Hajdu, P., Gaspar, R., Jr., Damjanovich, S., Horjales, E., . . . Panyi, G. (2001). "*Effects of toxins Pi2 and Pi3 on human T lymphocyte Kv1.3 channels: the role of Glu7 and Lys24*." J Membr Biol 179(1): 13-25.

Piccini, M., Vitelli, F., Seri, M., Galietta, L. J., Moran, O., Bulfone, A., . . . Renieri, A. (1999). "*KCNE1-like gene is deleted in AMME contiguous gene syndrome: identification and characterization of the human and mouse homologs*." Genomics 60(3): 251-257.

Pongs, O., Leicher, T., Berger, M., Roeper, J., Bahring, R., Wray, D., . . . Storm, J. F. (1999). "*Functional and molecular aspects of voltage-gated K+ channel beta subunits*." Ann N Y Acad Sci 868: 344-355.

Pongs, O. and Schwarz, J. R. (2010). "*Ancillary subunits associated with voltage-dependent K+ channels*." Physiol Rev 90(2): 755-796.

Post, M. A., Kirsch, G. E. and Brown, A. M. (1996). "*Kv2.1 and electrically silent Kv6.1 potassium channel subunits combine and express a novel current*." FEBS Lett 399(1-2): 177-182.

Pottosin, II, Valencia-Cruz, G., Bonales-Alatorre, E., Shabala, S. N. and Dobrovinskaya, O. R. (2007). "*Methyl-beta-cyclodextrin reversibly alters the gating of lipid rafts-associated Kv1.3 channels in Jurkat T lymphocytes*." Pflugers Arch 454(2): 235-244.

Poulsen, A. N. and Klaerke, D. A. (2007). "*The KCNE1 beta-subunit exerts a transient effect on the KCNQ1 K+ channel*." Biochem Biophys Res Commun 363(1): 133-139.

Pourrier, M., Schram, G. and Nattel, S. (2003). "*Properties, expression and potential roles of cardiac K+ channel accessory subunits: MinK, MiRPs, KChIP, and KChAP*." J Membr Biol 194(3): 141-152.

Preston, P., Wartosch, L., Gunzel, D., Fromm, M., Kongsuphol, P., Ousingsawat, J., . . . Jentsch, T. J. (2010). "*Disruption of the K+ channel beta-subunit KCNE3 reveals an important role in intestinal and tracheal Cl- transport*." J Biol Chem 285(10): 7165-7175.

Pusch, M. (1998). "*Increase of the single-channel conductance of KvLQT1 potassium channels induced by the association with minK*." Pflugers Arch 437(1): 172-174.

Pusch, M., Magrassi, R., Wollnik, B. and Conti, F. (1998). "*Activation and inactivation of homomeric KvLQT1 potassium channels*." Biophys J 75(2): 785-792.

Radicke, S., Cotella, D., Graf, E. M., Banse, U., Jost, N., Varro, A., . . . Wettwer, E. (2006). "*Functional modulation of the transient outward current Ito by KCNE beta-subunits and regional distribution in human non-failing and failing hearts*." Cardiovasc Res 71(4): 695-703.

Radicke, S., Vaquero, M., Caballero, R., Gomez, R., Nunez, L., Tamargo, J., . . . Delpon, E. (2008). "*Effects of MiRP1 and DPP6 beta-subunits on the blockade induced by flecainide of Kv4.3/KChIP2 channels*." Br J Pharmacol 154(4): 774-786.

Ramu, Y., Xu, Y. and Lu, Z. (2006). "*Enzymatic activation of voltage-gated potassium channels*." Nature 442(7103): 696-699.

Rangaraju, S., Chi, V., Pennington, M. W. and Chandy, K. G. (2009). "*Kv1.3 potassium channels as a therapeutic target in multiple sclerosis*." Expert Opin Ther Targets 13(8): 909-924.

Ravn, L. S., Aizawa, Y., Pollevick, G. D., Hofman-Bang, J., Cordeiro, J. M., Dixen, U., . . . Antzelevitch, C. (2008). "*Gain of function in IKs secondary to a mutation in KCNE5 associated with atrial fibrillation*." Heart Rhythm 5(3): 427-435.

Ravn, L. S., Hofman-Bang, J., Dixen, U., Larsen, S. O., Jensen, G., Haunso, S., . . . Christiansen, M. (2005). "*Relation of 97T polymorphism in KCNE5 to risk of atrial fibrillation*." Am J Cardiol 96(3): 405-407.

Razani, B., Woodman, S. E. and Lisanti, M. P. (2002). "*Caveolae: from cell biology to animal physiology*." Pharmacol Rev 54(3): 431-467.

Rettig, J., Heinemann, S. H., Wunder, F., Lorra, C., Parcej, D. N., Dolly, J. O. and Pongs, O. (1994). "*Inactivation properties of voltage-gated K+ channels altered by presence of beta-subunit*." Nature 369(6478): 289-294.

Robbins, J. (2001). "*KCNQ potassium channels: physiology, pathophysiology, and pharmacology*." Pharmacol Ther 90(1): 1-19.

Roepke, T. K., Kanda, V. A., Purtell, K., King, E. C., Lerner, D. J. and Abbott, G. W. (2011). "*KCNE2 forms potassium channels with KCNA3 and KCNQ1 in the choroid plexus epithelium*." FASEB J 25(12): 4264-4273.

Roepke, T. K., King, E. C., Reyna-Neyra, A., Paroder, M., Purtell, K., Koba, W., . . . Abbott, G. W. (2009). "*Kcne2 deletion uncovers its crucial role in thyroid hormone biosynthesis*." Nat Med 15(10): 1186-1194.

Roepke, T. K., Kontogeorgis, A., Ovanez, C., Xu, X., Young, J. B., Purtell, K., . . . Abbott, G. W. (2008). "*Targeted deletion of kcne2 impairs ventricular repolarization via disruption of I(K,slow1) and I(to,f)*." FASEB J 22(10): 3648-3660.

Roepke, T. K., Purtell, K., King, E. C., La Perle, K. M., Lerner, D. J. and Abbott, G. W. (2010). "*Targeted deletion of Kcne2 causes gastritis cystica profunda and gastric neoplasia*." PLoS One 5(7): e11451.

Romanenko, V. G., Rothblat, G. H. and Levitan, I. (2002). "*Modulation of endothelial inward-rectifier K+ current by optical isomers of cholesterol*." Biophys J 83(6): 3211-3222.

Rothberg, K. G., Heuser, J. E., Donzell, W. C., Ying, Y. S., Glenney, J. R. and Anderson, R. G. (1992). "*Caveolin, a protein component of caveolae membrane coats*." Cell 68(4): 673-682.

Roura-Ferrer, M., Etxebarria, A., Sole, L., Oliveras, A., Comes, N., Villarroel, A. and Felipe, A. (2009). "*Functional implications of KCNE subunit expression for the Kv7.5 (KCNQ5) channel*." Cell Physiol Biochem 24(5-6): 325-334.

Roura-Ferrer, M., Sole, L., Martinez-Marmol, R., Villalonga, N. and Felipe, A. (2008). "*Skeletal muscle Kv7 (KCNQ) channels in myoblast differentiation and proliferation*." Biochem Biophys Res Commun 369(4): 1094-1097.

Roura-Ferrer, M., Sole, L., Oliveras, A., Villarroel, A., Comes, N. and Felipe, A. (2012). "*Targeting of Kv7.5 (KCNQ5)/KCNE channels to surface microdomains of cell membranes*." Muscle Nerve 45(1): 48-54.

Roza, C. and Lopez-Garcia, J. A. (2008). "*Retigabine, the specific KCNQ channel opener, blocks ectopic discharges in axotomized sensory fibres*." Pain 138(3): 537-545.

Rus, H., Pardo, C. A., Hu, L., Darrah, E., Cudrici, C., Niculescu, T., . . . Calabresi, P. A. (2005). "*The voltage-gated potassium channel Kv1.3 is highly expressed on inflammatory infiltrates in multiple sclerosis brain*." Proc Natl Acad Sci U S A 102(31): 11094-11099.

Ruta, V., Chen, J. and MacKinnon, R. (2005). "*Calibrated measurement of gating-charge arginine displacement in the KvAP voltage-dependent K+ channel*." Cell 123(3): 463-475.

Ryan, J. J., Kalscheur, M., Dellefave, L., McNally, E. and Archer, S. L. (2012). "*A KCNE1 missense variant (V47I) causing exercise-induced long QT syndrome (Romano Ward)*." Int J Cardiol 156(2): e33-35.

Sachse, C. C., Kim, Y. H., Agsten, M., Huth, T., Alzheimer, C., Kovacs, D. M. and Kim, D. Y. (2013). "*BACE1 and presenilin/gamma-secretase regulate proteolytic processing of KCNE1 and 2, auxiliary subunits of voltage-gated potassium channels*." FASEB J 27(6): 2458-2467.

Salinas, M., Duprat, F., Heurteaux, C., Hugnot, J. P. and Lazdunski, M. (1997). "*New modulatory alpha subunits for mammalian Shab K+ channels*." J Biol Chem 272(39): 24371-24379.

Sampson, L. J., Davies, L. M., Barrett-Jolley, R., Standen, N. B. and Dart, C. (2007). "*Angiotensin II-activated protein kinase C targets caveolae to inhibit aortic ATP-sensitive potassium channels*." Cardiovasc Res 76(1): 61-70.

Sampson, L. J., Hayabuchi, Y., Standen, N. B. and Dart, C. (2004). "*Caveolae localize protein kinase A signaling to arterial ATP-sensitive potassium channels*." Circ Res 95(10): 1012-1018.

Sanguinetti, M. C., Curran, M. E., Zou, A., Shen, J., Spector, P. S., Atkinson, D. L. and Keating, M. T. (1996). "*Coassembly of K(V)LQT1 and minK (IsK) proteins to form cardiac I(Ks) potassium channel*." Nature 384(6604): 80-83.

Sanguinetti, M. C. and Jurkiewicz, N. K. (1990). "*Two components of cardiac delayed rectifier K+ current. Differential sensitivity to block by class III antiarrhythmic agents*." J Gen Physiol 96(1): 195-215.

Sargiacomo, M., Sudol, M., Tang, Z. and Lisanti, M. P. (1993). "*Signal transducing molecules and glycosyl-phosphatidylinositol-linked proteins form a caveolin-rich insoluble complex in MDCK cells*." J Cell Biol 122(4): 789-807.

Schenzer, A., Friedrich, T., Pusch, M., Saftig, P., Jentsch, T. J., Grotzinger, J. and Schwake, M. (2005). "*Molecular determinants of KCNQ (Kv7) K+ channel sensitivity to the anticonvulsant retigabine*." J Neurosci 25(20): 5051-5060.

Scherer, P. E., Lisanti, M. P., Baldini, G., Sargiacomo, M., Mastick, C. C. and Lodish, H. F. (1994). "*Induction of caveolin during adipogenesis and association of GLUT4 with caveolin-rich vesicles*." J Cell Biol 127(5): 1233-1243.

Scherer, P. E., Tang, Z., Chun, M., Sargiacomo, M., Lodish, H. F. and Lisanti, M. P. (1995). "*Caveolin isoforms differ in their N-terminal protein sequence and subcellular distribution. Identification and epitope mapping of an isoform-specific monoclonal antibody probe*." J Biol Chem 270(27): 16395-16401.

Schroeder, B. C., Hechenberger, M., Weinreich, F., Kubisch, C. and Jentsch, T. J. (2000). "*KCNQ5, a novel potassium channel broadly expressed in brain, mediates M-type currents*." J Biol Chem 275(31): 24089-24095.

Schroeder, B. C., Waldegger, S., Fehr, S., Bleich, M., Warth, R., Greger, R. and Jentsch, T. J. (2000). "*A constitutively open potassium channel formed by KCNQ1 and KCNE3*." Nature 403(6766): 196-199.

Schubert, A. L., Schubert, W., Spray, D. C. and Lisanti, M. P. (2002). "*Connexin family members target to lipid raft domains and interact with caveolin-1*." Biochemistry 41(18): 5754-5764.

Schulteis, C. T., Nagaya, N. and Papazian, D. M. (1998). "*Subunit folding and assembly steps are interspersed during Shaker potassium channel biogenesis*." J Biol Chem 273(40): 26210-26217.

Schulze-Bahr, E., Wang, Q., Wedekind, H., Haverkamp, W., Chen, Q., Sun, Y., . . . Funke, H. (1997). "*KCNE1 mutations cause jervell and Lange-Nielsen syndrome*." Nat Genet 17(3): 267-268.

Seebohm, G., Sanguinetti, M. C. and Pusch, M. (2003). "*Tight coupling of rubidium conductance and inactivation in human KCNQ1 potassium channels*." J Physiol 552(Pt 2): 369-378.

Seebohm, G., Scherer, C. R., Busch, A. E. and Lerche, C. (2001). "*Identification of specific pore residues mediating KCNQ1 inactivation. A novel mechanism for long QT syndrome*." J Biol Chem 276(17): 13600-13605.

Sesti, F., Abbott, G. W., Wei, J., Murray, K. T., Saksena, S., Schwartz, P. J., . . . Goldstein, S. A. (2000). "*A common polymorphism associated with antibiotic-induced cardiac arrhythmia*." Proc Natl Acad Sci U S A 97(19): 10613-10618.

Sewing, S., Roeper, J. and Pongs, O. (1996). "*Kv beta 1 subunit binding specific for shaker-related potassium channel alpha subunits*." Neuron 16(2): 455-463.

Shamgar, L., Haitin, Y., Yisharel, I., Malka, E., Schottelndreier, H., Peretz, A., . . . Attali, B. (2008). "*KCNE1 constrains the voltage sensor of Kv7.1 K+ channels*." PLoS One 3(4): e1943.

Shamgar, L., Ma, L., Schmitt, N., Haitin, Y., Peretz, A., Wiener, R., . . . Attali, B. (2006). "*Calmodulin is essential for cardiac IKS channel gating and assembly: impaired function in long-QT mutations*." Circ Res 98(8): 1055-1063.

Shamotienko, O. G., Parcej, D. N. and Dolly, J. O. (1997). "*Subunit combinations defined for K+ channel Kv1 subtypes in synaptic membranes from bovine brain*." Biochemistry 36(27): 8195-8201.

Shaul, P. W. and Anderson, R. G. (1998). "*Role of plasmalemmal caveolae in signal transduction*." Am J Physiol 275(5 Pt 1): L843-851.

Shen, Z., Liu, J., Marcus, D. C., Shiga, N. and Wangemann, P. (1995). "*DIDS increases K+ secretion through an IsK channel in apical membrane of vestibular dark cell epithelium of gerbil*." J Membr Biol 146(3): 283-291.

Shi, G., Nakahira, K., Hammond, S., Rhodes, K. J., Schechter, L. E. and Trimmer, J. S. (1996). "*Beta subunits promote K+ channel surface expression through effects early in biosynthesis*." Neuron 16(4): 843-852.

Shibata, R., Misonou, H., Campomanes, C. R., Anderson, A. E., Schrader, L. A., Doliveira, L. C., . . . Trimmer, J. S. (2003). "*A fundamental role for KChIPs in determining the molecular properties and trafficking of Kv4.2 potassium channels*." J Biol Chem 278(38): 36445-36454.

Sieben, C., Mikosch, M., Brandizzi, F. and Homann, U. (2008). "*Interaction of the K(+)-channel KAT1 with the coat protein complex II coat component Sec24 depends on a di-acidic endoplasmic reticulum export motif*." Plant J 56(6): 997-1006.

Silva, M. R., Chiamolera, M. I., Kasamatsu, T. S., Cerutti, J. M. and Maciel, R. M. (2004). "*[Thyrotoxic hypokalemic periodic paralysis, an endocrine emergency: clinical and genetic features in 25 patients]*." Arq Bras Endocrinol Metabol 48(1): 196-215.

Simons, K. and Ikonen, E. (1997). "*Functional rafts in cell membranes*." Nature 387(6633): 569-572.

Simons, K. and Toomre, D. (2000). "*Lipid rafts and signal transduction*." Nat Rev Mol Cell Biol 1(1): 31-39.

Snyders, D. J., Tamkun, M. M. and Bennett, P. B. (1993). "*A rapidly activating and slowly inactivating potassium channel cloned from human heart. Functional analysis after stable mammalian cell culture expression*." J Gen Physiol 101(4): 513-543.

Sobko, A., Peretz, A. and Attali, B. (1998). "*Constitutive activation of delayed-rectifier potassium channels by a src family tyrosine kinase in Schwann cells*." EMBO J 17(16): 4723-4734.

Soh, H. and Goldstein, S. A. (2008). "*I SA channel complexes include four subunits each of DPP6 and Kv4.2*." J Biol Chem 283(22): 15072-15077.

Solé, L., Roura-Ferrer, M., Perez-Verdaguer, M., Oliveras, A., Calvo, M., Fernandez-Fernandez, J. M. and Felipe, A. (2009). "*KCNE4 suppresses Kv1.3 currents by modulating trafficking, surface expression and channel gating*." J Cell Sci 122(Pt 20): 3738-3748.

Splawski, I., Shen, J., Timothy, K. W., Lehmann, M. H., Priori, S., Robinson, J. L., . . . Keating, M. T. (2000). "*Spectrum of mutations in long-QT syndrome genes. KVLQT1, HERG, SCN5A, KCNE1, and KCNE2*." Circulation 102(10): 1178-1185.

Splawski, I., Tristani-Firouzi, M., Lehmann, M. H., Sanguinetti, M. C. and Keating, M. T. (1997). "*Mutations in the hminK gene cause long QT syndrome and suppress IKs function*." Nat Genet 17(3): 338-340.

Starace, D. M. and Bezanilla, F. (2001). "*Histidine scanning mutagenesis of basic residues of the S4 segment of the shaker k+ channel*." J Gen Physiol 117(5): 469-490.

Starace, D. M. and Bezanilla, F. (2004). "*A proton pore in a potassium channel voltage sensor reveals a focused electric field*." Nature 427(6974): 548-553.

Staub, O., Gautschi, I., Ishikawa, T., Breitschopf, K., Ciechanover, A., Schild, L. and Rotin, D. (1997). "*Regulation of stability and function of the epithelial Na+ channel (ENaC) by ubiquitination*." EMBO J 16(21): 6325-6336.

Steele, D. F., Eldstrom, J. and Fedida, D. (2007). "*Mechanisms of cardiac potassium channel trafficking*." J Physiol 582(Pt 1): 17-26.

Sterling, H., Lin, D. H., Gu, R. M., Dong, K., Hebert, S. C. and Wang, W. H. (2002). "*Inhibition of protein-tyrosine phosphatase stimulates the dynamin-dependent endocytosis of ROMK1*." J Biol Chem 277(6): 4317-4323.

Sternberg, D., Tabti, N., Fournier, E., Hainque, B. and Fontaine, B. (2003). "*Lack of association of the potassium channel-associated peptide MiRP2-R83H variant with periodic paralysis*." Neurology 61(6): 857-859.

Strop, P., Bankovich, A. J., Hansen, K. C., Garcia, K. C. and Brunger, A. T. (2004). "*Structure of a human A-type potassium channel interacting protein DPPX, a member of the dipeptidyl aminopeptidase family*." J Mol Biol 343(4): 1055-1065.

Strutz-Seebohm, N., Pusch, M., Wolf, S., Stoll, R., Tapken, D., Gerwert, K., . . . Seebohm, G. (2011). "*Structural basis of slow activation gating in the cardiac I Ks channel complex*." Cell Physiol Biochem 27(5): 443-452.

Suginta, W., Karoulias, N., Aitken, A. and Ashley, R. H. (2001). "*Chloride intracellular channel protein CLIC4 (p64H1) binds directly to brain dynamin I in a complex containing actin, tubulin and 14-3-3 isoforms*." Biochem J 359(Pt 1): 55-64.

Sundivakkam, P. C., Kwiatek, A. M., Sharma, T. T., Minshall, R. D., Malik, A. B. and Tiruppathi, C. (2009). "*Caveolin-1 scaffold domain interacts with TRPC1 and IP3R3 to regulate Ca2+ store release-induced Ca2+ entry in endothelial cells*." Am J Physiol Cell Physiol 296(3): C403-413.

Sunose, H., Liu, J., Shen, Z. and Marcus, D. C. (1997). "*cAMP increases apical IsK channel current and K+ secretion in vestibular dark cells*." J Membr Biol 156(1): 25-35.

Swanson, R., Marshall, J., Smith, J. S., Williams, J. B., Boyle, M. B., Folander, K., . . . et al. (1990). "*Cloning and expression of cDNA and genomic clones encoding three delayed rectifier potassium channels in rat brain*." Neuron 4(6): 929-939.

Szabo, I., Bock, J., Grassme, H., Soddemann, M., Wilker, B., Lang, F., . . . Gulbins, E. (2008). "*Mitochondrial potassium channel Kv1.3 mediates Bax-induced apoptosis in lymphocytes*." Proc Natl Acad Sci U S A 105(39): 14861-14866.

Szabo, I., Bock, J., Jekle, A., Soddemann, M., Adams, C., Lang, F., . . . Gulbins, E. (2005). "*A novel potassium channel in lymphocyte mitochondria*." J Biol Chem 280(13): 12790-12798.

Szilagyi, O., Boratko, A., Panyi, G. and Hajdu, P. (2013). "*The role of PSD-95 in the rearrangement of Kv1.3 channels to the immunological synapse*." Pflugers Arch.

Tai, K. K. and Goldstein, S. A. (1998). "*The conduction pore of a cardiac potassium channel*." Nature 391(6667): 605-608.

Takimoto, K., Gealy, R. and Levitan, E. S. (1995). "*Multiple protein kinases are required for basal Kv1.5 K+ channel gene expression in GH3 clonal pituitary cells*." Biochim Biophys Acta 1265(1): 22-28.

Takumi, T., Moriyoshi, K., Aramori, I., Ishii, T., Oiki, S., Okada, Y., . . . Nakanishi, S. (1991). "*Alteration of channel activities and gating by mutations of slow ISK potassium channel*." J Biol Chem 266(33): 22192-22198.

Takumi, T., Ohkubo, H. and Nakanishi, S. (1988). "*Cloning of a membrane protein that induces a slow voltage-gated potassium current*." Science 242(4881): 1042-1045.

Tamkun, M. M., Knoth, K. M., Walbridge, J. A., Kroemer, H., Roden, D. M. and Glover, D. M. (1991). "*Molecular cloning and characterization of two voltage-gated K+ channel cDNAs from human ventricle*." FASEB J 5(3): 331-337.

Tamkun, M. M., O'Connell K, M. and Rolig, A. S. (2007). "*A cytoskeletal-based perimeter fence selectively corrals a sub-population of cell surface Kv2.1 channels*." J Cell Sci 120(Pt 14): 2413-2423.

Tang, N. L., Chow, C. C., Ko, G. T., Tai, M. H., Kwok, R., Yao, X. Q. and Cockram, C. S. (2004). "*No mutation in the KCNE3 potassium channel gene in Chinese thyrotoxic hypokalaemic periodic paralysis patients*." Clin Endocrinol (Oxf) 61(1): 109-112.

Tang, Z., Scherer, P. E., Okamoto, T., Song, K., Chu, C., Kohtz, D. S., . . . Lisanti, M. P. (1996). "*Molecular cloning of caveolin-3, a novel member of the caveolin gene family expressed predominantly in muscle*." J Biol Chem 271(4): 2255-2261.

Tao, X., Avalos, J. L., Chen, J. and MacKinnon, R. (2009). "*Crystal structure of the eukaryotic strong inward-rectifier K+ channel Kir2.2 at 3.1 A resolution*." Science 326(5960): 1668-1674.

Tapper, A. R. and George, A. L., Jr. (2000). "*MinK subdomains that mediate modulation of and association with KvLQT1*." J Gen Physiol 116(3): 379-390.

Tapper, A. R. and George, A. L., Jr. (2001). "*Location and orientation of minK within the I(Ks) potassium channel complex*." J Biol Chem 276(41): 38249-38254.

Temple, J., Frias, P., Rottman, J., Yang, T., Wu, Y., Verheijck, E. E., . . . Roden, D. M. (2005). "*Atrial fibrillation in KCNE1-null mice*." Circ Res 97(1): 62-69.

Teng, S., Ma, L., Zhen, Y., Lin, C., Bahring, R., Vardanyan, V., . . . Hui, R. (2003). "*Novel gene hKCNE4 slows the activation of the KCNQ1 channel*." Biochem Biophys Res Commun 303(3): 808-813.

Tester, D. J., Will, M. L., Haglund, C. M. and Ackerman, M. J. (2005). "*Compendium of cardiac channel mutations in 541 consecutive unrelated patients referred for long QT syndrome genetic testing*." Heart Rhythm 2(5): 507-517.

Tinel, N., Diochot, S., Borsotto, M., Lazdunski, M. and Barhanin, J. (2000). "*KCNE2 confers background current characteristics to the cardiac KCNQ1 potassium channel*." EMBO J 19(23): 6326-6330.

Toth, A., Szilagyi, O., Krasznai, Z., Panyi, G. and Hajdu, P. (2009). "*Functional consequences of Kv1.3 ion channel rearrangement into the immunological synapse*." Immunol Lett 125(1): 15-21.

Triantafilou, K. and Triantafilou, M. (2004). "*Lipid-raft-dependent Coxsackievirus B4 internalization and rapid targeting to the Golgi*." Virology 326(1): 6-19.

Tristani-Firouzi, M. and Sanguinetti, M. C. (1998). "*Voltage-dependent inactivation of the human K+ channel KvLQT1 is eliminated by association with minimal K+ channel (minK) subunits*." J Physiol 510 (Pt 1): 37-45.

Tsevi, I., Vicente, R., Grande, M., Lopez-Iglesias, C., Figueras, A., Capella, G., . . . Felipe, A. (2005). "*KCNQ1/KCNE1 channels during germ-cell differentiation in the rat: expression associated with testis pathologies*." J Cell Physiol 202(2): 400-410.

Tu, L., Wang, J., Helm, A., Skach, W. R. and Deutsch, C. (2000). "*Transmembrane biogenesis of Kv1.3*." Biochemistry 39(4): 824-836.

Tucker, K., Overton, J. M. and Fadool, D. A. (2008). "*Kv1.3 gene-targeted deletion alters longevity and reduces adiposity by increasing locomotion and metabolism in melanocortin-4 receptor-null mice*." Int J Obes (Lond) 32(8): 1222-1232.

Tzounopoulos, T., Guy, H. R., Durell, S., Adelman, J. P. and Maylie, J. (1995). "*min K channels form by assembly of at least 14 subunits*." Proc Natl Acad Sci U S A 92(21): 9593-9597.

Uebele, V. N., England, S. K., Chaudhary, A., Tamkun, M. M. and Snyders, D. J. (1996). "*Functional differences in Kv1.5 currents expressed in mammalian cell lines are due to the presence of endogenous Kv beta 2.1 subunits*." J Biol Chem 271(5): 2406-2412.

Um, S. Y. and McDonald, T. V. (2007). "*Differential association between HERG and KCNE1 or KCNE2*." PLoS One 2(9): e933.

Uysal, S., Vasquez, V., Tereshko, V., Esaki, K., Fellouse, F. A., Sidhu, S. S., . . . Kossiakoff, A. (2009). "*Crystal structure of full-length KcsA in its closed conformation*." Proc Natl Acad Sci U S A 106(16): 6644-6649.

Vacca, F., Amadio, S., Sancesario, G., Bernardi, G. and Volonte, C. (2004). "*P2X3 receptor localizes into lipid rafts in neuronal cells*." J Neurosci Res 76(5): 653-661.

Vallon, V., Grahammer, F., Richter, K., Bleich, M., Lang, F., Barhanin, J., . . . Warth, R. (2001). "*Role of KCNE1-dependent K+ fluxes in mouse proximal tubule*." J Am Soc Nephrol 12(10): 2003-2011.

Vallon, V., Grahammer, F., Volkl, H., Sandu, C. D., Richter, K., Rexhepaj, R., . . . Lang, F. (2005). "*KCNQ1-dependent transport in renal and gastrointestinal epithelia*." Proc Natl Acad Sci U S A 102(49): 17864-17869.

Vanoye, C. G., Welch, R. C., Daniels, M. A., Manderfield, L. J., Tapper, A. R., Sanders, C. R. and George, A. L., Jr. (2009). "*Distinct subdomains of the KCNQ1 S6 segment determine channel modulation by different KCNE subunits*." J Gen Physiol 134(3): 207-217.

Varga, Z., Csepany, T., Papp, F., Fabian, A., Gogolak, P., Toth, A. and Panyi, G. (2009). "*Potassium channel expression in human CD4+ regulatory and naive T cells from healthy subjects and multiple sclerosis patients*." Immunol Lett 124(2): 95-101.

Varga, Z., Hajdu, P. and Panyi, G. (2010). "*Ion channels in T lymphocytes: an update on facts, mechanisms and therapeutic targeting in autoimmune diseases*." Immunol Lett 130(1-2): 19-25.

Vendrame, F., Verrienti, A., Parlapiano, C., Filetti, S., Dotta, F. and Morano, S. (2008). "*Thyrotoxic periodic paralysis in an Italian man: clinical manifestation and genetic analysis*." Ann Clin Biochem 45(Pt 2): 218-220.

Vennekamp, J., Wulff, H., Beeton, C., Calabresi, P. A., Grissmer, S., Hansel, W. and Chandy, K. G. (2004). "*Kv1.3-blocking 5-phenylalkoxypsoralens: a new class of immunomodulators*." Mol Pharmacol 65(6): 1364-1374.

Vial, C. and Evans, R. J. (2005). "*Disruption of lipid rafts inhibits P2X1 receptor-mediated currents and arterial vasoconstriction*." J Biol Chem 280(35): 30705-30711.

Vicente, R., Escalada, A., Coma, M., Fuster, G., Sanchez-Tillo, E., Lopez-Iglesias, C., . . . Felipe, A. (2003). "*Differential voltage-dependent K+ channel responses during proliferation and activation in macrophages*." J Biol Chem 278(47): 46307-46320.

Vicente, R., Escalada, A., Soler, C., Grande, M., Celada, A., Tamkun, M. M., . . . Felipe, A. (2005). "*Pattern of Kv beta subunit expression in macrophages depends upon proliferation and the mode of activation*." J Immunol 174(8): 4736-4744.

Vicente, R., Escalada, A., Villalonga, N., Texido, L., Roura-Ferrer, M., Martin-Satue, M., . . . Felipe, A. (2006). "*Association of Kv1.5 and Kv1.3 contributes to the major voltage-dependent K+ channel in macrophages*." J Biol Chem 281(49): 37675-37685.

Vicente, R., Villalonga, N., Calvo, M., Escalada, A., Solsona, C., Soler, C., . . . Felipe, A. (2008). "*Kv1.5 association modifies Kv1.3 traffic and membrane localization*." J Biol Chem 283(13): 8756-8764.

Villalonga, N., Escalada, A., Vicente, R., Sanchez-Tillo, E., Celada, A., Solsona, C. and Felipe, A. (2007). "*Kv1.3/Kv1.5 heteromeric channels compromise pharmacological responses in macrophages*." Biochem Biophys Res Commun 352(4): 913-918.

Villalonga, N., Martinez-Marmol, R., Roura-Ferrer, M., David, M., Valenzuela, C., Soler, C. and Felipe, A. (2008). "*Cell cycle-dependent expression of Kv1.5 is involved in myoblast proliferation*." Biochim Biophys Acta 1783(5): 728-736.

Wang, D. T., Hill, A. P., Mann, S. A., Tan, P. S. and Vandenberg, J. I. (2011). "*Mapping the sequence of conformational changes underlying selectivity filter gating in the K(v)11.1 potassium channel*." Nat Struct Mol Biol 18(1): 35-41.

Wang, H., Yan, Y., Liu, Q., Huang, Y., Shen, Y., Chen, L., . . . Chai, J. (2007). "*Structural basis for modulation of Kv4 K+ channels by auxiliary KChIP subunits*." Nat Neurosci 10(1): 32-39.

Wang, H. S., Brown, B. S., McKinnon, D. and Cohen, I. S. (2000). "*Molecular basis for differential sensitivity of KCNQ and I(Ks) channels to the cognitive enhancer XE991*." Mol Pharmacol 57(6): 1218-1223.

Wang, H. S., Pan, Z., Shi, W., Brown, B. S., Wymore, R. S., Cohen, I. S., . . . McKinnon, D. (1998). "*KCNQ2 and KCNQ3 potassium channel subunits: molecular correlates of the M-channel*." Science 282(5395): 1890-1893.

Wang, J., Weigand, L., Wang, W., Sylvester, J. T. and Shimoda, L. A. (2005). "*Chronic hypoxia inhibits Kv channel gene expression in rat distal pulmonary artery*." Am J Physiol Lung Cell Mol Physiol 288(6): L1049-1058.

Wang, K., Terrenoire, C., Sampson, K. J., Iyer, V., Osteen, J. D., Lu, J., . . . Kass, R. S. (2011). "*Biophysical properties of slow potassium channels in human embryonic stem cell derived cardiomyocytes implicate subunit stoichiometry*." J Physiol 589(Pt 24): 6093-6104.

Wang, K. W. and Goldstein, S. A. (1995). "*Subunit composition of minK potassium channels*." Neuron 14(6): 1303-1309.

Wang, K. W., Tai, K. K. and Goldstein, S. A. (1996). "*MinK residues line a potassium channel pore*." Neuron 16(3): 571-577.

Wang, Q., Curran, M. E., Splawski, I., Burn, T. C., Millholland, J. M., VanRaay, T. J., . . . Keating, M. T. (1996). "*Positional cloning of a novel potassium channel gene: KVLQT1 mutations cause cardiac arrhythmias*." Nat Genet 12(1): 17-23.

Wang, W., Xia, J. and Kass, R. S. (1998). "*MinK-KvLQT1 fusion proteins, evidence for multiple stoichiometries of the assembled IsK channel*." J Biol Chem 273(51): 34069-34074.

Wang, X. L., Ye, D., Peterson, T. E., Cao, S., Shah, V. H., Katusic, Z. S., . . . Lee, H. C. (2005). "*Caveolae targeting and regulation of large conductance Ca(2+)-activated K+ channels in vascular endothelial cells*." J Biol Chem 280(12): 11656-11664.

Wangemann, P., Liu, J. and Marcus, D. C. (1995). "*Ion transport mechanisms responsible for K+ secretion and the transepithelial voltage across marginal cells of stria vascularis in vitro*." Hear Res 84(1-2): 19-29.

Wen, H. and Levitan, I. B. (2002). "*Calmodulin is an auxiliary subunit of KCNQ2/3 potassium channels*." J Neurosci 22(18): 7991-8001.

Weng, J., Cao, Y., Moss, N. and Zhou, M. (2006). "*Modulation of voltage-dependent Shaker family potassium channels by an aldo-keto reductase*." J Biol Chem 281(22): 15194-15200.

Wible, B. A., Yang, Q., Kuryshev, Y. A., Accili, E. A. and Brown, A. M. (1998). "*Cloning and expression of a novel K+ channel regulatory protein, KChAP*." J Biol Chem 273(19): 11745-11751.

Wiener, R., Haitin, Y., Shamgar, L., Fernandez-Alonso, M. C., Martos, A., Chomsky-Hecht, O., . . . Hirsch, J. A. (2008). "*The KCNQ1 (Kv7.1) COOH terminus, a multitiered scaffold for subunit assembly and protein interaction*." J Biol Chem 283(9): 5815-5830.

Williams, C. P., Hu, N., Shen, W., Mashburn, A. B. and Murray, K. T. (2002). "*Modulation of the human Kv1.5 channel by protein kinase C activation: role of the Kvbeta1.2 subunit*." J Pharmacol Exp Ther 302(2): 545-550.

Wissmann, R., Baukrowitz, T., Kalbacher, H., Kalbitzer, H. R., Ruppersberg, J. P., Pongs, O., . . . Fakler, B. (1999). "*NMR structure and functional characteristics of the hydrophilic N terminus of the potassium channel beta-subunit Kvbeta1.1*." J Biol Chem 274(50): 35521-35525.

Wollnik, B., Schroeder, B. C., Kubisch, C., Esperer, H. D., Wieacker, P. and Jentsch, T. J. (1997). "*Pathophysiological mechanisms of dominant and recessive KVLQT1 K+ channel mutations found in inherited cardiac arrhythmias*." Hum Mol Genet 6(11): 1943-1949.

Wong, W. and Schlichter, L. C. (2004). "*Differential recruitment of Kv1.4 and Kv4.2 to lipid rafts by PSD-95*." J Biol Chem 279(1): 444-452.

Wu, D., Delaloye, K., Zaydman, M. A., Nekouzadeh, A., Rudy, Y. and Cui, J. (2010). "*State-dependent electrostatic interactions of S4 arginines with E1 in S2 during Kv7.1 activation*." J Gen Physiol 135(6): 595-606.

Wu, D., Pan, H., Delaloye, K. and Cui, J. (2010). "*KCNE1 remodels the voltage sensor of Kv7.1 to modulate channel function*." Biophys J 99(11): 3599-3608.

Wu, D. M., Jiang, M., Zhang, M., Liu, X. S., Korolkova, Y. V. and Tseng, G. N. (2006). "*KCNE2 is colocalized with KCNQ1 and KCNE1 in cardiac myocytes and may function as a negative modulator of I(Ks) current amplitude in the heart*." Heart Rhythm 3(12): 1469-1480.

Wu, D. M., Lai, L. P., Zhang, M., Wang, H. L., Jiang, M., Liu, X. S. and Tseng, G. N. (2006). "*Characterization of an LQT5-related mutation in KCNE1, Y81C: implications for a role of KCNE1 cytoplasmic domain in IKs channel function*." Heart Rhythm 3(9): 1031-1040.

Wu, J., Shimizu, W., Ding, W. G., Ohno, S., Toyoda, F., Itoh, H., . . . Horie, M. (2010). "*KCNE2 modulation of Kv4.3 current and its potential role in fatal rhythm disorders*." Heart Rhythm 7(2): 199-205.

Wulff, H., Calabresi, P. A., Allie, R., Yun, S., Pennington, M., Beeton, C. and Chandy, K. G. (2003). "*The voltage-gated Kv1.3 K(+) channel in effector memory T cells as new target for MS*." J Clin Invest 111(11): 1703-1713.

Xia, F., Gao, X., Kwan, E., Lam, P. P., Chan, L., Sy, K., . . . Tsushima, R. G. (2004). "*Disruption of pancreatic beta-cell lipid rafts modifies Kv2.1 channel gating and insulin exocytosis*." J Biol Chem 279(23): 24685-24691.

Xu, J., Koni, P. A., Wang, P., Li, G., Kaczmarek, L., Wu, Y., . . . Desir, G. V. (2003). "*The voltage-gated potassium channel Kv1.3 regulates energy homeostasis and body weight*." Hum Mol Genet 12(5): 551-559.

Xu, J., Yu, W., Jan, Y. N., Jan, L. Y. and Li, M. (1995). "*Assembly of voltage-gated potassium channels. Conserved hydrophilic motifs determine subfamily-specific interactions between the alpha-subunits*." J Biol Chem 270(42): 24761-24768.

Yamada, E. (1955). "*The fine structure of the gall bladder epithelium of the mouse*." J Biophys Biochem Cytol 1(5): 445-458.

Yang, J. W., Vacher, H., Park, K. S., Clark, E. and Trimmer, J. S. (2007). "*Trafficking-dependent phosphorylation of Kv1.2 regulates voltage-gated potassium channel cell surface expression*." Proc Natl Acad Sci U S A 104(50): 20055-20060.

Yang, W. P., Levesque, P. C., Little, W. A., Conder, M. L., Shalaby, F. Y. and Blanar, M. A. (1997). "*KvLQT1, a voltage-gated potassium channel responsible for human cardiac arrhythmias*." Proc Natl Acad Sci U S A 94(8): 4017-4021.

Yang, Y. and Sigworth, F. J. (1998). "*Single-channel properties of IKs potassium channels*." J Gen Physiol 112(6): 665-678.

Yang, Y., Xia, M., Jin, Q., Bendahhou, S., Shi, J., Chen, Y., . . . Barhanin, J. (2004). "*Identification of a KCNE2 gain-of-function mutation in patients with familial atrial fibrillation*." Am J Hum Genet 75(5): 899-905.

Yao, X., Chang, A. Y., Boulpaep, E. L., Segal, A. S. and Desir, G. V. (1996). "*Molecular cloning of a glibenclamide-sensitive, voltage-gated potassium channel expressed in rabbit kidney*." J Clin Invest 97(11): 2525-2533.

Yarbrough, T. L., Lu, T., Lee, H. C. and Shibata, E. F. (2002). "*Localization of cardiac sodium channels in caveolin-rich membrane domains: regulation of sodium current amplitude*." Circ Res 90(4): 443-449.

Yellen, G. (2002). "*The voltage-gated potassium channels and their relatives*." Nature 419(6902): 35-42.

Yeung, S. Y., Lange, W., Schwake, M. and Greenwood, I. A. (2008). "*Expression profile and characterisation of a truncated KCNQ5 splice variant*." Biochem Biophys Res Commun 371(4): 741-746.

Yeung, S. Y., Pucovsky, V., Moffatt, J. D., Saldanha, L., Schwake, M., Ohya, S. and Greenwood, I. A. (2007). "*Molecular expression and pharmacological identification of a role for K(v)7 channels in murine vascular reactivity*." Br J Pharmacol 151(6): 758-770.

Ying, S. W., Kanda, V. A., Hu, Z., Purtell, K., King, E. C., Abbott, G. W. and Goldstein, P. A. (2012). "*Targeted deletion of Kcne2 impairs HCN channel function in mouse thalamocortical circuits*." PLoS One 7(8): e42756.

Yus-Najera, E., Munoz, A., Salvador, N., Jensen, B. S., Rasmussen, H. B., Defelipe, J. and Villarroel, A. (2003). "*Localization of KCNQ5 in the normal and epileptic human temporal neocortex and hippocampal formation*." Neuroscience 120(2): 353-364.

Yus-Najera, E., Santana-Castro, I. and Villarroel, A. (2002). "*The identification and characterization of a noncontinuous calmodulin-binding site in noninactivating voltage-dependent KCNQ potassium channels*." J Biol Chem 277(32): 28545-28553.

Zacharias, D. A., Violin, J. D., Newton, A. C. and Tsien, R. Y. (2002). "*Partitioning of lipid-modified monomeric GFPs into membrane microdomains of live cells*." Science 296(5569): 913-916.

Zagha, E., Ozaita, A., Chang, S. Y., Nadal, M. S., Lin, U., Saganich, M. J., . . . Rudy, B. (2005). "*DPP10 modulates Kv4-mediated A-type potassium channels*." J Biol Chem 280(19): 18853-18861.

Zagotta, W. N., Hoshi, T. and Aldrich, R. W. (1990). "*Restoration of inactivation in mutants of Shaker potassium channels by a peptide derived from ShB*." Science 250(4980): 568-571.

Zeng, Z., Tan, C., Teng, S., Chen, J., Su, S., Zhou, X., . . . Pu, J. (2007). "*The single nucleotide polymorphisms of I(Ks) potassium channel genes and their association with atrial fibrillation in a Chinese population*." Cardiology 108(2): 97-103.

Zerangue, N., Schwappach, B., Jan, Y. N. and Jan, L. Y. (1999). "*A new ER trafficking signal regulates the subunit stoichiometry of plasma membrane K(ATP) channels*." Neuron 22(3): 537-548.

Zhang, H., Craciun, L. C., Mirshahi, T., Rohacs, T., Lopes, C. M., Jin, T. and Logothetis, D. E. (2003). "*PIP(2) activates KCNQ channels, and its hydrolysis underlies receptor-mediated inhibition of M currents*." Neuron 37(6): 963-975.

Zhang, L., Foster, K., Li, Q. and Martens, J. R. (2007). "*S-acylation regulates Kv1.5 channel surface expression*." Am J Physiol Cell Physiol 293(1): C152-161.

Zhang, M., Jiang, M. and Tseng, G. N. (2001). "*minK-related peptide 1 associates with Kv4.2 and modulates its gating function: potential role as beta subunit of cardiac transient outward channel?*" Circ Res 88(10): 1012-1019.

Zhang, M., Wang, Y., Jiang, M., Zankov, D. P., Chowdhury, S., Kasirajan, V. and Tseng, G. N. (2012). "*KCNE2 protein is more abundant in ventricles than in atria and can accelerate hERG protein degradation in a phosphorylation-dependent manner*." Am J Physiol Heart Circ Physiol 302(4): H910-922.

Zheng, R., Thompson, K., Obeng-Gyimah, E., Alessi, D., Chen, J., Cheng, H. and McDonald, T. V. (2010). "*Analysis of the interactions between the C-terminal cytoplasmic domains of KCNQ1 and KCNE1 channel subunits*." Biochem J 428(1): 75-84.

Zhong, X. Z., Harhun, M. I., Olesen, S. P., Ohya, S., Moffatt, J. D., Cole, W. C. and Greenwood, I. A. (2010). "*Participation of KCNQ (Kv7) potassium channels in myogenic control of cerebral arterial diameter*." J Physiol 588(Pt 17): 3277-3293.

Zhou, M., Morais-Cabral, J. H., Mann, S. and MacKinnon, R. (2001). "*Potassium channel receptor site for the inactivation gate and quaternary amine inhibitors*." Nature 411(6838): 657-661.

Zhou, Y. and MacKinnon, R. (2003). "*The occupancy of ions in the K+ selectivity filter: charge balance and coupling of ion binding to a protein conformational change underlie high conduction rates*." J Mol Biol 333(5): 965-975.

Zhu, J., Gomez, B., Watanabe, I. and Thornhill, W. B. (2005). "*Amino acids in the pore region of Kv1 potassium channels dictate cell-surface protein levels: a possible trafficking code in the Kv1 subfamily*." Biochem J 388(Pt 1): 355-362.

Zhu, J., Watanabe, I., Gomez, B. and Thornhill, W. B. (2003). "*Heteromeric Kv1 potassium channel expression: amino acid determinants involved in processing and trafficking to the cell surface*." J Biol Chem 278(28): 25558-25567.

Zhu, J., Watanabe, I., Gomez, B. and Thornhill, W. B. (2003). "*Trafficking of Kv1.4 potassium channels: interdependence of a pore region determinant and a cytoplasmic C-terminal VXXSL determinant in regulating cell-surface trafficking*." Biochem J 375(Pt 3): 761-768.

Zuzarte, M., Rinne, S., Schlichthorl, G., Schubert, A., Daut, J. and Preisig-Muller, R. (2007). "*A di-acidic sequence motif enhances the surface expression of the potassium channel TASK-3*." Traffic 8(8): 1093-1100.

7. Resum

AVÍS IMPORTANT

El text d'aquest capítol ha estat retirat seguint instruccions de l'autora de la tesi, en existir participació d'empreses, existir conveni de confidencialitat o existeix la possibilitat de generar patents

AVISO IMPORTANTE

El texto de este capítulo ha sido retirado siguiendo instrucciones de la autora, al existir participación de empresas, convenio de confidencialidad o la posibilidad de generar patentes.

IMPORTANT NOTICE

The text of this chapter has been withdrawn on the instructions of the author, as there is participation of undertakings, confidentiality agreement or the ability to generate patent

8. Addendum

8.1. Methodology

8.1.1. Bacteria manipulation and culture

Competent XL1-Blue strain (*Escherichia coli*) has been used.

8.1.1.1. Transformation of competent bacteria

Either 5-25 ng of plasmid DNA or 1/3 of ligation reaction (see section 8.2.1. for more information) were mixed with 25μl XL1-Blue, in a sterile eppendorf tube on ice. After 30 minutes, a heat shock of 1 min 45 s at 42ºC was performed. Next, tubes were placed again on ice for 2 min. Finally, 300 μl of Super Optimal Broth (SOB) was added and bacteria were incubated for 45-60 min at 37ºC. Cultures were seeded on agar plates, supplemented with selected antibiotics (Ampicillin or Kanamycine). Plates were incubated overnight at 37ºC.

8.1.1.2. Bacterial cultures and purification of plasmid DNA

Transformed bacteria, either from glycerol stocks at -80ºC or from colonies in agar plates, were cultured overnight in Luria Broth (LB) supplemented with 100 μg/ml Ampicillin or 30 μg/ml Kanamycine. The culture was spun (5 min at 14000 rpm) at RT (room temperature) and the pellet was processed for the extraction of the plasmid DNA by using the GeneElute Plasmid DNA purification kit (Sigma), according to the manufacturer's instructions.

8.1.2. Chimeric proteins and constructs.

Many constructs were kindly given from other institutions or have been produced previously by others members of the group. Constructs can be generated either by subcloning a cDNA in a new vector or by mutagenesis of an existent construct. These two procedures will be explained briefly below, and see the tables 8.1 and 8.2 from the addendum for detailed information of all the constructs used.

8.1.2.1. Subcloning of a cDNA in a new plasmid.

In order to create a tagged cDNA, the normal protocol used was to amplify the desired fragment of the cDNA by the Polymerase Chain Reaction (PCR) with a pair of designed primers that will introduce the restriction enzyme's target of the final vector. The PCR was generally done with Phusion polymerase (ThermoScientific), following manufacturer's instructions. Then, the PCR reaction was purified using the ATP Gel/PCR Extraction kit (ATP Biotech Inc), following the manufacturer's instructions. Next, the purified PCR was digested by restriction enzymes (New England), following the manufacturer's instructions, usually at 37ºC over night. In parallel, the final vector was also digested with the same enzymes, plus Phosphatase Alkaline (Roche), in order to avoid possible posteriori re-

ligation of the vector without the insert. Once the digestions were done, all them were loaded in an 1-2 % agarose-TAE gel with 1/15,000 SyberSafe Gel Stain (Invitrogen), and the desired bands of insert (cDNA from the digested PCR) and vector (final vector) were cut and purified with the ATP Gel/PCR Extraction kit. Then, the purified vector and inserts were ligated doing the reaction with T4 DNA-Ligase (New England Biolab), according to the supplier's instructions, for 1 h at RT, or overnight at 4ºC or 16ºC. Finally, the ligation was transformed to competent bacteria (see section 8.1.1.) and processed in order to check positive clones.

8.1.2.2. Site-Directed Mutagenesis.

Mutagenesis reactions were performed by using Single site-Directed Mutagenesis or Multiple site-Directed Mutagensis kits from Strategene. Reactions were done following supplier's indications. Briefly, a PCR with the PfuTurbo polymerase and the primer pair will incorporate the mutation. Primers are longer than usual primers because a sequence of 10-15 nucleotides has to flank the mutation. Next, DNA is digested with Dpn I, which only recognizes and digests methilated DNA (parental, not-mutated DNA). Finally, the mutated DNA is transformed into competent bacteria supplied by the kit. After growing and selected clones are analyzed by sequenciation.

All constructs were analyzed by sequenciation with the Big Dye Terminator v3.1 kit (Applied Biosystems). Samples were processed by the Genomic's Facility of the Universitat de Barcelona. Sequences obtained were analyzed with Clone Manager Professional v7 software (Sci Ed Central software).

8.1.3. Cell culture and cell lines

Hek-293 cells have been used for heterologous expression. Jurkat T-lymphocytes, Raji B-lymphocytes and Raw 264.7 and Bone Marrow Derived macrophages have been used for native expression.

8.1.3.1. Hek-293

The human embryonic kidney (Hek-293) cell line has a fibroblastic morphology and apparently has neither endogenous ion channel expression or Kvβ auxiliary subunits (Uebele et al.,1996).

Hek-293 cells were cultured on DMEM (LONZA) containing 10% fetal bovine serum (FBS) supplemented with penicillin (10.000 U/ml), streptomycin (100 µg/ml) (GIBCO) and L-glutamine (4 mM). Cells were grown in 100-mm tissue culture dishes or on poly-D-lysine-coated coverslips.

8.1.3.2. Raw 264.7 macrophages

RAW 264.7 is a monocytic cell line derived from a murine ascitic tumor. Cells were cultured in RPMI medium containing 10% FBS supplemented with penicillin (10.000 U/ml), streptomycin (100 µg/ml), L-glutamine (4 mM) and HEPES 25mM. Macrophages were grown in 100-mm tissue culture dishes.

8.1.3.3. Jurkat T-lymphocytes

Jurkat T-cells are derived from a human acute T-cell leukemia. Cells cultured in RPMI medium containing 10% FBS supplemented with penicillin (10.000U/ml), streptomycin (100 µg/ml) L-glutamine (2 mM) and HEPES (25 mM). Jurkat T-cells, ,were grown in 25 and 75-cm^2 culture flasks.

8.1.3.4. Raji B-lymphocytes

Raji B-lymphocytes are derived from a human Burkitt's lymphoma. Cells were cultured in RPMI culture medium containing 10% FBS supplemented with penicillin (10.000 U/ml), streptomycin (100 µg/ml) L-glutamine (2 mM) and HEPES (25mM). Raji cells were grown in 25 or 75-cm^2 flasks.

8.1.3.5. Bone Marrow Derived Macrophages

Murine bone marrow-derived macrophages (BMDM) were extracted from 6- to 10-wk-old BALB/c mice (Charles River laboratories). Briefly, animals were sacrificed by cervical dislocation, and introduced in an alcohol glass. Once inside the hood, the femurs were extracted with pre-sterilized surgery material. The adherent tissue was removed to dissect both femurs. The ends of bones were cut off, and the marrow tissue was flushed using irrigation with medium. The marrow plugs were passed through a 25-gauge needle for dispersion. The cells were cultured in DMEM containing 20% FBS and 30% L-929 fibroblast (L-cell) conditioned media as a source of macrophage colony-stimulating factor (MCSF), need for these cells for survival and differentiation (Meerpohl et al. 1976). The macrophages were obtained as a homogeneous population of adherent cells in non-treated dishes, after 7 days of culture and maintained at 37°C in a humidified incubator under 5% CO_2.

The ethics committee from the University of Barcelona approved all methods for animal care and handling, and the experiments were conducted in accordance with EU regulations.

8.1.4. Transfection of mammalian cells

Cells were seeded (70-80 % of confluence), in dishes 24 h before transfection with selected cDNAs., Metafectene PRO (Biontex) was used for transfection according to the

supplier's instructions. 4 μg DNA in a 100 mm dish and 500 ng for each well of a 6-well dish (for coverslip use) was used. Next, 4-6 h after transfection, the mixture was removed and replaced with new fresh culture media. Unless indicated, all the experiments were performed 24 h after transfection.

For TIRF microscopy experiments, cells were electroporated for transfection. In those case, first cells from a confluent 100-mm dish were tryspinised and then electroporated with 25-100ng of the desired DNA plus 100ng of BirA DNA (biotin ligase to biotinylate the loopBAD-tag proteins) using a Bio-Rad Genepulser Xcell, with a 0.2-cm-gap cuvette and a single 110 V 25ms pulse. Transfected cells were the desired treated dishes (see section 8.13 for more information).

8.1.5. mRNA expression analysis by Real-time PCR.

We performed a mRNA expression analysis of KCNE4 and Kv1.3 by quantitative RT-PCR, in different cell lines, such as Raw462.7 macrophages and Jurkat T-cells. We previously extracted RNA from cells and the synthesis of the complementary DNA (cDNA) was performed.

8.1.5.1. RNA extraction and cDNA sintesis.

Total RNA was isolated by using Nucleospin RNAII (Machery-Nagel), which contains DNAseI. In most cases, the starting material was 100-mm dish or a 75-cm^2 flask nearly confluence. cDNA synthesis was performed, using transcriptor reverse transcriptase (Roche) with a random hexanucleotide and oligo(dT) according to the manufacturer's instructions, from 1-4 μg of RNA. Controls were performed in the absence of the reverse transcriptase reaction. The RNA was incubated at 65ºC for 5 min. Next, the retrotranscriptase, dNTPs, and inhibitor of RNAses were added. The cDNA synthesis last for 45 min at 55ºC. Finally, the retrotranscriptase activity was inhibited by incubating the sample at 80-90ºC for 10 min.

8.1.5.2. Real Time PCR.

Real-time PCR was performed using a LightCycler machine (Roche) and a 7500 Real Time PCR System (Applied Biosystems) with LightCycler FastStart DNA MasterPLUS SYBR Green I (Roche), according to the manufacturer's instructions. PCR primers, gene accession numbers, annealing conditions and amplicon lengths are listed in Table 8.3. Reactions were performed under the following conditions: an initial incubation at 95ºC at 10 min followed by cycling at 95°C for 5 sec, specific anhealing at T°C for 8 sec, and 72°C for 6-9 sec (depending on the amplicon length), followed by 10 min at 95°C, in order to get the melting curves to verify the specificity of the product. Ribosomal 18s was included as an internal

reference, as previously described (Villalonga et al., 2007). Results were analyzed with Light Cycler software 1.5 (Roche) and 7500 Software v2.01 (Applied Bioystems). For each primer set, a standard curve was generated and the slope factor calculated. Values were normalized to the corresponding 18S RNA. The corresponding real-time PCR efficiency (E) of one cycle in the exponential phase was calculated according to the equation: E=10(–1/slope). In the case of comparing the different KCNEs, the ratio KCNEx/KCNE1 was calculated taking into account the primer pair efficiencies as follows: Ratio=$(1+E)^{\Delta Ct(KCNEx)}$/ $(1+E)^{\Delta Ct(KCNE1)}$, where Ct signifies the threshold cycle.

8.1.6. Protein extraction.

8.1.6.1. Total protein.

To obtain a total protein lysate the starting material was always a pre-confluent 100-mm dish, or a 75-cm^2 flask (lymphocytes). The process was realized on ice to inhibit proteases. Cells were washed twice with 5 ml of cold PBS (1x). Next, cells were incubated for 5 min with 500 µl of Lysis Buffer (5 mM HEPES, 150 mM NaCl, 1% Triton X-100, pH 7.5) supplemented with 1 µg/ml aprotinin, 1 µg/ml leupeptin, 1 µg/ml pepstatin and 1 mM phenylmethylsulfonyl fluoride as protease inhibitors. Cells were next scrapped and transferred to a 1.5 ml-tube. Then they were incubated for 20 min at the orbital, and spun for 20 min at 14000 rpm. The supernatant was transferred to a new 1.5 ml-tube and stored at -20ºC until use.

In some experiments performed in presence of calcium or calcium chelators, the lysis buffer was further supplemented with 2mM $CaCl_2$, or 2mM EGTA plus 2mM EDTA, respectively.

Protein contents were determined by using the Bio-Rad Protein Assay (Bio-Rad).

8.1.7. Isolation of *lipid raft* membrane microdomains

The plasma membrane is a heterogeneous structure that contains multiple specialized microdomains. One of these microdomains are called lipid rafts, which are rich in cholesterol and sphingolipids. Their composition provides to these rafts the resistance to non-ionic detergents. The method used to isolate lipid rafts (Sargiacomo et al. 1993) treats the cells with a non-ionic detergent such as Triton X-100 followed by a centrifugation in a continuous sucrose density gradient. The non-solubilized rafts, with very low density with a high content of cholesterol and sphingolipids, float in the fractions of low density sucrose of the gradient.

The starting material was always four 100-mm dishes of HEK293 cells transfected with 4 µg/plate of DNA. The procedure was always performed on ice-cold conditions.

Cells were washed twice with cold PBS (1x), and scrapped with 2 ml of 1x PBS. The cell suspension was centrifuged 2 min at 1000 rpm. The pellet were resuspended in 1ml of 1x MBS lysis buffer (0.15 M NaCl, 25 mM 2-Morpholinoethanesulphonic acid (MES), pH 6.5) supplemented with 1% Titron X-100 and protease inhibitors (see chapter 1.5.1.). Cells were homogenized with a 2 ml loose-homogenizator (10 times) and 1 ml was transferred to a 12.5 ml ultracentrifuge tube. Three ml of 53.28% of sucrose was added on top and mixed carefully, generating a 40% sucrose final mixture. Finally, a continuous sucrose gradient density was added on top using 4.25 ml of 30% and 4.25 ml of 5% sucrose by a continuous gradient generator device. The gradients were centrifuged at 39000 rpm for 16-22 hours at 4ºC in a Beckman centrifuge, using the SW41TI rotor. Next, 1 ml fractions were collected from the top to the bottom of the gradient and stored at -20ºC until analysis by western blot. The expression of caveolin and clatrhin were used as positive and negative control markers for raft and non-raft microdomains, respectively.

8.1.8. Immunoprecipitation

Immunoprecipitation (IP) experiments were performed from a 100 mm dish of HEK293 cells transfected with 4 µg of DNA of each protein, 24 h after the transfection. All protocol has been realized on ice, whenever possible.

First, a total protein extraction was performed, following the protocol listed on the section 8.5.1. Next, 1000 µg of protein of each condition were used for IP. An IP in absence of antibody is performed as a negative control. Each sample was brought up to a volume of 500 ml with Lysis Buffer for IPs (150 mM NaCl, 50 mM HEPES, 1%Titron X-100, pH 7.4), supplemented with protease inhibitors.

Each sample was subjected to precleaning with 40 µl of protein G or A (depending on the antibody) sepharose beads (GE Healthcare) during 1 h at 4ºC. Next, samples were incubated in a column containing a selected antibody crosslinked to protein G/A sepharose beads (see table 8.4 from addendum for more information) for 2 h at RT, with continuous mixing. Some immunoprecipitations were performed overnight at 4ºC. Next, the columns were centrifuged 30 sec at 1000 g. The supernatant (SN), containing all free proteins, was kept and stored at -20ºC. Columns were washed four times with 500 µl of lysis buffer. Finally, bound proteins were eluted with 100 µl of 0.2 M glycine pH 2.5, and spun 30 sec at 1000 g. Eluted proteins (IP) were processed for western blot analysis by adding 20 µl of Loading Buffer (5x) and 5 µl of 1 M Tris-HCl pH 10.

After the elution, the columns were washed three times with 1x TBS (150 mM NaCl, 25 mM TRIS, pH 7.2) and stored in the fridge for maximum three weeks with 1x TBS and sodium azide 0.025 %, ready for being re-used.

8.1.8.1. Preparation of columns for immunoprecipitation.

The above protocol is based on columns for IPs, and is adapted from Qoronfleh et al. (J. Biomedicine and Biotechnology 2003) using small cromatogrophy columns (BioRad Micro spin Cromatography Columns). 500 µl of 1x PBS is added to the column. Next, 2.5 µg of the desired antibody is added to the +IP columns. Nothing is added to the -IP columns (negative control of the IP without antibody). Finally, 50 µl of protein G or A sheparose (see table 8.4 for antibodies and proteins G or A used) beads is added to each column (either + or -IP) and incubated 1 h at RT. Columns are further washed twice with Borat Buffer (0.2 mM Na-Borat, pH 9), and centrifuged at 1000 g for 30 sec. 500µl of Dimethyl pimelimidate (DMP, from Pierce) is added to each column, and incubated for 30 min at RT. Once the crosslinking is done, each column is washed four times with 500 µl of 1x TBS, in order to remove the excess of DMP or free not bound antibody. Further, the reaction is stopped by washing four times each column with 500 µl of 0.2 M glycine pH 2.5. Finally, columns are washed three more times with 1x TBS and they can be either stored at 4ºC with 1x TBS and 0.025 % sodium azide or equilibrated with 500 µl of Lysis Buffer for IPs and being ready to use for IP.

8.1.9. Western blot

Protein samples were prepared with 5x Laemmli buffer (1 M Tris, 10 % SDS, 50 % glicerol and 4 % bromophenol blue, pH 6.8) with 10 % of β-Mercaptoethanol, and boiled 5 min. 50 µg of total protein, 40 µl of lipid raft fractions and supernatants from IPs were analyzed.

Samples were loaded and separated in a 10–15 % SDS-polyacrilamide gel (SDS-PAGE). Next, proteins were transferred to a nitrocellulose PVDF membranes (Immobilon-P; Millipore) and blocked in 0.05 % Tween-20-PBS supplemented with 5 % dry milk 1 h at RT. Filters were immunobloted with selected primary antibodies in 0.5 % Tween-20-PBS supplemented with 5 % dry milk O/N at 4ºC. Membranes were incubated 1 h at RT with 0.5 % Tween-20-PBS secondary antibody conjugated to Horse Radish Peroxidase (BioRad). Primary and secondary antibodies details are in table 8.5 from addendum. After antibody incubation, 4-5 washes of 5 min were performed at RT with 0.05 % Tween-20-PBS.

Membranes were developed using ECL (Biological Industries), and Kodak photographic films (Rosex). Quantification was performed by ImageJ analysis.

8.1.10. Biotinylation of cell surface proteins

Cell surface biotinylation was carried out with the Pierce Cell Surface Protein Isolation Kit (Pierce) following manufacturer's instructions. HEK293 cells were transfected with the desired protein tagged with YFP or CRP and their temporal presence at the surface was analyzed by western blotting. At the desired times after transfection (at the end point measurement time was 24 hours), cell surface proteins were labeled with sulfo-succinimidyl-2-(biotinamido)ethyl-1,3-dithiopropionate (Sulfo-NHS-SS-biotin; Pierce). Briefly, cells were washed with ice-cold PBS twice, and Sulfo-NHS-SS-biotin was added and incubated at 4°C with constant rotation for 30 min. Excess biotin was quenched with quenching solution. Cells were treated with lysis buffer and centrifuged at 10,000 g for 2 min at 4°C. Clear supernatant was reacted with immobilized NeutrAvidin gel slurry in columns (Pierce) to isolate surface proteins. Columns were washed and protein eluted in sample buffer containing DTT. Surface proteins were resolved on a SDS-PAGE gel and the samples were analyzed by western blotting, as described in section 1.9.

8.1.11. Immunocytochemistry

In order to study the subcellular localization of selected proteins, immuno-cytochemistry studies have been performed in native and transfected cells.

Cells were seeded in poly-D-Lysine (Sigma) 20x20mm coverslips (Acefesa), transfected, and processed 24 h later. First, cells were quickly washed twice with 1x PBS without potassium and fixed with 4% paraformaldehyde (PFA) (Sigma) in PBS-K^+ for 10 minutes at RT. Cells were further washed three times with PBS-K^+ for 5 min. Next, cells were permebealized for 20 min with 0.1 % Triton X-100 PBS-K^+. After three washes with 0.05 % Triton X-100 PBS-K^+, cells where further incubated with a Blocking solution (5 % milk, 10 % goat serum in 0.05 % Triton X-100 PBS-K^+), for 1 h at RT. Next, cells were incubated with the primary antibody with 10 % goat serum, 0.05 % Triton X-100 PBS-K^+, for 1 h 45 min at RT. Cells were washed three times with 0.05 % Triton X-100 PBS-K^+, and further incubated with the secondary antibody (conjugated with a fluorophore) in 1 % BSA, 0.05 % Triton X-100 PBS-K^+, for 45 min at RT. See table 8.6 from addendum for detailed information about antibodies conditions. Finally, cells were washed tree times with PBS-K^+ for 5 min, and the

coverslips were mounted on microscope slides (Acefesa) with the mounting media (Molecular Probes). Coverslips were let dry at RT before being observed at the microscope.

In some experiments the immunocytochemistry should be done in non permeabilitzant conditions. Therefore, the permeabilitzation step was skipped and all the buffers used in the protocol were Triton X-100 free. When fluorescent tagged-proteins were used, cells were only washed, fixed, washed and mounted, as described before.

8.1.11.1. Induced-Patched Immunocytochemistry.

Antibody-induced patching Immunocytochemistry generates better signals. Cells are incubated with the primary antibody while stil alive. This will cause a rearrangement of the membrane, and it will tend to form protein aggregates in different regions of the plasma membrane. Whether this protein interacts with another protein, the later will also be rearranged, and both proteins follow the same pattern.

Cells were quickly washed with PBS-K^+ and incubated with the primary antibody in DMEM media supplemented with 30mM HEPES, for 1 h at 37 ºC. Next, cells were quickly washed twice with PBS-K^+, and incubated with the secondary antibody also in the same DMEM media, for 1 h at 4 ºC (to decrease the endocytosis of the complexes). Then cells were quickly washed three times and fixed with 4 % PFA for 10 min RT. Finally, cells were washed three times with PBS-K^+ and mounted as described before. When an extra labeling is needed (i.e. intracellular analysis of another protein), a second round of labeling with primary and secondary antibodies could be done after the fixation protocol, following the indications described in the section 8.11.

8.1.12. Analysis of cellular structures

8.1.12.1. Plasma membrane staining

- Wheat Germ Agglutinin-Texas Red (WGA) (Invitrogen) was used to stain the plasma membrane.

- β subunit of Cholera toxin-Alexa555 (CTXβ) (Invitrogen). was used to identify surface lipid raft microdomains.

The protocol used for both stainings is similar, and was always performed under non-permeabilized conditions. First, cells (on ice) were washed with PBS at 4°C and incubated with Alexa555-CTXβ (1/1000) or WGA-TexasRed (1/1500) in DMEM supplemented with 30mM Hepes for 30 and 15 min, respectively, at 4°C. Subsequently, cells were quickly

washed twice and fixed with 4% paraformaldehyde in PBS for 6 min. Further, cells can be processed as a normal immunocytochemistry (see section 8.11.)

8.12.2. Endoplasmatic Reticulum

A construction (pDs-Red-ER) that codifies for a DsRed (fluorofophore) fused to the endoplasmatic reticulum targeting aminoacid sequence of calreticulin protein was used.

8.12.3. Golgi Apparatus

A construction (pECFP) that codifies for the human protein β.1,4-galatosiltransferasa (which localizes in trans-medial Golgi complex) fused to the ciano fluorescent protein was used.

8.1.13. Microscope techniques

8.1.13.1. Confocal Microscope

Images were taken with a Leica TCS SL laser scanning confocal spectral microscope (Leica Microsystems), equipped with an Argon and Helium-Neon lasers. All the experiments were captured with a 63x oil-immersion objective lens (NA 1.32). Images with a resolution of 1024x1024 pixels were taken under the following conditions: 1 Airy Units (AU) of the pinhole, 4 line-average scanning (the laser scanned a region of the sample 4 times, and the average of all the scannings was used to generate the final image), with 400Hz of scanning velocity, and a zoom of 4x mainly was used.

As it has been described before, in order to analyze the distribution of a protein in a cell by microscope techniques, one can use to kind of fluorophores-tagging approaches: a chimera of the desired protein with a fluorescence protein such as GFP, YFP or CFP, Cherry, etc, or primary antibodies against the desired protein and secondary antibodies attached to a fluorophore. In both cases, this fluorophores will be only excited under a small range of wavelength light , and will emit less energetic light (higher wavelength). Thanks to the progression of science, nowadays, there are multiple kinds of fluorophores and fluorescent proteins with different excitation and emission characteristics that give us a lot of possibilities and possible combinations to be used.

8.1.13.1.1. Fluorescence Recovery After Photobleaching (FRAP)

FRAP analyses the cellular mobility of a fluorophore-tagged protein at the membrane evaluating the membrane dynamics. Fluorophores, which present in a determined region of the membrane, are irreversible bleached by applying the excitation laser at 100% of the

power. Then, the fluorescence recovery of the bleached region is analyzed for several minutes. The fluorescence recovery is caused by the movement or diffusion of the non-bleached fluorophores from the surrounded areas. The recovery time of the fluorescence will be faster or slower depending on the membrane composition (Fig. 1.).

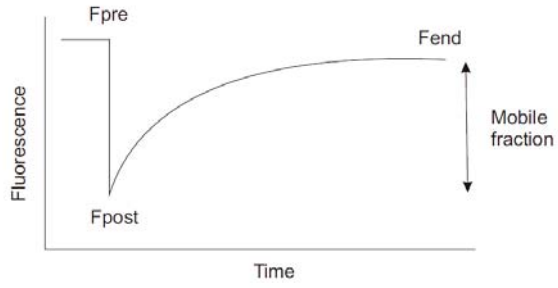

Fig. 1. *Graph showing the recovery of the fluorescene after the photobleaching.* Fpre, Fpost, Fend and the mobile fraction are indicated.

The technology and software coupled to the current confocal microscopes allows to monitor and quantify the fluorescence recuperation during time. Using a non-lineal fitting of the data obtained in FRAP experiments the mobile fraction and recovery half time parameters can be calculated..

Mobile fraction (MF): Percentage of fluorescence recovered from the initial value (F_{pre}) when the stationary estate is reached (F_{end}). The immobile fraction is the resting percentage until reach the initial value. High values of immobile fraction may suggest that the protein is localized in more compact regions of the membrane, such as lipid rafts. This parameter is calculated by the following formula:

$$MF= (F_{end}-F_{post})/(F_{pre}-F_{post})$$

Where MF is the mobile fraction, F_{end} corresponds to the fluorescence at the steady state, F_{post} corresponds to the fluorescence after the bleaching and F_{pre} corresponds to the fluorescence before the bleaching.

Recovery half time: The time that the fluorescence recovers half of the fluorescence at the steady state. This parameter indicates the dynamics of a protein in the membrane. When the fluorescence recovers very fast (smaller recovery half time) this suggests a protein localized in a region of the membrane that is not very structured or compacted. To calculate the recovery half time the recovery fluorescence curve is fitted to a simple exponential:

$$Y= Y_o + a*[1-\exp(-b*x)] \qquad t_{1/2} = (\ln 0.5)/b$$

Where

Y: fluorescence

Y_0: minimum of intensity (bleach)

a: maximum of intensity (steady state)

X: time

b: slope of the curve

$t_{1/2}$: recovery half time

FRAP experiments were performed 1 day after transfection at RT, with non-fixed cells. Dishes were replaced every 2 hours. The fluorophore in all the cases was YFP.

Experiments consisted in different time series: 20 scans before bleaching, which was accomplished by 20 iterations of bleaching with 100% laser power of the 514 nm line followed by 100 scans every 0.36 sec and 100 scans every sec (2.5 min in total) of the bleached region with 6% laser power. In each cell, a circular ROI of 6.57 μm^2 was bleached. Experiments were performed with n>15 cells per group. Fluorescence intensity was normalized to the prebleach intensity. Any loss of fluorescence during the recording was corrected with unbleached regions of the cell.

Cells were examined with a 63x oil immersion objective on a Leica TCS SL laser scanning confocal microscope, as mentioned before (section 1.13.1). The scanning speed was increased to 800Hz and images taken with a resolution of 512x128pixels. All offline image analysis was done using Leica confocal and Image J software and Sigmaplot.

8.1.13.1.2. Förster Resonance Energy Transfer (FRET)

FRET is a common technique to determine whether two proteins are physically associated. Two fluorophores (a donor and an acceptor) must have some overlapping between donor's emission spectrum and acceptor's excitation spectrum. If this two fluorophores are close enough (between 10-100 Aº), the donor excitation transfers its excited state energy to the acceptor, in a non-radiative way. This results in a light's emission by the acceptor fluorophore just by exciting the donor fluorophore (Fig. 2).

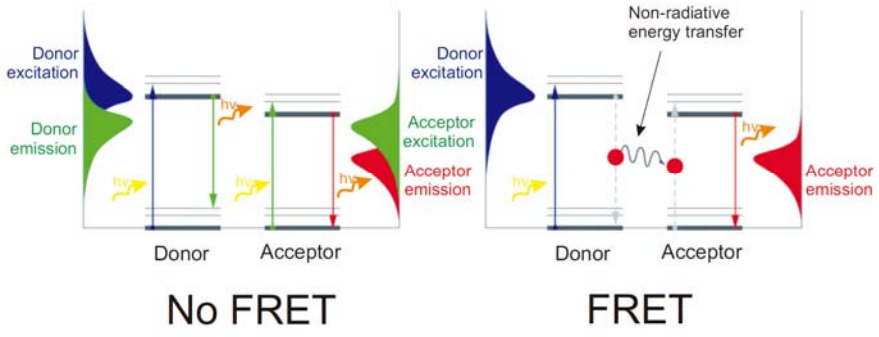

Fig. 2. *Jablonski diagrams of FRET*. The left diagram illustrates the energy transitions of the donor and acceptor in the case of no FRET, where there is no energy transfer between them. The right diagram illustrates the coupled transitions involved between the donor and acceptor absorbance when FRET occurs and that exciting the donor, an acceptor emission is emitted.

When the energy transference between different fluorophores occurs, it is manifest in many ways, on one hand, there is a sensibilization of the fluorescence of the acceptor (emission of the acceptor in absence of direct light exciting), but on the other hand, there is a quenching of donor's fluorescence (since its transferring its energy to the acceptor, and then it does not emit fluorescence). Furthermore, when FRET occurs, the halftime of the fluorophere (time that the excited electron stays in an excited state before releasing the energy) it is decreased. Depending in which of this events is analyzed, different kinds of FRET approaches can be done.

FRET Sensitized Emission consists in to analyze the fluorescence emitted by the acceptor fluorophore, when the donor is excited. Experiments of FRET SE must be done under some specific conditions with live cells.

FRET SE was used to measure the molecular proximity between Kv1.3 and KCNE4. A Leica TCS SL laser scanning confocal spectral microscope (Leica Microsystems) equipped with an argon laser, 63_oil immersion objective lens (NA 1.32) and a double dichroic filter (458/514 nm) was used. CFP was used as the donor fluorochrome paired with YFP, as the acceptor fluorochrome. To measure FRET, three images were acquired in the same order in all experiments through (1) the CFP channel (excitation 458 nm; emission 465–510 nm), (2) the FRET channel (excitation 458 nm; emission 525–600 nm) and (3) the YFP channel (excitation 514 nm; emission 525–600 nm). The background values were subtracted from the image values before performing FRET calculations. Control and experimental images were taken under the same photomultiplier gain conditions, offset and pinhole aperture. In order to calculate and eliminate non-FRET components from the FRET channel, images of cells transfected with either CFP or YFP alone were taken under the same conditions as for the experiments. The fraction of cross-over of CFP (*A*) and YFP (*B*) fluorescence was calculated for the different experimental conditions. Corrected FRET (FRETc) was calculated on a pixel-by-pixel basis for the entire image using the equation:

$$FRET_c = FRET–(A*CFP)–(B*YFP) \quad FRET_N=FRET_c/YFP$$

where FRET, CFP and YFP are the values for the background-subtracted images of cells expressing CFP and YFP acquired through the FRET, CFP and YFP channels,

respectively, and $FRET_N$ is FRET normalized. Mean $FRET_c$ values were calculated from mean fluorescence intensities for each selected region of interest (ROI) according to the above equation, and normalized ($FRET_N$) values for membrane regions were calculated according to the upper equation. All calculations were performed using the FRET sensitized emission wizard from Leica Confocal Software and Microsoft Excel. FRET values were expressed as the mean ± s.e.m. of $n>15$ cells for each group.

8.1.13.2. Total Internal Reflection Fluorescence Microscope (TIRFM)

For GFP bleaching experiments a TIRFM was used. Those experiments were performed with a Nikon Eclipse Ti Perfect-Focus equipped TIRF/wide-field fluorescence microscope equipped with AOTF-controlled 405, 488, 561 nm diode lasers, 100mW each, and an Intensilight wide-field light source. A 100xPlanApo TIRF, 1.49 NA, objective was used for image acquisition. Emission was collected through a Sutter Lambda 10–3 filter wheel containing the appropriate bandpass filters. This microscope is equipped with the Andor iXonEMCCD DU-897 camera, 512x512. For TIRF image acquisition, an incident angle of 63.3° was used.

Single bleaching steps counting is an approach which was first used by Isacoff and collaborators (Ulbrich and Isacoff 2007), and uses TIRF microscopy to visualize single GFP-tagged proteins on the cell surface. Since the photobleaching of a single GFP is a discrete process, the fluorescence intensity of a protein complex with one or several GFP molecules drops in a stepwise fashion and the number of steps reveals the number of GFP-tagged subunits in the complex.

HEK-293 cells transfected with GFP-tag were imaged within 24 h after electroporation in HEK physiological saline buffer consisting of (in mM): 146 NaCl, 4.7 KCl, 2.5 $CaCl_2$, 1 $MgCl_2$, 10 glucose, and 10 HEPES, pH 7.4. Videos were further processed and analyzed using Volocity software. Intensity of a 6x6 pixel ROIs were summed and calculated among all the duration of the videos. ROI's intensity was plot against the time. GFP bleaching steps were counted and statistically analyzed.

8.1.14. Electrophysiology

In this work there have been performed to types of electrophysiology recordings. Thus, an amphibian heterologous model such as *Xenopus laevis* oocytes were used for voltage-clamp experiments. Experoiments of pstch-clamp were performed in HEK-293 mammalian cells.

8.1.14.1. Xenopus oocytes

Channels and regulatory subunits were cloned to oocyte expression vectors (Roura-Ferrer phD thesis 2008). The expression in Xenopus oocytes is divided in three main steps: synthesis of the messangerRNA, preparation of the oocytes and microinjection of the oocytes with mRNAs.

First, a linearitzation of the cDNAs was done. Next, the mRNAs were generated with T7 and SP6 RNA polymerase by using the mMESSAGE mMACHINE kit, according to the manufacturer's instructions (Ambion).

Oocyte preparation was performed as described previously (Villarroel and Schwarz 1996). Stage V or VI oocytes were enzymatically defolliculated with collagenase (Sigma), 1 mg/ml in Ca^{2+}-free solution, in a solution containing, in mM, 82.5 NaCl, 2.5 KCl, 1 $MgCl_2$, and 5 HEPES, pH 7.5. They were then transferred to a Ca^{2+}-containing solution, ND96, consisting of, in mM, 96 NaCl, 2 KCl, 1.8 $CaCl_2$, 1 $MgCl_2$, and 5 HEPES, pH 7.5.

Finally, the oocytes were injected with 50 nl of the mRNA using a Drummond microinjector. The amount of mRNA used of the channels was 10 ng. In the case of the regulatory subunits, the amount of mRNA was 5 ng (for KCNE1-3) and 2.5 ng (for KCNE4-5). This amount was decreased due to their smaller weigth and some cytotoxic effect, as described in (Grunnet et al. 2003). Oocytes were kept in ND96 buffer at 18ºC and used for recording two to four days after injection.

Whole-cell currents were recorded in oocytes at RT (22ºC) with a two-electrode voltage clamp using a virtual-ground Geneclamp 500B amplifier (Axon Instruments). Borosilicate electrodes were filled with 3 M KCl and had resistances of 1 MΩ. The oocytes were perfused continuously in Xenopus saline comprising, in mM, 100 NaCl, 2.5 KCl, 1 $MgCl_2$, 2 $MnCl_2$, and 5 HEPES, pH 7.5. All chemicals, except where otherwise stated, were from Sigma. Data were acquired at a sampling rate of 1 KHz and filtered at 100 Hz.

Voltage-step protocols and current analysis were performed with pCLAMP8.2 software (Axon Instruments). The voltage activation was determined as follows: oocytes were clamped for 3 s from a holding potential of -50 mV to voltages between -100 to +60 mV in 10 mV steps, and followed by a constant pulse to -20 mV of 1 s duration. The current activated at different voltage test pulses was estimated by measuring the amplitude of corresponding tail currents at -20 mV. For each oocyte, the current (I), was normalized relative to its maximal value. To evaluate the voltage dependence of potassium channels, the mean values of currents (±SE) were plotted versus voltage, and the I/V relationship was fitted to a Boltzmann function of the form:

$$I = I_{max}/[1 + \exp((V_{1/2}-V_m)/slope)]$$

where Imax is the maximal current and $V_{1/2}$ is the membrane potential (V_m) at which $I=I_{max}/2$. Fits were made by treating Imax , $V_{1/2}$ and slope as free parameters, and the best values of constants were obtained by applying an iterative procedure of fitting to minimize the least-squares error between the data and the calculated fit point. Data were normalized in Excel

and plotted with SigmaPlot. For statistical evaluation, the unpaired Student's t-test was applied. A $p<0.05$ was considered significant.

8.1.14.2. Mammalian expression system: HEK-293.

Some 100 mm dishes of 70% confluent were transfected with 2 µg of each DNA. After 24 h cells were trypsinized and seed in 35mm dish in order to have individual cells to record. 24h later whole-cell currents were measured with a D-6100 Darmstadt amplifier (List Medical) using the patch clamp technique. Currents were low-pass filtered at 1 kHz. Series resistance compensation was always above 70%. The pClamp8 software (Axon Instruments) was used for pulse generation and data acquired using an Axon Digidata A/D interface and subsequent analysis.

Electrodes were fabricated from borosilicate glass capillaries (Clark Electromedical Instruments) using a Flaming-Brown (P-87) micropipette puller (Sutter Instruments) and fire polished. Pipettes had a resistance of 2-3 MW when filled with a solution containing (in mM): 144 KCl, 0.2 $CaCl_2$, 1.2 $MgCl_2$, 10 Hepes, 0.5 EGTA (pH 7.35 and 302 mosmoles/l). The extracellular solution contained (in mM): 150 NaCl, 4 KCl, 2 $CaCl_2$, 1 $MgCl_2$, 10 Hepes (pH 7.4 and 310 mosmoles/l).

Cells were clamped to a holding potential of –80 mV. To evoke voltage gated currents, all cells were stimulated with 200-millisecond square pulses ranging from –100 to +60 mV in 20 mV steps. All recordings were routinely subtracted for leak currents. To calculate inactivation time constants (t), cells were held at –80 mV and a +60 mV pulse potential of 5 seconds was applied. Inactivation adjustment was calculated from the peak of the current at 60 mV to the steady-state inactivation, and traces were fitted with Sigma Plot (SPSS, Chicago, IL). To analyze cumulative inactivation, currents were elicited by a train of 25 depolarizing voltage steps of 200 milliseconds to +60 mV once every 400 milliseconds.

REFERENCES

Grunnet, M., Rasmussen, H. B., Hay-Schmidt, A., Rosenstierne, M., Klaerke, D. A., Olesen, S. P. and Jespersen, T. (2003). "*KCNE4 is an inhibitory subunit to Kv1.1 and Kv1.3 potassium channels*." Biophys J 85(3): 1525-1537.

Meerpohl, H. G., Lohmann-Matthes, M. L. and Fischer, H. (1976). "*Studies on the activation of mouse bone marrow-derived macrophages by the macrophage cytotoxicity factor (MCF)*." Eur J Immunol 6(3): 213-217.

Sargiacomo, M., Sudol, M., Tang, Z. and Lisanti, M. P. (1993). "*Signal transducing molecules and glycosyl-phosphatidylinositol-linked proteins form a caveolin-rich insoluble complex in MDCK cells*." J Cell Biol 122(4): 789-807.

Ulbrich, M. H. and Isacoff, E. Y. (2007). "*Subunit counting in membrane-bound proteins*." Nat Methods 4(4): 319-321.

Villarroel, A. and Schwarz, T. L. (1996). "*Inhibition of the Kv4 (Shal) family of transient K+ currents by arachidonic acid*." J Neurosci 16(8): 2522-2532.

8.2. Tables

8.2.1. Table of constructions provided

Plasmid	Observations	Origin
Kv1.3 prc/CMV	Rat Kv1.3 in prc/CMV vector	T.C.Holmes (New York University)
Kv1.3-HA	Rat Kv1.3 with HA-tag between S3-S4 loop	B. Arnold (University of Southern California)
Kv1.3-YFP/CFP	Rat Kv1.3 in YFP or CFP-C1 plasmid	R. Vicente (phD thesis 2005 UB)
Kv1.5	Human Kv1.5 in pBK plasmid	M.M.Tamkun (Colorado State University)
Kv1.5-YFP/CFP	Rat Kv1.5 in YFP or CFP-C1 plasmid	R. Vicente (phD thesis 2005 UB)
Kv7.1	Human Kv7.1 in pTLN vector	T.Jentzsch (Instituto farmacológico molecular de Berlín)
Kv7.1-YFP/CFP	Human Kv7.1 in YFP or CFP-N1 vector	M. Roura-Ferrer (phD thesis 2008 UB)
Kv7.5	Human Kv7.5 in pTPN vector	Given by Dr. T. Jentzsch (Instituto farmacológico molecular de Berlín)
Kv7.5-YFP	Human Kv7.5 in YFP-N1 vector	Given by Dr. Shapiro (Texas University)
Kv7.5-CFP	Human Kv7.5 in CFP-N1 vector	Generated by Dra. Roura-Ferrer (thesis 2008)
KCNE1-CFP/YFP	Human KCNE1 in CFP or YFP-N1 plasmid	Generated by Dra. Roura-Ferrer (thesis 2008)
KCNE1-pXoom	Human KCNE1 in pXoom plasmid (for Xenopus oocytes expression)	Generated by Dra. Roura-Ferrer (thesis 2008)
HA-KCNE1	HA tag in the Nt of human KCNE1, in pCDNA plasmid	Given by Dra. De la Luna (Centre de Recerca Genòmica de Barcelona)
KCNE2-CFP/YFP	Mouse KCNE2 in CFP or YFP-N1 plasmid	Generated by Dra. Roura-Ferrer (thesis 2008)
KCNE2-pXoom	Human KCNE2 in pXoom plasmid	Generated by Dra. Roura-Ferrer (thesis 2008)
HA-KCNE2	HA tag in the Nt of human KCNE2, in pCDNA plasmid	Given by Dra. De la Luna (Centre de Recerca Genòmica de Barcelona)
KCNE3-CFP/YFP	Mouse KCNE3 in CFP or YFP-N1 plasmid	Generated by Dra. Roura-Ferrer (thesis 2008)
KCNE3-pXoom	Human KCNE3 in pXoom plasmid	Given by Dr. Jaques Barhanin (Instituto de Farmacología Molecular y Celular de Valbone)
HA-KCNE3	HA tag in the Nt of human	Generated by Dra. Roura-Ferrer (thesis

	KCNE3, in pCDNA plasmid	2008)
KCNE4-CFP/YFP	Mouse KCNE4 in CFP or YFP-N1 plasmid	Generated by Dra. Roura-Ferrer (thesis 2008)
KCNE4-pXoom	Human KCNE4 in pXoom plasmid	Given by Given by Dr. Jaques Barhanin (Instituto de Farmacología Molecular y Celular de Valbone)
HA-KCNE4	HA tag in the Nt of human KCNE4, in pCDNA plasmid	Generated by Dra. Roura-Ferrer (thesis 2008)
KCNE4-HA-IRES-GFP	Human KCNE4 tagged with 3xHA in the Ct, in an IRES plasmid that also express GFP	Given by Dr. George (Vanderbilt Univesity)
KCNE5-CFP/YFP	Human KCNE5 in CFP or YFP-N1 plasmid	Generated by Dra. Roura-Ferrer (thesis 2008)
KCNE5-pXoom	Human KCNE5 in pXoom plasmid	Given by Dr. Jaques Barhanin (Instituto de Farmacología Molecular y Celular de Valbone)
KCNE5-HA	HA tag in the Nt of human KCNE5, in pCDNA plasmid	Generated by Dra. Roura-Ferrer (thesis 2008)
YFP-Kv1.3_ΔC	rKv1.3 with a deletion of Ct, in YFP-C1 vector	Generated by Dr. Martínez-Mármol (thesis 2010)
YFP-Kv1.3_ΔN	rKv1.3 with a deletion of Nt, in YFP-C1 vector	Generated by Dr. Martínez-Mármol (thesis 2010)
YFP-Kv1.3_ΔP	rKv1.3 with a deletion of the pore, in YFP-C1 vector	Generated by Dr. Martínez-Mármol (thesis 2010)
YFP-Kv1.3_Ntermkv1.5	rKv1.3 with Nt of hKv1.5, in YFP-C1 vector (YFP-1.5-1.3-1.3)	Generated by Dr. Martínez-Mármol (thesis 2010)
YFP-Kv1.3_Ctermkv1.5	rKv1.3 with Ct of hKv1.5, in YFP-C1 vector (YFP-1.3-1.3-1.5)	Generated by Dr. Martínez-Mármol (thesis 2010)
CFP-Kv1.5_Ntermkv1.3	hKv1.5 with Nt of rKv1.3, in CFP-C1 vector (CFP-1.3-1.5-1.5)	Generated by Dr. Martínez-Mármol (thesis 2010)
CFP-Kv1.5_Ctermkv1.3	hKv1.5 with Ct of rKv1.3 (CFP-1.5-1.5-1.3)	Generated by Dr. Martínez-Mármol (thesis 2010)
YFP-Kv1.3_F492stop	rKv1.3-YFP with a stop at position 492 (aa)	Generated by Dr. Martínez-Mármol (thesis 2010)
YFP-Kv1.3_M487stop	rKv1.3-YFP with a stop at position 492 (aa)	Generated by Dr. Martínez-Mármol (thesis 2010)
YFP-Kv1.3_G483stop	rKv1.3-YFP with a stop at position 483 (aa)	Generated by Dr. Martínez-Mármol (thesis 2010)
YFP-Kv1.3_G478stop	rKv1.3-YFP with a stop at position 478 (aa)	Generated by Dr. Martínez-Mármol (thesis 2010)
YFP-Kv1.3_G442stop	rKv1.3-YFP with a stop at position 442 (aa)	Generated by Dr. Martínez-Mármol (thesis 2010)
YFP-Kv1.3_F433stop	rKv1.3-YFP with a stop at position	Generated by Dr. Martínez-Mármol

	433 (aa)	(thesis 2010)
YFP-Kv1.3_PDZstop	rKv1.3-YFP with a stop at position 522 (aa), before PDZ domain.	Generated by Dr. Martínez-Mármol (thesis 2010)
Calmodulin-YFP	YFP fused to Calmodulin, in a pCDNA3 plasmid	Given by Dr. Villarroel (Universidad País Vasco)
Calmodulin	Calmodulin in pCDNA3 vector	Given by Dr. Villarroel (Universidad País Vasco)
mCherry	Monomeric-Cherry-C1 vector	Given by Dr. Piston (Vanderbilt University)
mApple	Monomeric-Apple-C1 vector	Given by Dr. Piston (Vanderbilt University)

8.2. Table of constructs generated during this PhD

Construct	Comments	Insert	Vector	Restriction enzymes used	Primers used (5´-3' seq)
KCNE4-HA-IRES	KCNE4-HA-IRES no GFP expression. A STOP was introduced at the second aa of the GFP		KCNE4-HA-IRES-GFP		F: AATATGGCCACAACCATGTGAGCAAGGGCGAGGAGC R: GCTCCTCGCCCTTGCTCACATGGTTGTGGCCATATT
GFP-Kv1.3	Simple digestion of rKv1.3-YFP subcloned into GFP-C1.	rKv1.3	pEGFP-C1	Bgl II Hind III	
Apple-Kv1.3	rKv1.3 obtained by simple digestion of Kv1.3-YFP and cloned to a Apple-C1 plasmid.	rKv1.3	mApple-C1	Bgl II Hind III	
Cherry-Kv1.3	rKv1.3 obtained by simple digestion of Kv1.3-YFP and cloned to a Cherry-C1 plasmid.	rKv1.3	mCherry-C1	Bgl II Hind III	
KCNE4-GFP	GFP was amplified by PCR from EGFR-GFP-N1 plasmid and cloned to E4CFP plasmid (previously CFP also was removed by digestion)	GFP	KCNE4-CFP-C1	BamHI Not I	F: CTAGCGGATCCGGTCGCCACCATGGTGAGC R: GAGATCGCGGCCGCTACTTGTACAGCTCGT
KCNE4-Cherry	Cherry was amplified by PCR from Cherry-C1 plasmid and cloned to E4CFP plasmid (previously CFP also was removed by digestion)	Cherry	KCNE4-C1	BamHI Not I	Similar to KCNE4-GFP
YFP-Kv1.3-Kv1.3 tandem	Kv1.3 without Stop codon (previously removed by site-directed mutagenesis) was amplified by PCR from YFP-Kv1.3 plasmid and cloned next to another Kv1.3 in the same plasmid	Kv1.3-STOPless	YFP-Kv1.3-C1	Hind III Eco RI	Fmut: ATATTCACTGATGTCTTAAAGCTTCGAATTCTG Rmut: CAGAATTCGAAGCTTTAAGACATCAGTGAATAT F: CCCAAGCTTATGACCGTGGTG R:

					TTCACTCATGTCTAAGAATTCCGG
KCNE4-link-YFP-Kv1.3	mKCNE4 cloned with a flexible link of 16aa at Nt of YFP-Kv1.3. 2 pcrs done: first to introduce Nhe I target at Nt of KCNE4 and half of the link at Ct of KCNE4, and second to introduce the rest of the link.	mKCNE4 from KCNE4-CFP	YFP-Kv1.3 C1	Nhe I	For1: CTAGCTAGCCTATGCTAGAGGATGGAGCC Rev1: CTACCTCCTGATCCTCCACTACCACCCTCGGAATTCTGGTGGATGTTC For2 = For1 Rev2: CGGCTAGCCGACCTCCACTACCTCCGCTACCTCCTGATCCTCCACTACC
KCNE4-link-YFP-Kv1.3-Kv1.3	mKCNE4 cloned with a flexible link of 16aa at Nt of YFP-Kv1.3-Kv1.3 tandem.	mKCNE4 from KCNE4-CFP	YFP-Kv1.3-Kv1.3 C1	Nhe I	The same than for KCE4-link-YFP-Kv1.3
KCNE4-CFP NruI mut Ct	Mutant with NruI target at the beginning of Ct		KCNE4-CFP N1		F: CTGGACTTCTTCTCGCGACGCTTGGATTTCATGTAGCCR: GGCTACATGAAATCCAAGCGTCGCGAGAAGAAGTCCAG
KCNE2-CFP NruI mut Ct	Mutant with NruI target at the beginning of Ct		KCNE2-CFP N1		F: CACTGTGAAATCCAAGCGTCGCGAACACTCCAATGACCR: ATTGGAGTGTTCGCGACGCTTGGATTTCACAGTGCTCACCAG
KCNE4-4-2-CFP	KCNE4 with Ct of KCNE2, fused with CFP	Ct hKCNE2 from KCNE2-CFP	KCNE4-CFP NruI mut Ct	Nru I Bam HI	
KCNE2-2-4-CFP	KCNE2 with Ct of KCNE4, fused with CFP	Ct mKCNE4 from KCNE2-CFP	KCNE2-CFP NruI mut Ct	Nru I Bam HI	
KCNE4-CFP target MluI Nt and Ct	KCNE4 with two MluI targets flanking the transmembrane region, generated by multiple site mutagenesis		mKCNE4-CFP-N1		F1 (Mlu I target Nt): GTACAGCAGTGTAATGGCAACGCGTACTTCTATATTTTGGTC F2 (Mlu I target Ct): GATCGGAAATCATGCTGGGCACGCGTAAATCCAAGAGGCGG
KCNE2-CFP target MluI Nt and Ct	KCNE2 with two MluI targets flanking the transmembrane region, generated by multiple site mutagenesis.		hKCNE2-CFP-N1		F1 (Mlu I target Nt): GTTGATGCTGAGAACTACGCGTATGTCATCCTGTACCTCC F2 (Mlu I target Ct): CCATCCTGGTGAGCACGCGTAAATCCAAGAGACGGG
KCNE4-2-4-CFP	KCNE4 with the transmembrane of KCNE2, fused to CFP	Trasmembrane of hKCNE2-CFP	KCNE4-CFP target MluI Nt and Ct	Mlu I	
KCNE2-4-2-CFP	KCNE2 with the transmembrane of KCNE4, fused to CFP	Trasmembrane of mKCNE4-CFP	KCNE2-CFP target MluI Nt and Ct	Mlu I	
KCNE4-L(69-72)A-CFP	KCNE4 with leucines 69-79 mutated to alanines		mKCNE4-CFP-N1		F: GAGAAGAAGTCCAGCGCTGCGGCGGCGTACAAAGAC

					GAGGAG R: CTCCTCGTCTTTGTACGCC GCCGCAGCGCTGGACTTC TTCTC
KCNE2-2L-CFP	KCNE2 with aa 82 and 83 mutated to leucines		hKCNE2-CFP-N1		F: CAAGAGACGGGAACACTC CAGTTCCTTATACCACCAG TACAGTACATTGTAG R: CTACAATGTACTGGTGGTA TAAGGAACTGGAGTGTTCC CGTCTCTTG
KCNE2-LLLL-CFP	KCNE2 with 4 leucines (82-85 aa)		KCNE2-2L-CFP		F: GAACACTCCAGTTCCTTAT TACTCCTGTACATTGTAGA GGACTGGC R: GCCAGTCCTCTACAATGTA CAGGAGTAATAAGGAACTG GAGTGTTC
HA-KCNE4-105STOP	HA-KCNE4 with a stop codon at 105 bp position, just before transmembrane region. E35 → STOP		HA-KCNE4		F: GCGGCAATGGCAACTAGT ACTTCTACATTCTG R: CAGAATGTAGAAGTACTAG TTGCCATTGCCGC
HA-KCNE4-170STOP	HA-KCNE4 with a stop codon at 170 bp position, just after transmembrane region. Y57 → STOP		HA-KCNE4		F: AATCATGCTGGGCTGAATG AAATCCAAGAGG R: CCTCTTGGATTTCATTCAG CCCAGCATGATT
HA-KCNE4-204STOP	HA-KCNE4 with a stop codon at 204 bp position, just before the tetra-leucine motif. S68 → STOP		HA-KCNE4		F: GGGAGAAGAAGTCCTGAC TCCTGCTGCTGTAC R: GTACAGCAGCAGGAGTCA GGACTTCTTCTCCC
HA-KCNE4-219STOP	HA-KCNE4 with a stop codon at 219 bp position, just after the tetra-leucine motif. Y73 → STOP		HA-KCNE4		F: GCCTCCTGCTGCTGTAGAA AGACGAGGAGCG R: CGCTCCTCGTCTTTCTACA GCAGCAGGAGGC
HA-KCNE4-288STOP	HA-KCNE4 with a stop codon at 288 bp position. V96 → STOP		HA-KCNE4		F: CGGGCCTGAGGTCGTAGC AGGTGCCCCTGATG R: CATCAGGGGCACCTGCTA CGACCTCAGGCCCG
HA-KCNE4-375STOP	HA-KCNE4 with a stop codon at 375 bp position. V125→ STOP		HA-KCNE4		F: CCATGGAAGGGGACAGCT AGAGCTCCGAGTCCTC R: GAGGACTCGGAGCTCTAG CTGTCCCCTTCCATGG
HA-KCNE4-418STOP	HA-KCNE4 with a stop codon at 418 bp position. V140 → STOP		HA-KCNE4		F: GCACCTCACCATTTAGGAG GAGGGGGCAGACGATG R: CATCGTCTGCCCCCTCCTC CTAAATGGTGAGGTGC
HA-KCNE4-453STOP	HA-KCNE4 with a stop codon at 453 bp position. S151 → STOP		HA-KCNE4		F: GAGCTGGAGGAGACCTAG GAGACGCCCCTCAACG R: CGTTGAGGGGCGTCTCCT AGGTCTCCTCCAGCTC

8.3. Primers used for RT-PCR analysis

	5'-3' Sequence	Accession number	Annealing T (ºC)	Amplicon (bp)
Mouse KCNE1	For: TGA CAG CAA GCA GGA GGC GCT Rev: GAC ATA GCA AGC TCT GAA GC	NM_008424	58	210
Mouse KCNE2	For: GTC ATC CTG TAC CTC ATG GT Rev: TTC TCA TGG ATG GTG GCC TT	NM_134110	60	194
Mouse KCNE3	For: CGT AAT GAC AAC TCC TAC ATG Rev: TAC ACA TGA TAG GGG TCA CT'	NM_020574	67	127
Mouse KCNE4	For: TCC AGC AGC CCC CTC GAG TC Rev: AGG CTG GAC TTC TTC TCC CG (BMDC) For: CCT GAC AGA GAA GAG AAA CA Rev: TGA ACA GCA CAT ACC CCA G (Raw246.7)	NM_020574	60 55	158 139
Mouse KCNE5	For: ACC CCT ACC CCG CAT ATC CAA Rev: TTG GAC GTG CTG GAT TCT GTT	NM_021487	55	106
Human KCNE1	For: TGT GCC TGG GAA GTT TGA G Rev:GGG AAC CAC TGA CAG TCT ATC	NM_000219	70	634
Human KCNE2	For: ACG CCA GCA AGA AGG TTC A Rev: CTT GCT CAG CTG TTG TGT TC	NM_172201	60	183
Human KCNE3	For: GCT AAT ACA TGC AAT GTG GC Rev:TTC AAT GGG TAC TTC CAG G	NM_005472	55	137
Human KCNE4	Quantitect primer assay from Qiagen Ref QT00046676	NM_080671	55	105
Human KCNE5	For: CCT ACC CCG CAC ATC CAA CTG CAC Rev: TTG GAC GTG TTG GAT TCA GTT CC	NM_012282	62	104
Mouse Kv1.3	For: AGTATATGGTGATCGAAGAGG Rev: AGTGAATATCTTCTTGATGTT	NM_019270	55	136
18S	For: CGC AGA ATT CCC ACT CCC GAC CC Rev:CCC AAG ATC CAA CTA CGA GC	NR_003286 Human NR_003278 Mouse	55	210

8.4. List of antibodies used for co-immunoprecipitation experiments.

Antibody	Comercial brand	Developed in	Protein recommended for binding
GFP	Roche	Mouse	Protein G
GFP	GenScript	Rabbit	Protein A
HA	Sigma	Rabbit	Protein A
Calmodulin	Millipore	Mouse	Protein G

8.5. Table with the primary and secondary antibodies used for WB analysis

PRIMARY ANTIBODIES			
Antibody	**Developed in**	**Dilution used**	**Commercial brand**
Anti-β-actin	Mouse	1/50000	Sigma
Anti-Calmodulin	Mouse	1/600	Millipore
Anti-Caveolin	Rabbit	1/2500	BD Bioscience
Anti-Clathrin	Mouse	1/1000	BD Bioscience
Anti-GFP	Mouse	1/1000	Roche
Anti-HA	Rabbit	1/200	Sigma
Anti-KCNE4	Rabbit	1/800	Proteintech
Anti-Kv1.3	Mouse	1/1000	Neuromab
Anti-Kv7.1	Rabbit	1/200	Alomone
Anti-Kv7.5	Rabbit	1/500	Dr. Villarroel (in house)
Anti-Na/K ATPasa	Mouse	1/100	DSHB

SECONDARY ANTIBODIES (conjugated with HRP)		
Antibody	**Dilution used**	**Commercial brand**
Goat-anti-mouse	1/10000	Bio-Rad
Goat-anti-rabbit	1/3000	Bio-Rad

8.6. Table with the antibodies used for immunocytochemistry

PRIMARY ANTIBODIES			
Antibody	**Developed in**	**Working Dilution**	**Commercial Brand**
Anti-HA	Mouse	1/250	Covance
Anti-KCNE4	Rabbit		Proteintech
Anti-Kv1.3	Rabbit		Alomone

SECONDARY ANTIBODIES		
Antibody	**Working Dilution**	**Commercial Brand**
Goat-anti-mouse	1/100-1/1000	Molecular Probes
Goat-anti-rabbit	1/100-1/1000	Molecular Probes

8.7. List of chemical compounds used

Name	Function	Working dilution	Vehicle	Source
Brefeldin A (BFA)	Inhibits the anterograde transport of COPII type vesicles.	12.5 µg/ml (12 h)	DMSO	Sigma
Tunicamycin	N-glycosilation blocker via N-acteylglucosamine transferases.	12 µg/ml (24 h)	DMSO	Sigma
Lipopolysaccharide (LPS)	Generation of immunological responses via TLR4.	100 ng/ml (24 h)		Sigma
PMA	Phorbol esther PKC activator		DMSO	Sigma
PHA	Phytohematoglutinin		H_20	Sigma
M-CSF	Macrophage colony stimulating factor	1200 U/ml	H_20	
Dexamethasone (Dex)	Glucocorticoid	1 µM (24 h)	DMSO	Sigma
Poly-D-lysine	layer of positive charges promoting cell adhesion to the glass covers-slips.	1/500 of 0.1%	H_20	Sigma